



TECHNISCHE  
UNIVERSITÄT  
WIEN

D I S S E R T A T I O N

## Frequency-Dependent Complex-Scaled Infinite Elements for Exterior Helmholtz Resonance Problems

ausgeführt zum Zwecke der Erlangung des akademischen Grades  
eines Doktors der technischen Wissenschaften unter der Leitung von

**Assoc. Prof. Dr. Lothar Nannen**

E101-03 – Institut für Analysis und Scientific Computing,  
Forschungsbereich Scientific Computing and Modelling – TU Wien

eingereicht an der Technischen Universität Wien  
Fakultät für Mathematik und Geoinformation

von

**Dipl.-Ing. Markus Wess**

Matrikelnummer: 0725824

Wiedner Hauptstraße 106/1/5  
1050 Wien

Diese Dissertation haben begutachtet:

1. **Prof. Dr. Luka Grubišić**  
Department of Mathematics, University of Zagreb
2. **Assoc. Prof. Dr. Lothar Nannen**  
Institut für Analysis und Scientific Computing, TU Wien
3. **Prof. Dr. Achim Schädle**  
Mathematisches Institut, Heinrich-Heine-Universität Düsseldorf

Wien, am 22. Mai 2020



Die approbierte gedruckte Originalversion dieser Dissertation ist an der TU Wien Bibliothek verfügbar.  
The approved original version of this doctoral thesis is available in print at TU Wien Bibliothek.

# Kurzfassung

Resonanzphänomene können auftreten, wenn ein Wellensystem in gewissen Frequenzen angeregt wird. Für die mathematische Analysis von Resonanzen werden häufig zeitharmonische Wellen – Wellen mit einer gegebenen Kreisfrequenz – untersucht. In der vorliegenden Arbeit beschäftigen wir uns mit der numerischen Analysis der Helmholtz Gleichung – einer partiellen Differentialgleichung, die beispielsweise zeitharmonische akustische Wellen modelliert – auf unbeschränkten Gebieten und den zugehörigen Resonanzproblemen.

Eine beliebte Methode um solche Probleme zu behandeln ist die sogenannte komplexe Skalierung. Die Idee dieser Methode ist eine künstliche Dämpfung der Welle außerhalb eines gewählten Innenraums einzuführen, sodass keine zusätzlichen Reflexionen auftreten. Wenn sogenannte perfectly matched layers verwendet werden, wird der Außenraum, in welchem die Dämpfung eingeführt wurde, abgeschnitten und das – nun endliche – Gebiet beispielsweise mittels finiter Elemente diskretisiert. In der vorliegenden Arbeit analysieren, implementieren und testen wir einige Adaptierungen der beschriebenen Methode.

Um einen größeren Frequenzbereich mit vergleichbar guten Approximationen zu erhalten, verwenden wir Methodenparameter, die von der unbekanntenen Resonanzfrequenz abhängen. Dieser Ansatz führt zu nichtlinearen Eigenwertproblemen anstatt, wie üblich, zu linearen.

Für die Diskretisierung des Problems verwenden wir eine Methode, die auf der Zerlegung einer Welle in einen ausstrahlenden radialen und einen oszillierenden transversalen Teil basiert. Die Ansatzfunktionen für den ausstrahlenden Teil sind dabei Funktionen mit unbeschränktem Träger, welche in gewissem Sinne äquivalent zu den Ansatzfunktionen der Hardyraum infiniten Elemente sind. Durch die Verwendung dieser Funktionen vermeiden wir eine künstliche Beschränkung des Außenraums und erhalten superalgebraische Approximationseigenschaften. Außerdem macht es diese Zerlegung einfach die Methode an die gegebene Problemgeometrie anzupassen.

Schlussendlich präsentieren wir ein effizientes Verfahren um die Eigenwerte der resultierenden diskreten, nichtlinearen Eigenwertprobleme zu approximieren. Dieses Verfahren ist, verglichen mit entsprechenden Methoden für lineare Eigenwertprobleme, in seiner Anwendung nicht signifikant aufwändiger.

Numerische Experimente unterstreichen unsere Ergebnisse und zeigen die oben beschriebenen Vorteile unserer Methode.



Die approbierte gedruckte Originalversion dieser Dissertation ist an der TU Wien Bibliothek verfügbar.  
The approved original version of this doctoral thesis is available in print at TU Wien Bibliothek.

# Abstract

Resonance phenomena occur, when waves in a given system are excited at certain frequencies. For the mathematical analysis of resonances, time-harmonic waves (i.e., waves that are periodic in time, with respect to a given angular frequency) can be considered. In this work we are concerned with the numerical analysis of the Helmholtz equation – a partial differential equation that models, for example, time-harmonic acoustic waves – on unbounded domains and the numerical analysis of the according resonance problems.

A popular method for treating such problems is the so-called complex scaling. The idea of this method is to introduce an artificial damping of the waves outside of a chosen computational interior domain in a way that no additional reflections are induced. When so-called perfectly matched layers are used, the exterior domain (i.e., the part of the domain where the damping is introduced) is truncated to a bounded layer and discretized using, for instance, finite elements. In the work at hand, we analyze, implement, and test a number of improvements to the method described above.

To obtain a larger number of equally-well approximated resonances, we use method parameters that depend on the unknown resonance frequency. This approach leads to non-linear eigenvalue problems, instead of linear ones.

For the discretization of the problem, we use a method based on the decomposition of a wave into a propagating radial and an oscillating transversal part. The discrete ansatz functions for the propagating part are functions with unbounded support and are closely related to the ansatz functions of Hardy space infinite element methods and spectral element methods. Due to the use of these functions, we avoid the artificial truncation of the exterior domain and obtain super-algebraic approximation properties. Moreover, this decomposition makes it straightforward to adapt the method to the specific geometry of the given problem.

Lastly, we present an efficient method to approximate the eigenvalues of the resulting discrete, non-linear eigenvalue problems, which requires no significant extra computational effort, compared to similar methods for linear eigenvalue problems.

Numerical experiments underline our findings and exhibit the advantages of our method described above.



Die approbierte gedruckte Originalversion dieser Dissertation ist an der TU Wien Bibliothek verfügbar.  
The approved original version of this doctoral thesis is available in print at TU Wien Bibliothek.

# Acknowledgement

First and foremost I want to thank my adviser Assoc. Prof. Lothar Nannen for his guidance and support during these last few years. I can't remember any occasion where I left through his, always open, office door after a discussion, without the feeling of having made a huge step forward in understanding the problems I was tackling at the time.

Secondly, I would like to express my gratitude to Prof. Joachim Schöberl who sparked my interest in numerical analysis during his lectures and gave me the opportunity to be part of his, in the best possible way extraordinary, work group. Netgen/NGsolve made the implementation of the numerical methods possible and quite enjoyable!

Special thanks to Prof. Luka Grubišić and Prof. Achim Schädle for reading and reviewing my thesis and also to Martin Halla who suggested the use of frequency-dependent PMLs for resonance problems in the first place. Moreover, I acknowledge support from the Austrian Science Fund (FWF): P26252.

Since, coincidentally, a substantial amount of people I want to thank are called Michael, Matthias, or Martin, I representatively mention these names for all of my colleagues, my office mates, my dear friends, my brothers, family members (including a, more or less recent, Styrian addition) and everyone else who helped me keeping a healthy balance between hard mathematics and other, likewise enjoyable, things in life.

I would like to express my gratitude to my parents, who were the first ones to support me and thankfully have not stopped to do so ever since.

Most importantly I want to thank my girlfriend Vicky, whose contributions range from keeping me caffeinated in the afternoon, through constructively criticizing my working hours, to sitting out a full-grown pandemic with me. You have always been the perfect companion and I happily look forward to realizing all of our mutual plans!

Vienna, May 22, 2020

Markus Wess



Die approbierte gedruckte Originalversion dieser Dissertation ist an der TU Wien Bibliothek verfügbar.  
The approved original version of this doctoral thesis is available in print at TU Wien Bibliothek.



# Eidesstattliche Erklärung

Ich erkläre an Eides statt, dass ich die vorliegende Dissertation selbstständig und ohne fremde Hilfe verfasst, andere als die angegebenen Quellen und Hilfsmittel nicht benutzt bzw. die wörtlich oder sinngemäß entnommenen Stellen als solche kenntlich gemacht habe.

Wien, am 22. Mai 2020

---

Dipl. Ing. Markus Wess



Die approbierte gedruckte Originalversion dieser Dissertation ist an der TU Wien Bibliothek verfügbar.  
The approved original version of this doctoral thesis is available in print at TU Wien Bibliothek.

# Contents

<b>1. Introduction</b>	<b>1</b>
1.1. Time-harmonic waves	1
1.2. Existing methods	3
1.3. Methods based on complex scaling	4
1.4. Hardy space and complex-scaled infinite elements	6
1.5. Main ideas	7
1.6. Structure of the thesis	8
1.7. Some remarks on notation	9
<b>2. Problem Setting</b>	<b>13</b>
2.1. Helmholtz resonance problems on unbounded domains	13
2.2. Radiating solutions of the Helmholtz equation	14
<b>3. Complex Scaling</b>	<b>19</b>
3.1. Complex scaling in exterior coordinates	19
3.2. Analytic continuation of eigenfunctions	23
3.3. Exponential decay of complex-scaled eigenfunctions	28
3.4. Existence of square-integrable analytic continuations of eigenfunctions	31
<b>4. Numerical Results for Frequency-Dependent Perfectly Matched Layers</b>	<b>33</b>
4.1. Frequency-dependent PMLs in one dimension	33
4.2. Frequency-dependent PMLs in higher dimensions	37
<b>5. Analysis</b>	<b>41</b>
5.1. The weak formulation of the complex-scaled problem	43
5.2. Fredholmness and weak coercivity	49
5.3. The essential spectrum	53
5.4. Discussion of the analysis	65
<b>6. Discretization</b>	<b>67</b>
6.1. Galerkin methods	67
6.2. Discretization and coupling	68
6.3. Radial discretization	70
6.4. Complex-scaled and Hardy space infinite elements	73
6.5. Approximation results for infinite elements	76
<b>7. Implementation</b>	<b>91</b>
7.1. The complex-scaled Helmholtz equation in various exterior coordinates	91
7.2. Derivation of rational eigenvalue problems	99

7.3. Specific frequency-dependencies and their essential spectra . . . . .	102
7.4. Assembling the infinite element matrices . . . . .	106
<b>8. Non-Linear Eigenvalue Problems</b>	<b>111</b>
8.1. Generalized-linear eigenvalue problems . . . . .	112
8.2. Rational eigenvalue problems . . . . .	114
<b>9. Numerical Experiments</b>	<b>131</b>
9.1. Condition numbers . . . . .	131
9.2. Comparison of different scalings . . . . .	132
9.3. Comparison of infinite elements to PMLs . . . . .	134
<b>10. Conclusion and Outlook</b>	<b>141</b>
10.1. Conclusion . . . . .	141
10.2. Applications and extensions . . . . .	142
10.3. Further open questions . . . . .	145
<b>A. Appendix</b>	<b>147</b>
A.1. Special functions . . . . .	147
A.2. Further necessary results and technical computations . . . . .	151
<b>Bibliography</b>	<b>157</b>

# 1. Introduction

Wave phenomena in physics and engineering can, in many cases, be modeled by hyperbolic partial differential equations of the form

$$L(p)(t, \mathbf{x}) + \frac{\partial^2}{\partial t^2} p(t, \mathbf{x}) = s(t, \mathbf{x}), \quad (1.1)$$

where  $L$  is a second-order, elliptic differential operator,  $p$  is the unknown wave function, and  $s$  is a given source term. The simplest example of an equation along the lines of (1.1) is the so-called *wave equation*. This equation is given by

$$-\Delta_{\mathbf{x}} p(t, \mathbf{x}) + \frac{1}{c(\mathbf{x})^2} \frac{\partial^2}{\partial t^2} p(t, \mathbf{x}) = s(t, \mathbf{x}), \quad (1.2)$$

where  $c(\mathbf{x})$  is the wave speed of the medium. An example for an application of the wave equation is the modelling of acoustic waves, where the function  $p$  models the variation of the pressure.

Other examples of equations along the lines of (1.1) include the curl curl-formulation of Maxwell's equations and the elastic wave equation.

## 1.1. Time-harmonic waves

A classical approach for the analysis of wave-type equations is to use a time-harmonic ansatz of the form

$$p(t, \mathbf{x}) = \operatorname{Re}(u(\mathbf{x}) \exp(-i\omega t)) \quad (1.3)$$

for a fixed frequency  $\omega \in \mathbb{R}$ , an amplitude  $u$ , and a source term of the form

$$s(t, \mathbf{x}) = \operatorname{Re}(f(\mathbf{x}) \exp(-i\omega t)),$$

where  $f$  is the amplitude of the time-harmonic source. Plugging this ansatz into the wave equation (1.2), we obtain that the function (1.3) solves (1.2) if the amplitude  $u$  fulfills

$$-\Delta u(\mathbf{x}) - \omega^2(1 + \rho(\mathbf{x}))^2 u(\mathbf{x}) = f(\mathbf{x}) \quad (1.4)$$

for  $c(\mathbf{x})^2 = \frac{1}{(1+\rho(\mathbf{x}))^2}$ . Equation (1.4) is called the *Helmholtz equation*. If, for a given domain  $\Omega$ , the right-hand side  $f : \Omega \rightarrow \mathbb{R}$  and the frequency  $\omega$  of (1.4) are known, one can try to solve the Helmholtz equation with suitable boundary conditions on  $\partial\Omega$  and thereby gather information about the solution of the wave equation (1.2). This problem is called the Helmholtz *scattering problem* (cf. Figure 1.1).

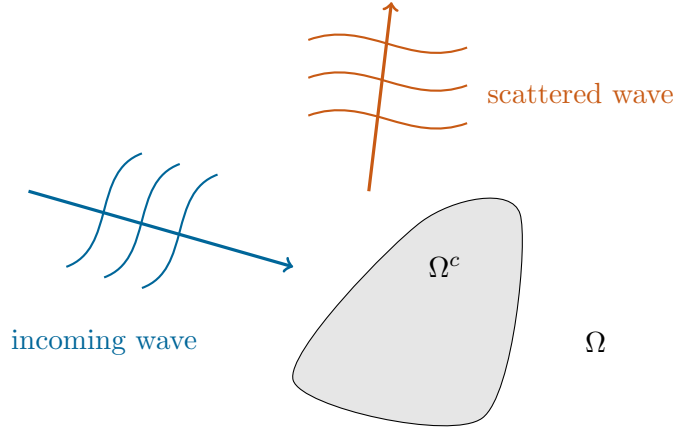


Figure 1.1.: Scattering of a wave by an obstacle.

Contrary to the scattering problem, the *resonance problem* is the task of finding frequencies  $\omega$  such that the scattering problem is not (uniquely) solvable. Helmholtz resonance problems are the main objects of research in this thesis. If, for a frequency  $\omega$ , there exists a function  $u_\omega \neq 0$  that solves the homogeneous Helmholtz equation

$$-\Delta u_\omega(\mathbf{x}) - \omega^2(1 + \rho(\mathbf{x}))^2 u_\omega(\mathbf{x}) = 0, \quad (1.5)$$

this frequency  $\omega$  and the function  $u_\omega$  are called an eigenfrequency and its respective eigenfunction or a resonance frequency and its respective resonance function. Suppose that there exists a complete orthonormal<sup>1</sup> system of eigenfunctions  $u_{\omega_n}, n \in \mathbb{N}_0$  of the operator  $-\Delta$  with suitable homogeneous boundary conditions<sup>2</sup>. Then the solutions of the scattering problem with  $\rho = 0$  can be written as a superposition of eigenfunctions

$$u(\mathbf{x}) = \sum_{n=0}^{\infty} \frac{(f, u_{\omega_n})}{\omega_n^2 - \omega^2} u_{\omega_n}(\mathbf{x}). \quad (1.6)$$

If the given frequency  $\omega$  is close to a resonance frequency  $\omega_n$  and  $(f, u_{\omega_n}) \neq 0$ , the according resonance function  $u_{\omega_n}$  is dominant in the expansion (1.6).

When a resonance  $\omega_n \in \mathbb{R}$  is excited over a period of time, the oscillation of the wave in question will increase up to a point where the system breaks down. In mechanics this phenomenon is known under the term *resonance catastrophe*. For a more comprehensive overview of the significance of resonances, we refer to [Zwo99].

### Helmholtz problems on unbounded domains

In many applications it is necessary to model the wave propagation in an unbounded domain (see Figure 1.1). Contrary to the case of bounded domains and non-lossy media,

<sup>1</sup>with respect to a suitable inner product  $(\cdot, \cdot)$

<sup>2</sup>Such orthonormal systems of eigenvectors exist, e.g., for compact operators and analogies can be derived for more general operators.

where the resonance frequencies are real, in the case of unbounded domains we have to expect complex resonances. In certain configurations it can be shown that the eigenvalues of (1.5) with suitable boundary and radiation conditions have non-positive imaginary parts ([N01, Theorem 2.6.1] and [SZ99]). The imaginary part of an eigenfrequency determines the decay over time of the wave corresponding to the according eigenfunction, where a smaller imaginary part results in a faster decay (cf. (1.3)). Therefore, and due to the fact that resonances close to the given frequency  $\omega$  dominate the resulting scattered wave (cf. (1.6)), the physically most interesting eigenvalues are the ones located close to the real axis.

Having to deal with unbounded domains is mathematically challenging for the following reasons: Due to the lack of an outer boundary, one has to specify a suitable radiation condition. This radiation condition is responsible for the selection of the physically meaningful solutions. We will see that, for frequencies with negative imaginary parts, the radiating eigenfunctions of (1.5) including boundary conditions are exponentially increasing in space for large arguments. Therefore, it is not straightforward to apply a classical  $L^2(\Omega)$ -framework for the analysis, as well as for the discretization of Helmholtz problems on unbounded domains.

Moreover, we want to apply finite element methods (see, e.g., [Cia02]) for the discretization of the problem, which are, in standard versions, only applicable on bounded domains. In the following section we briefly discuss several existing methods to overcome these difficulties.

## 1.2. Existing methods

One method for the treatment of waves in unbounded domains is to use absorbing boundary conditions on an, artificially chosen, exterior boundary. Such conditions can, for instance, be obtained by approximating the correct Dirichlet-to-Neumann operator (see [Giv01] for a review). Another approach is the use of boundary integral representations of the solution based on fundamental solutions (e.g., [SS11]). Moreover, there exists the relatively new method of half-space matching ([BDDFT18]), which is based on decomposing the exterior domain into overlapping half-spaces and constructing the overall solution out of the separate solutions on the half-spaces respectively.

Due to the fact that in the methods described above the dependency on the frequency is highly non-linear, applying these methods for resonance problems can be quite intricate (cf. [SU12] for boundary element methods for resonance problems).

In 1994 Bérenger proposed the so-called perfectly matched layers for time-dependent problems in [Ber94]. Perfectly matched layers were later recognized to be equivalent to a complex coordinate stretching or complex scaling when written in the frequency domain, a technique which was already known since the 1970s (e.g., [Sim79])<sup>3</sup>. Along the lines of the methods described above, the unbounded domain is decomposed into a bounded interior, surrounded by an unbounded exterior domain (cf. Figure 1.2). The complex scaling is applied to the exterior domain and is chosen in a way that the radiating solutions in question decay exponentially with respect to the spacial variable in the exterior domain. Thus, it can be expected that a truncation of the exterior domain will lead to small errors.

<sup>3</sup>For a more comprehensive historical overview we refer to [Hal19, Section 1.2].

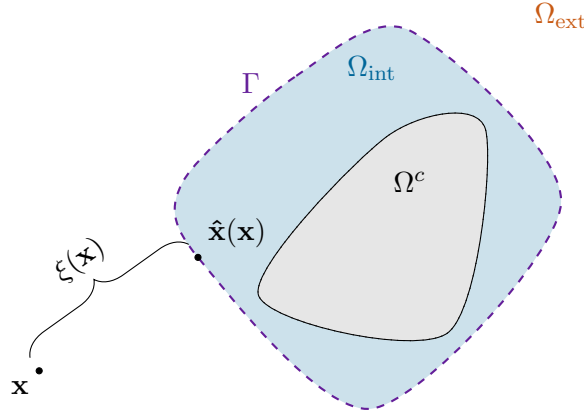


Figure 1.2.: The decomposition of the domain  $\Omega$  into an interior domain  $\Omega_{\text{int}}$  and an exterior domain  $\Omega_{\text{ext}}$  with interface  $\Gamma$  and exterior coordinates  $\xi(\mathbf{x}), \hat{\mathbf{x}}(\mathbf{x})$  of a point  $\mathbf{x} \in \Omega_{\text{ext}}$ .

Subsequently, the now both bounded interior and exterior domains are discretized using, for example, suitable finite elements or finite differences. The perfectly matched layers have been successfully applied to both, Helmholtz scattering and resonance problems (e.g., [Kim09, KP09, Kim14]).

Other methods are the use of Hardy space ([HN09]) or complex-scaled infinite elements ([NW19]). These methods will be discussed in more detail in Section 1.4.

### 1.3. Methods based on complex scaling

In the work at hand, we use methods based on complex scaling as briefly introduced in Section 1.2. In general these methods can be decomposed into the three single steps:

1. complex scaling,
2. discretization, and
3. solving the discrete problem.

In the following we discuss the state of the art of these three steps.

#### Complex scaling

As a preliminary step the unbounded domain  $\Omega$  is decomposed into a bounded interior domain  $\Omega_{\text{int}}$  and an unbounded exterior domain  $\Omega_{\text{ext}}$  (cf. Figure 1.2). The idea of the complex scaling is to utilize the fact that the solutions of the homogeneous Helmholtz equation (1.5) with analytic potential  $\rho$  allow an analytic continuation to a complex domain  $\Theta$  in a way that the real domain  $\Omega_{\text{ext}}$  is a subset of  $\Theta$ . One chooses a complex domain  $\tilde{\Omega}_{\text{ext}} \subset \Theta$  that has a one-to-one correspondence to  $\Omega_{\text{ext}}$ , so that the analytic continuations of the radiating solutions decrease exponentially in  $\tilde{\Omega}_{\text{ext}}$  for large arguments. Subsequently,



one derives an equation, called the complex-scaled equation, in a way that the analytic continuations to the complex domain  $\check{\Omega}_{\text{ext}}$  of the original radiating solutions are solutions of this new equation.

This procedure is helpful for the following reason: The exponentially decreasing solutions of the complex-scaled equation are elements of the Hilbert space  $H^1(\Omega)$  on the unbounded domain  $\Omega$ . This allows the derivation of a weak formulation which is essential for Galerkin methods, such as the finite element method.

The success and performance of the complex scaling depends on the choice of the complex domain  $\check{\Omega}_{\text{ext}}$ . In applications mostly scalings aligned with the cartesian coordinates are used ([Kim14, BP13, KP10b, KP10a]). This approach has the benefit of a straightforward derivation and implementation of the complex-scaled equation. Nevertheless, the analysis of such cartesian scalings can be quite challenging.

Another possible choice for the complex scaling is to choose the complexification in radial direction ([Hal19, CM98]). Generalizations of radial scalings include the choice of curvilinear coordinates ([LS01]) or generalized polar coordinates with respect to star-shaped interior domains ([Hal16]).

In addition to the scaling direction, a scaling profile has to be specified. This scaling profile determines the growth of the imaginary part of the complexified variable and therefore also the exponential decay of the solutions. Since this decay affects the quality of a possible approximation of the solution, a suitable choice of the scaling profile is substantial for the performance of the method. Here the choices range from simple linear scalings (e.g., [NW18]) to profiles which involve a singularity ([BHNPRr08]).

For scattering and time-dependent problems, it is common to use a complex coordinate transformation that depends on the frequency  $\omega$ . For resonance problems, on the other hand, this is usually omitted to preserve the linear structure of the resulting eigenvalue problem. Nevertheless, in [NW18] we successfully applied frequency-dependent scaling parameters to resonance problems as well, to also profit from the increased robustness and simplify the choice of parameters.

## Discretization

After applying the complex scaling, the resulting complex-scaled equation has to be discretized to obtain approximations to the solutions of the scattering or resonance problem.

The usual approach of the perfectly matched layer technique is to truncate the unbounded exterior domain to a bounded one. Since the solutions in question decay exponentially, one can expect that this truncation causes only an exponentially small error with respect to the size of the truncated domain. Subsequently the – now finite – domain can be meshed and standard finite elements can be used to discretize the truncated complex-scaled problem.

A way to avoid the additional truncation error is to remap the unbounded exterior domain to a bounded one, using a singular mapping, and to discretize the bounded mapped domain. This approach is related to the ideas in [BHNPRr08], where a scaling profile with singular imaginary part is used to evade truncation.

The approach we apply in the thesis at hand is to use ansatz functions with unbounded support, which are elements of  $H^1(\Omega)$ , to avoid the truncation of the exterior domain. For one-dimensional problems, similar ansatz functions are also used in spectral element

methods (e.g., [STW11]). The spaces spanned by these ansatz functions exhibit super-algebraic approximation properties for the solutions of the complex-scaled homogeneous Helmholtz equation with a linear scaling. Therefore, the use of more involved scaling profiles is not necessary in this case.

### Solvers for non-linear eigenvalue problems

The discretization of the frequency independently complex-scaled equation results in a large and sparse generalized-linear eigenvalue problem. For problems of this type, efficient algorithms, such as the Arnoldi algorithm ([Arn51]) or filtered subspace iteration (e.g., [TP14, GGO20]), are available for approximating eigenvalues. To obtain approximations to eigenvalues close to a given complex shift, a so-called shift-and-invert can be applied. For the application of this technique, in each step of the iteration the factorization of an inverse matrix has to be applied, which accounts for the main computational effort.

Contrary to the use of frequency-independent complex scalings, the application of frequency-dependent scalings with suitable frequency-dependencies leads to non-linear eigenvalue problems that are rational in the frequency .

Non-linear eigenvalue problems appear in a wide range of applications and numerical methods have been discussed for a long time (e.g., [Ruh73]). For an extensive collection of non-linear eigenvalue problems we refer to [BHM<sup>+</sup>13] and for a more recent overview of (mostly iterative projection methods) to [MV04]. A newer class of methods for holomorphic eigenvalue problems are methods based on contour integrals ([SS03, Bey12]). These contour-integration-based methods have also been combined with methods based on subspace iteration (e.g., [EG15]). Nevertheless, all of the methods above are less efficient compared to the methods for generalized-linear eigenvalue problems.

### 1.4. Hardy space and complex-scaled infinite elements

The method of Hardy space infinite elements (e.g., [HN09, Hal16]) is based on a radiation condition called the pole condition. This condition is a condition on the Laplace transformed solution with respect to the radial spacial variable and was introduced for time-dependent Schrödinger-type equations ([SD95, SY97]). Besides the method of Hardy space infinite elements, there exist various other numerical methods based on the pole condition (e.g., [HSZ03a, HSZ03b, RSS13, GS11]).

The idea of the Hardy space infinite element method is to approximate the Laplace transformed solution using suitable discrete spaces that are tensor products of discrete tangential spaces and discretizations of certain Hardy spaces. These Hardy spaces are chosen in a way that their elements fulfill the pole condition.

Using Hardy space infinite elements has numerous advantages over the standard perfectly matched layer method: Since it is based on a decomposition into (generalized) polar coordinates, it already takes into account the fact that the radial and the tangential part of the solutions behave differently. Moreover, due to the tensor product approach, no explicit meshing of the exterior domain is necessary. Since the solutions are approximated in the Laplace domain, no truncation is needed. Therefore, no additional error is introduced and the process of choosing a suitable truncation can be omitted. Furthermore, the Hardy

space infinite element method exhibits super-algebraic convergence rates with respect to the number of radial degrees of freedom.

In addition to the first versions of the Hardy space infinite elements from [HN09], there exist also more involved versions of this method ([HHNS16, HN18]). These modified versions allow also the treatment of problems that model waves with different signs of the phase- and group-velocities.

The cost for all these positive aspects is the fact that one has to deal with the unusual setting of Laplace transformed solutions and the according Hardy spaces. Moreover, there are no quadrature rules available for the numerical computation of the discretization matrices.

Complex-scaled infinite elements ([NW19]) use spaces of functions with unbounded support to discretize the complex-scaled problem. The radial parts of these ansatz functions are closely related to the Laguerre functions, which form a complete orthonormal system of the space  $L^2(\mathbb{R}_{>0})$ .

It can be shown that the complex-scaled infinite elements are, to some extent, equivalent to standard Hardy space infinite elements<sup>4</sup>. Thus, the complex-scaled infinite elements unite all the benefits of the perfectly matched layer method (easy implementation, standard framework for analysis, numerical integration) with the ones of the Hardy space infinite element method (tensor product discretization, super-algebraic convergence, no truncation, only linear scalings necessary).

## 1.5. Main ideas

In our work we present several additions and improvements to the existing methods for Helmholtz resonance problems based on complex scaling described in Section 1.3. They can be summarized under the three headings given below.

### Complex scaling in exterior coordinates

We describe a point  $\mathbf{x}$  in the exterior domain by a generalized-radial coordinate  $\xi(\mathbf{x}) \in \mathbb{R}_{>0}$  and a surface coordinate  $\hat{\mathbf{x}}(\mathbf{x}) \in \Gamma$ , where  $\Gamma$  denotes the interface between the interior and the exterior domain (see Figure 1.2 and Definition 3.1). The complex scaling is applied solely in the direction of the generalized-radial coordinate. By using exterior coordinates, it is possible to geometrically adapt the complex scaling to the given problem and avoid having to discretize an unnecessary large interior domain.

Moreover, the exterior coordinates can be employed for the discretization in the following way: We use suitable tensor product spaces of a discrete space on the interface  $\Gamma$  and generalized-radial ansatz functions defined on  $\mathbb{R}_{>0}$  (or on a bounded subset of  $\mathbb{R}_{>0}$  as in Section 6.2). The discrete space on the interface  $\Gamma$  is thereby already given by the  $\Gamma$ -traces of the discrete ansatz functions in the interior domain  $\Omega_{\text{int}}$ .

<sup>4</sup>In [GS11] a numerical method based on the pole condition was re-interpreted as a finite difference method. We emphasize that our approach is different since we construct a correspondence not only between the discretization matrices, but between the basis functions of the two methods.

### Frequency-dependent complex scaling

We choose the parameters of the complex scaling dependent on the frequency (Section 7.3). Although this can lead to a non-linearity in the frequency and therefore to non-linear eigenvalue problems, this approach can make the problem more robust and simplifies the choice of suitable parameters. We show in Sections 5.3 and 7.3 how the choice of the frequency-dependency affects the essential spectrum of the problem.

### Complex-scaled infinite elements

We discretize the generalized-radial part of the eigenfunctions in the exterior domain by using complex-scaled infinite elements (Section 6.3). They consist of generalized-radial ansatz functions that are linear combinations of generalized Laguerre functions. Advantages of these infinite elements over standard perfectly matched layers include the facts that no domain truncation is necessary and we obtain super-algebraic approximation properties.

The three concepts described above can be combined at will. It is, for example, possible to discretize the complex-scaled Helmholtz equation with a frequency-dependent scaling in exterior coordinates using perfectly matched layers (cf. [NW18]) or to apply complex-scaled infinite elements without a frequency-dependency (cf. [NW19]).

In addition to the ideas described above, we present a method for approximating rational eigenvalue problems. We apply an algorithm based on a shift-and-invert where the inverse matrix that has to be factorized has the same dimensions as the matrix of a corresponding generalized-linear problem. Since the factorization and application of this inverse matrix contributes the main computational effort, our method is not significantly more expensive, in terms of the computational costs, than algorithms for generalized-linear problems (Chapter 8).

## 1.6. Structure of the thesis

The remainder of this work is structured as follows: In Chapter 2 we properly define the Helmholtz resonance problems on unbounded domains, where Section 2.2 is dedicated to the discussion of the radiation condition we make use of.

Chapter 3 gives a definition of the exterior coordinates we employ to generate linear complex scalings. Moreover, in Section 3.2 we derive necessary assumptions for the eigenfunctions of the Helmholtz resonance problem to allow an analytic continuation to the complex-scaled domain. Furthermore, we prove in Section 3.3 under which conditions on the scaling the complex-scaled eigenfunctions are exponentially decreasing for large arguments.

For readers who are not familiar with [NW18], we briefly summarize the most important results thereof in Chapter 4 to motivate the use of frequency-dependent complex scalings and already exhibit some effects that will be important for understanding the successive chapters.

In Chapter 5 we analyze the weak formulation of the complex-scaled Helmholtz equation with a frequency-dependent scaling. We show that the problem is Fredholm for frequencies in a certain region of the complex plane depending on the given scaling. Moreover, we prove the existence of two different parts of the essential spectrum.

In Chapter 6 we discuss how the exterior domain is discretized using complex-scaled infinite elements and give some approximation results in Section 6.5. Moreover, we explain the correspondence between complex-scaled infinite elements and Hardy space infinite elements in Section 6.4.

For readers who are primarily interested in the implementation of frequency-dependent complex scalings, we present in Chapter 7 all the relevant weak formulations for some examples of exterior coordinates (Sections 7.1 and 7.2) and a variety of frequency-dependencies of the scaling parameter (Section 7.3). We also derive explicit formulas for the possible location of the essential spectrum.

Chapter 8 describes the algorithms used to efficiently solve the non-linear eigenvalue problems that result from the frequency-dependent complex scaling.

Chapter 9 gives a number of numerical results that exhibit the properties of our method derived in Chapters 5–7. Moreover, we perform numerical experiments that indicate that some results may be generalized and/or refined.

We close with a short conclusion, an outlook on possible applications and extensions, and address open questions in Chapter 10.

Appendix A contains some results that are necessary for the completeness of this thesis but are not contained in the main text to maintain a clean presentation.

## 1.7. Some remarks on notation

We use bold, lower-case letters for vectors and bold, capital letters for matrices. The entries of matrices/vectors are denoted by the same letter with subscript indices. Families of matrices/vectors denoted by the same letter are indexed by superscript indices. Thus, a subscript indexed bold letter mostly indicates a scalar quantity.

For  $\alpha \in \mathbb{C} \setminus \{0\}$  and  $\mathbf{x} \in \mathbb{C}^n$ , we use the notation

$$\frac{\mathbf{x}}{\alpha} := \frac{1}{\alpha} \mathbf{x}.$$

The letters  $\mathbf{n}$  and  $\mathbf{t}$  usually denote the (outward) normal and tangential vectors to manifolds. The symbol  $\mathbf{I}_X$  denotes the identity on some space  $X$ . If  $X$  is (a subspace) of  $\mathbb{C}^d$  we also write  $\mathbf{I}_d$ . Moreover, we use the symbol  $\mathbf{0}$  for vectors or matrices where all entries are zero. The dimensions of the zero vector/matrix can be deduced from the context or is given explicitly.

The Jacobian of a function  $f : \mathbb{R}^m \rightarrow \mathbb{R}^n$  is denoted by  $Df : \mathbb{R}^m \rightarrow \mathbb{R}^{n \times m}$  and for  $n = 1$  we denote its gradient by  $\nabla f = (Df)^\top : \mathbb{R}^m \rightarrow \mathbb{R}^m$ . We use similar notations for functions on complex domains and complex values. Moreover, we use the notation  $f(\cdot)$  to emphasize that we address the function as an object and not its value at a certain point.

We write  $\mathbb{N} := \{1, 2, \dots\}$  and  $\mathbb{N}_0 := \{0, 1, 2, \dots\}$ . We write  $\mathbb{R}_{\geq 0}$  for all real numbers larger or equal to zero and use similar notations for other subsets of the real numbers. Similarly

we write  $\mathbb{C}_{\text{Im}>0} := \{z \in \mathbb{C} : \text{Im}(z) > 0\}$  and so on, where  $\text{Re}(\cdot)$  and  $\text{Im}(\cdot)$  denote the real and the imaginary part of a complex number respectively.

The argument  $\arg(z)$  of a complex number  $z$  is its polar angle and we use the convention  $\arg(z) \in [0, 2\pi)$ . By default, the symbol  $\sqrt{\cdot}$  denotes the square root that is continuous from  $\mathbb{C} \setminus \mathbb{R}_{\leq 0}$  to  $\mathbb{C}_{\text{Re}>0}$  and maps negative real values to the positive imaginary axis. Whenever we want to emphasize the branch-cut of the square root we use the notation

$$\sqrt[\alpha]{z} = \sqrt[\alpha]{r \exp(i\varphi)} := \sqrt{r} \exp\left(\frac{i\varphi}{2}\right)$$

for the square root with the branch-cut at  $\alpha\mathbb{R}_{\geq 0}$ , where  $\alpha \in \mathbb{C} \setminus \{0\}$ ,  $r \geq 0$ , and  $\varphi \in (\arg \alpha - 2\pi, \arg \alpha]$  such that  $z = r \exp(i\varphi)$ .

For vectors  $\mathbf{x} \in \mathbb{C}^d$  or  $\mathbf{x} \in \mathbb{R}^d$ , the notation  $\|\cdot\|$ , without subscript, denotes the Euclidean norm

$$\|\mathbf{x}\| := \sqrt{\mathbf{x} \cdot \bar{\mathbf{x}}},$$

where  $\cdot$  denotes the real inner product without conjugation.

For a Hilbert space  $X$ , we use the symbol  $\mathcal{B}(X)$  for the set of all bounded operators that map  $X$  to itself. For  $x, y \in X$ , we write  $(x, y)_X$  and  $\|x\|_X$  for the  $X$ -inner product and the  $X$ -norm respectively.

We denote the open ball with center  $\mathbf{0}$  and radius  $R > 0$  in  $\mathbb{R}^d$  by

$$B_R^d := \left\{ \mathbf{x} \in \mathbb{R}^d : \|\mathbf{x}\| < R \right\}.$$

Moreover, we write

$$S_R^d = \partial B_R = \left\{ \mathbf{x} \in \mathbb{R}^d : \|\mathbf{x}\| = R \right\}.$$

Whenever the dimension  $d$  is clear, we omit the superscript  $d$ . We use the symbol  $\sim$  for the equivalence relation

$$f \sim g, \quad x \rightarrow a \quad \iff \quad \lim_{x \rightarrow a} \frac{f(x)}{g(x)} = 1$$

for some functions  $f, g : M \rightarrow \mathbb{C}$  on a set  $M$  such that the limit  $x \rightarrow a$  is defined for  $x \in M$ .

For two vectors  $\mathbf{x}, \mathbf{y} \in \mathbb{R}^d$ , we denote the angle enclosed by  $\mathbf{x}$  and  $\mathbf{y}$  by

$$\angle(\mathbf{x}, \mathbf{y}) := \arccos\left(\frac{\mathbf{x} \cdot \mathbf{y}}{\|\mathbf{x}\| \|\mathbf{y}\|}\right) \in [0, \pi].$$

For a (piecewise) smooth,  $d - 1$ -dimensional manifold  $\Gamma \subset \mathbb{R}^d$ , an integrable function  $f : \Gamma \rightarrow \mathbb{C}$ , and an embedding  $\varphi : M \subset \mathbb{R}^{d-1} \rightarrow \Gamma$ , we write

$$\int_{\varphi(M)} f(\hat{\mathbf{x}}) d\hat{\mathbf{x}} := \int_M (f \circ \varphi)(\eta) \sqrt{\det\left((D\varphi(\eta))^\top D\varphi(\eta)\right)} d\eta \quad (1.7)$$

for the integration by the surface measure of  $\Gamma$ . Moreover, we write  $\hat{\nabla}$  for the surface gradient

$$\left(\hat{\nabla} f\right)(\varphi(\eta)) := \left(D\varphi(\eta)^\dagger\right)^\top \nabla_\eta (f \circ \varphi)(\eta). \quad (1.8)$$

Here for a matrix  $\mathbf{A} \subset \mathbb{C}^{n \times m}$  with full rank and dimensions  $m \leq n$ ,

$$\mathbf{A}^\dagger := \left( \mathbf{A}^\top \mathbf{A} \right)^{-1} \mathbf{A}^\top$$

denotes the Moore-Penrose pseudo-inverse of a matrix.

The symbol  $(\cdot)!!$  denotes the double factorial defined by

$$(2n + 1)!! := 1 \cdot 3 \cdots (2n - 1) \cdot (2n + 1)$$

for  $n \in \mathbb{N}_0$ .

For a function  $f : M \rightarrow \mathbb{C}^n$  on some set  $M \subset \mathbb{C}^m$  and  $m, n \in \mathbb{N}$ , we denote its support by

$$\text{supp}(f) := \overline{\{\mathbf{x} \in M : |f(\mathbf{x})| > 0\}}.$$

We use the symbol  $\mathcal{P}_n$  for the set of polynomials up to the degree  $n \in \mathbb{N}_0$ .

Lastly, we use the terms *analytic* and *holomorphic* synonymously for complex differentiable functions on open domains.



Die approbierte gedruckte Originalversion dieser Dissertation ist an der TU Wien Bibliothek verfügbar.  
The approved original version of this doctoral thesis is available in print at TU Wien Bibliothek.



## 2. Problem Setting

This chapter is dedicated to the proper definition of Helmholtz resonance problems on unbounded domains. We have to pay special attention to the definition of a suitable radiation condition that replaces the – due to the unboundedness of the given domain – missing boundary condition. This radiation condition is responsible for selecting physically meaningful solutions and is defined in Section 2.2.1 for  $d = 1$  and in Section 2.2.2 for higher dimensions.

### 2.1. Helmholtz resonance problems on unbounded domains

In the following let  $d \in \{1, 2, 3\}$  denote the spacial dimension and  $\Omega_{\text{int}}, \Omega_{\text{ext}}, \Omega, \Omega_0, \Gamma, \Gamma_0 \subset \mathbb{R}^d$ . Moreover, we assume that these sets fulfill the following assumptions (see Figure 2.1 for a two-dimensional example):

- (D1)  $\Omega_{\text{int}}, \Omega_{\text{ext}}, \Omega, \Omega_0 \neq \emptyset$  are open domains and  $\Gamma, \Gamma_0$  are  $d - 1$ -dimensional manifolds without boundary,
- (D2) the sets  $\Omega_{\text{int}}, \Gamma$  and  $\Omega_{\text{ext}}$  are pairwise disjoint  $\Omega_{\text{int}} \cup \Gamma \cup \Omega_{\text{ext}} = \Omega$ , and  $\Gamma = \partial\Omega_{\text{ext}}$ ,
- (D3)  $\Omega^c$  and  $\Omega_{\text{int}}$  are bounded and  $\Omega^c \subset \Omega_{\text{ext}}^c$ ,
- (D4)  $\partial\Omega, \Gamma$  are locally Lipschitz, and
- (D5)  $\Omega^c \subset \Omega_0 \subset \Omega_{\text{ext}}^c$ ,  $\Gamma_0 = \partial\Omega_0$  is smooth, and  $\overline{\Omega_0} \cap \overline{\Omega_{\text{ext}}} = \emptyset$ .

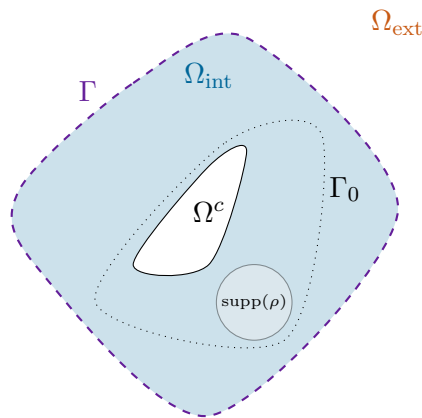


Figure 2.1.: An example of two-dimensional domains that fulfill (D1–5).

*Remark 2.1.* For  $d = 1$ , the interface  $\Gamma$  consists of two points  $\Gamma = \{R_l, R_r\}$  for some  $R_l, R_r \in \mathbb{R}$  such that  $R_l < R_r$ . The exterior domain  $\Omega_{\text{ext}}$  consists of the two disjoint sets  $\Omega_{\text{ext}}^l, \Omega_{\text{ext}}^r$  with  $\Omega_{\text{ext}}^l = (-\infty, R_l)$ ,  $\Omega_{\text{ext}}^r = (R_r, \infty)$ .

*Remark 2.2.* The conditions on the domains (D1–5) restrict our presentation to domains that are complements of compact sets. This excludes other interesting configurations, such as (open) waveguides and half-spaces. We point out that many of the ideas in our work can be applied to such configurations with, none or little, modifications as well.

On domains that fulfill the assumptions (D1–5), we study the following resonance problem:

**Problem 2.3.** Let  $\Omega, \Omega_{\text{int}}, \Omega_{\text{ext}}, \Omega_0, \Gamma, \Gamma_0 \subset \mathbb{R}^d$  fulfill (D1–5). Moreover, let  $\rho \in C(\Omega)$  be such that  $\text{supp}(\rho) \subset \Omega_0$  (see Figure 2.1) and  $\rho(\mathbf{x}) > -1$  for all  $\mathbf{x} \in \Omega$ . Then the problem to find  $\omega \in \mathbb{C}$  and  $u \in C^2(\Omega) \setminus \{0\}$  such that

$$-\Delta u(\mathbf{x}) = \omega^2(\rho(\mathbf{x}) + 1)^2 u(\mathbf{x}), \quad \mathbf{x} \in \Omega, \quad (2.1a)$$

$$u \text{ fulfills some homogeneous boundary condition,} \quad \mathbf{x} \in \partial\Omega, \quad (2.1b)$$

$$u \text{ is radiating,} \quad \|\mathbf{x}\| \rightarrow \infty \quad (2.1c)$$

is called the strong formulation of the *Helmholtz resonance problem*. A complex number  $\omega$  and a function  $u$  that fulfill (2.1) are called an *eigenvalue* and its corresponding *eigenfunction* or a *resonance frequency* and its corresponding *resonance function*.

The boundary condition (2.1b) can be a homogeneous Neumann, Dirichlet, or Robin boundary condition. Also a composition of these three types is possible. Unlike in the case of *scattering problems*, where for a given right-hand side and a given frequency the (unique) solution is sought after, in the case of resonance problems, also the corresponding eigenvalue or resonance frequency  $\omega$  is unknown. The eigenvalues of Problem 2.3 are values of  $\omega$  where the corresponding scattering problem is not uniquely solvable.

*Remark 2.4.* To keep the definition of the Helmholtz resonance problem as simple as possible, we confine ourselves to continuous potential functions  $\rho$  in Problem 2.3. Nevertheless, if suitable additional conditions are provided, more general, for example, piecewise continuous potentials can be used (cf. the experiments in Chapters 4 and 9).

*Remark 2.5.* Condition (D5) and the condition on  $\text{supp}(\rho)$  imply that there is a positive distance between  $\Gamma$  and  $\Gamma_0$ . This assumption ensures a certain regularity of the eigenfunctions of Problem 2.3 on the interface  $\Gamma$ . Sufficient weaker assumptions would be to require, for example, convexity and a certain regularity of the scatterer  $\Omega^c$ .

Next we have to specify the radiation condition (2.1c), namely, what we mean by the term *radiating*.

## 2.2. Radiating solutions of the Helmholtz equation

We define our radiation condition in the following order: In Section 2.2.1 we discuss the radiation conditions in one dimension and for positive frequencies  $\omega$  only. Subsequently, we extend our definition to complex frequencies. In Section 2.2.2 we define the radiation condition for  $d = 2, 3$ . We close this section with a brief discussion of radiation conditions (Section 2.2.3).

### 2.2.1. The radiation condition in one dimension

Although we will see that in one dimension the Helmholtz resonance problem behaves, in some respects, very differently from the problem in higher dimensions, it is, nevertheless, very instructive to consider this simple case first. Thus, we open this chapter with the definition and discussion of radiation conditions in one dimension. We focus on the case  $\omega > 0$  first.

In  $\Omega_{\text{ext}}^r = (R_r, \infty)$  (see Remark 2.1) all solutions to (2.1a) for  $\omega \neq 0$  are given by

$$u(x) = C_1 u_1(x) + C_2 u_2(x) \quad (2.2)$$

for some constants  $C_1, C_2 \in \mathbb{C}$ , where

$$u_{1,2}(x) := \exp(\pm i\omega x).$$

In Chapter 1 we derived the Helmholtz equation by looking for time-harmonic solutions of the wave equation given by

$$p(x, t) = \text{Re}(u(x) \exp(-i\omega t)). \quad (2.3)$$

By plugging (2.2) into (2.3), we obtain

$$p(x, t) = \text{Re}(C_1 \exp(i\omega(x - t)) + C_2 \exp(i\omega(-x - t))).$$

The first summand is an exponential that moves to the right over time, while the second summand moves to the left. Assuming that sources occur exclusively in  $\Omega_{\text{int}}$ , the physically reasonable assumption for radiating solutions is to consider only solutions with  $C_2 = 0$  in  $\Omega_{\text{ext}}^r$  and  $C_1 = 0$  in  $\Omega_{\text{ext}}^l$ . A mathematically precise formulation of this is to impose that the averaged outward energy flux

$$J(u) := -\frac{1}{2\omega} \text{Im} \left( \int_{\Gamma} u(\hat{\mathbf{x}}) \overline{\nabla u(\hat{\mathbf{x}})} \cdot \mathbf{n}(\hat{\mathbf{x}}) d\hat{\mathbf{x}} \right) \quad (2.4)$$

is positive for solutions  $u$  for every possible source in the interior. This means that the averaged outward energy flux for both,  $u_1$  and  $u_2$ , has to be positive. Because of

$$J(\exp(\pm i\omega \cdot)) = -\frac{1}{2\omega} \text{Im} \left( \mp i\omega |\exp(\pm i\omega R_r)|^2 \right) = \pm \frac{1}{2},$$

this energy flux at  $R_r$  is positive for  $u_1$  and negative for  $u_2$ . A similar calculation shows that it is negative for  $u_1$  and positive for  $u_2$  at  $R_l$ .

Thus, for  $d = 1$ , the radiation condition in (2.1c) in Problem 2.3 can be stated as follows:

**Definition 2.6.** For  $d = 1$  and  $\omega \in \mathbb{C} \setminus \{0\}$ , we call a solution  $u$  of (2.1a) *radiating*, if there exist constants  $\alpha_l, \alpha_r \in \mathbb{C} \setminus \{0\}$  such that

$$\begin{aligned} u(x) &= \alpha_l \exp(-i\omega x), & x &\in \Omega_{\text{ext}}^l, \\ u(x) &= \alpha_r \exp(i\omega x), & x &\in \Omega_{\text{ext}}^r. \end{aligned}$$

Note that, although we motivated Definition 2.6 by the use of the averaged outward energy flux, which is only meaningful for positive real frequencies, Definition 2.6 remains also valid for complex frequencies.

Definition 2.6 is, by far, not the only way to define a useful radiation condition. In fact, there are many different ways to do so. While Definition 2.6 explicitly imposes a condition on the solution in the whole exterior domain, another possibility is to only impose a condition on the asymptotic behavior of the solution. An example for this is the so-called *Sommerfeld* condition ([CK98, Definition 2.3] and (2.9)).

Another way to state a radiation condition is to impose a condition merely at the interface  $\Gamma$ . For  $d = 1$ , this can be done by imposing

$$u'(R_r) - i\omega u(R_r) = 0, \quad u'(R_l) + i\omega u(R_l) = 0. \quad (2.5)$$

Note that (2.5) is equivalent to the radiation condition from Definition 2.6.

### 2.2.2. The radiation condition in higher dimensions

Similar to the one-dimensional case, we choose to specify our radiation condition by giving an explicit representation of the radiating eigenfunctions in  $\Omega_{\text{ext}}$ . While for  $d = 1$  the solutions to the homogeneous Helmholtz equation in  $\Omega_{\text{ext}}$  are given by superpositions of exponentials with positive and negative signs (2.2), for higher dimensions, they can be written down in terms of (spherical) Hankel functions and cylindrical/spherical harmonics.

Using these special functions (Section A.1.1), we are in the position to properly define the radiation condition (2.1c) for  $d = 2, 3$  (cf. [CK98, Theorem 2.4]<sup>1</sup>).

**Definition 2.7.** For  $d = 2, 3$  and  $\omega \in \mathbb{C} \setminus \{0\}$ , we call a solution  $u$  of (2.1a) *radiating* if

$$u(\mathbf{x}) = \frac{i}{4} \int_{\Gamma_0} u(\mathbf{y}) \nabla G_{\mathbf{x}}(\mathbf{y}) \cdot \mathbf{n}(\mathbf{y}) - \nabla u(\mathbf{y}) \cdot \mathbf{n}(\mathbf{y}) G_{\mathbf{x}}(\mathbf{y}) \, d\mathbf{y} \quad (2.6)$$

for all  $\mathbf{x} \in \mathbb{R}^d \setminus \overline{\Omega_0}$ , where

$$G_{\mathbf{x}}(\mathbf{y}) := \begin{cases} H_0^{(1)}(\omega \|\mathbf{x} - \mathbf{y}\|), & d = 2, \\ \frac{\omega}{\pi} h_0^{(1)}(\omega \|\mathbf{x} - \mathbf{y}\|), & d = 3. \end{cases} \quad (2.7)$$

The integration in (2.6) has to be understood as integration with respect to the surface measure of  $\Gamma_0$  as defined in (1.7).

Proposition 2.8 shows that a function  $u$  given by (2.6) allows an expansion in (spherical) Hankel functions of the first kind and cylindrical/spherical harmonics.

**Proposition 2.8.** *A solution  $u$  of (2.1), for  $d = 2, 3$  and  $\omega \in \mathbb{C} \setminus \{0\}$ , is radiating, in the sense of Definition 2.7, if there exist  $\alpha_k, \beta_{k,j} \in \mathbb{C}$ , and  $R > 0$  such that*

$$u(\mathbf{x}) = \begin{cases} \sum_{k=-\infty}^{\infty} \alpha_k H_{|k|}^{(1)}(\omega \|\mathbf{x}\|) \Phi_k\left(\frac{\mathbf{x}}{\|\mathbf{x}\|}\right), & d = 2, \\ \sum_{k=0}^{\infty} \sum_{j=-k}^k \beta_{k,j} h_k^{(1)}(\omega \|\mathbf{x}\|) Y_k^j\left(\frac{\mathbf{x}}{\|\mathbf{x}\|}\right), & d = 3 \end{cases} \quad (2.8)$$

<sup>1</sup>Note that in [CK98] the Sommerfeld radiation condition is used and (2.6) is derived as a theorem. For resonance problems, this is not an option since the Sommerfeld condition is not feasible for frequencies with negative imaginary part (see Remark 2.9).

for all  $\|\mathbf{x}\| > R$ . This expansion is valid for all  $\|\mathbf{x}\| > \max\{\|\mathbf{y}\| : \mathbf{y} \in \Gamma_0\}$ . The sums converge uniformly on compact subsets of  $\{\mathbf{x} \in \Omega : \|\mathbf{x}\| > \max\{\|\mathbf{y}\| : \mathbf{y} \in \Gamma_0\}\}$ .

*Proof.* This is proven by a transformation of the Helmholtz equation in polar coordinates and a Fourier decomposition of the solution into spherical/cylindrical harmonics, which form a complete orthogonal system of  $H^1(S_1)$ . For  $d = 3$ , see [CK98, Thm. 2.14].  $\square$

For  $d = 2, 3$ , the (spherical) Hankel functions of the first kind adopt the role of the exponential with the correct sign in one dimension. It can be shown that functions that satisfy (2.8) have a positive averaged outward energy flux (2.4) through the interface  $\Gamma$  (see [Nan17]). Functions composed of (spherical) Hankel functions of the second kind, on the other hand, have a negative energy flux.

### 2.2.3. A brief discussion of radiation conditions

Apart from the radiation conditions introduced in Section 2.2.1 and Section 2.2.2, there exist a variety of other radiation conditions. For an overview, we refer to [Nan17].

The so-called Sommerfeld condition ([CK98, Definition 2.3]) imposes a condition on the asymptotic behavior of the solution for large arguments. It can be stated by

$$\lim_{\|\mathbf{x}\| \rightarrow \infty} \|\mathbf{x}\|^{(d-1)/2} \left( \frac{\partial}{\partial \|\mathbf{x}\|} - i\omega \right) u(\mathbf{x}) = 0, \quad \text{uniformly in } \frac{\mathbf{x}}{\|\mathbf{x}\|}. \quad (2.9)$$

For  $d = 1$ , (2.9) is obviously equivalent to the condition defined in Definition 2.6 for all frequencies  $\omega \in \mathbb{C} \setminus \{0\}$ . For higher dimensions, Remark 2.9 shows that this is not the case for frequencies with a negative imaginary part.

A generalization of (2.5) to higher dimensions is given by

$$\nabla u(\hat{\mathbf{x}}) \cdot \mathbf{n}(\hat{\mathbf{x}}) - i\omega u(\hat{\mathbf{x}}) = 0, \quad \hat{\mathbf{x}} \in \Gamma, \quad (2.10)$$

where  $\mathbf{n}$  is the outward normal of the interface  $\Gamma$  pointing into  $\Omega_{\text{ext}}$ . Condition (2.10) is called the *first-order absorbing boundary condition*. Although in higher dimensions this condition is not equivalent to other radiation conditions, it is widely used as an approximation since it is straightforward to implement (cf., e.g., [Ihl98, Giv01, Giv04]).

*Remark 2.9.* For  $d = 3$  and  $\omega \in \mathbb{C} \setminus \{0\}$ , plugging  $u(\mathbf{x}) = h_0^{(1)}(\omega \|\cdot\|) Y_0^0\left(\frac{\cdot}{\|\cdot\|}\right)$  into the expression inside the limit of the left-hand side of (2.9) and using  $h_0^{(1)}(x) = \frac{\exp(ix)}{ix}$  gives

$$\begin{aligned} \|\mathbf{x}\| \left( \frac{\partial}{\partial \|\mathbf{x}\|} - i\omega \right) u(\mathbf{x}) &= \|\mathbf{x}\| Y_0^0\left(\frac{\mathbf{x}}{\|\mathbf{x}\|}\right) \omega \left( \left( h_0^{(1)} \right)'(\omega \|\mathbf{x}\|) - i h_0^{(1)}(\omega \|\mathbf{x}\|) \right) \\ &= \|\mathbf{x}\| Y_0^0\left(\frac{\mathbf{x}}{\|\mathbf{x}\|}\right) \omega \exp(i\omega \|\mathbf{x}\|) \left( \frac{1}{\omega \|\mathbf{x}\|} + \frac{i}{\omega^2 \|\mathbf{x}\|^2} - \frac{1}{\omega \|\mathbf{x}\|} \right) \\ &= Y_0^0\left(\frac{\mathbf{x}}{\|\mathbf{x}\|}\right) \frac{i \exp(i\omega \|\mathbf{x}\|)}{\omega \|\mathbf{x}\|}. \end{aligned}$$

While for  $\text{Im}(\omega) \geq 0$  this tends to zero for  $\|\mathbf{x}\| \rightarrow \infty$ , it is unbounded for  $\text{Im}(\omega) < 0$ . Therefore, the Sommerfeld radiation condition (2.9) is not equivalent to the radiation condition specified in Definition 2.7 for frequencies with negative imaginary part.

## 2. Problem Setting

---

The so-called *pole condition* ([SHK<sup>+</sup>07]) imposes a condition on the Laplace transformed solution with respect to the radial variable in  $\Omega_{\text{ext}}$ . The Hardy space infinite element method ([HN09] and Sections 1.4 and 6.4) is based on this condition.

Transparent boundary conditions are conditions on the solution at the interface  $\Gamma$  only (e.g., [Giv04]). They are often based on representations of the Dirichlet-to-Neumann operator, which maps the Dirichlet trace of a function on  $\Gamma$  to its Neumann trace.

Nevertheless, many of these transparent boundary conditions are not straightforward to employ in the context of finite element approximations to Helmholtz resonance problems. One difficulty here is the fact that the representation of the solution in the exterior and on the interface  $\Gamma$  depends highly non-linear on the frequency  $\omega$ . This makes the computation of discrete resonances very challenging. Moreover, the fact that the eigenfunctions of the Helmholtz resonance problem are not square-integrable on  $\Omega$ , due to the unboundedness of the exterior domain, poses an obstacle in deriving a variational formulation of Problem 2.3. We overcome this by using the technique of complex scaling. In the following chapters, we will derive the weak formulation of an equation with eigenfunctions that are square-integrable and the restrictions of analytic continuations of the sought-after eigenfunctions on a complexified exterior domain.

## 3. Complex Scaling

The main topic of this chapter is the proper definition of the complex scaling technique. In particular we focus on linear scaling functions which are sufficient for the use of complex-scaled infinite elements. Moreover, we deal with the question of analytic continuation of radiating eigenfunctions and show under which assumptions such continuations to a set containing the complex-scaled domain exist. In Section 3.3 we show that the complex-scaled eigenfunctions decrease exponentially for large arguments and are, therefore, square-integrable on  $\Omega$ . Although we will use a frequency-dependent scaling parameter later on, we omit this dependency in this chapter since all the definitions of this chapter can be stated without modifications for the frequency-dependent case as well.

### 3.1. Complex scaling in exterior coordinates

In Chapter 2 we have already imposed the assumptions (D1–5) on the domains in question to be able to define the Helmholtz resonance problem. We define exterior coordinates for such domains as follows:

**Definition 3.1.** Let  $d \in \{1, 2, 3\}$  and  $\Omega, \Omega_{\text{int}}, \Omega_{\text{ext}}, \Gamma \subset \mathbb{R}^d$  be such that (D1–4) are fulfilled. Moreover, let  $\mathbf{v} : \Gamma \rightarrow \mathbb{R}^d$  be continuous and piecewise smooth such that  $D\mathbf{v} \in L^\infty(\Gamma)$ . Additionally, we assume that

(C1) the mapping

$$\Psi : \begin{cases} \mathbb{R}_{>0} \times \Gamma & \rightarrow \Omega_{\text{ext}}, \\ (\xi, \hat{\mathbf{x}}) & \mapsto \hat{\mathbf{x}} + \xi \mathbf{v}(\hat{\mathbf{x}}) \end{cases}$$

is a bijection and

(C2)

$$(\hat{\mathbf{x}} - \mathbf{y}) \cdot \mathbf{v}(\hat{\mathbf{x}}) \geq 0$$

for all  $\hat{\mathbf{x}} \in \Gamma, \mathbf{y} \in \Gamma_0$ .

Then we call the mapping  $\Psi$  an *exterior coordinatization* of  $\Omega_{\text{ext}}$ . The mappings  $\xi, \hat{\mathbf{x}}$ , given by

$$(\xi(\mathbf{x}), \hat{\mathbf{x}}(\mathbf{x})) := \Psi^{-1}(\xi, \hat{\mathbf{x}}),$$

are called *exterior coordinates* (see Figure 3.1). Note that, in the following chapters, we will use the symbol  $\Psi$  also for complex and negative arguments  $\xi$ .

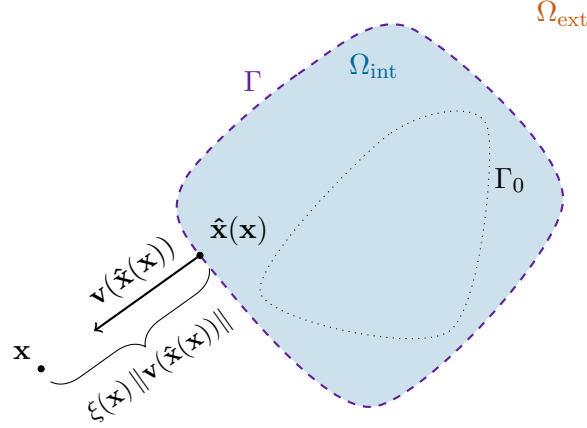


Figure 3.1.: An example of exterior coordinates.

Condition (C1) guarantees that we have indeed a parametrization of  $\Omega_{\text{ext}}$ , while we will see later on that condition (C2) ensures that our eigenfunctions allow an analytic continuation to a sufficiently large complex domain (Section 3.2). Note that (C2) implies

$$\angle(\hat{\mathbf{x}} - \mathbf{y}, \mathbf{v}(\hat{\mathbf{x}})) \in \left[0, \frac{\pi}{2}\right]$$

and the function  $(\hat{\mathbf{x}}, \mathbf{y}) \mapsto \angle(\hat{\mathbf{x}} - \mathbf{y}, \mathbf{v}(\hat{\mathbf{x}}))$  is continuous on the compact set  $\Gamma \times \Gamma_0$ . Thus, we may define

$$\mu := \max\{\angle(\hat{\mathbf{x}} - \mathbf{y}, \mathbf{v}(\hat{\mathbf{x}})), \hat{\mathbf{x}} \in \Gamma, \mathbf{y} \in \Gamma_0\} \in \left[0, \frac{\pi}{2}\right]. \quad (3.1)$$

Moreover, by condition (C1) it is clear that

$$\mathbf{v}(\hat{\mathbf{x}}) \neq 0$$

for all  $\hat{\mathbf{x}} \in \Gamma$ .

*Remark 3.2.* For  $d = 1$ , we have  $\Gamma = \{R_l, R_r\}$  with  $R_l < R_r$  (as in Remark 2.1). Thus,  $\mathbf{v}(R_l) = v_l \in \mathbb{R}_{<0}$  and  $\mathbf{v}(R_r) = v_r \in \mathbb{R}_{>0}$ .

*Example 3.3.* The simplest form of exterior coordinates that comes to mind are polar coordinates. In the notation of exterior coordinates they correspond to the configuration  $\Gamma = S_1$  and  $\mathbf{v}(\hat{\mathbf{x}}) = \hat{\mathbf{x}}$ . In this case the exterior coordinates of a point  $\mathbf{x} \in \Omega_{\text{ext}}$  are explicitly given by

$$\xi(\mathbf{x}) = \|\mathbf{x}\| - 1, \quad \hat{\mathbf{x}}(\mathbf{x}) = \frac{\mathbf{x}}{\|\mathbf{x}\|}.$$

In Chapter 5 we will provide an analysis of our method for this case and  $d = 3$ .

We use exterior coordinates to define linear complex scalings as follows:



**Definition 3.4.** Let  $\Omega, \Omega_{\text{int}}, \Omega_{\text{ext}}, \Gamma$  and  $\Psi, \mathbf{v}$  be as in Definition 3.1. Then, for  $\sigma \in \mathbb{C} \setminus \{0\}$ , we define the mapping

$$\Psi^\sigma : \begin{cases} \mathbb{R}_{>0} \times \Gamma & \rightarrow \mathbb{C}^d, \\ (\xi, \hat{\mathbf{x}}) & \mapsto \hat{\mathbf{x}} + \sigma \xi \mathbf{v}(\hat{\mathbf{x}}) \end{cases} \quad (3.2)$$

and call  $\check{\Omega}_{\text{ext}} := \Psi^\sigma(\mathbb{R}_{>0}, \Gamma)$  the *complex-scaled exterior domain*. Moreover, we write  $\check{\Omega} := \Omega_{\text{int}} \cup \Gamma \cup \check{\Omega}_{\text{ext}}$  for the whole complex-scaled domain. If we want to emphasize the scaling parameter  $\sigma$  of a complex-scaled domain, we also write  $\check{\Omega}_{\text{ext}}^\sigma$  and  $\check{\Omega}^\sigma$ .

The complex-scaled domain is a continuous and piecewise smooth  $d$ -dimensional manifold in  $\mathbb{C}^d$  with a possible kink at  $\Gamma$  and possible kinks at  $\Psi^\sigma(\mathbb{R}_{>0}, \hat{\mathbf{x}})$  for  $\hat{\mathbf{x}}$  where  $\mathbf{v}$  and/or  $\Gamma$  is/are not smooth.

We also write

$$\check{\mathbf{x}}(\mathbf{x}) := \begin{cases} \mathbf{x}, & \mathbf{x} \in \Omega_{\text{int}} \cup \Gamma, \\ \Psi^\sigma(\xi(\mathbf{x}), \hat{\mathbf{x}}(\mathbf{x})), & \mathbf{x} \in \Omega_{\text{ext}} \end{cases}$$

for a complex-scaled point  $\check{\mathbf{x}}(\mathbf{x}) \in \check{\Omega}$  corresponding to the original point  $\mathbf{x} \in \Omega$ .

*Remark 3.5.* In this work we use complex-scaled infinite elements (see Chapter 6) for the discretization of the exterior domain. For these infinite elements, only linear scalings of the form (3.2) are necessary. When perfectly matched layers (i.e., standard finite elements for the complex-scaled problem and potentially a domain truncation) are applied, frequently more involved scaling profiles are used. In the setting of exterior coordinates, this corresponds to a mapping

$$\Psi^\tau : \begin{cases} \mathbb{R}_{>0} \times \Gamma & \rightarrow \mathbb{C}^d, \\ (\xi, \hat{\mathbf{x}}) & \mapsto \hat{\mathbf{x}} + \tau(\xi) \mathbf{v}(\hat{\mathbf{x}}) \end{cases}$$

with a suitable smooth scaling function  $\tau : \mathbb{R}_{>0} \rightarrow \mathbb{C}$  that fulfills  $\lim_{\xi \rightarrow 0} \tau(\xi) = 0$ ,  $\text{Im}(\tau(\xi)) > 0$ , and  $\text{Im}(\tau(\xi))$  and  $\text{Re}(\tau(\xi))$  are non-decreasing (cf. [Hal19, Assumption 2.10]).

To be able to uniquely map complex-scaled eigenfunctions (3.5) to the original ones and vice versa, we have to show that the mapping  $\mathbf{x} \mapsto \check{\mathbf{x}}(\mathbf{x})$  is invertible. Therefore, we state the following theorem:

**Theorem 3.6.** Let  $\Omega, \check{\Omega}, \Gamma, \Psi, \Psi^\sigma, \mathbf{v}, \check{\mathbf{x}}$  be as in Definition 3.4 for some  $\sigma \in \mathbb{C} \setminus \mathbb{R}_{\leq 0}$ . Then the mapping  $\mathbf{x} \mapsto \check{\mathbf{x}}(\mathbf{x})$  is a bijection from  $\Omega$  to  $\check{\Omega}$ .

*Proof.* Let  $\hat{\mathbf{x}}, \hat{\mathbf{y}} \in \Gamma$  and  $\xi_1, \xi_2 \in \mathbb{R}_{>0}$  such that

$$\Psi^\sigma(\xi_1, \hat{\mathbf{x}}) = \Psi^\sigma(\xi_2, \hat{\mathbf{y}}).$$

By the definition of  $\Psi^\sigma$  given in (3.2), this is equivalent to

$$\hat{\mathbf{x}} - \hat{\mathbf{y}} = -\sigma (\xi_1 \mathbf{v}(\hat{\mathbf{x}}) - \xi_2 \mathbf{v}(\hat{\mathbf{y}})).$$

### 3. Complex Scaling

If  $\sigma \notin \mathbb{R}$ , we take the (component-wise) imaginary part and find

$$0 = \text{Im}(\hat{\mathbf{x}} - \hat{\mathbf{y}}) = -\text{Im}(\sigma) (\xi_1 \mathbf{v}(\hat{\mathbf{x}}) - \xi_2 \mathbf{v}(\hat{\mathbf{y}})).$$

Since  $\text{Im}(\sigma) \neq 0$ , this gives  $\xi_1 \mathbf{v}(\hat{\mathbf{x}}) - \xi_2 \mathbf{v}(\hat{\mathbf{y}}) = 0$  and thus

$$0 = -\sigma (\xi_1 \mathbf{v}(\hat{\mathbf{x}}) - \xi_2 \mathbf{v}(\hat{\mathbf{y}})) = \hat{\mathbf{x}} - \hat{\mathbf{y}}.$$

Therefore, we have  $\hat{\mathbf{x}} = \hat{\mathbf{y}}$ . It follows that  $\mathbf{v}(\hat{\mathbf{x}}) = \mathbf{v}(\hat{\mathbf{y}}) \neq 0$  and therefore also  $\xi_1 = \xi_2$ .

For  $\sigma \in \mathbb{R}_{>0}$ , the mapping  $x \mapsto \sigma x$  is a bijection from  $\mathbb{R}_{>0}$  to itself. Since  $\Psi$  is a bijection, in this case also  $\Psi^\sigma(\cdot, \cdot) = \Psi(\sigma \cdot, \cdot)$  is a bijection from  $\mathbb{R}_{>0} \times \Gamma$  to  $\check{\Omega}_{\text{ext}}$  (which, in this case, is identical to  $\Omega_{\text{ext}}$ ).

A similar reasoning as above gives that the sets  $\check{\Omega}_{\text{ext}}$  and  $\Omega_{\text{int}}$  are disjoint. We have that the mapping  $\mathbf{x} \mapsto \check{\mathbf{x}}(\mathbf{x})$  restricted to  $\Omega_{\text{int}} \cup \Gamma$  is a bijection since it is the identity. Since we have just proven that  $\Psi^\sigma$  is bijective from  $\mathbb{R}_{>0} \times \Gamma$  to  $\check{\Omega}_{\text{ext}}$  and  $\Psi$  is bijective from  $\mathbb{R}_{>0} \times \Gamma$  to  $\Omega_{\text{ext}}$  by assumption (C1), we have that

$$\check{\mathbf{x}}(\cdot) = (\Psi^\sigma \circ \Psi^{-1})(\cdot)$$

is a bijection from  $\Omega_{\text{ext}}$  to  $\check{\Omega}_{\text{ext}}$ . □

Due to Theorem 3.6 we may also write

$$\mathbf{x}(\check{\mathbf{x}}) := \begin{cases} \check{\mathbf{x}}, & \check{\mathbf{x}} \in \Omega_{\text{int}} \cup \Gamma, \\ (\Psi \circ (\Psi^\sigma)^{-1})(\check{\mathbf{x}}), & \check{\mathbf{x}} \in \check{\Omega}_{\text{ext}}. \end{cases}$$

The lemma below states that the complex-scaled domains for two parameters coincide if their polar angles are equal.

**Lemma 3.7.** *Let  $\sigma_1, \sigma_2 \in \mathbb{C} \setminus \{0\}$  such that  $\arg(\sigma_1) = \arg(\sigma_2)$ . Then we have  $\check{\Omega}^{\sigma_1} = \check{\Omega}^{\sigma_2}$ .*

*Proof.* It follows from  $\arg(\sigma_1) = \arg(\sigma_2)$  that

$$\frac{\sigma_1}{\sigma_2} \in \mathbb{R}_{>0}.$$

Because of

$$\Psi^{\sigma_1}(\xi, \hat{\mathbf{x}}) = \hat{\mathbf{x}} + \xi \sigma_1 \mathbf{v}(\hat{\mathbf{x}}) = \hat{\mathbf{x}} + \xi \sigma_2 \frac{\sigma_1}{\sigma_2} \mathbf{v}(\hat{\mathbf{x}}) = \Psi^{\sigma_2} \left( \frac{\sigma_1}{\sigma_2} \xi, \hat{\mathbf{x}} \right)$$

and the fact that  $\xi \mapsto \frac{\sigma_1}{\sigma_2} \xi$  is a bijection from  $\mathbb{R}_{>0}$  to itself, we have

$$\check{\Omega}^{\sigma_1} = \{ \Psi^{\sigma_1}(\xi, \hat{\mathbf{x}}), \xi \in \mathbb{R}_{>0}, \hat{\mathbf{x}} \in \Gamma \} = \{ \Psi^{\sigma_2}(\xi, \hat{\mathbf{x}}), \xi \in \mathbb{R}_{>0}, \hat{\mathbf{x}} \in \Gamma \} = \check{\Omega}^{\sigma_2}. \quad \square$$

Since we want to use the analytic continuation of the radiating eigenfunctions of the Helmholtz resonance problem to the complex-scaled domain, we need to examine under which conditions such a continuation exists for the complex scalings in question.

### 3.2. Analytic continuation of eigenfunctions

The representation of the radiating eigenfunctions (2.6) for  $\mathbf{x} \in \Omega_{\text{ext}}$  contains the expression  $\|\mathbf{y} - \mathbf{x}\|$  for  $\mathbf{y} \in \Gamma_0$  and  $\mathbf{x} \in \Omega_{\text{ext}}$ . Thus, we have to study whether an analytic continuation of this expression in  $\mathbf{x}$  to a complex set containing  $\check{\Omega}_{\text{ext}}$  exists. To this end we state the following two lemmas.

**Lemma 3.8.** *Let  $\mathbf{x}_1, \mathbf{x}_2 \in \mathbb{R}^d \setminus \{0\}$  and  $\theta \in [0, 2\pi)$  such that  $\mathbf{x}_1 \cdot \mathbf{x}_2 \geq 0$ . Then the function*

$$h : \begin{cases} \mathbb{R}_{\geq 0} & \rightarrow \mathbb{C}, \\ \xi & \mapsto (\mathbf{x}_1 + \exp(i\theta) \xi \mathbf{x}_2) \cdot (\mathbf{x}_1 + \exp(i\theta) \xi \mathbf{x}_2) \end{cases}$$

fulfills

$$\left| \frac{h(\xi)}{\xi^2} - \exp(i\theta) \|\mathbf{x}_2\|^2 \right| \leq \frac{\|\mathbf{x}_1\|^2 + 2\mathbf{x}_1 \cdot \mathbf{x}_2}{\xi}$$

for all  $\xi \geq 1$ .

If  $\theta \in [0, 2\pi) \setminus [\pi - \angle(\mathbf{x}_1, \mathbf{x}_2), \pi + \angle(\mathbf{x}_1, \mathbf{x}_2)]$ , we additionally have

$$|h(\xi)| > 0$$

for all  $\xi \geq 0$ .

In this case, if  $\theta \in [0, \pi - \angle(\mathbf{x}_1, \mathbf{x}_2))$ , there exists some  $\delta_1 < 2\pi$  such that

$$\arg(h(\xi)) \notin [\delta_1, 2\pi)$$

for all  $\xi \geq 0$ .

If  $\theta \in (\pi + \angle(\mathbf{x}_1, \mathbf{x}_2), 2\pi) \cup \{0\}$ , there exists some  $\delta_2 \in \mathbb{R}$  with  $0 < \delta_2 < 2\pi$  such that

$$\arg(h(\xi)) \notin (0, \delta_2]$$

for all  $\xi \geq 0$ .

*Proof.* We restate the definition of  $h$  by

$$h(\xi) = (\mathbf{x}_1 + \exp(i\theta) \xi \mathbf{x}_2) \cdot (\mathbf{x}_1 + \exp(i\theta) \xi \mathbf{x}_2) \quad (3.3a)$$

$$= \|\mathbf{x}_1\|^2 + 2 \exp(i\theta) \xi \mathbf{x}_1 \cdot \mathbf{x}_2 + \exp(i\theta)^2 \xi^2 \|\mathbf{x}_2\|^2 \quad (3.3b)$$

$$= \|\mathbf{x}_1\|^2 + 2 \operatorname{Re}(\exp(i\theta)) \xi \mathbf{x}_1 \cdot \mathbf{x}_2 + (\operatorname{Re}(\exp(i\theta))^2 - \operatorname{Im}(\exp(i\theta))^2) \xi^2 \|\mathbf{x}_2\|^2 + 2i \operatorname{Im}(\exp(i\theta)) (\xi \mathbf{x}_1 \cdot \mathbf{x}_2 + \operatorname{Re}(\exp(i\theta)) \xi^2 \|\mathbf{x}_2\|^2). \quad (3.3c)$$

Because, for all  $\xi \geq 1$ , we have

$$\begin{aligned} \left| \frac{h(\xi)}{\xi^2} - \exp(i\theta) \|\mathbf{x}_2\|^2 \right| &= \left| \frac{\|\mathbf{x}_1\|^2}{\xi^2} + \frac{2 \exp(i\theta) \mathbf{x}_1 \cdot \mathbf{x}_2}{\xi} \right| \\ &\leq \frac{\|\mathbf{x}_1\|^2}{\xi^2} + \frac{|2 \exp(i\theta) \mathbf{x}_1 \cdot \mathbf{x}_2|}{\xi} \\ &\leq \frac{\|\mathbf{x}_1\|^2 + 2\mathbf{x}_1 \cdot \mathbf{x}_2}{\xi}, \end{aligned}$$

the first claim is proven.

For the remainder, we begin with the assumption  $\theta \in [0, \pi - \angle(\mathbf{x}_1, \mathbf{x}_2))$  and distinguish four cases (cf. Figure 3.2).

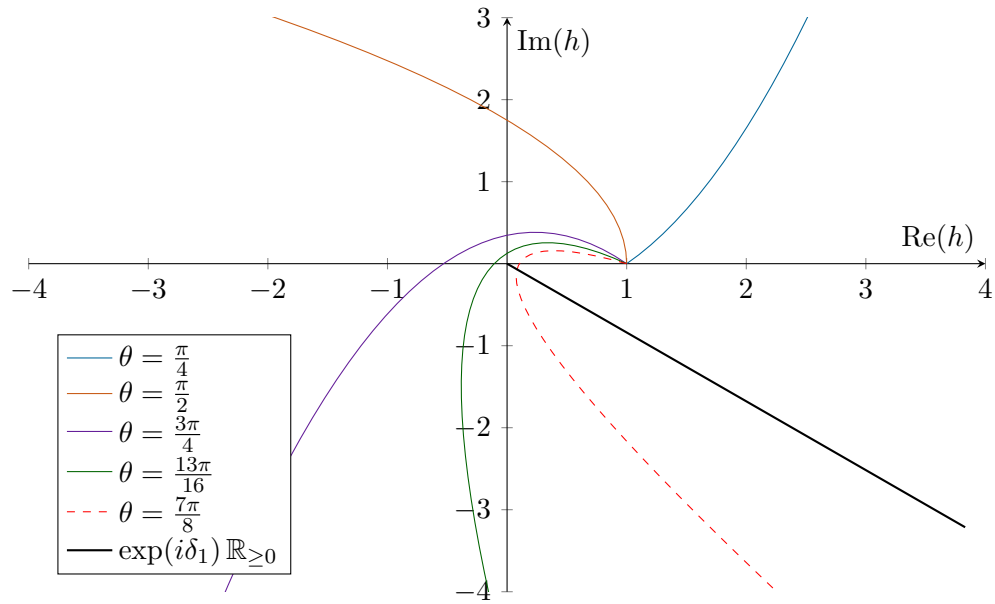


Figure 3.2.: The graph of the function  $h$  from Lemma 3.8 in the complex plane, with  $\|\mathbf{x}_1\| = 1$ ,  $\|\mathbf{x}_2\| = 0.8$ ,  $\mathbf{x}_1 \cdot \mathbf{x}_2 = 0.7$ , and different values of  $\theta$ . For  $\theta = \frac{7\pi}{8}$ , the condition  $\theta < \pi - \angle(\mathbf{x}_1, \mathbf{x}_2)$  is violated. Therefore, the graph crosses the positive real axis and the line  $\exp(i\delta_1) \mathbb{R}_{\geq 0}$ .

**Case 1:**  $\theta = 0$  :

Then  $\exp(i\theta) = 1$  and therefore, by (3.3b),  $h$  is real-valued and increasing. Thus,

$$\arg(h(\xi)) = 0$$

and

$$|h(\xi)| = h(\xi) > \|\mathbf{x}_1\|^2 > 0$$

for all  $\xi \geq 0$ , since  $h(0) = \|\mathbf{x}_1\|^2$ .

**Case 2:**  $\theta \in (0, \frac{\pi}{2})$  :

Then  $\text{Re}(\exp(i\theta)) > 0$ ,  $\text{Im}(\exp(i\theta)) > 0$  and therefore, by (3.3c),

$$\begin{aligned} \text{Im}(h(\xi)) &= 2\text{Im}(\exp(i\theta)) (\xi \mathbf{x}_1 \cdot \mathbf{x}_2 + \xi^2 \text{Re}(\exp(i\theta)) \|\mathbf{x}_2\|^2) \\ &\geq 2\text{Im}(\exp(i\theta)) \xi^2 \text{Re}(\exp(i\theta)) \|\mathbf{x}_2\|^2 > 0 \end{aligned}$$

for all  $\xi > 0$  since  $\mathbf{x}_1 \cdot \mathbf{x}_2 \geq 0$  and  $\|\mathbf{x}_2\| > 0$  by assumption.

Together with  $h(0) = \|\mathbf{x}_1\|^2 > 0$ , we obtain

$$0 \leq \arg(h(\xi)) < \pi$$

and

$$|h(\xi)| \geq \text{Im}(h(\xi)) > 0$$

for all  $\xi \geq 0$ .

**Case 3:**  $\theta = \frac{\pi}{2}$  :

In this case  $\exp(i\theta) = i$ . If  $\mathbf{x}_1 \cdot \mathbf{x}_2 = 0$ , we would have  $\theta < \pi - \angle(\mathbf{x}_1, \mathbf{x}_2) = \frac{\pi}{2}$  which would contradict the assumption that  $\theta = \frac{\pi}{2}$ . Otherwise,

$$\operatorname{Im}(h(\xi)) = 2\xi \mathbf{x}_1 \cdot \mathbf{x}_2 > 0$$

for  $\xi > 0$  and as above

$$0 \leq \arg(h(\xi)) < \pi$$

and

$$|h(\xi)| \geq \operatorname{Im}(h(\xi)) > 0$$

for all  $\xi \geq 0$ .

**Case 4:**  $\theta \in (\frac{\pi}{2}, \pi - \angle(\mathbf{x}_1, \mathbf{x}_2))$  :

Then  $\operatorname{Re}(\exp(i\theta)) < 0$  and  $\operatorname{Im}(\exp(i\theta)) > 0$ . Like in the previous case, we can assume that  $\mathbf{x}_1 \cdot \mathbf{x}_2 > 0$  and therefore also  $\|\mathbf{x}_1\| > 0$ . Apart from

$$h(0) = \|\mathbf{x}_1\|^2,$$

by (3.3c), the graph of  $h$  intersects the real axis only at  $h(\xi_1)$ , with

$$\xi_1 = -\frac{\mathbf{x}_1 \cdot \mathbf{x}_2}{\operatorname{Re}(\exp(i\theta)) \|\mathbf{x}_2\|^2} > 0.$$

Plugging this into (3.3c) gives

$$\begin{aligned} h(\xi_1) &= \|\mathbf{x}_1\|^2 - \frac{2(\mathbf{x}_1 \cdot \mathbf{x}_2)^2}{\|\mathbf{x}_2\|^2} + \frac{(\operatorname{Re}(\exp(i\theta))^2 - \operatorname{Im}(\exp(i\theta))^2)(\mathbf{x}_1 \cdot \mathbf{x}_2)^2}{\operatorname{Re}(\exp(i\theta))^2 \|\mathbf{x}_2\|^2} \\ &= \|\mathbf{x}_1\|^2 - \frac{(\mathbf{x}_1 \cdot \mathbf{x}_2)^2}{\|\mathbf{x}_2\|^2} \left( 1 + \frac{\operatorname{Im}(\exp(i\theta))^2}{\operatorname{Re}(\exp(i\theta))^2} \right) \\ &= \|\mathbf{x}_1\|^2 \left( 1 - \frac{\cos(\angle(\mathbf{x}_1, \mathbf{x}_2))^2}{\cos(\theta)^2} \right). \end{aligned}$$

Since we assumed that  $\theta \in (\frac{\pi}{2}, \pi - \angle(\mathbf{x}_1, \mathbf{x}_2))$ , we have

$$|\cos(\angle(\mathbf{x}_1, \mathbf{x}_2))| > |\cos(\theta)|$$

and therefore  $h(\xi_1) < 0$ . Thus,  $h$  has no roots and we have

$$|h(\xi)| > 0$$

for all  $\xi \geq 0$ .

Due to the fact that

$$\operatorname{Im}(h'(0)) = 2\operatorname{Im}(\exp(i\theta)) \mathbf{x}_1 \cdot \mathbf{x}_2 > 0,$$

### 3. Complex Scaling

---

we have

$$\arg(h(\xi)) \in [0, \pi]$$

for  $\xi \in [0, \xi_1]$ . Moreover, due to the asymptotic behavior of  $h$  given by

$$\lim_{\xi \rightarrow \infty} \frac{h(\xi)}{\xi^2} = \exp(i\theta)^2 \|\mathbf{x}_2\|^2,$$

we can find  $\xi_m > \xi_1$  and  $\beta_1 < 2\pi$  such that

$$\arg(h(\xi)) < \beta_1$$

for all  $\xi > \xi_m$ . The continuous function  $\arg(h(\xi))$  takes a maximum  $\beta_2$  smaller than  $2\pi$  on the compact interval  $[0, \xi_m]$ . Thus,

$$\arg(h(\xi)) \in [0, \delta_1)$$

for  $\max\{\beta_1, \beta_2\} < \delta_1 < 2\pi$  and all  $\xi \in \mathbb{R}_{\geq 0}$ .

The proof for  $\theta \in (\pi + \angle(\mathbf{x}_1, \mathbf{x}_2), 2\pi) \cup \{0\}$  works similarly.  $\square$

We use Lemma 3.9 to prove that the norm on  $\mathbb{R}^d$  has an analytic continuation to a complex set containing  $\Omega_{\text{ext}}$  and  $\check{\Omega}_{\text{ext}}$ .

**Lemma 3.9.** *Let  $\Omega_{\text{ext}}, \Gamma, \Gamma_0$ , and  $\mathbf{v}$  be as in Definition 3.1 and  $\mu$  be as in (3.1). Then, for fixed  $\mathbf{y} \in \Gamma_0$ , the function*

$$\begin{cases} \Omega_{\text{ext}} & \rightarrow \mathbb{R}, \\ \mathbf{x} & \mapsto \|\mathbf{x} - \mathbf{y}\| \end{cases}$$

*allows analytic continuations to the sets*

$$\Theta_+ := \{\hat{\mathbf{x}} + \sigma \xi \mathbf{v}(\hat{\mathbf{x}}) : \hat{\mathbf{x}} \in \Gamma, \sigma \in \mathbb{C} \setminus \{0\}, \arg(\sigma) \in [0, \pi - \mu], \xi \in \mathbb{R}_{>0}\},$$

$$\Theta_- := \{\hat{\mathbf{x}} + \sigma \xi \mathbf{v}(\hat{\mathbf{x}}) : \hat{\mathbf{x}} \in \Gamma, \sigma \in \mathbb{C} \setminus \{0\}, \arg(\sigma) \in (\pi + \mu, 2\pi) \cup \{0\}, \xi \in \mathbb{R}_{>0}\}.$$

*Moreover, the images of these analytic continuations are contained in the set  $\mathbb{C} \setminus \mathbb{R}_{\leq 0}$  for all  $\mathbf{y} \in \Gamma_0$ .*

*Proof.* We treat  $\mathbf{x} \in \Theta_+$  first. Because of Lemma 3.7, we have

$$\Theta_+ = \{\hat{\mathbf{x}} + \exp(i\theta) \xi \mathbf{v}(\hat{\mathbf{x}}) : \hat{\mathbf{x}} \in \Gamma, \theta \in [0, \pi - \mu], \xi \in \mathbb{R}_{>0}\}.$$

We define the function  $f : \Gamma_0 \times \Gamma \times [0, \pi - \mu] \times \mathbb{R}_{\geq 0} \rightarrow \mathbb{C}$  by

$$f(\mathbf{y}, \hat{\mathbf{x}}, \theta, \xi) = (\hat{\mathbf{x}} + \exp(i\theta) \xi \mathbf{v}(\hat{\mathbf{x}}) - \mathbf{y}) \cdot (\hat{\mathbf{x}} + \exp(i\theta) \xi \mathbf{v}(\hat{\mathbf{x}}) - \mathbf{y}).$$

For fixed  $\mathbf{y}, \hat{\mathbf{x}}, \theta$ , this is exactly the function  $h$  from Lemma 3.8, with  $\mathbf{x}_1 = \hat{\mathbf{x}} - \mathbf{y}$  and  $\mathbf{x}_2 = \mathbf{v}(\hat{\mathbf{x}})$  and Lemma 3.8 gives

$$\left| \frac{f(\mathbf{y}, \hat{\mathbf{x}}, \theta, \xi)}{\xi^2} - \exp(i\theta)^2 \|\mathbf{v}(\hat{\mathbf{x}})\|^2 \right| \leq \frac{\|\hat{\mathbf{x}} - \mathbf{y}\|^2 + 2(\hat{\mathbf{x}} - \mathbf{y}) \cdot \mathbf{v}(\hat{\mathbf{x}})}{\xi}$$

for all  $\xi \geq 1$ . The function  $(\mathbf{y}, \hat{\mathbf{x}}) \mapsto \|\hat{\mathbf{x}} - \mathbf{y}\|^2 + 2(\hat{\mathbf{x}} - \mathbf{y}) \cdot \mathbf{v}(\hat{\mathbf{x}})$  is continuous and positive on the compact set  $\Gamma_0 \times \Gamma$ . Therefore, it takes a global maximum  $C > 0$  depending only on the domains and  $\mathbf{v}$ . Thus, we have

$$\lim_{\xi \rightarrow \infty} \frac{f(\mathbf{y}, \hat{\mathbf{x}}, \theta, \xi)}{\xi^2} = \exp(i\theta)^2 \|\mathbf{v}(\hat{\mathbf{x}})\|^2,$$

uniformly on  $\Gamma_0 \times \Gamma \times [0, \pi - \mu)$ . It follows that also

$$\lim_{\xi \rightarrow \infty} \arg(f(\mathbf{y}, \hat{\mathbf{x}}, \theta, \xi)) = 2\theta, \quad \lim_{\xi \rightarrow \infty} |f(\mathbf{y}, \hat{\mathbf{x}}, \theta, \xi)| = +\infty,$$

uniformly on  $\Gamma_0 \times \Gamma \times [0, \pi - \mu)$ . Therefore, we can find  $\xi_m > 0$  such that

$$\arg(f(\mathbf{y}, \hat{\mathbf{x}}, \theta, \xi)) < 2\pi - \mu$$

for all  $\mathbf{y} \in \Gamma_0$ ,  $\hat{\mathbf{x}} \in \Gamma$ ,  $\theta \in [0, \pi - \mu)$ , and  $\xi \geq \xi_m$ . Moreover, Lemma 3.8 gives us that  $|f| > 0$  and  $f$  does not cross the positive real axis for  $\xi > 0$ . Thus,  $\arg(f)$  is continuous on the compact set  $\Gamma_0 \times \Gamma \times [0, \pi - \mu - \varepsilon] \times [0, \xi_m]$  for arbitrary  $\varepsilon > 0$  and therefore takes a maximum  $\delta < 2\pi$  there. Thus, we can pick the branch of the square root that is a continuation of the positive square root on  $\mathbb{R}_{>0}$  and has its branch-cut at  $\alpha\mathbb{R}_{\geq 0}$ , with

$$\alpha := \exp\left(i \max\left\{\pi + \frac{\delta}{2}, 2\pi - \mu\right\}\right).$$

It follows that the function

$$\mathbf{x} \mapsto \sqrt[\alpha]{(\mathbf{x} - \mathbf{y}) \cdot (\mathbf{x} - \mathbf{y})}$$

is analytic on  $\Theta_+$ . Moreover, we have that  $\arg\left(\sqrt[\alpha]{(\mathbf{x} - \mathbf{y}) \cdot (\mathbf{x} - \mathbf{y})}\right) \in [0, \pi)$  for all  $\mathbf{x} \in \Theta_+$ . Similar arguments can be repeated for the set  $\Theta_-$ .  $\square$

*Remark 3.10.* To distinguish between the Euclidean norm of a vector  $\mathbf{x} \in \mathbb{C}^d$ , given by  $\|\mathbf{x}\| = \sqrt{\mathbf{x} \cdot \bar{\mathbf{x}}}$ , and the analytic continuation of the Euclidean norm on  $\mathbb{R}^d$  to a complex domain, as in Lemma 3.9, we denote this analytic continuation by  $r$ .

Lemma 3.9 immediately leads to the following theorem:

**Theorem 3.11.** *Let  $\Omega, \Gamma, \Gamma_0, \Omega_{\text{int}}, \Omega_{\text{ext}}$ , and  $\mathbf{v}$  be as in Definition 3.1 and  $\omega \in \mathbb{C} \setminus \{0\}$ . Then the Green's function  $\mathbf{x} \mapsto G_{\mathbf{x}}(\mathbf{y})$  and the function  $\mathbf{x} \mapsto \nabla G_{\mathbf{x}}(\mathbf{y})$  allow an analytic continuation to the sets*

$$\begin{aligned} \Theta_+ &:= \{\hat{\mathbf{x}} + \sigma\xi\mathbf{v}(\hat{\mathbf{x}}) : \hat{\mathbf{x}} \in \Gamma, \sigma \in \mathbb{C} \setminus \{0\}, \arg(\sigma) \in [0, \pi - \mu), \xi \in \mathbb{R}_{>0}\}, \\ \Theta_- &:= \{\hat{\mathbf{x}} + \sigma\xi\mathbf{v}(\hat{\mathbf{x}}) : \hat{\mathbf{x}} \in \Gamma, \sigma \in \mathbb{C} \setminus \{0\}, \arg(\sigma) \in (\pi + \mu, 2\pi) \cup \{0\}, \xi \in \mathbb{R}_{>0}\}, \end{aligned}$$

in a sense that the norm  $\|\cdot\|$  in (2.7) is continued as in Lemma 3.9. Moreover, a function  $u \in C^1(\Omega_{\text{ext}})$  that fulfills

$$u(\mathbf{x}) = \frac{i}{4} \int_{\Gamma_0} u(\mathbf{y}) \nabla G_{\mathbf{x}}(\mathbf{y}) \cdot \mathbf{n}(\mathbf{y}) - \nabla u(\mathbf{y}) \cdot \mathbf{n}(\mathbf{y}) G_{\mathbf{x}}(\mathbf{y}) \, dy \quad (3.4)$$

### 3. Complex Scaling

for all  $\mathbf{x} \in \Omega_{\text{ext}}$ , has an analytic continuation  $U$  to the sets  $\Theta_{\pm}$  given by

$$U(\check{\mathbf{x}}) = \frac{i}{4} \int_{\Gamma_0} u(\mathbf{y}) \nabla G_{\check{\mathbf{x}}}(\mathbf{y}) \cdot \mathbf{n}(\mathbf{y}) - \nabla u(\mathbf{y}) \cdot \mathbf{n}(\mathbf{y}) G_{\check{\mathbf{x}}}(\mathbf{y}) \, d\mathbf{y}$$

for all  $\check{\mathbf{x}} \in \Theta_{\pm}$ .

*Proof.* The function  $G_{\mathbf{x}}$  is holomorphic on  $\mathbb{C} \setminus \{0\}$ , with a possible branch-cut at 0. Since the analytic continuations  $r(\cdot - \mathbf{y})$  of  $\|\cdot - \mathbf{y}\|$  from  $\Omega_{\text{ext}}$  to the sets  $\Theta_{\pm}$  map to  $\mathbb{C} \setminus \mathbb{R}_{\leq 0}$  for all  $\mathbf{y} \in \Gamma_0$  by Lemma 3.9, the function  $\mathbf{x} \mapsto G_{\mathbf{x}}(\mathbf{y})$  is also analytic. Thus, we can define for  $\check{\mathbf{x}} \in \Theta_{\pm}$

$$U(\check{\mathbf{x}}) = \frac{i}{4} \int_{\Gamma_0} u(\mathbf{y}) \nabla G_{\check{\mathbf{x}}}(\mathbf{y}) \cdot \mathbf{n}(\mathbf{y}) - \nabla u(\mathbf{y}) \cdot \mathbf{n}(\mathbf{y}) G_{\check{\mathbf{x}}}(\mathbf{y}) \, d\mathbf{y}.$$

Clearly,  $U$  is a continuation of  $u$ . Since  $U$  is also complex differentiable by the bounded convergence theorem, it is an analytic continuation.  $\square$

Theorem 3.11 states that, as long as  $\sigma \in \{z \in \mathbb{C} : \arg(z) \notin [\pi - \mu, \pi + \mu]\}$ , radiating eigenfunctions  $u$  of the Helmholtz resonance problem (Problem 2.3) allow an analytic continuation to a complex set, containing  $\Omega$  and  $\check{\Omega}$ . Moreover, we define the complex-scaled solution, for fixed  $\sigma$ , by

$$\check{u} : \begin{cases} \Omega & \rightarrow \mathbb{C}, \\ \mathbf{x} & \mapsto u(\check{\mathbf{x}}(\mathbf{x})). \end{cases} \quad (3.5)$$

Note that, although the complex continuation of  $u$  is an analytic function on a superset of  $\check{\Omega}_{\text{ext}}$ , the complex-scaled solution  $\check{u}$  is not smooth at points  $\mathbf{x}$  with corresponding points  $\check{\mathbf{x}}(\mathbf{x})$ , where the complex-scaled domain  $\check{\Omega}$  is not smooth (i.e., at  $\Gamma$  and at points  $\mathbf{x}$  where  $\mathbf{v}(\hat{\mathbf{x}}(\mathbf{x}))$  is not smooth or  $\hat{\mathbf{x}}(\mathbf{x})$  is a kink of  $\Gamma$ ).

*Remark 3.12.* Similar results for the analytic continuation of solutions to the Helmholtz equation can be found in [Tja19, Chapter 5] for cartesian scalings, where the complex scaling is combined with the technique of half-space matching.

### 3.3. Exponential decay of complex-scaled eigenfunctions

Since we want to use the complex scaling to obtain complex-scaled eigenfunctions (3.5) that are square-integrable on  $\Omega$ , we need to make sure that they decay sufficiently fast for  $\|\mathbf{x}\| \rightarrow \infty$ . The lemma below deals with the asymptotic behavior of the Green's function  $G_{\mathbf{x}}$  for large parameters  $\mathbf{x}$ .

**Lemma 3.13.** *Let  $\Gamma, \Gamma_0, \mathbf{v}, \Psi^{\sigma}$  be as in Definition 3.4 and  $\omega, \sigma \in \mathbb{C}$  be such that  $\text{Im}(\omega\sigma) > 0$  and  $\arg(\sigma) \notin [\pi - \mu, \pi + \mu]$ , with  $\mu$  given by (3.1).*

*Then there exist constants  $C_1, C_2, \varepsilon_1, \varepsilon_2 > 0$  such that*

$$\begin{aligned} |G_{\Psi^{\sigma}(\xi, \hat{\mathbf{x}})}(\mathbf{y})|, |\nabla_{\mathbf{y}} G_{\Psi^{\sigma}(\xi, \hat{\mathbf{x}})}(\mathbf{y}) \cdot \mathbf{n}(\mathbf{y})| &\leq C_1 \exp(-\varepsilon_1 \xi), \\ \|\nabla_{\xi, \hat{\mathbf{x}}} G_{\Psi^{\sigma}(\xi, \hat{\mathbf{x}})}(\mathbf{y})\|, \|\nabla_{\xi, \hat{\mathbf{x}}} (\nabla_{\mathbf{y}} G_{\Psi^{\sigma}(\xi, \hat{\mathbf{x}})}(\mathbf{y}) \cdot \mathbf{n}(\mathbf{y}))\| &\leq C_2 (1 + \xi) \exp(-\varepsilon_2 \xi) \end{aligned}$$

for all  $\xi \in \mathbb{R}_{>0}$ ,  $\hat{\mathbf{x}} \in \Gamma$ ,  $\mathbf{y} \in \Gamma_0$ .



*Proof.* From Section 3.2 we know that, under our assumptions, the Green's function  $G_{\mathbf{x}}$  is analytic in their parameter  $\mathbf{x}$ .

We have to bound the terms  $G_{\Psi^\sigma(\xi, \hat{\mathbf{x}})}, \nabla G_{\Psi^\sigma(\xi, \hat{\mathbf{x}})} \cdot \mathbf{n}, \nabla_{\xi, \hat{\mathbf{x}}} G_{\Psi^\sigma(\xi, \hat{\mathbf{x}})}, \nabla_{\xi, \hat{\mathbf{x}}} (\nabla G_{\Psi^\sigma(\xi, \hat{\mathbf{x}})} \cdot \mathbf{n})$  uniformly in  $\mathbf{y}, \hat{\mathbf{x}}$ .

The analytic continuation  $r$  (Remark 3.10) of the norm  $\|\cdot\|$  also fulfills

$$\nabla r(\mathbf{x}) = \frac{\mathbf{x}}{r(\mathbf{x})}. \quad (3.6)$$

Using (3.6) and

$$\nabla_{\xi, \hat{\mathbf{x}}} \Psi^\sigma(\xi, \hat{\mathbf{x}}) = \begin{pmatrix} \sigma \mathbf{v}(\hat{\mathbf{x}})^\top \\ \mathbf{I}_d + \sigma \xi D\mathbf{v}(\hat{\mathbf{x}})^\top \end{pmatrix},$$

we have, for  $\mathcal{H} = H_0^{(1)}, h_0^{(1)}$ , that

$$\begin{aligned} \nabla_{\mathbf{y}} \mathcal{H}(\omega r(\Psi^\sigma(\xi, \hat{\mathbf{x}}) - \mathbf{y})) &= \omega \mathcal{H}'(\omega r(\Psi^\sigma(\xi, \hat{\mathbf{x}}) - \mathbf{y})) \frac{\mathbf{y} - \Psi^\sigma(\xi, \hat{\mathbf{x}})}{r(\Psi^\sigma(\xi, \hat{\mathbf{x}}) - \mathbf{y})}, \\ \nabla_{\xi, \hat{\mathbf{x}}} \mathcal{H}(\omega r(\Psi^\sigma(\xi, \hat{\mathbf{x}}) - \mathbf{y})) &= \omega \mathcal{H}'(\omega r(\Psi^\sigma(\xi, \hat{\mathbf{x}}) - \mathbf{y})) \mathbf{g}(\xi, \hat{\mathbf{x}}), \end{aligned}$$

where we used the notation

$$\mathbf{g}(\xi, \hat{\mathbf{x}}) := \begin{pmatrix} \sigma \mathbf{v}(\hat{\mathbf{x}})^\top \\ \mathbf{I}_d + \sigma \xi D\mathbf{v}(\hat{\mathbf{x}})^\top \end{pmatrix} \frac{\Psi^\sigma(\xi, \hat{\mathbf{x}}) - \mathbf{y}}{r(\Psi^\sigma(\xi, \hat{\mathbf{x}}) - \mathbf{y})}.$$

Moreover, we obtain

$$\begin{aligned} \nabla_{\xi, \hat{\mathbf{x}}} (\nabla_{\mathbf{y}} \mathcal{H}(\omega r(\Psi^\sigma(\xi, \hat{\mathbf{x}}) - \mathbf{y})) \cdot \mathbf{n}(\mathbf{y})) &= \nabla_{\xi, \hat{\mathbf{x}}} \left( \omega \mathcal{H}'(\omega r(\Psi^\sigma(\xi, \hat{\mathbf{x}}) - \mathbf{y})) \frac{(\mathbf{y} - \Psi^\sigma(\xi, \hat{\mathbf{x}})) \cdot \mathbf{n}(\mathbf{y})}{r(\Psi^\sigma(\xi, \hat{\mathbf{x}}) - \mathbf{y})} \right) \\ &= -\mathbf{g}(\xi, \hat{\mathbf{x}}) \omega \mathcal{H}'(\omega r(\Psi^\sigma(\xi, \hat{\mathbf{x}}) - \mathbf{y})) \left( \mathbf{n}(\mathbf{y}) + \frac{(\mathbf{y} - \Psi^\sigma(\xi, \hat{\mathbf{x}})) \cdot \mathbf{n}(\mathbf{y})}{(\Psi^\sigma(\xi, \hat{\mathbf{x}}) - \mathbf{y}) \cdot (\Psi^\sigma(\xi, \hat{\mathbf{x}}) - \mathbf{y})} \right) \\ &\quad + \mathbf{g}(\xi, \hat{\mathbf{x}}) \omega^2 \mathcal{H}''(\omega r(\Psi^\sigma(\xi, \hat{\mathbf{x}}) - \mathbf{y})) \frac{(\mathbf{y} - \Psi^\sigma(\xi, \hat{\mathbf{x}})) \cdot \mathbf{n}(\mathbf{y})}{r(\Psi^\sigma(\xi, \hat{\mathbf{x}}) - \mathbf{y})}. \end{aligned}$$

Because of the (component-wise) asymptotic behavior

$$\begin{aligned} r(\Psi^\sigma(\xi, \hat{\mathbf{x}}) - \mathbf{y}) &\sim \sigma \xi \|\mathbf{v}(\hat{\mathbf{x}})\|, & \xi \rightarrow \infty, \\ \mathbf{y} - \Psi^\sigma(\xi, \hat{\mathbf{x}}) &\sim -\sigma \xi \mathbf{v}(\hat{\mathbf{x}}), & \xi \rightarrow \infty, \\ \mathbf{I}_d + \sigma \xi D\mathbf{v}(\hat{\mathbf{x}}) &\sim \sigma \xi D\mathbf{v}(\hat{\mathbf{x}}), & \xi \rightarrow \infty, \end{aligned}$$

the fact that  $\|\mathbf{v}(\hat{\mathbf{x}})\|$  and  $\|D\mathbf{v}(\hat{\mathbf{x}})\|$  are bounded in  $\Gamma$ , and the asymptotic behavior of (the derivatives) of the (spherical) Hankel functions from Proposition A.3, we obtain

$$\begin{aligned} |G_{\Psi^\sigma(\xi, \hat{\mathbf{x}})}(\mathbf{y})|, |\nabla_{\mathbf{y}} G_{\Psi^\sigma(\xi, \hat{\mathbf{x}})}(\mathbf{y}) \cdot \mathbf{n}(\mathbf{y})| &\leq C_1 \exp(-\varepsilon_1 \xi), \\ \|\nabla_{\xi, \hat{\mathbf{x}}} G_{\Psi^\sigma(\xi, \hat{\mathbf{x}})}(\mathbf{y})\|, \|\nabla_{\xi, \hat{\mathbf{x}}} (\nabla_{\mathbf{y}} G_{\Psi^\sigma(\xi, \hat{\mathbf{x}})}(\mathbf{y}) \cdot \mathbf{n}(\mathbf{y}))\| &\leq C_2 (1 + \xi) \exp(-\varepsilon_2 \xi), \end{aligned}$$

uniformly in  $\mathbf{y}, \hat{\mathbf{x}}$  for some constants  $C_1, C_2, \varepsilon_1, \varepsilon_2 > 0$ . □

### 3. Complex Scaling

Using Lemma 3.13, we can prove the theorem below, which states that complex-scaled eigenfunctions and their derivatives decay exponentially in the radial variable.

**Theorem 3.14.** *Let  $\Gamma, \Gamma_0, \mathbf{v}, \Psi, \Psi^\sigma$  be as in Definition 3.4 and  $\sigma, \omega \in \mathbb{C}$  such that  $\text{Im}(\omega\sigma) > 0$ . For  $d = 2, 3$  we additionally assume that  $\arg(\sigma) \notin [\pi - \mu, \pi + \mu]$ , with  $\mu$  as in (3.1). Then there exist  $\varepsilon_1, \varepsilon_2, C_1, C_2 > 0$  such that, for a complex-scaled radiating eigenfunction  $\check{u}$  given by (3.5) of Problem 2.3, we have*

$$|\check{u} \circ \Psi(\xi, \hat{\mathbf{x}})| \leq C_1 \exp(-\varepsilon_1 \xi)$$

and

$$\|\nabla_{\xi, \hat{\mathbf{x}}} \check{u} \circ \Psi(\xi, \hat{\mathbf{x}})\| \leq (1 + \xi) C_2 \exp(-\varepsilon_2 \xi)$$

for all  $\hat{\mathbf{x}} \in \Gamma$  and  $\xi > 0$ .

*Proof.* For  $d = 1$  and  $x = x(\xi, R_r) \in \Omega_{\text{ext}}^r = (R_r, +\infty)$  (Remark 2.1), we have by (2.6) that

$$\begin{aligned} |\check{u}(x(\xi, R_r))| &= |\alpha_r \exp(i\omega \check{x}(x(\xi, R_r)))| \\ &= |\alpha_r \exp(i\omega (R_r + \sigma \xi v_r))| \\ &= |\alpha_r| \exp(-R_r \text{Im}(\omega)) \exp(-\text{Im}(\omega\sigma) v_r \xi) \\ &\leq C_r \exp(-\varepsilon \xi), \end{aligned}$$

with  $C_r = |\alpha_r| \exp(-R_r \text{Im}(\omega))$  and  $\varepsilon = \text{Im}(\omega\sigma) v_r > 0$ . A similar constant  $C_l$  can be found to bound  $|\alpha_l \exp(i\omega \check{x}(x(\xi, R_l)))|$  in  $\Omega_{\text{ext}}^l$ .

For  $d = 2, 3$  and fixed  $\xi, \hat{\mathbf{x}}$ , we use the analytic continuation of the integral representation (2.6) of the initial solution  $u$  to obtain

$$\begin{aligned} |\check{u}(\Psi(\xi, \hat{\mathbf{x}}))| &= \left| \frac{i}{4} \int_{\Gamma_0} u(\mathbf{y}) \nabla G_{\Psi^\sigma(\xi, \hat{\mathbf{x}})}(\mathbf{y}) \cdot \mathbf{n}(\mathbf{y}) - \nabla u(\mathbf{y}) \cdot \mathbf{n}(\mathbf{y}) G_{\Psi^\sigma(\xi, \hat{\mathbf{x}})}(\mathbf{y}) \, d\mathbf{y} \right| \\ &\leq \frac{1}{4} \int_{\Gamma_0} |u(\mathbf{y}) \nabla G_{\Psi^\sigma(\xi, \hat{\mathbf{x}})}(\mathbf{y}) \cdot \mathbf{n}(\mathbf{y})| + |\nabla u(\mathbf{y}) \cdot \mathbf{n}(\mathbf{y}) G_{\Psi^\sigma(\xi, \hat{\mathbf{x}})}(\mathbf{y})| \, d\mathbf{y} \\ &\leq \frac{1}{4} (\|u\|_{L^2(\Gamma_0)} \|\nabla G_{\Psi^\sigma(\xi, \hat{\mathbf{x}})}\|_{L^2(\Gamma_0)} + \|\nabla u\|_{L^2(\Gamma_0)} \|G_{\Psi^\sigma(\xi, \hat{\mathbf{x}})}\|_{L^2(\Gamma_0)}). \end{aligned}$$

For  $\nabla_{\xi, \hat{\mathbf{x}}} \check{u}$  we obtain

$$\begin{aligned} |\nabla_{\xi, \hat{\mathbf{x}}} \check{u} \circ \Psi(\xi, \hat{\mathbf{x}})| &= \left| \frac{i}{4} \int_{\Gamma_0} u(\mathbf{y}) \nabla_{\xi, \hat{\mathbf{x}}} (\nabla G_{\Psi^\sigma(\xi, \hat{\mathbf{x}})}(\mathbf{y}) \cdot \mathbf{n}(\mathbf{y})) - \nabla u(\mathbf{y}) \cdot \mathbf{n}(\mathbf{y}) \nabla_{\xi, \hat{\mathbf{x}}} G_{\Psi^\sigma(\xi, \hat{\mathbf{x}})}(\mathbf{y}) \, d\mathbf{y} \right| \\ &\leq \frac{1}{4} (\|u\|_{L^2(\Gamma_0)} \|\nabla_{\xi, \hat{\mathbf{x}}} \nabla G_{\Psi^\sigma(\xi, \hat{\mathbf{x}})}\|_{L^2(\Gamma_0)} + \|\nabla u\|_{L^2(\Gamma_0)} \|\nabla_{\xi, \hat{\mathbf{x}}} G_{\Psi^\sigma(\xi, \hat{\mathbf{x}})}\|_{L^2(\Gamma_0)}). \end{aligned}$$

Now, Lemma 3.13 yields the claim for  $\check{u}$  since  $u$  and  $\nabla u$  are continuous on the compact domain  $\Gamma_0$ .  $\square$

*Remark 3.15.* The rate of the bound on the decay of complex-scaled eigenfunctions in Theorem 3.14 can be improved due to the term in the denominator of the asymptotic expansion of the (spherical) Hankel functions in Proposition A.3. Nevertheless, Theorem 3.14 is sharp in a sense that a complex-scaled radiating eigenfunction of Problem 2.3, with

a scaling parameter  $\sigma$  and an eigenfrequency  $\omega$  that fulfill  $\text{Im}(\omega\sigma) < 0$  is exponentially increasing for large  $\xi(\mathbf{x})$ .

Similar to Definitions 2.6, 2.7, and Proposition 2.8, one could define a radiation condition using the exponential with negative sign (in one dimension) and (spherical) Hankel functions of the second kind (in higher dimensions). Eigenfunctions satisfying this inverted radiation condition would transfer energy from infinity to the interior (in the sense of (2.4)) and, therefore, be physically unfeasible. Nevertheless, if an analytic continuation is possible, complex-scaled versions of these non-radiating eigenfunctions are exponentially decreasing for  $\omega, \sigma$ , with  $\text{Im}(\omega\sigma) < 0$ . Therefore these functions will be eigenfunctions of the weak formulation of the complex-scaled equation in this region of the complex plane.

### 3.4. Existence of square-integrable analytic continuations of eigenfunctions

Theorems 3.11 and 3.14 show that there exist two limitations for the analytic continuation of a radiating eigenfunction  $u$  to be square-integrable on  $\check{\Omega}$ :

(S1) Theorem 3.11 gives us the condition

$$\arg(\sigma) \notin \left[ \pi - \max_{\hat{\mathbf{x}} \in \Gamma, \mathbf{x} \in \Gamma_0} \angle(\hat{\mathbf{x}} - \mathbf{y}, \mathbf{v}(\hat{\mathbf{x}})), \pi + \max_{\hat{\mathbf{x}} \in \Gamma, \mathbf{x} \in \Gamma_0} \angle(\hat{\mathbf{x}} - \mathbf{y}, \mathbf{v}(\hat{\mathbf{x}})) \right].$$

This is a condition solely on the choice of the complex scaling, namely, a condition for  $\sigma$  and the exterior coordinates. If this condition is violated, a complex continuation of an eigenfunction might have singularities in  $\check{\Omega}_{\text{ext}}$ . For the use of frequency-independent complex scalings with  $\sigma \equiv \sigma_0$ , the only restriction this condition poses is the fact that the parameter  $\sigma_0$  of the complex scaling has to be chosen properly.

Since we also use frequency-dependent complex scaling functions  $\sigma(\omega)$ , we have less control over the behavior of  $\sigma$ . Therefore, the limitations on the  $\sigma$  are more relevant in our case.

(S2) Theorem 3.14, on the other hand, gives us the condition

$$\text{Im}(\sigma\omega) > 0.$$

This is a condition on the combination of  $\sigma$  and  $\omega$ . If this condition is not met, a complex-scaled eigenfunction is, although still analytic, not square-integrable any more.

Note that condition (S1) is only significant for  $d = 2, 3$ , while condition (S2) is also important for  $d = 1$ .

We will see in Section 5.3 that in regions of the complex plane where said conditions are violated an essential spectrum might occur.

*Remark 3.16.* Complex scalings can also be used for the definition of radiation conditions in the following way: A function  $u$  is called radiating with respect to this condition if the according complex-scaled function  $\check{u}$  is square-integrable on  $\check{\Omega}_{\text{ext}}$ . This condition is only equivalent to the radiation condition defined in Section 2.2 for frequencies  $\omega$  that fulfill (S1) and (S2) (see Remark 3.15).



Die approbierte gedruckte Originalversion dieser Dissertation ist an der TU Wien Bibliothek verfügbar.  
The approved original version of this doctoral thesis is available in print at TU Wien Bibliothek.

## 4. Numerical Results for Frequency-Dependent Perfectly Matched Layers

In the previous Chapter 3, we have introduced the technique of complex scaling. It is one of the main ideas of this thesis to choose the parameter  $\sigma$  of the complex scaling (Definition 3.4) dependent on the frequency  $\omega$ . In the context of resonance problems, this was introduced first in [NW18]. Therein we have shown by numerous numerical experiments that using frequency-dependent scalings indeed simplifies the choice of the scaling parameters and makes the method more robust with respect to the frequency.

In the following we briefly reproduce the most important results from [NW18], to underline why pursuing this approach is a promising idea and to motivate some of the theoretical studies in Chapter 5. In Section 4.1 we show results for  $d = 1$  and move on to results for  $d = 2$  in Section 4.2. Differing from the fact that in the work at hand we are mainly concerned with complex-scaled infinite elements (Chapter 6), we use standard perfectly matched layers, or short, PMLs (i.e., a domain truncation and mesh-based finite elements) for the discretization of the exterior problem. Although there exist more involved scaling functions, we confine ourselves the linear scaling functions defined in Definition 3.4. All the numerical experiments were implemented using the software package Netgen/NGsolve [Sch97, Sch14].

We emphasize again that the following is just a short recapitulation of some of the effects of the frequency scaled PML and refer to [NW18] for a more comprehensive read.

### 4.1. Frequency-dependent PMLs in one dimension

Let  $R > R_0 > 0$  and  $\rho$  be given by

$$\rho : \begin{cases} \rho_0, & x \in (0, R_0], \\ 0, & x \in (R_0, \infty) \end{cases}$$

for some  $\rho_0 > 0$ . Then, for a given function  $\sigma : \Lambda \subset \mathbb{C} \rightarrow \mathbb{C} \setminus \{0\}$  and the domains  $\Omega := (0, \infty)$ ,  $\Omega_{\text{int}} := (0, R)$ ,  $\Gamma := \{R\}$ , and  $\Omega_{\text{ext}} := (R, \infty)$ , with a homogeneous Neumann boundary condition at 0, we consider the complex-scaled Helmholtz resonance problem to

find  $\check{u} \in C(\Omega) \cap L^2(\Omega) \setminus \{0\}$ , with  $\check{u} \in C^2(\Omega \setminus \{R_0, R\})$  and  $\omega \in \mathbb{C}$  such that

$$-\check{u}''(x) - \omega^2(1 + \rho(x))^2\check{u}(x) = 0, \quad x \in \Omega_{\text{int}}, \quad (4.1a)$$

$$-\frac{1}{\sigma(\omega)}\check{u}''(x) - \sigma(\omega)\omega^2\check{u}(x) = 0, \quad x \in \Omega_{\text{ext}}, \quad (4.1b)$$

$$\lim_{x \rightarrow R_-} \sigma(\omega)\check{u}'(x) = \lim_{x \rightarrow R_+} u'(x), \quad (4.1c)$$

$$\check{u}'(0) = 0. \quad (4.1d)$$

We also impose that  $\check{u}$  is continuous and differentiable at  $R_0$ . The interface condition (4.1c) is chosen in a way that the solution has the correct kink at  $x = R$  to be the evaluation of the analytic continuation of the radiating eigenfunction of Problem 2.3 along the path

$$\begin{cases} \mathbb{R}_{>0} & \rightarrow \mathbb{C}, \\ t & \mapsto \begin{cases} t, & t \leq R, \\ t + \sigma(t - R)t, & t > R. \end{cases} \end{cases}$$

It follows from straightforward calculations that the resonances and resonance functions of (4.1) are given by

$$\omega_k := \frac{1}{2R_0(\rho_0 + 1)} \left( -i \ln \left( \frac{\rho_0 + 2}{\rho_0} \right) + 2\pi k \right), \quad k \in \mathbb{Z}, \quad (4.2a)$$

$$\check{u}_k := \begin{cases} C \cos(\omega_k \rho_0 x), & x \in (0, R_0], \\ c \sin(\omega_k x) + d \cos(\omega_k x), & x \in (R_0, R], \\ g \exp(i\omega_k(x + \sigma(\omega_k)(R - x))), & x \in \Omega_{\text{ext}}, \end{cases} \quad (4.2b)$$

with

$$\begin{aligned} c &= C \cos(\omega \rho_0 R_0) \sin(\omega R_0) - C \rho_0 \cos(\omega R_0) \sin(\omega \rho_0 R_0), \\ d &= C \cos(\omega \rho_0 R_0) \cos(\omega R_0) + C \rho_0 \sin(\omega R_0) \sin(\omega \rho_0 R_0), \\ g &= C \frac{c \sin(\omega R) + d \cos(\omega R)}{\exp(i\omega R)} \end{aligned}$$

and arbitrary constants  $C \in \mathbb{C} \setminus \{0\}$ . The resonance functions (4.2b) decay exponentially, and are therefore elements of  $H^1(\Omega)$ , if and only if  $\text{Im}(\omega_k \sigma(\omega_k)) > 0$  (cf. Figure 4.1). If we truncate the exterior domain  $\Omega_{\text{ext}} = (R, \infty)$  to a finite domain  $\Omega_{\text{pml}} := (R, T)$  for some  $T > R$ , multiply (4.1a) and (4.1b) by a test function  $v \in H^1((0, T))$ , integrate, and apply integration by parts, we obtain the weak formulation of (4.1). Namely, the problem to

find  $\check{u}_T \in H^1(\Omega) \setminus \{0\}$  and  $\omega \in \mathbb{C}$  such that

$$\begin{aligned} & \int_0^R \check{u}'_T(x) v'(x) dx - \omega^2 \int_0^R (1 + \rho(x))^2 \check{u}_T(x) v(x) dx \\ & + \frac{1}{\sigma(\omega)} \int_R^T \check{u}'_T(x) v'(x) dx - \omega^2 \sigma(\omega) \int_R^T \check{u}_T(x) v(x) dx = 0. \end{aligned} \quad (4.3)$$

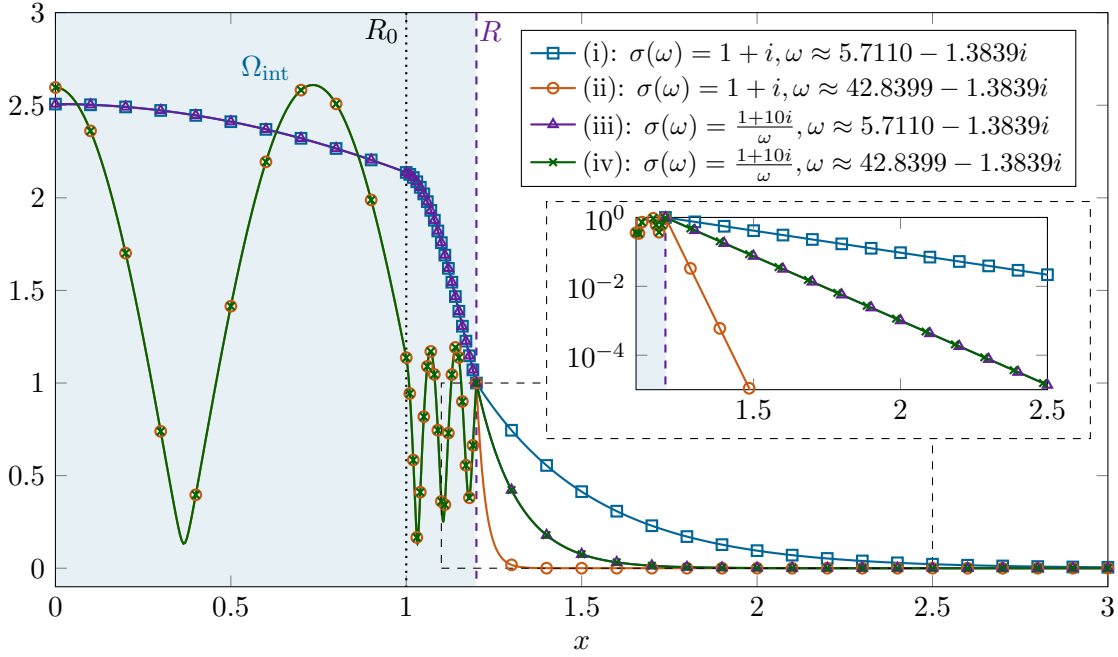


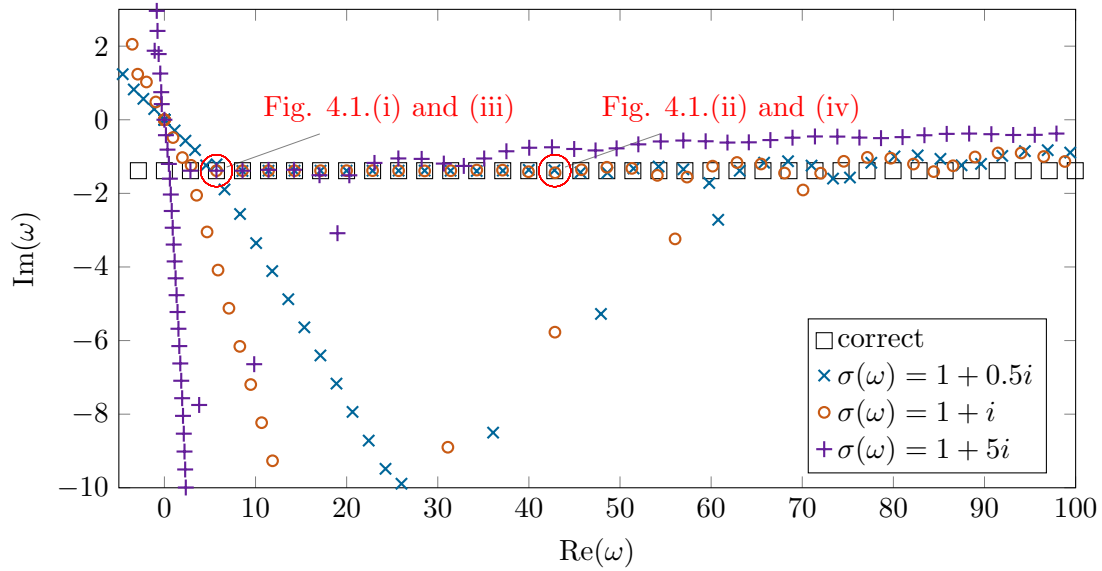
Figure 4.1.: Absolute values of the eigenfunctions  $\check{u}_k$  from (4.2b) of the un-truncated one-dimensional complex-scaled problem (4.1), with  $\rho_0 = 0.1$ ,  $R_0 = 1$ ,  $R = 1.2$ , different scalings, and different frequencies.

Note that for a rational function  $\sigma(\cdot)$ , the weak formulation (4.3) is a rational eigenvalue problem in the frequency  $\omega$  in the sense of Problem 8.1. Therefore, it can be treated using the methods from Chapter 8.

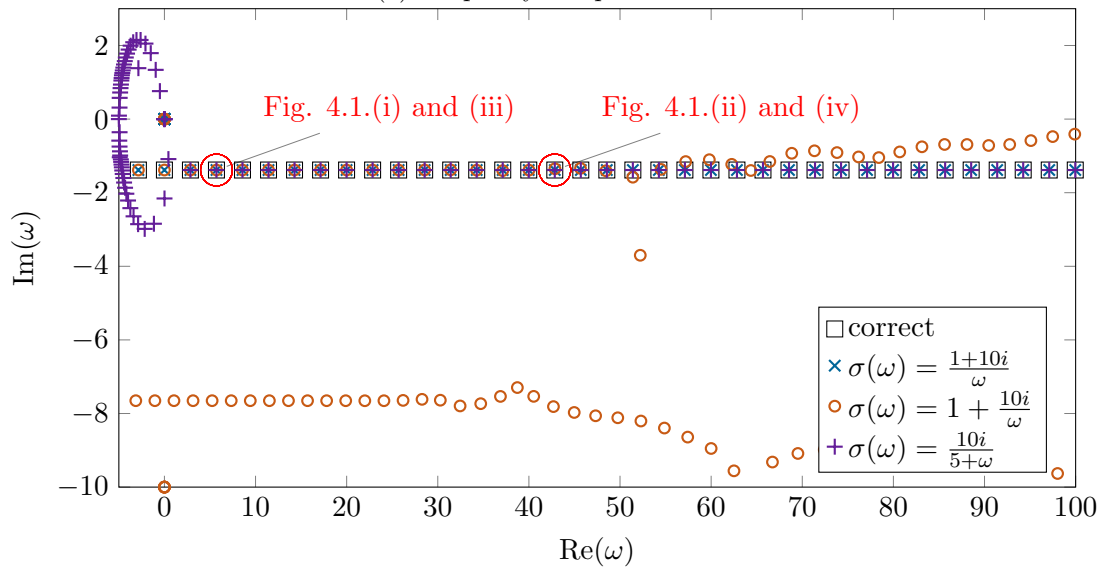
Figure 4.2 shows the resonances of a discretization of (4.3). We used high-order finite elements and a significantly finer discretization in  $\Omega_{\text{int}}$  than in  $\Omega_{\text{pml}}$ , to ensure that the error of the exterior discretization dominates.

Figure 4.2a shows approximated resonances by the use of the frequency-independent complex scaling  $\sigma(\omega) \equiv \sigma_0$  for different scaling parameters  $\sigma_0 \in \mathbb{C} \setminus \{0\}$ . We observe that the number of resonances which are well-approximated depends heavily on the choice of the parameter  $\sigma_0$ . Moreover, we observe a number of resonances that are no approximations to the resonances given in (4.2a): The eigenvalues that lie on a straight line crossing the origin are an approximation to the essential spectrum  $\Sigma_{\text{dec}}$  (see Sections 5.3.2, 7.3 and Figure 7.4) and approximate the boundary of the region where (S2) is fulfilled. For  $h \rightarrow 0$  and  $T \rightarrow \infty$ , they will approximate the set  $\{\omega \in \Lambda : \text{Im}(\sigma(\omega)\omega) = 0\}$ . We observe two reasons for poor approximations:

- Resonances close to the essential spectrum are not approximated well since, due to their slow decay, the truncation error dominates (see Figure 4.1.(i)).
- The quality of the approximation of eigenvalues with larger real parts deteriorates since their exponential decay is too fast to be approximated well (see Figure 4.1.(ii)).



(a) Frequency-independent PMLs.



(b) Frequency-dependent PMLs.

Figure 4.2.: Comparison of the frequency-dependent and frequency-independent PMLs for  $\rho_0 = 0.1$ ,  $R_0 = 1$ ,  $R = 1.2$ ,  $T = 2.5$ , mesh-sizes  $h_{\text{int}} = 0.01$  and  $h_{\text{ext}} = 0.1$ , and polynomial order 6.



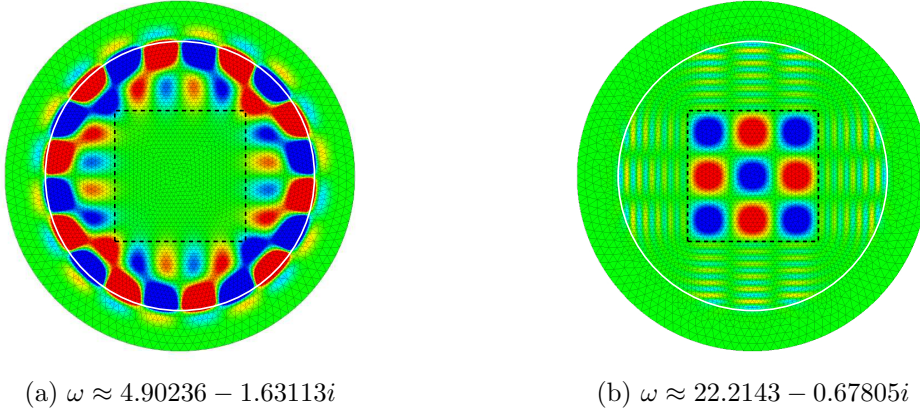


Figure 4.3.: Real parts of resonance functions of the two-dimensional problem, with  $\rho = -0.8\chi_{[-1.5,1.5]^2}$ ,  $\Omega_{\text{int}} = B_3$ , and  $\Omega_{\text{pml}} = B_4$ . The dashed square marks the jump in the potential  $\rho$  and the white circle the interface  $\Gamma$ . The colors red, blue, and green colors correspond to positive, negative, and neutral values respectively.

Moreover, we observe spurious resonances, which are artifacts of the discretization and will move farther away from the origin for better discretizations (see [NW18, Section 4]).

Figure 4.2b shows approximated resonances for different frequency-dependent complex scalings. We observe that the scalings where the limit  $\lim_{|\omega| \rightarrow \infty} \sigma(\omega)\omega$  is bounded yield also good approximations for resonances with large real parts. The reason for this is that their exponential decay in  $\Omega_{\text{ext}}$  is uniform with respect to  $\omega$  (cf. Figure 4.1.(iii,iv)). We also observe approximations to the essential spectra  $\Sigma_{\text{dec}}$ , which take different shapes depending on the respective scaling  $\sigma$  (see Section 7.3 and Figures 7.5, 7.6 and 7.7).

## 4.2. Frequency-dependent PMLs in higher dimensions

To undertake numerical experiments for  $d = 2$ , we choose the domains  $\Omega = \mathbb{R}^2$ ,  $\Omega_{\text{ext}} = \overline{B_R^c}$ ,  $\Gamma = S_R$ , and  $\Omega_{\text{int}} = B_R$  with  $R > 0$ . Moreover, we choose a potential  $\rho$  which is, again, piecewise constant. For the discretization of the problem, we pick the truncated domain  $\Omega_{\text{pml}} = \Omega_{\text{ext}} \cap B_T$ , with  $T > R$ .

Since the weak formulation of the complex-scaled Helmholtz equation for higher dimensions will be discussed at length in Chapters 5 and 7, we omit stating it at this place. For the weak formulation used for the frequency-dependent PML, we refer to [NW18, Formula (3.9)] and merely present numerical results.

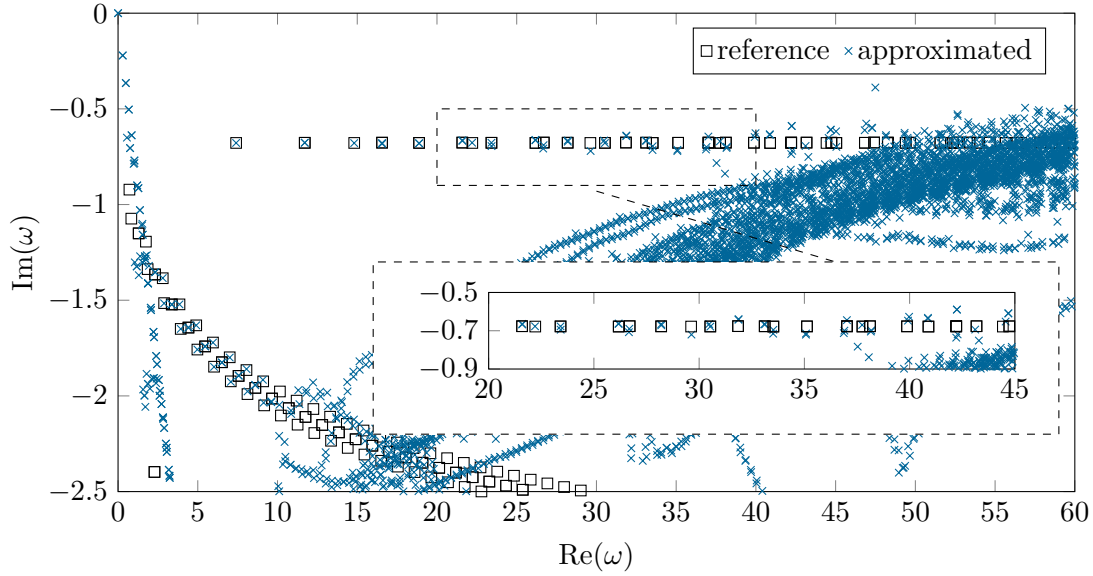
Figure 4.4 shows resonances of the two-dimensional problem approximated by mesh-based discretizations in  $\Omega_{\text{int}}$  and  $\Omega_{\text{pml}}$  (see Figure 4.3). The reference resonances were obtained by using a finer mesh, a larger truncated domain, and a higher polynomial order.

In Figure 4.4a we used a frequency-independent scaling. Again we can observe the approximation of the essential spectrum  $\Sigma_{\text{dec}}$  and spurious resonances due to the discretization. In Figure 4.4b we used a frequency-dependent scaling parameter. In this case we obtain a considerably larger number of well-approximated resonances and spurious reso-

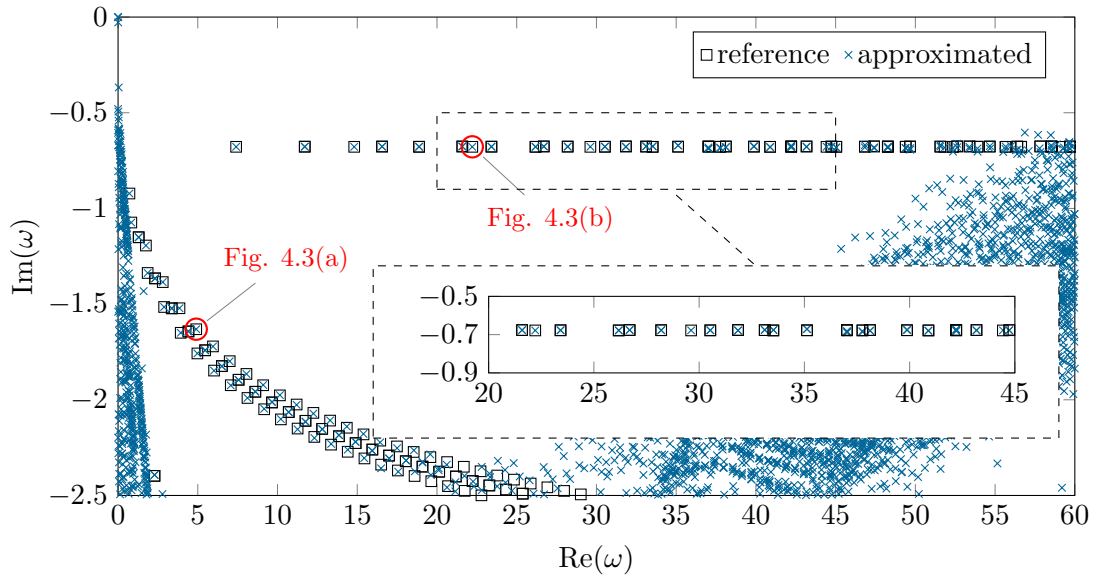
nances, which are located farther away from the origin than in the frequency-independent case.

Contrary to the one-dimensional case, we observe a new set of resonances close to the negative imaginary axis in the frequency-dependent case (Figure 4.4b). We will later see that these resonances are located within the area where condition (S1) is violated and are a discretization of the essential spectrum  $\Sigma_{\text{sing}}$  (see Sections 5.3.1, 7.3 and Figure 7.5). Note that corresponding eigenvalues were not present in the one-dimensional case since condition (S1) is only relevant for higher dimensions.

We emphasize that the superior results in the frequency-dependent case are obtained by using identical discrete spaces and numbers of unknowns. They are merely a result of the more pleasant behavior of the complex-scaled eigenfunctions in  $\Omega_{\text{ext}}$  due to the frequency-dependency.



(a) Frequency-independent PML, with  $\sigma(\omega) = 1 + 3i$ .



(b) Frequency-dependent PML, with  $\sigma(\omega) = \frac{9+9i}{\omega}$ .

Figure 4.4.: Comparison of frequency-dependent and frequency-independent PMLs for  $\rho = -0.8\chi_{[-1.5,1.5]^2}$ ,  $R = 3$ ,  $T = 4$ , mesh-sizes  $h_{\text{int}} = 0.1$  and  $h_{\text{ext}} = 0.2$ , and polynomial order 4.



Die approbierte gedruckte Originalversion dieser Dissertation ist an der TU Wien Bibliothek verfügbar.  
The approved original version of this doctoral thesis is available in print at TU Wien Bibliothek.

## 5. Analysis

In this chapter we present an analysis of the complex-scaled Helmholtz resonance problem for frequency-dependent spherical scalings in three dimensions. We allow arbitrary frequency-dependencies  $\sigma(\cdot)$ , where  $\sigma : \Lambda \rightarrow \mathbb{C} \setminus \{0\}$  is a holomorphic function on some domain  $\Lambda \subset \mathbb{C}$ .

A key tool to analyze resonance problems like Problem 2.3 is the Riesz-Fredholm theory (e.g., [Kre99, Chapters 3 and 4]). This theory can be applied to operators that are the values of functions that map complex frequencies to bounded operators, mapping  $H^1(\Omega)$  to itself. These so-called operator functions are associated with the sesquilinear forms of the weak formulations of Problem 2.3 by the Riesz representation theorem.

The fact that the function  $\sigma$ , and therefore also the associated operator function, is holomorphic in  $\omega$  will not be essential for the analysis of the continuous problem since here only results for fixed frequencies  $\omega$  are required. The holomorphy of  $\sigma(\cdot)$  is, however, crucial for analyzing the stability of Galerkin approximations of operator functions (see [Kar96a, Kar96b] and [Hal19, Theorem 3.17]).

In Section 5.1 we derive a weak formulation of the complex-scaled problem. We show that an eigenfunction of this weak formulation is the analytic continuation of an eigenfunction of the strong formulation (Problem 2.3) to the complex-scaled domain and vice versa.

An important ingredient for the analysis of holomorphic operator functions is Fredholmness (Definition 5.8). In Section 5.2 we show that the operator function induced by the weak formulation is weakly coercive and therefore Fredholm, at least, for certain  $\omega \in \Lambda$  such that the conditions (S1) and (S2) established in Chapter 3 are fulfilled. In Section 5.3 we show that an essential spectrum indeed exists for certain  $\omega \in \Lambda$  such that the conditions (S1) and (S2) are violated. Although, for the sake of a clear presentation, we present our analysis merely for spherical scalings and  $d = 3$ , we indicate how to extend our results to more general settings.

For the remainder of this chapter, we assume that (see Figure 5.1 for a sketch in two dimensions)

$$\Omega_{\text{ext}} := \overline{B_1}^c \subset \mathbb{R}^3, \quad \Gamma := S_1, \quad \mathbf{v}(\hat{\mathbf{x}}) := \hat{\mathbf{x}}. \quad (5.1)$$

Note that in this case the exterior coordinatization and the coordinates of a point  $\mathbf{x} \in \Omega_{\text{ext}}$  are given explicitly by

$$\Psi(\xi, \hat{\mathbf{x}}) = (1 + \xi)\hat{\mathbf{x}}, \quad \xi(\mathbf{x}) = \|\mathbf{x}\| - 1, \quad \hat{\mathbf{x}}(\mathbf{x}) = \frac{\mathbf{x}}{\|\mathbf{x}\|}.$$

The maximal angle  $\mu$  defined in (3.1) is given by

$$\mu = \arcsin(\max \{\|\mathbf{y}\| : \mathbf{y} \in \Gamma_0\}) \in \left(0, \frac{\pi}{2}\right]. \quad (5.2)$$

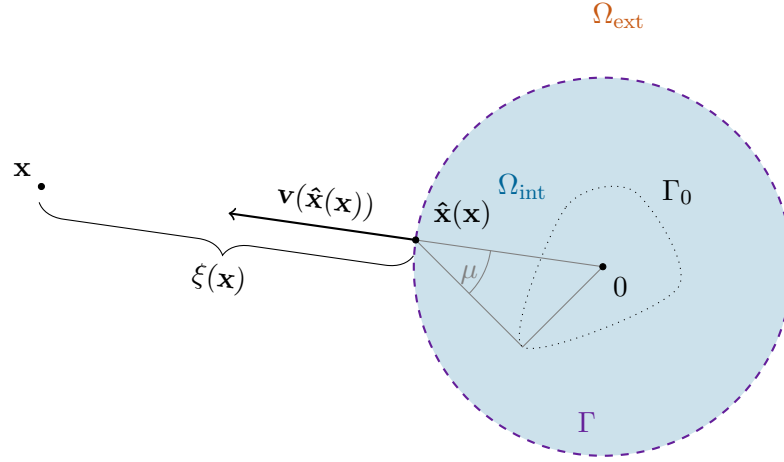


Figure 5.1.: Spherical coordinates in two dimensions.

Moreover, the gradient and the Laplace operator in polar coordinates for a function  $f \in C^2(\Omega_{\text{ext}})$  at a point  $\Psi(\xi, \hat{\mathbf{x}})$  are given by

$$(\nabla f)(\Psi(\xi, \hat{\mathbf{x}})) = \frac{\partial f \circ \Psi}{\partial \xi}(\xi, \hat{\mathbf{x}}) \hat{\mathbf{x}} + \frac{1}{1 + \xi} \left( \hat{\nabla} f \circ \Psi \right)(\xi, \hat{\mathbf{x}}), \quad (5.3a)$$

$$(\Delta f)(\Psi(\xi, \hat{\mathbf{x}})) = \frac{\partial^2 f \circ \Psi}{\partial \xi^2}(\xi, \hat{\mathbf{x}}) + \frac{2}{1 + \xi} \frac{\partial f \circ \Psi}{\partial \xi}(\xi, \hat{\mathbf{x}}) + \frac{1}{(1 + \xi)^2} \left( \hat{\nabla} \cdot \hat{\nabla} f \circ \Psi \right)(\xi, \hat{\mathbf{x}}) \quad (5.3b)$$

for  $\xi > 0$ ,  $\hat{\mathbf{x}} \in \Gamma$  (Remark 7.7), where  $\hat{\nabla}$  denotes the surface gradient on  $\Gamma$  (see (1.8)).

It is straightforward to verify, by transforming the integral to polar coordinates, that

$$\|f\|_{L^2(\Omega)}^2 = \int_{\Omega_{\text{int}}} |f(\mathbf{x})|^2 d\mathbf{x} + \int_{\mathbb{R}_{>0} \times \Gamma} (1 + \xi)^2 |(f \circ \Psi)(\xi, \hat{\mathbf{x}})|^2 d(\xi, \hat{\mathbf{x}}) \quad (5.4)$$

and

$$\begin{aligned} \|f\|_{H^1(\Omega)}^2 &= \int_{\Omega_{\text{int}}} \|\nabla f(\mathbf{x})\|^2 + |f(\mathbf{x})|^2 d\mathbf{x} \\ &+ \int_{\mathbb{R}_{>0} \times \Gamma} (1 + \xi)^2 \left| \frac{\partial}{\partial \xi} (f \circ \Psi)(\xi, \hat{\mathbf{x}}) \right|^2 + \left\| \hat{\nabla} (f \circ \Psi)(\xi, \hat{\mathbf{x}}) \right\|^2 d(\xi, \hat{\mathbf{x}}) \\ &+ \int_{\mathbb{R}_{>0} \times \Gamma} (1 + \xi)^2 |(f \circ \Psi)(\xi, \hat{\mathbf{x}})|^2 d(\xi, \hat{\mathbf{x}}) \end{aligned} \quad (5.5)$$

for functions  $f \in L^2(\Omega)$  and  $f \in H^1(\Omega)$  respectively. A function  $f$  is in  $L^2(\Omega)$  or  $H^1(\Omega)$  respectively if and only if the right-hand side of (5.4) or (5.5) is finite. For functions  $f, g \in L^2(\Omega)$ , the  $L^2(\Omega)$ -inner product is given by

$$(f, g)_{L^2(\Omega)} = \int_{\Omega_{\text{int}}} f(\mathbf{x}) \overline{g(\mathbf{x})} d\mathbf{x} + \int_{\mathbb{R}_{>0} \times \Gamma} (1 + \xi)^2 (f \circ \Psi)(\xi, \hat{\mathbf{x}}) \overline{(g \circ \Psi)(\xi, \hat{\mathbf{x}})} d(\xi, \hat{\mathbf{x}}).$$

Similarly, for functions  $f, g \in H^1(\Omega)$ , the  $H^1(\Omega)$ -inner product is given by

$$\begin{aligned}
 (f, g)_{H^1(\Omega)} &= \int_{\Omega_{\text{int}}} \nabla f(\mathbf{x}) \cdot \overline{\nabla g(\mathbf{x})} \, d\mathbf{x} + \int_{\Omega_{\text{int}}} f(\mathbf{x}) \overline{g(\mathbf{x})} \, d\mathbf{x} \\
 &+ \int_{\mathbb{R}_{>0} \times \Gamma} (1 + \xi)^2 \frac{\partial}{\partial \xi} (f \circ \Psi)(\xi, \hat{\mathbf{x}}) \overline{\frac{\partial}{\partial \xi} (g \circ \Psi)(\xi, \hat{\mathbf{x}})} \, d(\xi, \hat{\mathbf{x}}) \\
 &+ \int_{\mathbb{R}_{>0} \times \Gamma} \hat{\nabla} (f \circ \Psi)(\xi, \hat{\mathbf{x}}) \cdot \overline{\hat{\nabla} (g \circ \Psi)(\xi, \hat{\mathbf{x}})} \, d(\xi, \hat{\mathbf{x}}) \\
 &+ \int_{\mathbb{R}_{>0} \times \Gamma} (1 + \xi)^2 (f \circ \Psi)(\xi, \hat{\mathbf{x}}) \overline{(g \circ \Psi)(\xi, \hat{\mathbf{x}})} \, d(\xi, \hat{\mathbf{x}}).
 \end{aligned}$$

## 5.1. The weak formulation of the complex-scaled problem

In Chapter 3 we have established that, under certain conditions, the eigenfunctions of the Helmholtz resonance problem (Problem 2.3) allow an analytic continuation to a set containing the complex-scaled domain  $\check{\Omega}$ . In the following we derive the weak formulation of an equation such that the complex-scaled eigenfunctions  $\check{u}$ , given by (3.5), are eigenfunctions of this equation. We refer to the according problem as the *complex-scaled Helmholtz resonance problem* for the remainder of this text.

We shall see that the weak formulation of the complex-scaled equation is given by the following sesquilinear form:

**Definition 5.1.** Let (5.1) hold and  $\Lambda \subset \mathbb{C}$ ,  $\sigma : \Lambda \rightarrow \mathbb{C} \setminus \{0\}$ . Then, for  $\omega \in \Lambda$ , we define a sesquilinear form  $a_\sigma(\omega)$  for  $f, g \in H^1(\Omega)$  by

$$\begin{aligned}
 a_\sigma(\omega)(f, g) &:= \int_{\Omega_{\text{int}}} \nabla f(\mathbf{x}) \cdot \overline{\nabla g(\mathbf{x})} \, d\mathbf{x} - \omega^2 \int_{\Omega_{\text{int}}} (1 + \rho(\mathbf{x}))^2 f(\mathbf{x}) \overline{g(\mathbf{x})} \, d\mathbf{x} \\
 &+ \frac{1}{\sigma(\omega)} \int_{\mathbb{R}_{>0} \times \Gamma} (1 + \xi \sigma(\omega))^2 \frac{\partial}{\partial \xi} (f \circ \Psi)(\xi, \hat{\mathbf{x}}) \overline{\frac{\partial}{\partial \xi} (g \circ \Psi)(\xi, \hat{\mathbf{x}})} \, d(\xi, \hat{\mathbf{x}}) \\
 &+ \sigma(\omega) \int_{\mathbb{R}_{>0} \times \Gamma} \hat{\nabla} (f \circ \Psi)(\xi, \hat{\mathbf{x}}) \cdot \overline{\hat{\nabla} (g \circ \Psi)(\xi, \hat{\mathbf{x}})} \, d(\xi, \hat{\mathbf{x}}) \\
 &- \sigma(\omega) \omega^2 \int_{\mathbb{R}_{>0} \times \Gamma} (1 + \sigma(\omega) \xi)^2 (f \circ \Psi)(\xi, \hat{\mathbf{x}}) \overline{(g \circ \Psi)(\xi, \hat{\mathbf{x}})} \, d(\xi, \hat{\mathbf{x}}).
 \end{aligned}$$

In the lemma below we show that the sesquilinear form  $a_\sigma(\omega)$  is continuous for all  $\omega \in \Lambda$  with respect to the  $H^1(\Omega)$ -norm.

**Lemma 5.2.** Let  $\omega \in \Lambda$  and  $a_\sigma(\omega)$  be as in Definition 5.1. Then there exists a constant  $C(\sigma(\omega)) > 0$  such that

$$|a_\sigma(\omega)(f, g)| \leq C(\sigma(\omega)) \|f\|_{H^1(\Omega)} \|g\|_{H^1(\Omega)}$$

for all  $f, g \in H^1(\Omega)$ .

*Proof.* We use the triangle inequality to obtain

$$\begin{aligned}
 |a_\sigma(\omega)(f, g)| &\leq \underbrace{\left| \int_{\Omega_{\text{int}}} \nabla f(\mathbf{x}) \cdot \overline{\nabla g(\mathbf{x})} \, d\mathbf{x} \right| + |\omega|^2 \left| \int_{\Omega_{\text{int}}} (1 + \rho(\mathbf{x}))^2 f(\mathbf{x}) \overline{g(\mathbf{x})} \, d\mathbf{x} \right|}_{(i)} \\
 &\quad + \underbrace{\left| \frac{1}{|\sigma(\omega)|} \int_{\mathbb{R}_{>0} \times \Gamma} (1 + \xi\sigma(\omega))^2 \frac{\partial}{\partial \xi} (f \circ \Psi)(\xi, \hat{\mathbf{x}}) \overline{\frac{\partial}{\partial \xi} (g \circ \Psi)(\xi, \hat{\mathbf{x}})} \, d(\xi, \hat{\mathbf{x}}) \right|}_{(ii)} \\
 &\quad + \underbrace{|\sigma(\omega)| \left| \int_{\mathbb{R}_{>0} \times \Gamma} \hat{\nabla} (f \circ \Psi)(\xi, \hat{\mathbf{x}}) \cdot \overline{\hat{\nabla} (g \circ \Psi)(\xi, \hat{\mathbf{x}})} \, d(\xi, \hat{\mathbf{x}}) \right|}_{(iii)} \\
 &\quad + \underbrace{|\sigma(\omega)| |\omega|^2 \left| \int_{\mathbb{R}_{>0} \times \Gamma} (1 + \sigma(\omega)\xi)^2 (f \circ \Psi)(\xi, \hat{\mathbf{x}}) \overline{(g \circ \Psi)(\xi, \hat{\mathbf{x}})} \, d(\xi, \hat{\mathbf{x}}) \right|}_{(iv)}.
 \end{aligned}$$

We can bound the term (i) by

$$\begin{aligned}
 (i) &\leq \int_{\Omega_{\text{int}}} |\nabla f(\mathbf{x}) \cdot \nabla g(\mathbf{x})| \, d\mathbf{x} + |\omega|^2 \int_{\Omega_{\text{int}}} |(1 + \rho(\mathbf{x}))^2 f(\mathbf{x}) g(\mathbf{x})| \, d\mathbf{x} \\
 &\leq \max \left\{ 1, |\omega|^2 \|(1 + \rho)^2\|_{L^\infty(\Omega_{\text{int}})} \right\} \int_{\Omega_{\text{int}}} |\nabla f(\mathbf{x}) \cdot \nabla g(\mathbf{x})| + |f(\mathbf{x}) g(\mathbf{x})| \, d\mathbf{x}.
 \end{aligned}$$

Because there exists a constant  $D(\sigma(\omega)) > 0$  such that

$$\left| \frac{1 + \xi\sigma(\omega)}{1 + \xi} \right|^2 \leq D(\sigma(\omega))$$

for all  $\xi > 0$ , we obtain

$$\begin{aligned}
 (ii) &\leq \frac{1}{|\sigma(\omega)|} \int_{\mathbb{R}_{>0} \times \Gamma} \left| \frac{1 + \xi\sigma(\omega)}{1 + \xi} \right|^2 (1 + \xi)^2 \left| \frac{\partial}{\partial \xi} (f \circ \Psi)(\xi, \hat{\mathbf{x}}) \frac{\partial}{\partial \xi} (g \circ \Psi)(\xi, \hat{\mathbf{x}}) \right| \, d(\xi, \hat{\mathbf{x}}) \\
 &\leq \frac{D(\sigma(\omega))}{|\sigma(\omega)|} \int_{\mathbb{R}_{>0} \times \Gamma} (1 + \xi)^2 \left| \frac{\partial}{\partial \xi} (f \circ \Psi)(\xi, \hat{\mathbf{x}}) \frac{\partial}{\partial \xi} (g \circ \Psi)(\xi, \hat{\mathbf{x}}) \right| \, d(\xi, \hat{\mathbf{x}}).
 \end{aligned}$$

Similarly, we can bound (iv) by

$$(iv) \leq |\sigma(\omega)| |\omega|^2 D(\sigma(\omega)) \int_{\mathbb{R}_{>0} \times \Gamma} (1 + \xi)^2 |(f \circ \Psi)(\xi, \hat{\mathbf{x}}) (g \circ \Psi)(\xi, \hat{\mathbf{x}})| \, d(\xi, \hat{\mathbf{x}}).$$

The bound for (iii) is trivial. Combining the terms (i) – (iv) and applying the Cauchy-Schwarz inequality, we obtain

$$|a_\sigma(\omega)(f, g)| \leq C(\sigma(\omega)) (f, g)_{H^1(\Omega)} \leq C(\sigma(\omega)) \|f\|_{H^1(\Omega)} \|g\|_{H^1(\Omega)},$$

with

$$C(\sigma(\omega)) := \max \left\{ 1, |\omega|^2 \|(1 + \rho)^2\|_{L^\infty(\Omega_{\text{int}})}, \frac{D(\sigma(\omega))}{|\sigma(\omega)|}, |\sigma(\omega)|, |\sigma(\omega)| |\omega|^2 D(\sigma(\omega)) \right\}.$$

□



Because the sesquilinear form  $a_\sigma(\omega)$  is bounded, we can define the operator  $A_\sigma(\omega) \in \mathcal{B}(H^1(\Omega))$ , where  $\mathcal{B}(H^1(\Omega))$  denotes the set of all bounded linear operators from  $H^1(\Omega)$  to itself, by

$$(A_\sigma(\omega) f, g)_{H^1(\Omega)} = a_\sigma(\omega)(f, g) \quad (5.6)$$

using the Riesz representation theorem. It is clear that  $A_\sigma(\omega)$  is bounded with respect to the operator norm  $\|\cdot\|_{\mathcal{B}(H^1(\Omega))}$  with

$$\|A_\sigma(\omega)\|_{\mathcal{B}(H^1(\Omega))} \leq \max \left\{ 1, |\omega|^2 \|(1 + \rho)^2\|_{L^\infty(\Omega_{\text{int}})}, \frac{D(\sigma(\omega))}{|\sigma(\omega)|}, |\sigma(\omega)|, |\sigma(\omega)| |\omega|^2 D(\sigma(\omega)) \right\}.$$

Using the operator  $A_\sigma(\omega)$  and/or the sesquilinear form  $a_\sigma(\omega)$ , we define the complex-scaled problem as follows:

**Problem 5.3.** Let (5.1) hold,  $a_\sigma$  be as in Definition 5.1, and  $A_\sigma$  be as in (5.6). Then the equivalent problems to

$$\text{find } \omega \in \Lambda \text{ and } \check{u} \in H^1(\Omega) \setminus \{0\} \text{ such that } A_\sigma(\omega) \check{u} = 0$$

and to

$$\text{find } \omega \in \Lambda \text{ and } \check{u} \in H^1(\Omega) \setminus \{0\} \text{ such that } a_\sigma(\omega)(\check{u}, v) = 0 \text{ for all } v \in H^1(\Omega)$$

are called the *weak formulation of the complex-scaled Helmholtz resonance problem*.

In the case that  $(\omega, \check{u})$  solves this problem, we call  $\omega$  an eigenvalue and  $\check{u}$  the corresponding eigenfunction of  $A_\sigma(\cdot)$  and  $a_\sigma(\cdot)$ .

The theorems below show that sufficiently smooth eigenfunctions of Problem 5.3 are the complex-scaled eigenfunctions of Problem 2.3 and vice versa.

**Theorem 5.4.** Let (5.1) hold,  $\sigma : \Lambda \subset \mathbb{C} \rightarrow \mathbb{C} \setminus \{0\}$ , and  $\omega \in \Lambda$  be such that  $\text{Im}(\sigma(\omega)\omega) > 0$  and  $\arg(\sigma(\omega)) \notin [\pi - \mu, \pi + \mu]$ , with  $\mu$  as in (5.2). Moreover, let  $u \in C^2(\Omega)$  be a radiating eigenfunction as in Definition 2.7 corresponding to the eigenvalue  $\omega$  of Problem 2.3 with homogeneous Neumann boundary conditions on  $\partial\Omega$ . Then

(i) the function  $u|_{\Omega_{\text{ext}}}$  allows an analytic continuation  $U$  to a set  $\Theta \subset \mathbb{C}^3$  such that  $\check{\Omega}_{\text{ext}}, \Omega_{\text{ext}} \subset \Theta$ , and

(ii) the complex-scaled eigenfunction

$$\check{u} : \begin{cases} \Omega & \rightarrow \mathbb{C}, \\ \mathbf{x} & \mapsto \begin{cases} u(\mathbf{x}), & \mathbf{x} \in \Omega_{\text{int}} \cup \Gamma, \\ U(\check{\mathbf{x}}(\mathbf{x})), & \mathbf{x} \in \Omega_{\text{ext}} \end{cases} \end{cases} \quad (5.7)$$

solves Problem 5.3.

*Proof.* We know, by Theorem 3.11, that  $u|_{\Omega_{\text{ext}}}$  allows an analytic continuation  $U$  to the set  $\Theta = \Theta_{\pm}$ , where we choose the appropriate set such that  $\check{\Omega}_{\text{ext}}^{\sigma(\omega)} \subset \Theta$ . Moreover,

$$0 = -\Delta U(\check{\mathbf{x}}) - \omega^2 U(\check{\mathbf{x}})$$

for all  $\check{\mathbf{x}} \in \Theta$ , since the function on the right-hand side is analytic on  $\Theta$  and coincides with zero on  $\Omega_{\text{ext}}$ . The same holds for the equation in polar coordinates (cf. (5.3b)) at a point  $\check{\mathbf{x}} = \Psi^\sigma(\xi, \hat{\mathbf{x}}) = \Psi(\sigma\xi, \hat{\mathbf{x}}) = (1 + \sigma\xi)\hat{\mathbf{x}}$ , with  $\sigma = \sigma(\omega)$ , namely,

$$\begin{aligned} 0 &= -\frac{\partial^2 U \circ \Psi}{\partial \xi^2}(\sigma\xi, \hat{\mathbf{x}}) - \frac{2}{1 + \sigma\xi} \frac{\partial U \circ \Psi}{\partial \xi}(\sigma\xi, \hat{\mathbf{x}}) \\ &\quad - \frac{1}{(1 + \sigma\xi)^2} \left( \hat{\nabla} \cdot \hat{\nabla} U \circ \Psi \right)(\sigma\xi, \hat{\mathbf{x}}) - \omega^2 (U \circ \Psi)(\sigma\xi, \hat{\mathbf{x}}) \\ &= -\frac{1}{\sigma^2} \frac{\partial^2 U \circ \Psi^\sigma}{\partial \xi^2}(\xi, \hat{\mathbf{x}}) - \frac{2}{\sigma(1 + \sigma\xi)} \frac{\partial U \circ \Psi^\sigma}{\partial \xi}(\xi, \hat{\mathbf{x}}) \\ &\quad - \frac{1}{(1 + \sigma\xi)^2} \left( \hat{\nabla} \cdot \hat{\nabla} U \circ \Psi^\sigma \right)(\xi, \hat{\mathbf{x}}) - \omega^2 (U \circ \Psi^\sigma)(\xi, \hat{\mathbf{x}}). \end{aligned} \tag{5.8}$$

Moreover, we know by Theorem 3.14 that the functions  $U \circ \Psi^\sigma$  and  $\nabla_{\xi, \hat{\mathbf{x}}}(U \circ \Psi^\sigma)$  decay exponentially for  $\xi \rightarrow \infty$ . Thus, the function  $\check{u}$ , defined by (5.7), fulfills  $\check{u} \in H^1(\Omega) \cap C(\Omega)$ .

For a test function  $v \in H^1(\Omega) \cap C(\Omega)$  we multiply

$$0 = -\Delta \check{u} - (1 + \rho)^2 \omega^2 \check{u}$$

by  $\bar{v}$  in  $\Omega_{\text{int}}$  and equation (5.8) by  $(1 + \sigma\xi)^2 \overline{\sigma v \circ \Psi^\sigma(\xi, \hat{\mathbf{x}})}$  in  $\Omega_{\text{ext}}$ . Then we integrate over  $\Omega_{\text{int}}$  and  $\mathbb{R}_{>0} \times \Gamma$  respectively to obtain

$$\begin{aligned} 0 &= \int_{\Omega_{\text{int}}} -\Delta \check{u}(\mathbf{x}) \overline{v(\mathbf{x})} - \omega^2 (1 + \rho(\mathbf{x}))^2 \check{u}(\mathbf{x}) \overline{v(\mathbf{x})} \, d\mathbf{x} \\ &\quad - \frac{1}{\sigma} \int_{\mathbb{R}_{>0} \times \Gamma} (1 + \sigma\xi)^2 \frac{\partial^2 \check{u} \circ \Psi^\sigma}{\partial \xi^2}(\xi, \hat{\mathbf{x}}) \overline{v \circ \Psi^\sigma(\xi, \hat{\mathbf{x}})} \, d(\xi, \hat{\mathbf{x}}) \\ &\quad - 2 \int_{\mathbb{R}_{>0} \times \Gamma} (1 + \sigma\xi) \frac{\partial \check{u} \circ \Psi^\sigma}{\partial \xi}(\xi, \hat{\mathbf{x}}) \overline{v \circ \Psi^\sigma(\xi, \hat{\mathbf{x}})} \, d(\xi, \hat{\mathbf{x}}) \\ &\quad - \sigma \int_{\mathbb{R}_{>0} \times \Gamma} \left( \hat{\nabla} \cdot \hat{\nabla} \check{u} \circ \Psi^\sigma \right)(\xi, \hat{\mathbf{x}}) \overline{v \circ \Psi^\sigma(\xi, \hat{\mathbf{x}})} \, d(\xi, \hat{\mathbf{x}}) \\ &\quad - \sigma \omega^2 \int_{\mathbb{R}_{>0} \times \Gamma} (1 + \sigma\xi)^2 (\check{u} \circ \Psi^\sigma)(\xi, \hat{\mathbf{x}}) \overline{v \circ \Psi^\sigma(\xi, \hat{\mathbf{x}})} \, d(\xi, \hat{\mathbf{x}}) \\ &= a_\sigma(\omega)(\check{u}, v) - \int_{\Gamma \cup \partial\Omega} \nabla \check{u}(\hat{\mathbf{x}}) \cdot \mathbf{n}(\hat{\mathbf{x}}) \overline{v(\hat{\mathbf{x}})} \, d\hat{\mathbf{x}} \\ &\quad - \frac{1}{\sigma} \left[ \int_{\Gamma} (1 + \sigma\xi)^2 \frac{\partial \check{u} \circ \Psi^\sigma}{\partial \xi}(\xi, \hat{\mathbf{x}}) \overline{v \circ \Psi^\sigma(\xi, \hat{\mathbf{x}})} \, d\xi \right]_{\xi=0}^{\xi=\infty}, \end{aligned}$$

where we applied integration by parts. The evaluation of the boundary integral at  $\xi = 0, \infty$  has to be understood as taking the positive limit. Because of the asymptotic behavior of the

radial derivative of  $U \circ \Psi^\sigma$  from Theorem 3.14 and the fact that we imposed homogeneous Neumann boundary conditions on  $\partial\Omega$ , we obtain

$$0 = a_\sigma(\omega)(\check{u}, v) + \int_\Gamma \left( \frac{1}{\sigma} \lim_{\xi \rightarrow 0_+} \frac{\partial U \circ \Psi^\sigma}{\partial \xi}(\xi, \hat{\mathbf{x}}) - \nabla u(\hat{\mathbf{x}}) \cdot \mathbf{n}(\hat{\mathbf{x}}) \right) \overline{v(\hat{\mathbf{x}})} d\hat{\mathbf{x}} \\ - \int_{\partial\Omega} \nabla u(\mathbf{y}) \cdot \mathbf{n}(\mathbf{y}) \overline{v(\mathbf{y})} d\mathbf{y}.$$

Since  $u$  is also analytic in a neighborhood of  $\Gamma$  by Proposition 2.8, we obtain by application of the chain rule

$$\lim_{\xi \rightarrow 0_+} \frac{\partial U \circ \Psi^\sigma}{\partial \xi}(\xi, \hat{\mathbf{x}}) = \lim_{\xi \rightarrow 0_+} \sigma \hat{\mathbf{x}} \cdot (\nabla U)(\Psi^\sigma(\xi, \hat{\mathbf{x}})) = \sigma \nabla u(\hat{\mathbf{x}}) \cdot \hat{\mathbf{x}}.$$

Because of  $\mathbf{n}(\hat{\mathbf{x}}) = \hat{\mathbf{x}}$  on  $\Gamma$ , the first boundary term vanishes. The second term vanishes since we imposed homogeneous Neumann boundary conditions on  $\partial\Omega$ .

The density of  $C(\Omega) \cap H^1(\Omega)$  in  $H^1(\Omega)$  concludes the proof.  $\square$

**Theorem 5.5.** *Let (5.1) hold,  $\sigma : \Lambda \subset \mathbb{C} \rightarrow \mathbb{C} \setminus \{0\}$ , and  $\omega \in \Lambda$  be such that  $\text{Im}(\sigma(\omega)\omega) > 0$  and  $\arg(\sigma(\omega)) \notin [\pi - \mu, \pi + \mu]$ , with  $\mu$  as in (5.2). Moreover, let  $\check{u} \in C(\Omega)$  such that  $\check{u}|_{\Omega_{\text{int}}} \in C^2(\Omega_{\text{int}})$  and  $\check{u}|_{\Omega_{\text{ext}}} \in C^2(\Omega_{\text{ext}})$  be a solution to Problem 5.3. Then*

(i) *the function  $\check{\mathbf{x}} \mapsto \check{u}(\mathbf{x}(\check{\mathbf{x}}))$  is analytic in  $\check{\Omega}_{\text{ext}}$  and allows an analytic continuation  $U$  to a set  $\Theta \subset \mathbb{C}^3$  such that  $\Omega_{\text{ext}}, \check{\Omega}_{\text{ext}} \subset \Theta$  and*

(ii) *the function*

$$\begin{cases} \Omega & \rightarrow \mathbb{C}, \\ \mathbf{x} & \mapsto \begin{cases} \check{u}(\mathbf{x}), & \mathbf{x} \in \Omega_{\text{int}} \cup \Gamma, \\ U(\mathbf{x}), & \mathbf{x} \in \Omega_{\text{ext}} \end{cases} \end{cases} \quad (5.9)$$

*solves Problem 2.3 with homogeneous Neumann boundary conditions on  $\partial\Omega$ .*

*Proof.* Since  $\Omega_{\text{ext}} = \Psi(\mathbb{R}_{>0}, \Gamma) \subset \Omega_0^c$  and  $\Omega_0$  has a positive distance to  $\partial\Omega_{\text{ext}} = \Gamma$ , by (D5), we can find  $\varepsilon > 0$  such that  $\Psi(\mathbb{R}_{>-\varepsilon}, \Gamma) \subset \Omega_0^c$ . Note that here we have enlarged the domain of  $\Psi(\cdot, \hat{\mathbf{x}})$  to negative numbers.

For every  $\xi \in \mathbb{R}_{>-\varepsilon}$  we decompose  $\check{u} \circ \Psi$  into spherical harmonics by

$$\check{u}(\Psi(\xi, \hat{\mathbf{x}})) = \sum_{k=0}^{\infty} \sum_{j=-k}^k u_{k,j}(\xi) Y_k^j(\hat{\mathbf{x}}) \quad (5.10)$$

for some unknown functions  $u_{k,j} : \mathbb{R}_{>-\varepsilon} \rightarrow \mathbb{C}$ . Since the spherical harmonics form a complete orthonormal system of  $L^2(\Gamma)$  for each  $\xi \in \mathbb{R}_{>-\varepsilon}$ , the series

$$\sum_{k=0}^{\infty} \sum_{j=-k}^k |u_{k,j}(\xi)|^2$$

converges. Because for fixed  $k, j$  the function  $\check{u}(\Psi(\xi, \hat{\mathbf{x}})) Y_k^j(\hat{\mathbf{x}})$  is differentiable in  $\xi$  and uniformly bounded in  $\hat{\mathbf{x}}$ , we can apply the dominated convergence theorem to obtain

$$\int_{\Gamma} \frac{\partial}{\partial \xi} \check{u} \circ \Psi(\xi, \hat{\mathbf{x}}) Y_k^j(\hat{\mathbf{x}}) d\hat{\mathbf{x}} = \frac{\partial}{\partial \xi} \int_{\Gamma} \check{u} \circ \Psi(\xi, \hat{\mathbf{x}}) Y_k^j(\hat{\mathbf{x}}) d\hat{\mathbf{x}} = u'_{k,j}(\xi).$$

A similar argument can be made for the second derivative. Plugging a test function  $v$  with  $v(\Psi(\xi, \hat{\mathbf{x}})) = \tilde{v}(\xi) Y_k^j(\hat{\mathbf{x}})$  for  $\xi > -\varepsilon$  and  $\hat{\mathbf{x}} \in \Gamma$  (continued by zero on  $\Omega \setminus \Psi(\mathbb{R}_{>-\varepsilon}, \Gamma)$ ) for fixed  $k, j$  and  $\tilde{v} \in C_0^\infty(\mathbb{R}_{>-\varepsilon}) = \{f \in C^\infty(\mathbb{R}_{>-\varepsilon}) : f(-\varepsilon) = 0\}$  into the weak formulation

$$a_\sigma(\check{u}, v) = 0,$$

we obtain by using integration by parts that each function  $u_{k,j}$  solves the complex-scaled spherical Bessel's equation

$$\begin{aligned} -\frac{\partial^2}{\partial \xi^2} \tilde{u}(\xi) - \frac{2}{1+\xi} \frac{\partial}{\partial \xi} \tilde{u}(\xi) - \frac{k(k+1)}{(1+\xi)^2} \tilde{u}(\xi) - \omega^2 \tilde{u}(\xi) &= 0, & \xi \in (-\varepsilon, 0), \\ -\frac{1}{\sigma^2} \frac{\partial^2}{\partial \xi^2} \tilde{u}(\xi) - \frac{2}{\sigma(1+\sigma\xi)} \frac{\partial}{\partial \xi} \tilde{u}(\xi) - \frac{k(k+1)}{(1+\sigma\xi)^2} \tilde{u}(\xi) - \omega^2 \tilde{u}(\xi) &= 0, & \xi > 0, \\ \sigma \lim_{\xi \rightarrow 0^-} \frac{\partial}{\partial \xi} \tilde{u}(\xi) &= \lim_{\xi \rightarrow 0^+} \frac{\partial}{\partial \xi} \tilde{u}(\xi). \end{aligned}$$

It can be easily checked that every solution of the complex-scaled spherical Bessel's equation for  $\xi > 0$  is given by

$$u_{k,j}(\xi) = \alpha_{k,j} h_k^{(1)}(\omega(1+\sigma\xi)) + \beta_{k,j} h_k^{(2)}(\omega(1+\sigma\xi))$$

for some constants  $\alpha_{k,j}, \beta_{k,j}$ . Due to the asymptotic behavior of the spherical Hankel functions of the first and the second kind (Proposition A.3) and the fact that  $\check{u}$  is square-integrable, we immediately obtain that  $\beta_{k,j} = 0$ . Due to the continuity and the condition on the derivative at  $\xi = 0$ , we obtain that

$$u_{k,j}(\xi) = \begin{cases} \alpha_{k,j} h_k^{(1)}(\omega(1+\xi)), & \xi \in (-\varepsilon, 0), \\ \alpha_{k,j} h_k^{(1)}(\omega(1+\sigma\xi)), & \xi > 0. \end{cases}$$

Since the series (5.10) converges for  $\xi > -\varepsilon$ , due to the asymptotic behavior of the spherical Hankel functions in the index also the series

$$U(\mathbf{x}) := \sum_{k=0}^{\infty} \sum_{j=-k}^k \alpha_{k,j} h_k^{(1)}(\omega(1+\xi(\mathbf{x}))) Y_k^j(\hat{\mathbf{x}}(\mathbf{x}))$$

converges uniformly on compact sets (cf. [CK98, Theorem 2.14]). Therefore,  $U$  is an analytic continuation of  $\check{u}(\mathbf{x}(\check{\mathbf{x}}))$ . By construction it is clear that the function defined in (5.9) solves Problem 2.3. □

*Remark 5.6.* For  $d = 1$ , Theorems 5.4 and 5.5 hold without the restriction on  $\arg(\sigma(\omega))$ .

*Remark 5.7.* Here the fact that we restricted ourselves to the spherical scaling in three dimensions does not pose any limitation. In fact, Theorems 5.4 and 5.5 and their respective proofs also hold for the more generalized scalings defined in Chapter 3. Of course, the weak formulation of the complex-scaled problem 5.3 has to be replaced by the according weak formulation derived in Chapter 7. Similarly, the weak formulation has to be modified for different boundary conditions. If the boundary  $\Gamma$  and/or the mapping  $\mathbf{v}$  is not smooth, the fact that the complex-scaled eigenfunctions have kinks has to be taken into account as well.

## 5.2. Fredholmness and weak coercivity

An important role in the analysis of the approximation of eigenvalues of holomorphic operator functions play the properties of Fredholmness and (weak  $T$ -)coercivity. We define these concepts as follows:

**Definition 5.8.** Let  $X$  be a Hilbert space and let  $\mathcal{B}(X)$  denote the space of all bounded linear operators  $X \rightarrow X$ . Then the index  $\text{ind}(A) \in \mathbb{Z} \cup \{\pm\infty\}$  of an operator  $A \in \mathcal{B}(X)$  is defined by

$$\text{ind}(A) := \dim(\ker(A)) - \dim(\text{ran}(A)^\perp).$$

An operator  $A \in \mathcal{B}(X)$  is called

- (i) *coercive* if there exists a constant  $C > 0$  such that for all  $f \in X$

$$|(Af, f)_X| \geq C \|f\|_X,$$

- (ii) *weakly coercive* if there exists a compact operator  $K \in \mathcal{B}(X)$  such that  $A - K$  is coercive,
- (iii) *weakly  $T$ -coercive* if there exists a bijective operator  $T \in \mathcal{B}(X)$  such that  $T^*A$  is weakly coercive, and
- (iv) *Fredholm* if its index is finite.

An operator function  $\omega \mapsto A(\omega)$  is called one of the above if the evaluation at every point has the according attribute. A bounded bilinear or sesquilinear form is called one of the above if the associated operator has the according attribute.

It is a well-known fact (e.g., [Kat95, § 5]) that compact perturbations do not change the index of an operator. Thus, any operator  $A$  that can be written as a compact perturbation of an invertible operator is Fredholm with index zero. Therefore, every coercive operator is also weakly coercive, every weakly coercive operator is also weakly  $T$ -coercive, and every weakly  $T$ -coercive operator is also Fredholm with index zero.

Although we have shown in Section 5.1 that for given  $\omega$  in a certain region, a sufficiently smooth eigenfunction corresponding to the eigenvalue  $\omega$  of the complex-scaled weak formulation 5.3 is a complex-scaled eigenfunction of our initial strong formulation and vice versa, it is not clear for which  $\omega \in \Lambda$  the operator function  $\omega \mapsto A_\sigma(\omega)$  is Fredholm. Therefore, it is not clear for which  $\omega \in \Lambda$  the approximation theory for holomorphic operator functions

[Kar96a, Kar96b] is valid and where we have to expect an essential spectrum (Definition 5.12).

In [Hal19, Theorem 3.17] it is stated that holomorphic operator functions that are weakly  $T$ -coercive are feasible for Galerkin discretizations. Thus, this section is dedicated to examining for which  $\omega \in \Lambda$  the operator  $A_\sigma(\omega)$  is weakly coercive and therefore also Fredholm.

The lemma below is helpful for showing compactness of an operator.

**Lemma 5.9.** *Let  $\Omega \in \mathbb{R}^d$  and  $m \in L^\infty(\Omega)$  such that*

$$\lim_{R \rightarrow \infty} \|m\|_{L^\infty(\Omega \cap B_R^c)} = 0.$$

*Then the multiplication operator defined by*

$$M_m : \begin{cases} H^1(\Omega) & \rightarrow L^2(\Omega), \\ f & \mapsto m(\cdot) f(\cdot) \end{cases}$$

*is compact.*

*Proof.* [Hal19, Lemma 4.3] with  $Y = H^1(\Omega)$ ,  $\eta_1 \equiv 1$ , and  $\eta_2 = m$ . □

The theorem below is a special case of [Hal19, Theorem 4.5] for linear scalings.

**Theorem 5.10.** *Let (5.1) hold,  $\sigma : \Lambda \rightarrow \mathbb{C} \setminus \{0\}$ , and  $\omega \in \Lambda \cap \mathbb{C}_{\text{Im} \leq 0}$  such that  $\text{Im}(\sigma(\omega)\omega) > 0$  and  $\arg(\sigma(\omega)) \in [0, \frac{\pi}{2})$ . Then the operator  $A_\sigma(\omega)$  defined in (5.6) is weakly coercive.*

*Proof.* We define the sesquilinear forms  $b_\sigma(\omega)$ ,  $k_\sigma(\omega)$  by

$$\begin{aligned} b_\sigma(\omega)(f, g) &:= \int_{\Omega_{\text{int}}} \nabla f(\mathbf{x}) \cdot \overline{\nabla g(\mathbf{x})} \, d\mathbf{x} \\ &\quad + \frac{1}{\sigma(\omega)} \int_{\mathbb{R}_{>0} \times \Gamma} (1 + \xi \sigma(\omega))^2 \frac{\partial}{\partial \xi} (f \circ \Psi)(\xi, \hat{\mathbf{x}}) \overline{\frac{\partial}{\partial \xi} (g \circ \Psi)(\xi, \hat{\mathbf{x}})} \, d(\xi, \hat{\mathbf{x}}) \\ &\quad + \sigma(\omega) \int_{\mathbb{R}_{>0} \times \Gamma} \hat{\nabla} (f \circ \Psi)(\xi, \hat{\mathbf{x}}) \cdot \overline{\hat{\nabla} (g \circ \Psi)(\xi, \hat{\mathbf{x}})} \, d(\xi, \hat{\mathbf{x}}) \\ &\quad - \sigma(\omega)^3 \omega^2 \int_{\mathbb{R}_{>0} \times \Gamma} (1 + \xi)^2 (f \circ \Psi)(\xi, \hat{\mathbf{x}}) \overline{(g \circ \Psi)(\xi, \hat{\mathbf{x}})} \, d(\xi, \hat{\mathbf{x}}) \end{aligned}$$

and

$$\begin{aligned} k_\sigma(\omega)(f, g) &:= -\omega^2 \int_{\Omega_{\text{int}}} (1 + \rho(\mathbf{x}))^2 f(\mathbf{x}) \overline{g(\mathbf{x})} \, d\mathbf{x} \\ &\quad - \sigma(\omega) \omega^2 \int_{\mathbb{R}_{>0} \times \Gamma} \left[ (1 + \sigma(\omega) \xi)^2 - \sigma(\omega)^2 (1 + \xi)^2 \right] (f \circ \Psi)(\xi, \hat{\mathbf{x}}) \overline{(g \circ \Psi)(\xi, \hat{\mathbf{x}})} \, d(\xi, \hat{\mathbf{x}}) \end{aligned}$$

for  $f, g \in H^1(\Omega)$ .

Clearly,

$$a_\sigma(\omega) = b_\sigma(\omega) + k_\sigma(\omega).$$

The sesquilinear form  $k_\sigma(\omega)$  can be rewritten by

$$k_\sigma(\omega)(f, g) = (f, M_{\bar{m}}g)_{L^2(\Omega)},$$

with the function  $m \in L^\infty(\Omega)$  given by

$$m(\mathbf{x}) = \begin{cases} -\omega^2(1 + \rho)^2, & \mathbf{x} \in \Omega_{\text{int}}, \\ -\sigma(\omega) \omega^2 \frac{(1 + \sigma(\omega)(\|\mathbf{x}\| - 1))^2 - \sigma(\omega)^2 \|\mathbf{x}\|^2}{\|\mathbf{x}\|^2}, & \mathbf{x} \in \Omega_{\text{ext}}, \end{cases}$$

and  $M_{\bar{m}} : H^1(\Omega) \rightarrow L^2(\Omega)$  is the multiplication operator by  $\bar{m}$ , where we remind the reader that  $\xi(\mathbf{x}) = \|\mathbf{x}\| - 1$ . Since

$$\lim_{\xi \rightarrow \infty} m(\mathbf{x}(\xi, \hat{\mathbf{x}})) = 0,$$

uniformly in  $\hat{\mathbf{x}} \in \Gamma$ , we can apply Lemma 5.9 and obtain that  $M_{\bar{m}}$  is compact. By [Kat95, Theorem 4.10] the adjoint of a compact operator is also compact. Therefore, also

$$K_\sigma(\omega) := M_{\bar{m}}^*|_{H^1(\Omega)} : H^1(\Omega) \rightarrow H^1(\Omega),$$

is compact. Clearly,  $K_\sigma(\omega)$  is the operator induced by the sesquilinear form  $k_\sigma(\omega)$ .

It is easy to check that the sesquilinear form  $b_\sigma(\omega)$  is bounded with respect to the  $H^1(\Omega)$ -norm. Thus, by means of the Riesz representation theorem we can define a bounded operator  $B_\sigma(\omega)$  such that

$$(B_\sigma(\omega) f, g)_{H^1(\Omega)} := b_\sigma(\omega)(f, g)$$

for all  $f, g \in H^1(\Omega)$ .

Next we show that  $B_\sigma(\omega)$  is coercive. Since we assumed that  $\arg(\sigma(\omega)) \in [0, \frac{\pi}{2})$ ,  $\text{Im}(\omega) \leq 0$ , and  $\text{Im}(\sigma(\omega)\omega) > 0$ , we obtain

$$\arg(\sigma(\omega)\omega) \in \left(0, \frac{\pi}{2}\right),$$

and therefore also

$$\text{Im}\left(\sigma(\omega)^2 \omega^2\right) > 0.$$

Because of this and  $\text{Re}\left(\frac{i}{\sigma(\omega)^2}\right) > 0$  we can find  $0 < \varepsilon < \frac{\pi}{2}$  such that

$$\text{Re}\left(\frac{i \exp(-i\varepsilon)}{\sigma(\omega)^2}\right) > 0$$

and

$$\text{Im}\left(\exp(-i\varepsilon) \sigma(\omega)^2 \omega^2\right) > 0.$$

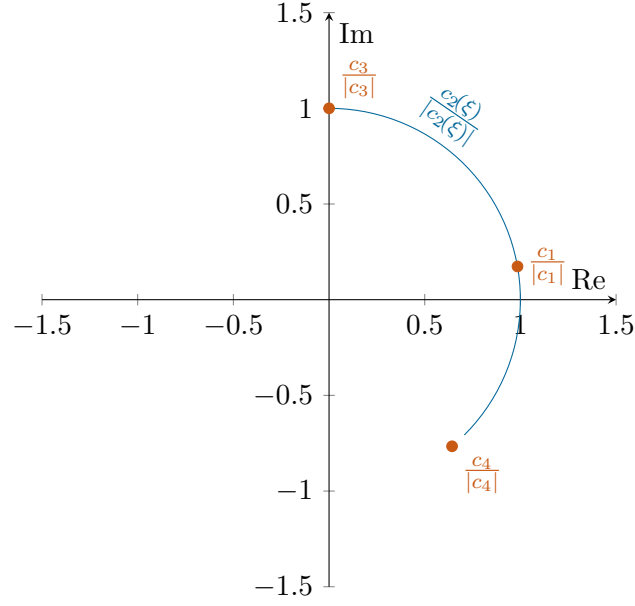


Figure 5.2.: Exemplary sketch of the normalized coefficients of the sesquilinear form  $b_\sigma(\omega)$  with  $c_1 = \frac{i}{\sigma(\omega)}$ ,  $c_2(\xi) = \frac{i(1+\xi\sigma(\omega))^2}{\sigma^2(\omega)(1+\xi)^2}$ ,  $c_3 = i$ , and  $c_4 = -i\sigma(\omega)^2\omega^2$  for  $\sigma(\omega) = \exp(i\frac{4\pi}{9})$  and  $\omega = \exp(-i\frac{\pi}{3})$ .

We use this to calculate

$$\begin{aligned} \left| \frac{b_\sigma(\omega)(f, f)}{\sigma(\omega)} \right| &\geq \operatorname{Re} \left( \frac{i \exp(-i\varepsilon)}{\sigma(\omega)} b_\sigma(\omega)(f, f) \right) \\ &= \operatorname{Re} \left( \frac{i \exp(-i\varepsilon)}{\sigma(\omega)} \right) \int_{\Omega_{\text{int}}} \|\nabla f(\mathbf{x})\|^2 d\mathbf{x} \\ &\quad + \int_{\mathbb{R}_{>0} \times \Gamma} \operatorname{Re} \left( \frac{i \exp(-i\varepsilon) (1 + \xi\sigma(\omega))^2}{\sigma(\omega)^2 (1 + \xi)^2} \right) (1 + \xi)^2 \left| \frac{\partial}{\partial \xi} (f \circ \Psi)(\xi, \hat{\mathbf{x}}) \right|^2 d(\xi, \hat{\mathbf{x}}) \\ &\quad + \operatorname{Re}(i \exp(-i\varepsilon)) \int_{\mathbb{R}_{>0} \times \Gamma} \left\| \hat{\nabla} (f \circ \Psi)(\xi, \hat{\mathbf{x}}) \right\|^2 d(\xi, \hat{\mathbf{x}}) \\ &\quad - \operatorname{Re} \left( i \exp(-i\varepsilon) \sigma(\omega)^2 \omega^2 \right) \int_{\mathbb{R}_{>0} \times \Gamma} (1 + \xi)^2 |(f \circ \Psi)(\xi, \hat{\mathbf{x}})|^2 d(\xi, \hat{\mathbf{x}}) \end{aligned}$$

for  $f \in H^1(\Omega)$ . Since (see Figure 5.2)

$$\begin{aligned} \operatorname{Re} \left( \frac{i \exp(-i\varepsilon)}{\sigma(\omega)} \right) &= \frac{\sin(\varepsilon) \operatorname{Re}(\sigma(\omega)) + \cos(\varepsilon) \operatorname{Im}(\sigma(\omega))}{|\sigma(\omega)|^2} > 0, \\ \operatorname{Re} \left( \frac{i \exp(-i\varepsilon) (1 + \xi\sigma(\omega))^2}{\sigma(\omega)^2 (1 + \xi)^2} \right) &\geq \min \left\{ \operatorname{Re} \left( \frac{i \exp(-i\varepsilon)}{\sigma(\omega)^2} \right), \operatorname{Re}(i \exp(-i\varepsilon)) \right\} > 0 \end{aligned}$$

for all  $\xi \geq 0$ , and

$$-\operatorname{Re} \left( i \exp(-i\varepsilon) \sigma(\omega)^2 \omega^2 \right) = \operatorname{Im} \left( \exp(-i\varepsilon) \sigma(\omega)^2 \omega^2 \right) > 0,$$



we have that  $b_\sigma(\omega)$ , and therefore also  $B_\sigma(\omega)$ , is coercive.  $\square$

Theorem 5.10 gives us that the operator function

$$A_\sigma : \{\omega \in \Lambda \cap \mathbb{C}_{\text{Im} \leq 0} : \text{Re}(\sigma(\omega)) > 0, \text{Im}(\sigma(\omega)\omega) > 0\} \rightarrow \mathcal{B}(H^1(\Omega)),$$

is Fredholm with index 0. Note that the conditions from Chapter 3, the numerical experiments from Chapter 9, and the construction of the essential spectrum  $\Sigma_{\text{sing}}$  in Section 5.3 suggest that this is also the case for  $\omega \in \Lambda$  such that  $\arg(\sigma(\omega)) \in [\frac{\pi}{2}, \pi - \mu)$ , with  $\mu$  as in (5.2). However, it is not clear how this can be shown. We also neglected frequencies with positive imaginary part since we are mostly interested in the ones below the positive real axis and refer to [Hal19], where it is proven that the operator function is  $T$ -coercive for these frequencies.

*Remark 5.11.* The fact that  $A_\sigma$  is a Fredholm operator function gives us additional regularity of our eigenfunctions. This means that we have a one-to-one correspondence between solutions of the weak formulation (Problem 5.3) and the strong formulation (Problem 2.3). Since, by Theorem 5.10,

$$a_\sigma(\omega) = b_\sigma(\omega) + k_\sigma(\omega),$$

where  $b_\sigma(\omega)$  is elliptic and  $k_\sigma(\omega)$  is given by an  $L^2$ -inner product with an additional coefficient, we can use standard elliptic regularity theory (e.g., [Eva10, Chapters 6.3 and 6.5]) to show that a complex-scaled eigenfunction  $\check{u}$  is smooth in  $\Omega_{\text{ext}}$  and regular in  $\Omega_{\text{int}}$  depending on the regularity of  $\rho$ . Thus, the assumption on the regularity in Theorem 5.5 is fulfilled.

### 5.3. The essential spectrum

We know from Section 5.2 that the operator function  $A_\sigma(\omega)$  defined in (5.6) is Fredholm for certain values of  $\omega$ . For these values we can apply the approximation theory of Karma (see [Kar96a] and [Kar96b]). The question remains how the operator behaves for frequencies  $\omega$  where we have not shown Fredholmness. The considerations from Chapter 3, particularly from Section 3.2, and the conditions (S1) and (S2) suggest that for frequencies  $\omega$  where these conditions are violated the operator are not Fredholm. Simply put, this happens because the candidates for the complex-scaled eigenfunctions corresponding to these frequencies are no elements of the space  $H^1(\Omega)$ . Nevertheless, there might exist so-called singular sequences, which fulfill the eigenvalue equation in the limit. The elements of these singular sequences will also be approximated by a discretization scheme.

In this section we show the converse result of Theorem 5.10 for a special configuration of domains, namely, that if one of the conditions (S1) and (S2) is violated, the operator is not Fredholm. Points where an operator function is not Fredholm constitute the so-called *essential spectrum* (see, e.g., [Dav02, Section 3]) which we define as follows:

**Definition 5.12.** Let  $X$  be a Hilbert space,  $\Lambda \subset \mathbb{C}$  and  $A : \Lambda \rightarrow \mathcal{B}(X)$  be an operator function. Then we define the essential spectrum  $\Sigma_e(A(\cdot))$  as the set of all  $\omega \in \Lambda$  such that  $A(\omega)$  is not Fredholm.

*Remark 5.13.* In the literature the definition of the essential spectrum is very ambiguous. Another possible way to define the essential spectrum as the spectrum of the operator minus all eigenvalues of finite multiplicity ([HS96, Definition 1.4]). This essential spectrum is a superset of  $\Sigma_e$  from in Definition 5.12. Differing from this, Kato defines the essential spectrum as the set of all points where the operator function is not semi-Fredholm ([Kat95, IV. §5.6]). This set is a subset of  $\Sigma_e$ . For an overview of the various definitions of the essential spectrum we refer to [EE87, Chapters I and IX]. Regardless of the choice of the definition of the essential spectrum, it is always a closed set ([EE87, Section I.4]).

Note that in all the given sources the essential spectrum is only defined for operator functions of the form  $\omega \mapsto T - \omega \mathbf{I}_X$  for a fixed operator  $T \in \mathcal{B}(X)$ . Nevertheless, these definitions can be extended to the case of more general operator functions in a straightforward manner.

An important tool to characterize non-Fredholmness of an operator, and therefore points in the essential spectrum of an operator function, are so-called singular sequences.

**Theorem 5.14.** *Let  $A \in \mathcal{B}(X)$  for some Hilbert space  $X$ . Moreover, let  $s_n \in X, n \in \mathbb{N}$  be a sequence of normalized vectors such that*

1.  $\lim_{n \rightarrow \infty} \|As_n\|_X = 0$  and
2. *there exists no converging subsequence of  $s_n$ .*

*Then  $A$  is not Fredholm and the sequence  $s_n$  is called a singular sequence.*

*Proof.* This is proven, for instance, in [Hal19, Thm. 3.3] and [EE87, Chapter IX, Theorem 1.3].  $\square$

*Remark 5.15.* A term worth mentioning at this point is the so-called *pseudo spectrum* (see, e.g., [Dav02, Section 2]). For an operator function  $A(\cdot)$  and fixed  $\varepsilon > 0$ , it consists of all values  $\omega$  such that there exists a vector  $f \in X$ , called pseudo eigenvector, that satisfies

$$\|A(\omega) f\|_X < \varepsilon \|f\|_X.$$

It is clear that every singular sequence for the operator  $A(\omega)$  contains pseudo eigenvectors corresponding to the pseudo eigenvalue  $\omega$ . Thus, every point  $\omega$  such that there exists a singular sequence for  $A(\omega)$  is part of the pseudo spectrum. Approximations of pseudo eigenpairs will often be eigenpairs of discretizations of the according resonance problem with approximation quality  $\varepsilon$  (see Chapter 9).

In the following two sections, we will construct singular sequences for frequencies  $\omega$  such that the conditions (S1) and (S2) are violated. We denote the set of frequencies  $\omega \in \Sigma_e$  connected to the violation of (S1) by  $\Sigma_{\text{sing}}$ . Similarly, we denote the set of frequencies in  $\Sigma_e$  corresponding to the violation of (S2) by  $\Sigma_{\text{dec}}$ .

### 5.3.1. The set $\Sigma_{\text{sing}}$

In this section we construct a singular sequence for the operator  $A_\sigma(\omega)$  when (S1) is not fulfilled (i.e., if  $\arg(\sigma(\omega)) \in [\pi - \mu, \pi + \mu]$ ). Remember that  $\mu$  is the maximal angle defined in (3.1) and in the spherical case given by (5.2).

To simplify our presentation we consider a special case first: We assume that our domain solely consists of an exterior domain, namely,

$$\Omega = \Omega_{\text{ext}} = \overline{B_1}^c, \quad \Gamma = S_1. \quad (5.11)$$

Note that, in this case, we have  $\mu = \frac{\pi}{2}$ .

**Lemma 5.16.** *Let (5.11) hold,  $a_\sigma, A_\sigma$  be as in Definition 5.1 and (5.6),  $\sigma : \Lambda \subset \mathbb{C} \rightarrow \mathbb{C} \setminus \{0\}$ , and  $\sigma(\omega) \notin \mathbb{R}_{<0}$ . For  $\omega \in \Lambda$  and fixed  $n \in \mathbb{N}_0$ ,  $m \in \mathbb{Z}$  such that  $|m| \leq n$ , we define the function  $u_{n,m} : \Omega \rightarrow \mathbb{C}$  by*

$$u_{n,m}(\mathbf{x}) := h_n^{(1)}(\omega\gamma(\xi(\mathbf{x}))) Y_n^m(\hat{\mathbf{x}}(\mathbf{x})), \quad (5.12)$$

with  $\gamma(\xi) := 1 + \sigma(\omega)\xi$ . Then  $u_{n,m} \in H^1(\Omega)$  if and only if  $\text{Im}(\omega\sigma(\omega)) > 0$  (i.e., if (S2) is fulfilled). In this case

$$a_\sigma(\omega)(u_{n,m}, g) = (A_\sigma(\omega) u_{n,m}, g)_{H^1(\Omega)} = -\omega \left( h_n^{(1)} \right)'(\omega) \int_\Gamma Y_n^m(\hat{\mathbf{x}}) \overline{\text{tr}_\Gamma g(\hat{\mathbf{x}})} d\hat{\mathbf{x}}$$

for all  $g \in H^1(\Omega)$  and there exists a constant  $c > 0$  independent of  $n, m, \sigma, \omega$  such that

$$\|A_\sigma(\omega) u_{n,m}\|_{H^1(\Omega)} \leq c \left| \omega \left( h_n^{(1)} \right)'(\omega) \right|.$$

*Proof.* The first claim is clear because of the exponential term in the spherical Hankel functions (Proposition A.2) and the formula for the  $H^1$ -norm in polar coordinates (5.5). Note that the assumption  $\sigma(\omega) \notin \mathbb{R}_{<0}$  prevents the complex-scaled spherical Hankel function from having a singularity.

Using a test function  $g \in H^1(\Omega)$ , we obtain

$$\begin{aligned} a_\sigma(\omega)(u_{n,m}, g) &= \underbrace{\int_0^\infty \omega\gamma(\xi)^2 \left( h_n^{(1)} \right)'(\omega\gamma(\xi)) \int_\Gamma Y_n^m(\hat{\mathbf{x}}) \overline{\frac{\partial g \circ \Psi}{\partial \xi}(\xi, \hat{\mathbf{x}})} d\hat{\mathbf{x}} d\xi}_{(*)} \\ &\quad + \sigma(\omega) \int_0^\infty h_n^{(1)}(\omega\gamma(\xi)) \int_\Gamma \hat{\nabla} Y_n^m(\hat{\mathbf{x}}) \cdot \overline{\hat{\nabla} (g \circ \Psi)(\xi, \hat{\mathbf{x}})} d\hat{\mathbf{x}} d\xi \\ &\quad - \omega^2 \sigma(\omega) \int_0^\infty \gamma(\xi)^2 h_n^{(1)}(\omega\gamma(\xi)) \int_\Gamma Y_n^m(\hat{\mathbf{x}}) \overline{g(\Psi(\xi, \hat{\mathbf{x}}))} d\hat{\mathbf{x}} d\xi. \end{aligned}$$

Performing integration by parts on the first term, gives

$$\begin{aligned} (*) &= - \int_0^\infty \omega \frac{\partial}{\partial \xi} \left( \gamma(\xi)^2 \left( h_n^{(1)} \right)'(\omega\gamma(\xi)) \right) \int_\Gamma Y_n^m(\hat{\mathbf{x}}) \overline{g(\Psi(\xi, \hat{\mathbf{x}}))} d\hat{\mathbf{x}} d\xi \\ &\quad + \left[ \omega\gamma(\xi)^2 \left( h_n^{(1)} \right)'(\omega\gamma(\xi)) \int_\Gamma Y_n^m(\hat{\mathbf{x}}) \overline{g(\Psi(\xi, \hat{\mathbf{x}}))} d\hat{\mathbf{x}} \right]_{\xi=0}^{\xi=\infty} \\ &= - \sigma(\omega) \int_0^\infty \left( 2\omega\gamma(\xi) \left( h_n^{(1)} \right)'(\omega\gamma(\xi)) + \omega^2 \gamma(\xi)^2 \left( h_n^{(1)} \right)''(\omega\gamma(\xi)) \right) \int_\Gamma Y_n^m(\hat{\mathbf{x}}) \overline{g(\Psi(\xi, \hat{\mathbf{x}}))} d\hat{\mathbf{x}} d\xi \\ &\quad - \omega \left( h_n^{(1)} \right)'(\omega) \int_\Gamma Y_n^m(\hat{\mathbf{x}}) \overline{\text{tr}_\Gamma g(\hat{\mathbf{x}})} d\hat{\mathbf{x}}, \end{aligned}$$

since the functions  $(h_n^{(1)})'(\omega\gamma(\xi))$  decay exponentially for  $\xi \rightarrow \infty$ . Using the fact that the spherical harmonics are the eigenfunctions of the surface Laplacian, we obtain

$$\begin{aligned} a_\sigma(\omega)(u_{n,m}, g) &= -\sigma(\omega) \int_0^\infty (T_n h_n^{(1)})'(\omega\gamma(\xi)) \int_\Gamma Y_n^m(\hat{\mathbf{x}}) \overline{g(\mathbf{x}(r, \hat{\mathbf{x}}))} d\hat{\mathbf{x}} d\xi \\ &\quad - \omega (h_n^{(1)})'(\omega) \int_\Gamma Y_n^m(\hat{\mathbf{x}}) \overline{\text{tr}_\Gamma g(\hat{\mathbf{x}})} d\hat{\mathbf{x}}, \end{aligned}$$

with

$$(T_n u)(z) := z^2 u''(z) + 2z u'(z) - (z^2 - n(n+1)) u(z),$$

which is the differential operator of the spherical Bessel's equation (A.1) with index  $n$ . The fact that  $h_n^{(1)}$  solves  $T_n u = 0$  yields the second claim.

For the last claim we calculate

$$\begin{aligned} \|A_\sigma(\omega) u_{n,m}\|_{H^1(\Omega)} &= \sup_{\substack{g \in H^1(\Omega) \\ \|g\|_{H^1(\Omega)}=1}} |(A_\sigma(\omega) u_{n,m}, g)_{H^1(\Omega)}| \\ &= \sup_{\substack{g \in H^1(\Omega) \\ \|g\|_{H^1(\Omega)}=1}} \left| (Y_n^m, \text{tr}_\Gamma g)_{L^2(\Gamma)} (h_n^{(1)})'(\omega) \omega \right| \\ &\leq \underbrace{\|Y_n^m\|_{L^2(\Gamma)}}_{=1} \left| (h_n^{(1)})'(\omega) \omega \right| \sup_{\substack{g \in H^1(\Omega) \\ \|g\|_{H^1(\Omega)}=1}} \|\text{tr}_\Gamma g\|_{L^2(\Gamma)} \\ &\leq \|\text{tr}_{\partial\Omega}\| \left| \omega (h_n^{(1)})'(\omega) \right|, \end{aligned}$$

where the inequality for the trace holds because of Theorem A.12.  $\square$

Note that this situation is actually not covered by our theory since in (D1–5) we required a positive distance between  $\Gamma$  and  $\partial\Omega$  (see Remark 2.5). This assumption was necessary to ensure that the eigenfunctions are smooth at the interface  $\Gamma$ . In the case of (5.11) the regularity of the eigenfunctions is not an issue since an eigenfunction is given by only one single spherical Hankel function times a single spherical harmonic and not by an infinite sum.

Lemma 5.16 shows that the roots of  $(h_n^{(1)})'$  are eigenvalues of  $a_\sigma(\omega)$  and  $u_{n,m}$  for  $|m| \leq n$  the corresponding eigenfunctions. If  $\omega$  is no root of  $(h_n^{(1)})'$ , the construction above does not lead to eigenvalues. Nevertheless, if  $(h_n^{(1)})'(\omega)$  is small, it helps us to construct a singular sequence. The main idea here is that, for  $\sigma(\omega)$  with  $\arg(\sigma(\omega)) \in (\frac{\pi}{2}, \pi)$ , the functions  $|h_n^{(1)}(\omega(1 + \sigma(\omega) \cdot))|$  take their unique, global maximum at a point  $\xi_0 > 0$  (cf. Figure 5.4). Due to the asymptotic behavior of the spherical Hankel functions, this peak dominates the behavior of the function at  $\xi = 0$  for large  $n$  making it an approximate eigenfunction

(Lemma 5.16). Thus, our singular sequence will be defined by

$$s_n(\mathbf{x}) := \frac{h_n^{(1)}(\omega\gamma(\xi(\mathbf{x}))) Y_n^0(\hat{\mathbf{x}}(\mathbf{x}))}{\left\| h_n^{(1)}(\omega\gamma(\xi(\cdot))) Y_n^0(\hat{\mathbf{x}}(\cdot)) \right\|_{H^1(\Omega)}}.$$

To characterize the behavior of the functions  $s_n$ , we need the following technical lemma:

**Lemma 5.17.** *Let  $\sigma \in \mathbb{C} \setminus \{0\}$ . Then the function*

$$\begin{cases} \mathbb{R} & \rightarrow \mathbb{C}, \\ \xi & \mapsto |\gamma(\xi)|^2 = |1 + \sigma\xi|^2 \end{cases}$$

takes its unique, global minimum  $m := |\gamma(\xi_0)|^2 = \sin(\arg \sigma)^2$  at  $\xi_0 := -\frac{\operatorname{Re}(\sigma)}{|\sigma|^2}$  (see Figure 5.3).

*Proof.* We differentiate  $|\gamma(\cdot)|^2$  to obtain

$$\frac{\partial}{\partial \xi} |\gamma(\xi)|^2 = \frac{\partial}{\partial \xi} \left( \gamma(\xi) \overline{\gamma(\xi)} \right) = \frac{\partial}{\partial \xi} (1 + (\sigma + \bar{\sigma})\xi + |\sigma|^2 \xi^2) = 2\operatorname{Re}(\sigma) + 2|\sigma|^2 \xi,$$

which has its unique root at  $\xi_0 := -\frac{\operatorname{Re}(\sigma)}{|\sigma|^2}$ . Since  $|\gamma(\xi)|^2$  is a positive, quadratic function in  $\xi$ , this is the global minimum and its value is

$$\begin{aligned} |\gamma(\xi_0)|^2 &= 1 + 2\operatorname{Re}(\sigma) \xi_0 + |\sigma|^2 \xi_0^2 = 1 + 2\operatorname{Re}(\sigma) \left( -\frac{\operatorname{Re}(\sigma)}{|\sigma|^2} \right) + |\sigma|^2 \left( \frac{\operatorname{Re}(\sigma)}{|\sigma|^2} \right)^2 \\ &= 1 - \frac{\operatorname{Re}(\sigma)^2}{|\sigma|^2} = 1 - \cos(\arg(\sigma))^2 = \sin(\arg(\sigma))^2. \end{aligned}$$

□

A main ingredient for the construction of the singular sequence is the fact that the norms of the functions  $s_n$  mainly depend on their behavior at the peak. This can be justified by the so-called Laplace's Method.

**Theorem 5.18** (Laplace's Method). *For a finite or infinite open interval  $I$ , let  $\phi, f \in L_2(I) \cap C^\infty(I)$  be such that  $f$  takes its unique, global maximum at  $x_0 \in I$ . Then*

$$\int_I \phi(x) f(x)^j dx \sim \phi(x_0) f(x_0)^{j+1/2} \sqrt{-\frac{2\pi}{j f''(x_0)}}, \quad j \rightarrow \infty.$$

*Proof.* See, for example, [Won01, Chapter II.1].

□

Using Lemma 5.17 and Theorem 5.18 we can prove, by the construction of a singular sequence, that frequencies  $\omega$  that violate condition (S1) are elements of the essential spectrum.

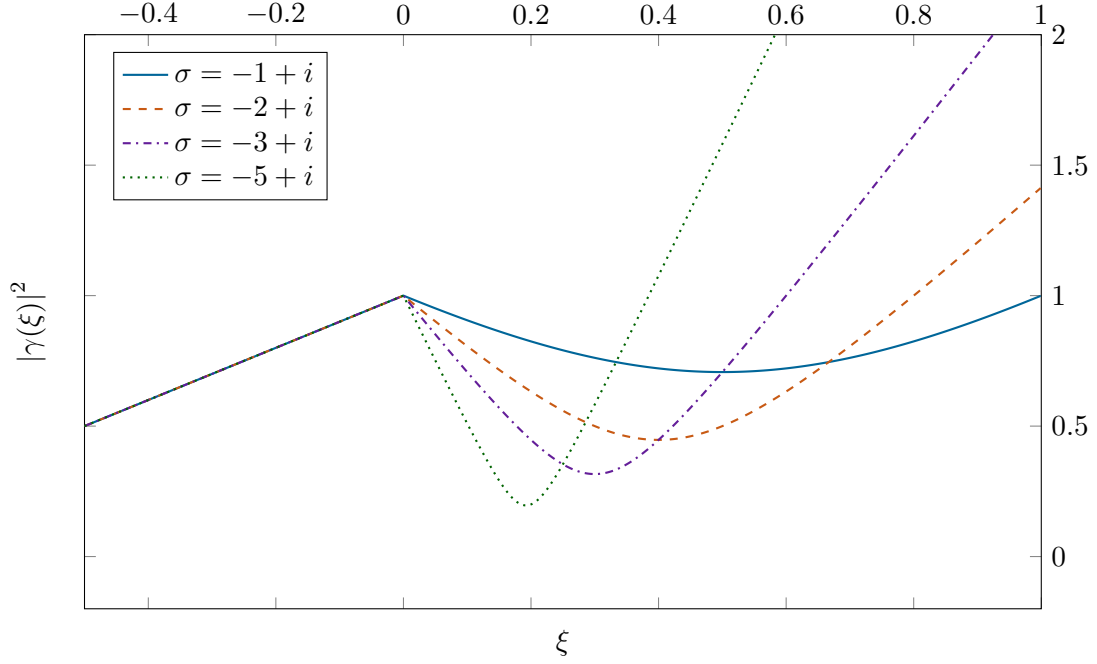


Figure 5.3.: The functions  $|\gamma(\cdot)|^2$  from the Lemmas 5.17 (for  $\xi > 0$ ) and 5.21 for different values of  $\sigma$ .

**Theorem 5.19.** *Let (5.1) hold,  $\sigma : \Lambda \subset \mathbb{C} \rightarrow \mathbb{C} \setminus \{0\}$ , and  $A_\sigma$  as in (5.6). Moreover, let  $\omega \in \Lambda$  such that  $\operatorname{Re}(\sigma(\omega)) < 0$ ,  $\sigma(\omega) \notin \mathbb{R}_{<0}$ , and  $\operatorname{Im}(\sigma(\omega)\omega) > 0$ . Then  $\omega \in \Sigma_e(A_\sigma)$ .*

*Proof.* Since the functions  $h_n^{(1)}(\omega\gamma(\xi(\cdot)))$  are in  $H^1(\Omega)$ , we may define a sequence for functions  $s_n \in H^1(\Omega)$  by

$$s_n(\mathbf{x}) := \frac{h_n^{(1)}(\omega\gamma(\xi(\mathbf{x}))) Y_n^0(\hat{\mathbf{x}}(\mathbf{x}))}{\left\| h_n^{(1)}(\omega\gamma(\xi(\cdot))) Y_n^0(\hat{\mathbf{x}}(\cdot)) \right\|_{H^1(\Omega)}}$$

for  $\mathbf{x} \in \Omega$ . Let  $\xi_0 = -\frac{\operatorname{Re}(\sigma(\omega))}{|\sigma(\omega)|^2}$  be the point where  $|\gamma(\cdot)|^2$  takes its unique minimum by Lemma 5.17. Then we have  $\xi_0 > 0$  since  $\operatorname{Re}(\sigma(\omega)) < 0$ . We pick  $\xi_1 > \xi_0$  and  $0 < \varepsilon < 1$ . Due to the asymptotic behavior of the spherical Hankel functions (Proposition A.4), we know that there exists an index  $N \in \mathbb{N}$  such that

$$(1 - \varepsilon) \frac{(2n - 1)!!}{|\omega\gamma(\xi)|^{n+1}} \leq |h_n(\omega\gamma(\xi))| \leq (1 + \varepsilon) \frac{(2n - 1)!!}{|\omega\gamma(\xi)|^{n+1}}$$

for all  $n > N_0$  and  $\xi \in [0, \xi_1]$ . We can bound the norm of  $h_n^{(1)}(\omega\gamma(\xi(\cdot))) Y_n^0(\hat{\mathbf{x}}(\cdot))$  from

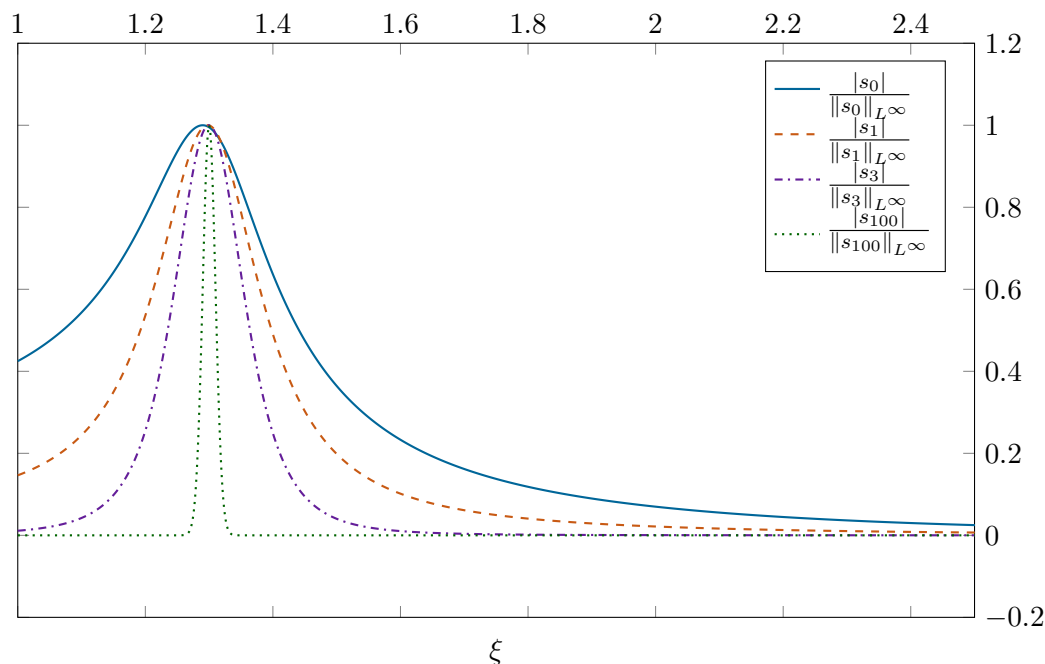


Figure 5.4.: The functions  $s_n(\Psi(\cdot, \hat{\mathbf{x}}))$  for  $\sigma = -3 + i$ , normalized at their peak.

below by

$$\begin{aligned}
 \left\| h_n^{(1)}(\omega\gamma(\xi(\cdot))) Y_n^0(\hat{\mathbf{x}}(\cdot)) \right\|_{H^1(\Omega)}^2 &\geq \left\| h_n^{(1)}(\omega\gamma(\xi(\cdot))) Y_n^0(\hat{\mathbf{x}}(\cdot)) \right\|_{L^2(\Omega)}^2 \\
 &= \underbrace{\int_{\Gamma} |Y_n^0(\hat{\mathbf{x}})|^2 d\hat{\mathbf{x}}}_{=1} \int_0^\infty |h_n^{(1)}(\omega\gamma(\xi)) (1 + \xi)|^2 d\xi \\
 &\geq \int_0^{\xi_1} |h_n^{(1)}(\omega\gamma(\xi)) (1 + \xi)|^2 d\xi \\
 &\geq \frac{(1 - \varepsilon)^2 ((2n - 1)!!)^2}{|\omega|^{2n+2}} \int_0^{\xi_1} \frac{(1 + \xi)^2}{|\gamma(\xi)|^{2n+2}} d\xi.
 \end{aligned}$$

Next we apply Theorem 5.18 with  $\phi(\xi) = (1 + \xi)^2$ ,  $f(\xi) = |\gamma(\xi)|^{-2}$ ,  $j = n + 1$ , and  $I = (0, \xi_1)$  and obtain

$$\int_0^{\xi_1} \frac{(1 + \xi)^2}{|\gamma(\xi)|^{2n+2}} d\xi \sim \frac{(1 + \xi_0)^2}{|\gamma(\xi_0)|^{2n+3}} \sqrt{\frac{2\pi}{(n + 1)f''(\xi_0)}}$$

and thus,

$$\int_0^{\xi_1} \frac{(1 + \xi)^2}{|\gamma(\xi)|^{2n+2}} d\xi \geq \frac{C_1}{\sqrt{n + 1} |\gamma(\xi_0)|^{2n+3}}$$

with  $n > N_1$  for some  $N_1 \in \mathbb{N}$  and  $C_1 = (1 - \varepsilon)(1 + \xi_0)^2 \sqrt{-\frac{2\pi}{f''(\xi_0)}} > 0$ . Note that  $C_1$  depends only on  $\sigma(\omega)$  and  $\varepsilon$  and is independent of  $n$ . The index  $N_1$  depends on  $\sigma(\omega)$ ,  $\varepsilon$  and  $\xi_1$ . All in all, we obtain

$$\left\| h_n^{(1)}(\omega\gamma(\xi(\cdot))) Y_n^0(\hat{\mathbf{x}}(\cdot)) \right\|_{H^1(\Omega)}^2 \geq \frac{(1 - \varepsilon)^3 C_1 ((2n - 1)!)^2}{|\omega|^{2n+2} |\gamma(\xi_0)|^{2n+3} \sqrt{n+1}} \quad (5.13)$$

for  $n > N_1$ .

Let  $\xi \neq \xi_0$ . Then we can find an index  $N_2 \in \mathbb{N}$  such that for all  $n > N_2$

$$\begin{aligned} |s_n(\mathbf{x}(\xi, \hat{\mathbf{x}}))| &\leq \frac{(1 + \varepsilon)(2n - 1)!! |\omega|^{n+1} |\gamma(\xi_0)|^{n+3/2} (n + 1)^{1/4}}{|\omega\gamma(\xi)|^{n+1} (1 - \varepsilon)^{3/2} \sqrt{C_1} (2n - 1)!!} \sup_{\hat{\mathbf{x}} \in \Gamma} |Y_n^0(\hat{\mathbf{x}})| \\ &\leq C_2 \left| \frac{\gamma(\xi_0)}{\gamma(\xi)} \right|^{n+1} \sqrt{2n+1} (n+1)^{1/4}, \end{aligned}$$

since  $|Y_n^0|$  is bounded by  $\sqrt{2n+1}$  (Proposition A.6). Again, we put all the factors independent of  $n$  in the constant  $C_2 = \frac{(1+\varepsilon)}{(1-\varepsilon)^{3/2}} \frac{|\gamma(\xi_0)|^{1/2}}{\sqrt{C_1}} > 0$  depending on  $\varepsilon$  and  $\sigma(\omega)$  and independent of  $n$ .

Since  $\left| \frac{\gamma(\xi_0)}{\gamma(\xi)} \right| < 1$ , this gives

$$\lim_{n \rightarrow \infty} |s_n(\mathbf{x})| = 0$$

for all  $\mathbf{x} \in \Omega$  such that  $\|\mathbf{x}\| \neq 1 + \xi_0$ . Using the second part of 5.16 we find

$$\begin{aligned} \|A_\sigma(\omega) s_n\|_{H^1(\Omega)} &= \frac{\left\| A_\sigma(\omega) \left( h_n^{(1)}(\omega\gamma(\xi(\cdot))) Y_n^0(\hat{\mathbf{x}}(\cdot)) \right) \right\|_{H^1(\Omega)}}{\left\| h_n^{(1)}(\omega\gamma(\xi(\cdot))) Y_n^0(\hat{\mathbf{x}}(\cdot)) \right\|_{H^1(\Omega)}} \\ &\leq c \frac{\left| \omega \left( h_n^{(1)} \right)'(\omega) \right|}{\left\| h_n^{(1)}(\omega\gamma(\xi(\cdot))) Y_n^0(\hat{\mathbf{x}}(\cdot)) \right\|_{H^1(\Omega)}} \end{aligned}$$

for some  $c > 0$  independent of  $n$ . Using the asymptotic behavior of  $\left( h_n^{(1)} \right)'$  and the lower bound of the norm in the denominator (5.13) we obtain

$$\begin{aligned} \|A_\sigma(\omega) s_n\|_{H^1(\Omega)} &\leq c \left| (1 + \varepsilon) \frac{(2n - 1)!! (n + 1) \omega \omega^{n+1} \gamma(\xi_0)^{n+3/2} (n + 1)^{1/4}}{i \omega^{n+2} (1 - \varepsilon)^{3/2} \sqrt{C_1} (2n - 1)!!} \right| \\ &= \frac{c(1 + \varepsilon)}{(1 - \varepsilon)^{3/2} \sqrt{C_1}} |\gamma(\xi_0)|^{n+3/2} (n + 1)^{3/4} \end{aligned}$$

for large  $n$ .

Because of  $|\gamma(\xi_0)| < |\gamma(0)| = 1$  this shows that

$$\lim_{n \rightarrow \infty} \|A_\sigma(\omega) s_n\|_{H^1(\Omega)} = 0.$$

To show that there exists no converging subsequence of  $s_n$ , let  $s_{n_k}$  be an arbitrary subsequence. Then  $s_{n_k}$  converges to zero pointwise almost everywhere. Thus, the only possible limit would be the zero function. This cannot be the case since  $\|s_{n_k}\|_{H^1(\Omega)} = 1$ .  $\square$



### Adding an interior domain

Until now, we have proven the existence of an essential spectrum for frequencies  $\omega$  such that  $\operatorname{Re}(\sigma(\omega)) < 0$  for the domain  $\Omega = \overline{B_1}^c$ . The situation is a little different when we add an interior domain  $\Omega_{\text{int}} = B_1 \setminus \overline{B_R}$  for some  $0 < R < 1$ .

In this case the eigenfunctions of  $A_\sigma$  can be constructed similarly to Lemma 5.16.

**Lemma 5.20.** *Let  $0 < R < 1$ ,  $\Omega = \overline{B_R}^c$ ,  $\Gamma = \partial B_1$ ,  $\Omega_{\text{int}} = \Omega \cap B_1$ , and  $\Omega_{\text{ext}} = \overline{B_1}^c$ . Moreover, let  $\sigma : \Lambda \subset \mathbb{C} \rightarrow \mathbb{C} \setminus \{0\}$  and  $A_\sigma$  be as in (5.6). Then, for fixed  $\omega \in \Lambda$  and  $n \in \mathbb{N}_0$ ,  $m \in \mathbb{Z}$  such that  $|m| \leq n$ , we define a function*

$$u_{n,m}(\mathbf{x}) := h_n^{(1)}(\omega\gamma(\xi(\mathbf{x}))) Y_n^m(\hat{\mathbf{x}}(\mathbf{x})),$$

where

$$\gamma : \begin{cases} \mathbb{R}_{\geq R-1} & \rightarrow \mathbb{C}, \\ \xi & \mapsto \begin{cases} 1 + \xi, & \xi < 0, \\ 1 + \sigma(\omega)\xi, & \xi \geq 0. \end{cases} \end{cases} \quad (5.14)$$

Then  $u_{n,m} \in H^1(\Omega)$  if and only if  $\operatorname{Im}(\omega\sigma) > 0$  and  $\sigma(\omega) \notin \mathbb{R}_{<0}$ . In this case

$$a_\sigma(\omega)(u_{n,m}, g) = (A_{\sigma,\omega} u_{n,m}, g)_{H^1(\Omega)} = -\omega \left( h_n^{(1)} \right)'(R\omega) \int_{\Gamma} Y_n^m(\hat{\mathbf{x}}) g(\hat{\mathbf{x}}) d\hat{\mathbf{x}}$$

for all  $g \in H^1(\Omega) \cap C(\overline{\Omega})$  and there exists a constant  $c > 0$  independent of  $n, m, \sigma, \omega$  such that

$$\|A_\sigma(\omega) u_{n,m}\|_{H^1(\Omega)} \leq c \left| \omega \left( h_n^{(1)} \right)'(R\omega) \right|.$$

*Proof.* After a transformation into polar coordinates of the interior part of  $a_\sigma(\omega)$ , the proof works exactly along the lines of the proof of Lemma 5.16.  $\square$

In this case the same construction as before will only lead to a singular sequence if the peaks of  $h_n(\omega\gamma(\cdot))$  dominate the behavior of  $h_n'(\omega R)$ . This is quantified by the following lemma:

**Lemma 5.21.** *Let  $0 < R < 1$ ,  $\sigma \in \{z \in \mathbb{C} \setminus \{0\} : \arg z \in (\pi - \sin^{-1}(R), \pi + \sin^{-1}(R))\}$  and  $\gamma$  as in (5.14). Then the function  $|\gamma(\cdot)|^2$  takes its global minimum  $m := \sin(\arg(\sigma))^2$  at  $\xi_0 := -\frac{\operatorname{Re}(\sigma)}{|\sigma|^2}$  (see Figure 5.3).*

*Proof.* By Lemma 5.17, the global minimum of  $|\gamma|^2 \Big|_{\mathbb{R}_{\geq 0}}$  is  $\sin(\arg(\sigma))^2$  at the point  $\xi_0 = -\frac{\operatorname{Re}(\sigma)}{|\sigma|^2}$ . For  $\xi \in [R-1, 0]$ , we have

$$|\gamma(\xi)|^2 = (1 + \xi)^2 \geq R^2 = \sin(\pi \pm \sin^{-1}(R))^2 > \sin(\arg(\sigma))^2.$$

$\square$

**Theorem 5.22.** *Let  $0 < R < 1$ ,  $\Omega = \overline{B_R^c}$ ,  $\Gamma = \partial B_1$ ,  $\Omega_{\text{int}} = \Omega \cap B_1$ ,  $\Omega_{\text{ext}} = \overline{B_1^c}$ ,  $\sigma : \Lambda \subset \mathbb{C} \rightarrow \mathbb{C} \setminus \{0\}$ , and  $A_\sigma$  be as in (5.6). Moreover, let  $\omega \in \Lambda$  such that*

$$\arg(\sigma(\omega)) \in (\pi - \sin^{-1}(R), \pi) \cup (\pi, \pi + \sin^{-1}(R))$$

and  $\text{Im}(\omega\sigma(\omega)) > 0$ . Then we have  $\omega \in \Sigma_e(A_\sigma(\cdot))$ .

*Proof.* The singular sequence can be defined exactly as in Theorem 5.19 with extended domain to  $\Omega_{\text{int}}$ . The proof works accordingly, where we use Lemma 5.20 instead of Lemma 5.16.  $\square$

*Remark 5.23.* In Theorems 5.19 and 5.22 we assumed  $\text{Im}(\sigma(\omega)\omega) > 0$  to obtain that the functions  $h_n^{(1)}(\omega\gamma(\cdot))$  are exponentially decreasing and to use them for the construction of the singular sequence. The same line of proof can be repeated for  $\text{Im}(\sigma(\omega)\omega) < 0$  and the spherical Hankel functions of the second kind.

Moreover, we excluded the case  $\sigma(\omega) \in \mathbb{R}_{\leq 0}$  to avoid having to deal with complex-scaled eigenfunctions with a singularity. Nevertheless, for continuous scaling functions  $\sigma : \Lambda \rightarrow \mathbb{C} \setminus \{0\}$ , the set  $\{\omega \in \Lambda : \sigma(\omega) \in \mathbb{R}_{\leq 0}\}$  is always part of the essential spectrum  $\Sigma_e$  since  $\Sigma_e$  is a closed set (see Remark 5.13).

An alternative way to prove this is to construct a singular sequence for  $\sigma(\omega) \in \mathbb{R}_{< 0}$ , by approximating the function  $u_n$  given in  $\Omega_{\text{ext}}$  by

$$u_n := h_n^{(1)}(\omega\gamma(\xi(\cdot))) Y_n^0(\hat{\mathbf{x}}(\cdot)),$$

which is not regular, by an appropriate sequence of  $H^1(\Omega)$  functions.

A similar line of proof for as in Theorems 5.19 and 5.22 works for a domain  $\Omega$  such that  $B_R \subset \Omega^c$  and potential functions  $\rho$  that vanish on  $B_R^c$ . Note, however, that the essential spectrum could, in theory, be larger for problems with an interior domain. In any case the essential spectrum  $\Sigma_{\text{sing}}$  is always a subset of  $\{\omega \in \Lambda : \text{Re}(\sigma(\omega)) \leq 0\}$  since otherwise the corresponding operator function is Fredholm. By the reasoning from Remark 5.23, on the other hand,  $\Sigma_{\text{sing}}$  always contains the set  $\{\omega \in \Lambda : \sigma(\omega) \in \mathbb{R}_{< 0}\}$ .

### 5.3.2. The set $\Sigma_{\text{dec}}$

In this section we construct a singular sequence for  $\omega \in \Lambda$  such that  $\text{Im}(\sigma(\omega)\omega) = 0$  and therefore show that  $A_\sigma(\omega)$  is not Fredholm at the boundary of the domain where (S2) is fulfilled. Contrary to Section 5.3.1 we consider general domains of the form (5.1). The theorem below and its proof are basically a special case of [Hal19, Theorem 4.6]. Nevertheless, we rephrase the proof for the sake of completeness and due to the fact that we consider merely the case of linear complex scalings.

**Theorem 5.24.** *Let  $\sigma : \Lambda \subset \mathbb{C} \rightarrow \mathbb{C} \setminus \{0\}$ ,  $A_\sigma$  as in (5.6), and  $\omega \in \Lambda$  such that  $\text{Im}(\sigma(\omega)\omega) = 0$  and  $\sigma(\omega) \notin \mathbb{R}_{< 0}$ . Then  $\omega \in \Sigma_{\text{dec}}(A_\sigma)$ .*

*Proof.* We pick a smooth cut-off function  $\zeta : \mathbb{R} \rightarrow \mathbb{R}$  such that  $\text{supp}(\zeta) \subset [-1, 1]$ ,  $\zeta(x) \in [0, 1]$  for  $x \in \mathbb{R}$ , and  $\zeta(x) = 1$  for  $x \in (-\frac{1}{2}, \frac{1}{2})$ . Such a function can be constructed, for

instance, by using mollifiers (e.g., [Eva10, Appendix C.4]). Moreover, we define

$$\zeta_n(\xi) := \zeta\left(\frac{\xi - n^2}{n}\right), \quad u_0(\xi) := h_0^{(1)}(\omega\gamma(\xi)),$$

where we used the notation  $\gamma(\xi) = 1 + \sigma(\omega)\xi$ . The functions  $\zeta_n$  fulfill

$$\text{supp}(\zeta_n) = [n^2 - n, n^2 + n]$$

and  $\zeta_n(\xi) = 1$  for  $\xi \in [n^2 - n/2, n^2 + n/2]$ . Now we define the elements of our singular sequence  $s_n \in H^1(\Omega)$  by

$$s_n(\mathbf{x}) := \begin{cases} 0, & \mathbf{x} \in \Omega_{\text{int}} \cup \Gamma, \\ \frac{\zeta_n(\xi(\mathbf{x}))u_0(\xi(\mathbf{x}))}{\|\zeta_n(\xi(\cdot))u_0(\xi(\cdot))\|_{H^1(\Omega_{\text{ext}})}}, & \mathbf{x} \in \Omega_{\text{ext}} \end{cases} \quad (5.15)$$

for  $n \in \mathbb{N}$ .

We can bound the  $H^1(\Omega)$ -norm in the denominator of (5.15) from below by

$$\begin{aligned} \|\zeta_n(\xi(\cdot))u_0(\xi(\cdot))\|_{H^1(\Omega_{\text{ext}})}^2 &\geq \|\zeta_n(\xi(\cdot))u_0(\xi(\cdot))\|_{L^2(\Omega)}^2 \\ &= \int_{\mathbb{R}_{>0} \times \Gamma} (1 + \xi)^2 |\zeta_n(\xi)u_0(\xi)|^2 d(\xi, \hat{\mathbf{x}}) \\ &= \frac{4\pi}{3} \int_0^\infty (1 + \xi)^2 |\zeta_n(\xi)u_0(\xi)|^2 d\xi. \end{aligned}$$

Because of  $\zeta_n(\xi) = \zeta\left(\frac{\xi - n^2}{n}\right) = 1$  for  $\xi \in (n^2 - \frac{n}{2}, n^2 + \frac{n}{2})$  and  $h_0^{(1)}(z) = \frac{\exp(iz)}{iz}$ , we can continue to calculate

$$\begin{aligned} \|\zeta_n(\xi(\cdot))u_0(\xi(\cdot))\|_{H^1(\Omega_{\text{ext}})}^2 &\geq \frac{4\pi}{3} \int_{n^2 - n/2}^{n^2 + n/2} (1 + \xi)^2 \left| \frac{\exp(i\omega\gamma(\xi))}{i\omega\gamma(\xi)} \right|^2 d\xi \\ &= \frac{4\pi \exp(\text{Re}(i\omega))^2}{3|\omega|^2} \int_{n^2 - n/2}^{n^2 + n/2} \left| \frac{1 + \xi}{1 + \sigma(\omega)\xi} \right|^2 d\xi, \end{aligned}$$

since

$$|\exp(i\omega\sigma(\omega)\xi)| = |\exp(-\text{Im}(\sigma(\omega)\omega)\xi)| = 1$$

for all  $\xi \in \mathbb{R}_{>0}$  by assumption. Because of

$$\lim_{\xi \rightarrow \infty} \frac{1 + \xi}{1 + \sigma(\omega)\xi} = \frac{1}{\sigma(\omega)},$$

we can find an index  $N \in \mathbb{N}$  such that

$$\left| \frac{1 + \xi}{1 + \sigma(\omega)\xi} \right|^2 \geq \frac{1}{2|\sigma(\omega)|^2}$$

for all  $\xi > n^2 - \frac{n}{2}$  and  $n > N$ . All in all we have

$$\|\zeta_n(\xi(\cdot))u_0(\xi(\cdot))\|_{H^1(\Omega_{\text{ext}})} \geq C\sqrt{n},$$

with  $C = \sqrt{\frac{2\pi}{3} \frac{\exp(\operatorname{Re}(i\omega))}{|\sigma(\omega)\omega|}}$  for all  $n > N$ .

For any test function  $g \in H^1(\Omega)$ , we have for  $n > N$  (see (5.5))

$$\begin{aligned} C\sqrt{n} |a_\sigma(\omega)(s_n, g)| &\leq \left| \int_{\mathbb{R}_{>0} \times \Gamma} \frac{\gamma(\xi)^2}{\sigma(\omega)} \frac{\partial}{\partial \xi} (\zeta_n(\xi) u_0(\xi)) \frac{\partial}{\partial \xi} \overline{g \circ \Psi(\xi, \hat{\mathbf{x}})} d(\xi, \hat{\mathbf{x}}) \right. \\ &\quad \left. - \omega^2 \sigma(\omega)^3 \int_{\mathbb{R}_{>0} \times \Gamma} \gamma(\xi)^2 \zeta_n(\xi) u_0(\xi) \overline{g \circ \Psi(\xi, \hat{\mathbf{x}})} d(\xi, \hat{\mathbf{x}}) \right| \\ &\leq |a_\sigma(\omega)(u_0(\xi(\cdot)), \zeta_n(\xi(\cdot)) g)| \\ &\quad + \frac{1}{|\sigma(\omega)|} \underbrace{\int_{\mathbb{R}_{>0} \times \Gamma} \left| \gamma(\xi)^2 \zeta_n'(\xi) u_0(\xi) \frac{\partial}{\partial \xi} \overline{g \circ \Psi(\xi, \hat{\mathbf{x}})} \right| d(\xi, \hat{\mathbf{x}})}_{= (*)} \\ &\quad + \frac{1}{|\sigma(\omega)|} \underbrace{\int_{\mathbb{R}_{>0} \times \Gamma} \left| \gamma(\xi)^2 \zeta_n'(\xi) u_0'(\xi) \overline{g \circ \Psi(\xi, \hat{\mathbf{x}})} \right| d(\xi, \hat{\mathbf{x}})}_{= (**)}, \end{aligned}$$

where we extended the functions  $\zeta_n(\xi(\cdot))$ ,  $u_0(\xi(\cdot))$  to  $\Omega_{\text{int}}$  by zero and  $u_0(0)$  respectively and used

$$\begin{aligned} \frac{\partial}{\partial \xi} (u_0(\xi) \zeta_n(\xi)) \frac{\partial}{\partial \xi} \overline{g \circ \Psi(\xi, \hat{\mathbf{x}})} &= u_0'(\xi) \frac{\partial}{\partial \xi} (\zeta_n(\xi) \overline{g \circ \Psi(\xi, \hat{\mathbf{x}})}) \\ &\quad - u_0'(\xi) \zeta_n'(\xi) \overline{g \circ \Psi(\xi, \hat{\mathbf{x}})} + u_0(\xi) \zeta_n'(\xi) \frac{\partial}{\partial \xi} \overline{g \circ \Psi(\xi, \hat{\mathbf{x}})}. \end{aligned}$$

Note that  $a_\sigma(\omega)(u_0(\xi(\cdot)), \zeta_n(\xi(\cdot)) g) = 0$  for  $n > 1$  (Lemma 5.16, where we use the fact that  $\operatorname{tr}_\Gamma(\zeta_n(\xi(\cdot)) g) = 0$ ).

Using a constant  $D > 0$  such that

$$\left| \frac{1 + \sigma(\omega) \xi}{1 + \xi} \right|^2 < D$$

for all  $\xi \geq 0$ , the terms (\*) and (\*\*) can be bounded by

$$\begin{aligned} (*) &\leq D \left( \zeta_n'(\xi(\cdot)) u_0(\xi(\cdot)), \left( \frac{\partial}{\partial \xi} g \circ \Psi \right) (\xi(\cdot), \hat{\mathbf{x}}(\cdot)) \right)_{L^2(\Omega)} \\ &\leq D \left\| \zeta_n'(\xi(\cdot)) u_0(\xi(\cdot)) \right\|_{L^2(\Omega)} \left\| \frac{\partial}{\partial \xi} g \circ \Psi \right\|_{L^2(\Omega)}, \\ (** ) &\leq D \left( \zeta_n'(\xi(\cdot)) u_0'(\xi(\cdot)), g \right)_{L^2(\Omega)} \\ &\leq D \left\| \zeta_n'(\xi(\cdot)) u_0'(\xi(\cdot)) \right\|_{L^2(\Omega)} \|g\|_{L^2(\Omega)}. \end{aligned}$$

Due to fact that

$$\zeta_n'(\xi) = \frac{1}{n} \zeta' \left( \frac{\xi - n^2}{n} \right),$$

we can bound

$$\|\zeta'_n(\xi(\cdot)) u_0(\xi(\cdot))\|_{L^2(\Omega)}^2 \leq \frac{4\pi}{3n} \|\zeta'\|_{L^\infty(-1,1)}^2 \int_{n^2-n}^{n^2+n} (1+\xi)^2 \left| \frac{\exp(i\omega\gamma(\xi))}{i\omega\gamma(\xi)} \right|^2 d\xi \leq E$$

for some constant  $E > 0$  independent of  $n$  and  $n$  large enough. The term containing

$$u'_0(\xi) = \left( \frac{\exp(i\omega\gamma(\xi))}{i\omega\gamma(\xi)} \right)' = i\omega\sigma(\omega) \exp(i\omega\gamma(\xi)) \left( \frac{i\omega\gamma(\xi) - 1}{(i\omega\gamma(\xi))^2} \right)$$

can be bounded similarly. Collecting all the terms, we obtain

$$|a_\sigma(\omega)(s_n, g)| \leq \frac{F}{\sqrt{n}} \|g\|_{H^1(\Omega)}$$

for  $n$  large enough and some constant  $F > 0$  and therefore

$$\lim_{n \rightarrow \infty} \|A_\sigma(\omega) s_n\|_{H^1(\Omega)} = 0.$$

The sequence  $s_n$  has no convergent subsequence since  $\text{supp } s_n \cap \text{supp } s_m = \emptyset$  for  $n \neq m$ .  $\square$

## 5.4. Discussion of the analysis

We have seen in Theorems 5.4 and 5.5 and Remark 5.11 that in the region of frequencies where the operator function  $A_\sigma$  is Fredholm, we have a one-to-one correspondence of eigenpairs of the complex-scaled weak formulation (Problem 5.3) and the strong formulation (Problem 2.3). Moreover, we can apply the approximation theory of weakly  $T$ -coercive operator functions to obtain spectral convergence of Galerkin discretizations of the complex-scaled weak formulation. This allows us to approximate eigenvalues and eigenfunctions of the Helmholtz resonance problem.

For other regions we have constructed singular sequences and, therefore, we have shown that the operator function is not Fredholm there. In these regions we expect the discretized problem to exhibit a discretization of the essential spectrum (cf. Remark 5.15).

Note, however, that our analysis is only complete for the case where  $\Omega = \overline{B_1^c}$  and  $\Gamma = S_1$ . In this case, for a scaling function  $\sigma : \Lambda \rightarrow \mathbb{C} \setminus \{0\}$ , we can decompose  $\Lambda$  into the disjoint sets

$$\Lambda = \Xi^+ \cup \Xi^- \cup \Sigma_e,$$

with

$$\Sigma_e = \Sigma_{\text{sing}} \cup \Sigma_{\text{dec}}, \quad \Sigma_{\text{sing}} = \{\omega \in \Lambda : \sigma(\omega) \in \mathbb{C}_{\text{Re} \leq 0}\}, \quad \Sigma_{\text{dec}} = \{\omega \in \Lambda : \omega\sigma(\omega) \in \mathbb{R}\},$$

and

$$\begin{aligned} \Xi^+ &= \{\omega \in \Lambda : \sigma(\omega) \in \mathbb{C}_{\text{Re} > 0}, \text{Im}(\omega\sigma(\omega)) > 0\}, \\ \Xi^- &= \{\omega \in \Lambda : \sigma(\omega) \in \mathbb{C}_{\text{Re} > 0}, \text{Im}(\omega\sigma(\omega)) < 0\}. \end{aligned} \tag{5.16}$$

Here  $\Xi^+$  and  $\Xi^-$  denote the sets where we can expect approximations to radiating and non-radiating resonances respectively (cf. Remarks 3.15 and 3.16).

For the case where we add an interior domain  $\Omega_{\text{int}} = \overline{B_R^c} \cap B_1$  for some  $0 < R < 1$ , we showed that

$$\{\omega \in \Lambda : \arg(\sigma(\omega)) \in [\pi - \sin^{-1}(R), \pi + \sin^{-1}(R)]\} \subset \Sigma_e,$$

which is smaller than the corresponding set in the previous case. The set  $\Sigma_{\text{dec}}$  remains unchanged. Note that these sets correspond exactly to the sets where the conditions (S1) and (S2) are violated. However, for a comprehensive analysis of this case it still remains to show Fredholmness of the operator functions in question for  $\omega \in \Lambda$  such that  $\arg(\sigma(\omega)) \in [\frac{\pi}{2}, \pi - \sin^{-1}(R)) \cup (\pi + \sin^{-1}(R), \frac{3\pi}{2}]$ .

For more general interior domains we will see in our numerical experiments in Chapter 9 that, for examples with a general interior domain, similar to the case of the interior domain with the cut-out sphere, we may expect a larger region where resonances are approximated than the one given in (5.16).

## 6. Discretization

In this chapter we define and analyze the discretization of the complex-scaled Helmholtz resonance problems (Problem 5.3 and Section 7.1) by the use of complex-scaled infinite elements. To this end we closely follow [NW19, Sections 4 and 5]. Since the frequency-dependency  $\sigma$  of the scaling function does not affect the discretization, we omit the frequency-dependency and write  $\sigma = \sigma(\omega)$  for this entire chapter.

We assume that the exterior part of the sesquilinear form  $a_\sigma(\omega)$  (cf. Definition 5.1), corresponding to the weak formulation of the complex-scaled equation, can be decomposed into generalized-radial and tangential parts in the following sense: For functions  $f, g \in H^1(\Omega)$  that can be written as products of a generalized-radial and a tangential part in  $\Omega_{\text{ext}}$ , namely,

$$f \circ \Psi(\xi, \hat{\mathbf{x}}) = \tilde{f}(\xi) \hat{f}(\hat{\mathbf{x}}), \quad g \circ \Psi(\xi, \hat{\mathbf{x}}) = \tilde{g}(\xi) \hat{g}(\hat{\mathbf{x}})$$

for  $\xi \in \mathbb{R}_{>0}$ ,  $\hat{\mathbf{x}} \in \Gamma$  and some functions  $\tilde{f}, \tilde{g} : \mathbb{R}_{>0} \rightarrow \mathbb{C}$  and  $\hat{f}, \hat{g} : \Gamma \rightarrow \mathbb{C}$ , we assume that

$$\begin{aligned}
 a_{\text{ext}}(\omega)(f, g) &:= a_\sigma(\omega)(f, g) - \int_{\Omega_{\text{int}}} \nabla f(\mathbf{x}) \cdot \overline{\nabla g(\mathbf{x})} \, d\mathbf{x} + \omega^2 \int_{\Omega_{\text{int}}} (1 + \rho(\mathbf{x}))^2 f(\mathbf{x}) \overline{g(\mathbf{x})} \, d\mathbf{x} \\
 &= \sum_{j=0}^J \tilde{a}_j(\tilde{f}, \tilde{g}) \hat{a}_j(\hat{f}, \hat{g})
 \end{aligned} \tag{6.1}$$

for some  $J \in \mathbb{N}_0$  and some sesquilinear form  $\tilde{a}_j, \hat{a}_j$  that act on functions  $\mathbb{R}_{>0} \rightarrow \mathbb{C}$  and  $\Gamma \rightarrow \mathbb{C}$  respectively. For the case that  $\Omega_{\text{ext}}$  is the complement of a sphere, the sesquilinear form  $a_\sigma(\omega)$  from Definition 5.1 allows such a decomposition. For more general cases we refer to Section 7.1. Additionally, we assume that a similar decomposition is possible for the  $L^2(\Omega_{\text{ext}})$  and  $H^1(\Omega_{\text{ext}})$ -inner products and norms in the respective exterior coordinates.

### 6.1. Galerkin methods

The finite element method belongs to the class of Galerkin methods. In the following we give a short introduction to these methods. We refer to [Cia02] for an introduction to the finite element method for elliptic problems and to [Ihl98] for the finite element method for scattering problems.

For the resonance problem to

$$\text{find } \omega \in \Lambda, f \in X \setminus \{0\} \text{ such that } A(\omega) f = 0$$

for a given operator function  $A : \Lambda \subset \mathbb{C} \rightarrow \mathcal{B}(X)$  on a Hilbert space  $X$ , the idea of Galerkin methods is to pick a finite-dimensional subspace  $X_h \subset X$  and consider the discrete problem to

$$\text{find } \omega \in \Lambda, f_h \in X_h \setminus \{0\} \text{ such that } \Pi_h A(\omega) f_h = 0. \quad (6.2)$$

Here  $\Pi_h : X \rightarrow X_h$  denotes the orthogonal projection. In the case where the operator function  $A$  is induced by a sesquilinear form valued function  $a$  via the Riesz representation theorem, the discrete problem (6.2) can be shown to be equivalent to the problem to

$$\text{find } \omega \in \Lambda, f_h \in X_h \setminus \{0\} \text{ such that } a(\omega)(f_h, g_h) = 0 \text{ for all } g_h \in X_h. \quad (6.3)$$

For a given basis  $B = \{b_0, \dots, b_N\}$  of  $X_h$ , any vector  $f_h \in X_h$  can be uniquely written as

$$f_h = \sum_{j=0}^N c_j b_j$$

for some coefficients  $c_0, \dots, c_N \in \mathbb{C}$ . Again, the discrete problems (6.2) and (6.3) are equivalent to the problem to

$$\text{find } \omega \in \Lambda \text{ and a vector } \mathbf{c} = (c_0, \dots, c_N)^\top \neq \mathbf{0} \text{ such that } \mathbf{M}(\omega) \mathbf{c} = \mathbf{0}. \quad (6.4)$$

Here  $\mathbf{M} = (\mathbf{M}_{i,j})_{i,j=0,\dots,N}$  is the matrix valued function with

$$\mathbf{M}_{i,j}(\omega) := a(\omega)(b_j, b_i)$$

for all  $\omega \in \Lambda$ .

Thus, for the application of a Galerkin method, an appropriate subspace  $X_h$  and a suitable basis  $b_0, \dots, b_N$  have to be defined. Subsequently, the resulting matrix eigenvalue problem (6.4) has to be solved using an appropriate algorithm (see Chapter 8).

By assumption (6.1) the resonance problem in  $\Omega_{\text{ext}}$  is already formulated in exterior coordinates  $(\xi, \hat{\mathbf{x}}) \in \mathbb{R}_{>0} \times \Gamma$ . Thus, in the exterior domain we use discrete tensor product spaces which are composed of finite-dimensional subspaces  $\tilde{\mathcal{X}} \subset H^1(\mathbb{R}_{>0})$  and  $\hat{\mathcal{X}} \subset H^1(\Gamma)$ . For discretizing the problem in the interior domain we use standard  $H^1$ -conforming, high order finite element spaces.

Since most of the available algorithms for solving matrix eigenvalue problems are based on the evaluation (and inversion) of the matrix function at one or more frequencies, we have to be able to assemble the matrix  $\mathbf{M}(\omega_0)$  for a given frequency  $\omega_0 \in \Lambda$ . It is one of the core ideas of the finite element method to choose the basis in a way that the resulting matrices are sparse (i.e., have few non-zero entries). Naturally, we want to choose subspaces that also exhibit this quality. Moreover, it is evident that the subspaces should approximate the eigenfunctions well. All of these requirements for our subspaces and basis functions are summarized in (R1–6).

## 6.2. Discretization and coupling

In this section we give a general outline on how we define our discretization without explicitly specifying the discrete bases and spaces. The radial bases and spaces will be defined in Section 6.3.



### 6.2.1. Interior discretization

For discretizing the problem in the interior domain  $\Omega_{\text{int}}$ , basically, any discrete space

$$\mathcal{X}_{\text{int}} = \text{span}\{b_j : j = 0, \dots, L\} \subset H^1(\Omega_{\text{int}})$$

such that  $\mathcal{X}_{\text{int}}|_{\Gamma} := \{\text{tr}_{\Gamma} f : f \in \mathcal{X}_{\text{int}}\} \subset H^1(\Gamma)$  can be used. The trace space of this interior discrete space is then used for the interface discretization, namely,

$$\hat{\mathcal{X}}_M := \mathcal{X}_{\text{int}}|_{\Gamma} = \text{span}\{\text{tr}_{\Gamma} b_j : j = 0, \dots, L\} \subset H^1(\Gamma). \quad (6.5)$$

A basis of  $\hat{\mathcal{X}}_M$  is given by  $\hat{B}_M := \{\text{tr}_{\Gamma} b_{j(0)}, \dots, \text{tr}_{\Gamma} b_{j(M)}\}$ , where the functions  $j(\cdot)$  choose a subset of all the traces such that the elements of  $\hat{B}_M$  are linearly independent and span the space  $\hat{\mathcal{X}}_M$ .

*Remark 6.1.* An obvious choice for  $\mathcal{X}_{\text{int}}$  is a standard high-order conforming finite element space. Since in this case all of the basis functions corresponding to inner nodes in  $\Omega_{\text{int}}$  have vanishing traces on the interface  $\Gamma$ , we expect the dimension of  $\hat{\mathcal{X}}_M$  to be considerably smaller than the dimension of  $\mathcal{X}_{\text{int}}$ .

Note that the definition of high-order finite element spaces for arbitrary surfaces  $\Gamma$  is not straightforward. For the construction of surface finite elements we refer to [DE13]. Commonly, for instance, a piecewise polynomial approximation  $\Gamma_h$  of  $\Gamma$  is considered. Nevertheless, if  $\Gamma_h$  fulfills the assumptions on the interface from Definition 3.1, we can simply work with  $\Gamma_h$ .

### 6.2.2. Exterior discretization by tensor product spaces

Let  $N \in \mathbb{N}_0$  and

$$\tilde{B}_N := \{\phi_n : n = 0, \dots, N\} \subset \{f : \mathbb{R}_{>0} \rightarrow \mathbb{C} : f(\xi(\cdot)) \in H^1(\Omega_{\text{ext}})\}$$

be a family of linearly independent functions and

$$\tilde{\mathcal{X}}_N := \text{span}(\tilde{B}_N)$$

the discrete space spanned by  $\tilde{B}_N$ . To discretize the exterior problem, we use a tensor product basis and space of the form

$$\begin{aligned} \tilde{\mathcal{X}}_N \otimes \hat{\mathcal{X}}_M &:= \text{span}(\tilde{B}_N \otimes \hat{B}_M), \\ \tilde{B}_N \otimes \hat{B}_M &:= \{\phi \otimes b := (\xi, \hat{\mathbf{x}}) \mapsto \phi(\xi) b(\hat{\mathbf{x}}) : \phi \in \tilde{B}_N, b \in \hat{B}_M\}, \end{aligned}$$

where  $\hat{\mathcal{X}}_M$  is the trace space of the interior space defined in (6.5).

It is easy to check that for a function  $g \in \tilde{\mathcal{X}}_N \otimes \hat{\mathcal{X}}_M$ , the function  $g \circ \Psi^{-1}$  is an element of  $H^1(\Omega_{\text{ext}})$ . Thus, we can define

$$\mathcal{X}_{N,M} := \left\{ g \circ \Psi^{-1} : g \in \tilde{\mathcal{X}}_N \otimes \hat{\mathcal{X}}_M \right\}.$$

### 6.2.3. Coupling the interior and the exterior problem

Since we want to create a conforming discrete space for the whole problem on  $\Omega$ , we need to couple our interior and exterior discrete spaces in a manner that the resulting space is equivalent to a subspace of  $H^1(\Omega)$ . We achieve this by using

$$\mathcal{X}_{\mathcal{N}} := \{f \in H^1(\Omega) : f|_{\Omega_{\text{int}}} \in \mathcal{X}_{\text{int}}, f|_{\Omega_{\text{ext}}} \in \mathcal{X}_{N,M}, \text{tr}_{\Gamma}(f|_{\Omega_{\text{int}}}) = \text{tr}_{\Gamma}(f|_{\Omega_{\text{ext}}})\},$$

with  $\mathcal{X}_{N,M}$  and  $\mathcal{X}_{\text{int}}$  as in Sections 6.2.2 and 6.2.1 respectively. To obtain a basis of  $\mathcal{X}_{\mathcal{N}}$  we have to couple the basis functions in a way that the resulting functions are continuous at the interface  $\Gamma$ . Under the assumption that the radial basis functions  $\phi_n$  are continuous with  $\phi_0(0) = 1$  and  $\phi_n(0) = 0$  for all  $n \in \mathbb{N}$ , this can be done as follows: Let  $b_j$  be an interior basis function with non-vanishing trace on  $\Gamma$ . Then  $\phi_0 \otimes \text{tr}_{\Gamma} b_j$  is also an element of  $\mathcal{X}_{N,M}$  and the function

$$\begin{cases} \Omega & \rightarrow \mathbb{C}, \\ \mathbf{x} & \mapsto \begin{cases} b_j(\mathbf{x}), & \mathbf{x} \in \Omega_{\text{int}} \cup \Gamma, \\ b_j(\hat{\mathbf{x}}(\mathbf{x})) \phi_0(\xi(\mathbf{x})), & \mathbf{x} \in \Omega_{\text{ext}}, \end{cases} \end{cases}$$

is continuous on  $\Omega$  and an element of  $\mathcal{X}_{\mathcal{N}}$ . Identifying the corresponding basis functions in this way results in a basis of the discrete space  $\mathcal{X}_{\mathcal{N}}$ . If there exist multiple basis functions of the radial space with non-vanishing trace at 0, we have to add more basis functions or use a non-conforming method.

### 6.3. Radial discretization

Our goal in this section is to construct a suitable finite basis  $\tilde{B}_N = \{\phi_j : j = 0, \dots, N\} \subset \{f : \mathbb{R}_{>0} \rightarrow \mathbb{C} : f(\xi(\cdot)) \in H^1(\Omega_{\text{ext}})\}$  and the according suitable finite-dimensional space

$$\tilde{\mathcal{X}}_N = \text{span}(\tilde{B}_N) \subset \{f : \mathbb{R}_{>0} \rightarrow \mathbb{C} : f(\xi(\cdot)) \in H^1(\Omega_{\text{ext}})\}.$$

Our requirements for the basis functions  $\phi_n$  and the discrete space  $\tilde{\mathcal{X}}_N$  are:

- (R1) It is easy to couple the interior and the exterior problem,
- (R2) the discretization matrices are sparse,
- (R3) the basis functions  $\phi_n$  are easy to evaluate numerically stable,
- (R4) the integrals<sup>1</sup>  $\int_{\mathbb{R}_{>0}} q(\xi) \phi_n^{(\alpha)}(\xi) \phi_j^{(\beta)}(\xi) d\xi$  are easy to compute (numerically) for polynomials  $q$  and  $\alpha, \beta \in \{0, 1\}$ ,
- (R5) the generalized-radial part of the eigenfunctions can be well approximated by functions from  $\tilde{\mathcal{X}}_N$ , and
- (R6) the condition numbers of the discretization matrices behave well for large values of  $N$ .

<sup>1</sup>where  $\cdot^{(n)}$  denotes the  $n$ -th derivative

### 6.3.1. Perfectly matched layers

The idea of perfectly matched layers is to use a finite-dimensional subspace  $\mathcal{X}_h \subset H^1(\Omega_{\text{ext}})$  of functions which are supported only in a finite domain  $\Omega_{\text{pml}} \subset \Omega_{\text{ext}}$ .

*Remark 6.2.* A usual implementation of a perfectly matched layer (for resonance problems see, e.g., [Hal19, KP09]) consists of meshing  $\Omega_{\text{pml}}$  and using standard finite element basis functions for  $H^1(\Omega_{\text{pml}})$ . To apply this idea to the coordinates from Definition 3.1, we have to transform the respective weak formulations back to cartesian coordinates after applying the complex scaling. To be able to do so, it is necessary to explicitly know the inverse coordinate mapping  $\Psi^{-1}(\mathbf{x}) = (\xi(\mathbf{x}), \hat{\mathbf{x}}(\mathbf{x}))$ . Although this is the case, for instance, for spherical coordinates (cf. Example 3.3), in more general cases these mappings are not available in closed forms.

Contrary to the usual implementation of perfectly matched layers described in Remark 6.2, one can also use the exterior coordinates and tensor product approach explained in Section 6.2. In the context of perfectly matched layers this corresponds to choosing a one-dimensional mesh on the truncated generalized-radial domain  $(0, T)$  for some  $T > 0$  and using a finite element space

$$\mathcal{X}_h \subset H_T^1((0, T)) := \{f \in H^1(\mathbb{R}_{>0}) : \text{supp}(f) \subset [0, T]\}.$$

For this approach merely the sesquilinear form in exterior coordinates of the form (6.1) has to be known. Usual one-dimensional finite element bases and spaces fulfill all the requirements (R1–6).

### 6.3.2. Complex-scaled infinite Elements

Complex scaling leads to anisotropic solutions. In the interior domain  $\Omega_{\text{int}}$ , as well as in the surface direction of the exterior domain, the oscillating behavior of the function dominates, whereas in the generalized-radial direction of the exterior domain the exponential decay is more significant. Therefore, it is natural to choose suitable different basis functions for the different parts of the solution respectively.

For the radial discretization we use the space of generalized Laguerre functions (Definition A.10). These functions are used as basis functions for spectral methods for equations on unbounded domains with exponentially decreasing solutions (see, e.g., [STW11, Section 7.4]). We will see in the following that they are a suitable choice considering our requirements (R1–6).

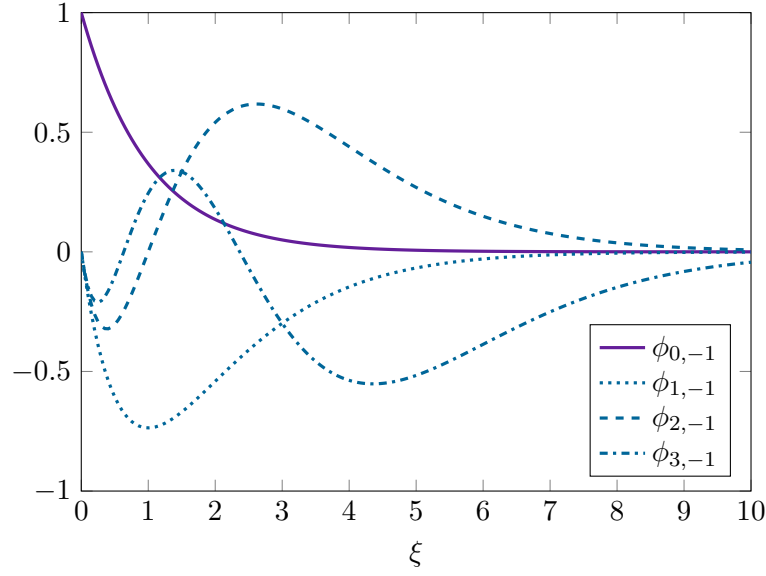
**Definition 6.3.** For  $N \in \mathbb{N}_0$  we define the radial basis and space by

$$\tilde{B}_N := \{\phi_0, \dots, \phi_N\}, \quad \tilde{\mathcal{X}}_N := \text{span}(\tilde{B}_N),$$

where  $\phi_n := \phi_{n,-1}$  are the generalized Laguerre functions with index  $-1$  given by

$$\phi_n(\xi) = \exp(-\xi) L_{n,-1}(2\xi) = \exp(-\xi) \sum_{k=0}^n \binom{n-1}{n-k} \frac{(-2\xi)^k}{k!}$$

for  $\xi > 0$  (Definitions A.7, A.10 and Figure 6.1).

Figure 6.1.: The first few basis functions  $\phi_j = \phi_{j,-1}$ .

The first few basis functions  $\phi_j$  are given by

$$\begin{aligned}\phi_0(\xi) &= \exp(-\xi), \\ \phi_1(\xi) &= -2\xi \exp(-\xi), \\ \phi_2(\xi) &= (2\xi^2 - 2\xi) \exp(-\xi), \\ \phi_3(\xi) &= \left(-\frac{4\xi^3}{3} + 4\xi^2 - 2\xi\right) \exp(-\xi).\end{aligned}$$

Since for any  $m \in \mathbb{Z}$  the function  $L_{n,m}$  is a polynomial of order  $n$  with non-zero leading coefficient (see Remark A.8), the space  $\tilde{\mathcal{X}}_N$  can also be described by

$$\tilde{\mathcal{X}}_N = \{\exp(-x) p_j(x) : p_j \in \mathcal{P}_N\} = \text{span}(\{\phi_{j,m} : j = 0, \dots, N\}),$$

for any  $m \in \mathbb{Z}$ . We proceed to study whether the space  $\tilde{\mathcal{X}}_N$  and the basis  $B_N$  from Definition 6.3 satisfy the requirements (R1–6).

For the approximation properties and the condition numbers, we refer to Sections 6.5 and 9.1 respectively.

### Coupling

By Proposition A.11.(iv) we have (cf. Figure 6.1)

$$\phi_0(0) = 1, \quad \phi_n(0) = 0$$

for all  $n \in \mathbb{N}$ . Thus, as described in Section 6.2.3, we only have to couple the basis functions that contain the generalized-radial basis function  $\phi_0$ . Therefore, (R1) is fulfilled.

### Sparsity

By A.11.(v) we have that the radial integrals vanish for radial basis functions  $\phi_j, \phi_k$  and  $|j - k|$  large enough, as long as the coefficients of the radial part of the sesquilinear forms are polynomials (see also the matrices in Section 7.4.1). This is the case for the radial sesquilinear forms corresponding to all the coordinates we consider (cf. Definition 5.1 and Section 7.1).

### Stable evaluation and numerical integration

The generalized Laguerre functions can be evaluated numerically stable by using the recursion given in Proposition A.11.(vi). We use Gauss rules for  $(0, \infty)$  with weighting function  $\exp(-\cdot)$  to obtain exact quadrature rules for the Laguerre functions (see [STW11, Chapter 7.1.2] and Section 7.4.2).

*Remark 6.4.* This enables us to also deal with inhomogeneous potentials in the exterior domain which is not possible in a straightforward way using classical Hardy space infinite elements (see Section 10.2.1).

## 6.4. Complex-scaled and Hardy space infinite elements

The method of Hardy space infinite elements (short HSIEM) was introduced by Hohage and Nannen in 2009 (see [HN09]) and is based on a radiation condition called the pole condition ([HSZ03a, HSZ03b, SHK<sup>+</sup>07]).

In the following we give a short introduction to the HSIEM for one-dimensional problems. The pole condition imposes a condition on the analytic continuation of the Laplace transform  $\mathcal{L}$  of a solution  $u$  given by

$$\mathcal{L}(u)(s) := \int_0^\infty u(x) \exp(-xs) dx.$$

To state the weak formulation on which the Hardy space infinite element method is based, we need the following definition:

**Definition 6.5.** For  $\sigma \in \mathbb{C} \setminus \{0\}$  we define the right Hardy space  $\mathcal{H}(\frac{i}{\sigma}\mathbb{R})$  as the set of all functions  $f : \frac{i}{\sigma}\mathbb{R} \rightarrow \mathbb{C}$  such that there exists a volume function  $f_{\text{vol}} : \frac{i}{\sigma}\mathbb{C}_{\text{Im} \leq 0} \rightarrow \mathbb{C}$  with  $f = f_{\text{vol}}|_{\frac{i}{\sigma}\mathbb{R}}$  and the integrals

$$\int_{\mathbb{R}} \left| f_{\text{vol}}\left(s + \frac{y}{\sigma}\right) \right|^2 ds$$

are uniformly bounded for  $y \in \mathbb{R}_{>0}$ . Moreover, we define operators  $\mathcal{T}_m^\sigma, \mathcal{T}_s^\sigma : \mathbb{C} \times \mathcal{H}(\frac{i}{\sigma}\mathbb{R}) \rightarrow$

$\mathcal{H}(\frac{i}{\sigma}\mathbb{R})$  and a bilinear form  $q^\sigma : \mathcal{H}(\frac{i}{\sigma}\mathbb{R}) \times \mathcal{H}(\frac{i}{\sigma}\mathbb{R}) \rightarrow \mathbb{C}$  by

$$\begin{aligned}\mathcal{T}_m^\sigma(u_0, U)^\top &:= \frac{u_0 + U(s)}{s + \frac{1}{\sigma}}, \\ \mathcal{T}_s^\sigma(u_0, U)^\top &:= \frac{-\frac{u_0}{\sigma} + sU(s)}{s + \frac{1}{\sigma}}, \\ q^\sigma(U, V) &:= \frac{1}{2i\pi} \int_{\frac{i}{\sigma}\mathbb{R}} U(s) V(-s) ds.\end{aligned}$$

Now the weak formulation for the HSIEM of a one-dimensional problem on the domain  $\Omega := (-R, \infty)$  for some  $R > 0$  can be stated as follows:

**Problem 6.6.** Let  $\sigma \in \mathbb{C} \setminus \{0\}$ ,  $R > 0$ ,  $\Omega_{\text{int}} := (-R, 0)$  and  $\mathcal{H}(\frac{i}{\sigma}\mathbb{R})$ ,  $\mathcal{T}_m^\sigma$ ,  $\mathcal{T}_s^\sigma$ ,  $q^\sigma$  as in Definition 6.5. Then we consider the problem to

$$\begin{aligned}\text{find } \omega \in \mathbb{C} \setminus \{0\}, \text{ and } 0 \neq (u, U) \in H^1(\Omega_{\text{int}}) \times \mathcal{H}\left(\frac{i}{\sigma}\mathbb{R}\right) \text{ such that} \\ (u', v')_{L^2(\Omega_{\text{int}})} + q^\sigma \left( \mathcal{T}_s^\sigma(\text{tr}_0 u, U)^\top, \mathcal{T}_s^\sigma(\text{tr}_0 v, V)^\top \right) \\ = \omega^2 \left( ((1 + \rho)^2 u, v)_{L^2(\Omega_{\text{int}})} + q^\sigma \left( \mathcal{T}_m^\sigma(\text{tr}_0 u, U)^\top, \mathcal{T}_m^\sigma(\text{tr}_0 v, V)^\top \right) \right) \\ \text{for all } v \in H^1(\Omega_{\text{int}}), V \in \mathcal{H}\left(\frac{i}{\sigma}\mathbb{R}\right).\end{aligned}$$

The correspondence in  $\Omega_{\text{ext}}$  between the eigenfunctions  $(u, U)^\top$  of Problem 6.6 and eigenfunctions  $w$  of the Helmholtz resonance problem is given by

$$\mathcal{L}(w|_{\Omega_{\text{ext}}}) = \mathcal{T}_m^\sigma(u(0), U)^\top.$$

It can be shown that Problem 6.6 is equivalent to Problem 2.3 for frequencies  $\omega$  with  $\text{Im}(\omega\sigma) > 0$ . For an exhaustive reference we refer to [HN18, HHNS16]<sup>2</sup> The parameter  $s_0$  used therein is related to  $\sigma$  by the formula  $s_0 = -\frac{1}{\sigma}$ . To discretize Problem 6.6 we use basis functions (cf. [HN18, 3.7] with  $s_0 = -\frac{1}{\sigma}$ )

$$\begin{aligned}\beta_{-1}^\sigma &:= \begin{pmatrix} 1 \\ 0 \end{pmatrix}, \\ \beta_n^\sigma &:= \begin{pmatrix} 0 \\ -\frac{2}{\sigma+1} \left( \frac{\sigma-1}{\sigma+1} \right)^n \end{pmatrix}\end{aligned}\tag{6.6}$$

for  $n = 0, \dots, N-1$ .

One key observation is the following correspondence between the generalized Laguerre functions and the basis functions defined above.

<sup>2</sup>Note that these papers use more involved basis functions and Hardy spaces respectively. Nevertheless, we refer to these, more recent publications since the presentation therein is closer to our understanding of infinite elements, whereas in publications like [HN09, Hal16, HN15b], in addition to the Laplace transform, a Möbius transform is used.

**Lemma 6.7.** For  $\sigma \in \mathbb{C} \setminus \{0\}$ , let  $\beta_j$ ,  $j \in \mathbb{Z}_{\geq -1}$  be as in (6.6),  $\mathcal{T}_m^\sigma$ ,  $\mathcal{T}_s^\sigma$  as in Definition 6.5, and  $\phi_j$ ,  $j \in \mathbb{N}_0$  be as in Definition 6.3. Then for  $s \in \mathbb{R}$  and  $n \in \mathbb{N}_0$

$$\mathcal{L}(\phi_n)(s) = \frac{1}{\sigma} \mathcal{T}_m^\sigma(\beta_{n-1}^\sigma) \left( \frac{s}{\sigma} \right)$$

and

$$\mathcal{L}(\phi'_n)(s) = \mathcal{T}_s^\sigma(\beta_{n-1}^\sigma) \left( \frac{s}{\sigma} \right).$$

*Proof.* For  $n = 0$  we have

$$\mathcal{L}(\phi_0)(s) = \mathcal{L}(\exp(-\cdot))(s) = \frac{1}{s+1} = \mathcal{T}_m^1(\beta_{-1}^1)(s).$$

For  $n > 0$  using  $\mathcal{L}(\exp(-\cdot) \cdot^k) = \frac{k!}{(s+1)^{k+1}}$  and  $\binom{n-1}{n} = 0$  we obtain

$$\begin{aligned} \mathcal{L}(\phi_n)(s) &= \sum_{k=0}^n \binom{n-1}{n-k} \frac{(-2)^k}{k!} \mathcal{L}(\exp(-\cdot) \cdot^k)(s) \\ &= \sum_{k=1}^n \binom{n-1}{n-k} \frac{(-2)^k}{(s+1)^{k+1}} \\ &= -\frac{2}{(s+1)^2} \sum_{k=1}^n \binom{n-1}{k-1} \frac{(-2)^{k-1}}{(s+1)^{k-1}} \\ &= -\frac{2}{(s+1)^2} \left( 1 - \frac{2}{s+1} \right)^{n-1} \\ &= \mathcal{T}_m^1(\beta_{n-1}^1)(s). \end{aligned}$$

Moreover, we have

$$\mathcal{T}_m^1(\beta_{n-1}^1)(s) = \frac{1}{\sigma} \mathcal{T}_m^\sigma(\beta_{n-1}^\sigma) \left( \frac{s}{\sigma} \right)$$

which leads to the first statement. The second claim can be obtained by similar computations or, alternatively, by the use of [HN18, 2.15].  $\square$

The theorem below states that the discretization matrices of the HSIEM and the complex-scaled infinite element method defined in 6.3.2 are identical.

**Theorem 6.8.** For  $\sigma \in \mathbb{C} \setminus \{0\}$ , let  $\beta_j$ ,  $j \in \mathbb{Z}_{\geq -1}$  be as in (6.6),  $\mathcal{T}_m^\sigma$ ,  $\mathcal{T}_s^\sigma$  as in Definition 6.5, and  $\phi_j$ ,  $j \in \mathbb{N}_0$  as in Definition 6.3. Then, for  $n, k \in \mathbb{N}_0$ ,

$$\begin{aligned} \sigma \int_0^\infty \phi_n(\xi) \phi_k(\xi) d\xi &= q^\sigma(\mathcal{T}_m^\sigma(\beta_{n-1}^\sigma), \mathcal{T}_m^\sigma(\beta_{k-1}^\sigma)), \\ \frac{1}{\sigma} \int_0^\infty \phi'_n(\xi) \phi'_k(\xi) d\xi &= q^\sigma(\mathcal{T}_s^\sigma(\beta_{n-1}^\sigma), \mathcal{T}_s^\sigma(\beta_{k-1}^\sigma)). \end{aligned}$$

*Proof.* We have

$$\begin{aligned}
\sigma \int_0^\infty \phi_n(\xi) \phi_k(\xi) d\xi &= \frac{\sigma}{2\pi} \int_{-\infty}^\infty \mathcal{L}(\phi_n)(is) \mathcal{L}(\phi_k)(-is) ds \\
&= \frac{\sigma}{2\pi} \int_{-\infty}^\infty \frac{1}{\sigma} \mathcal{T}_m^\sigma(\beta_{n-1}^\sigma) \left( \frac{is}{\sigma} \right) \frac{1}{\sigma} \mathcal{T}_m^\sigma(\beta_{k-1}^\sigma) \left( -\frac{is}{\sigma} \right) ds \\
&= \frac{1}{2i\pi} \int_{\frac{i}{\sigma}\mathbb{R}} \mathcal{T}_m^\sigma(\beta_{n-1}^\sigma)(s) \mathcal{T}_m^\sigma(\beta_{k-1}^\sigma)(-s) ds \\
&= q^\sigma(\mathcal{T}_m^\sigma(\beta_{n-1}^\sigma), \mathcal{T}_m^\sigma(\beta_{k-1}^\sigma)),
\end{aligned}$$

where we used the equality

$$\int_0^\infty f(x)g(x) dx = \frac{1}{2\pi} \int_{-\infty}^\infty \mathcal{L}(f)(is)\mathcal{L}(g)(-is) ds,$$

from [HN09, Lemma A.1], which can be shown to hold for the basis functions  $\phi_j$ . The proof for the derivatives works similarly.  $\square$

## 6.5. Approximation results for infinite elements

In this section we deal with the stability of the complex-scaled infinite element method. The main results for this analysis are contained in the work of Karma [Kar96a, Kar96b] on the approximation of holomorphic Fredholm operator functions. The main theorems therein are [Kar96a, Theorem 2] and [Kar96b, Theorems 2 and 3].

[Kar96a, Theorem 2] states that for certain discrete approximation schemes, the cluster points of sequences of eigenvalues of the discretized problems are exactly the eigenvalues of the initial problem. [Kar96b, Theorems 2 and 3] state that the convergence rates of the approximation of eigenvalues and eigenvectors are governed by the best approximation error of the eigenvectors.

In [Hal19, Section 3] it is proven that Galerkin discretization schemes fulfill the necessary assumptions of [Kar96a, Kar96b] on the discrete approximation schemes. The results are summarized in [Hal19, Theorem 3.17] in the context of weakly  $T(\cdot)$ -coercive operator functions.

In the following we study the approximation of eigenfunctions, given by (2.8), by the discrete functions defined in Section 6.3.

### Radial approximation error

Along the lines of Chapter 5, we consider the case of three-dimensional polar coordinates and the according scaling, namely,

$$\Omega_{\text{ext}} = \mathbb{R}^3 \setminus \overline{B_1}, \quad \Gamma = S_1,$$

and

$$\hat{\mathbf{x}}(\mathbf{x}) = \frac{\mathbf{x}}{\|\mathbf{x}\|}, \quad \xi(\mathbf{x}) = \|\mathbf{x}\| - 1, \quad \mathbf{v}(\hat{\mathbf{x}}) = \hat{\mathbf{x}}.$$



As a motivation for the following Sections 6.5.1 and 6.5.2, we undertake the following considerations: Let

$$v(\xi, \hat{\mathbf{x}}) := \sum_{k=0}^{\infty} \sum_{j=-k}^k \beta_{k,j} h_k^{(1)}(\omega(1 + \sigma\xi)) Y_k^j(\hat{\mathbf{x}}) = \sum_{l=0}^{\infty} \tilde{u}_l(\xi) \hat{u}_l(\hat{\mathbf{x}})$$

be a complex-scaled eigenfunction in polar coordinates in  $\Omega_{\text{ext}}$  (Proposition 2.8 and Theorem 5.5) for some scaling parameter  $\sigma \in \mathbb{C} \setminus \{0\}$  and a frequency  $\omega \in \mathbb{C}$  such that  $\omega, \sigma$  fulfill (S1) and (S2). Here  $\hat{u}_l = Y_{j(l)}^{k(l)}$  and  $(k(l), j(l))$  is the inverse of the bijection

$$l : \begin{cases} \{(k, j) \in \mathbb{N}_0 \times \mathbb{Z} : |j| \leq k\} & \rightarrow \mathbb{N}_0, \\ (k, j) & \mapsto k^2 + k + j. \end{cases}$$

Then the infinite sum converges uniformly on compact sets (Proposition 2.8) and  $v \circ \Psi^{-1} \in C^\infty(\overline{\Omega_{\text{ext}}})$ .

We pick an index  $K \in \mathbb{N}$  and truncate the infinite series to

$$u(\xi, \hat{\mathbf{x}}) := \sum_{l=0}^K \tilde{u}_l(\xi) \hat{u}_l(\hat{\mathbf{x}}) = v(\xi, \hat{\mathbf{x}}) - \sum_{l=K+1}^{\infty} \tilde{u}_l(\xi) \hat{u}_l(\hat{\mathbf{x}}).$$

In the following we discuss the approximation error of the truncated solution  $u$ . Note that the truncation of the series is not part of our method but merely a tool to motivate the following modal analysis. Also note that for a complete analysis of the approximation error an estimate that is uniform in  $K$  would be necessary.

*Remark 6.9.* The error caused by the truncation of the series can be analyzed using the reasoning we sketch in the following: Since  $v \in C^\infty(\overline{\Omega_{\text{ext}}})$ , we also have  $v(1, \cdot) \in H^n(\Gamma)$  for every  $n \in \mathbb{N}_0$ . From the fact that the spherical harmonics form a complete orthogonal system with respect to the  $H^1(\Gamma)$ -norm we obtain that (cf. [Hal19, (2.6)])

$$|v(1, \cdot)|_{H^n(\Gamma)}^2 = \sum_{k=0}^{\infty} (k(k+1))^n \sum_{j=-k}^k |\beta_{k,j} h_k^{(1)}(\omega)|^2,$$

where  $|\cdot|_{H^n(\Gamma)}$  denotes the  $H^n(\Gamma)$ -seminorm. Since this holds for any  $n \in \mathbb{N}_0$ , the coefficients  $\beta_{k,j} h_k^{(1)}(\omega)$  decay super-algebraically for  $k \rightarrow \infty$ .

In the following let

$$u_{N,M}(\xi, \hat{\mathbf{x}}) = \sum_{l=0}^K \tilde{u}_l^N(\xi) \hat{u}_l^M(\hat{\mathbf{x}}),$$

$$u_N(\xi, \hat{\mathbf{x}}) = \sum_{l=0}^K \tilde{u}_l^N(\xi) \hat{u}_l(\hat{\mathbf{x}})$$

for some approximations  $\tilde{u}_l^N \approx \tilde{u}_l$ ,  $\hat{u}_l^M \approx \hat{u}_l$  and  $l = 0, \dots, K$ .

Then we can bound the approximation error of  $u$  by

$$\begin{aligned} & \|u_{N,M}(\xi(\cdot), \hat{\mathbf{x}}(\cdot)) - u\|_{H^1(\Omega_{\text{ext}})} \\ & \leq \underbrace{\|u_{N,M}(\xi(\cdot), \hat{\mathbf{x}}(\cdot)) - u_N(\xi(\cdot), \hat{\mathbf{x}}(\cdot))\|_{H^1(\Omega_{\text{ext}})}}_{=:\hat{\varepsilon}} + \underbrace{\|u_N(\xi(\cdot), \hat{\mathbf{x}}(\cdot)) - u\|_{H^1(\Omega_{\text{ext}})}}_{=:\tilde{\varepsilon}} \end{aligned}$$

and obtain for the tangential error  $\hat{\varepsilon}$

$$\begin{aligned} \hat{\varepsilon}^2 &= \int_0^\infty (1+\xi)^2 \int_\Gamma \left| \sum_{l=0}^K (\tilde{u}_l^N)'(\xi) (\hat{u}_l^M(\hat{\mathbf{x}}) - \hat{u}_l(\hat{\mathbf{x}})) \right|^2 d\hat{\mathbf{x}} d\xi \\ &+ \int_0^\infty \int_\Gamma \left\| \sum_{l=0}^K \tilde{u}_l^N(\xi) \hat{\nabla} (\hat{u}_l^M(\hat{\mathbf{x}}) - \hat{u}_l(\hat{\mathbf{x}})) \right\|^2 d\hat{\mathbf{x}} d\xi \\ &+ \int_0^\infty (1+\xi)^2 \int_\Gamma \left| \sum_{l=0}^K \tilde{u}_l^N(\xi) (\hat{u}_l^M(\hat{\mathbf{x}}) - \hat{u}_l(\hat{\mathbf{x}})) \right|^2 d\hat{\mathbf{x}} d\xi \\ &\leq \left( \sum_{l=0}^K \int_0^\infty (1+\xi)^2 |(\tilde{u}_l^N)'(\xi)|^2 d\xi \right) \left( \sum_{l=0}^K \int_\Gamma |\hat{u}_l^M(\hat{\mathbf{x}}) - \hat{u}_l(\hat{\mathbf{x}})|^2 d\hat{\mathbf{x}} \right) \\ &+ \left( \sum_{l=0}^K \int_0^\infty |\tilde{u}_l^N(\xi)|^2 d\xi \right) \left( \sum_{l=0}^K \int_\Gamma \|\hat{\nabla} (\hat{u}_l^M(\hat{\mathbf{x}}) - \hat{u}_l(\hat{\mathbf{x}}))\|^2 d\hat{\mathbf{x}} \right) \\ &+ \left( \sum_{l=0}^K \int_0^\infty (1+\xi)^2 |\tilde{u}_l^N(\xi)|^2 d\xi \right) \left( \sum_{l=0}^K \int_\Gamma |\hat{u}_l^M(\hat{\mathbf{x}}) - \hat{u}_l(\hat{\mathbf{x}})|^2 d\hat{\mathbf{x}} \right). \end{aligned}$$

If we assume approximation properties of the tangential space of the form

$$\begin{aligned} \|\hat{u}_l^M - \hat{u}_l\|_{L^2(\Gamma)} &\leq \hat{C}(M) \|\hat{u}_l\|_{L^2(\Gamma)}, \\ \|\hat{\nabla}(\hat{u}_l^M - \hat{u}_l)\|_{L^2(\Gamma)} &\leq \hat{C}(M) \|\hat{\nabla}\hat{u}_l\|_{L^2(\Gamma)} \end{aligned}$$

for some functions  $\hat{C}$ , independent of  $\hat{u}_l$ , and the radial approximation to be continuous with constant  $\tilde{D} > 0$ , namely,

$$\|\tilde{u}_l^N\|_{H^1(\mathbb{R}_{>0})} \leq \tilde{D} \|\tilde{u}_l\|_{H^1(\mathbb{R}_{>0})},$$

we obtain

$$\hat{\varepsilon} \leq \tilde{D} \hat{C}(M) \|u(\xi(\cdot), \hat{\mathbf{x}}(\cdot))\|_{H^1(\Omega_{\text{ext}})},$$

since the  $H^1(\Omega_{\text{ext}})$ -norm of  $u(\xi(\cdot), \hat{\mathbf{x}}(\cdot))$  is given by

$$\begin{aligned}
 \|u(\xi(\cdot), \hat{\mathbf{x}}(\cdot))\|_{H^1(\Omega_{\text{ext}})}^2 &= \sum_{m,l=0}^K \int_0^\infty (1+\xi)^2 \tilde{u}'_l(\xi) \overline{\tilde{u}'_m(\xi)} d\xi \int_\Gamma \hat{u}_l(\hat{\mathbf{x}}) \hat{u}_m(\hat{\mathbf{x}}) d\hat{\mathbf{x}} \\
 &\quad + \int_0^\infty \tilde{u}_l(\xi) \overline{\tilde{u}_m(\xi)} d\xi \int_\Gamma \hat{\nabla} \hat{u}_l \cdot \hat{\nabla} \hat{u}_m d\hat{\mathbf{x}} \\
 &\quad + \int_0^\infty (1+\xi)^2 \tilde{u}_l(\xi) \overline{\tilde{u}_m(\xi)} d\xi \int_\Gamma \hat{u}_l(\hat{\mathbf{x}}) \hat{u}_m(\hat{\mathbf{x}}) d\hat{\mathbf{x}} \quad (6.7) \\
 &= \sum_{l=0}^K \int_0^\infty (1+\xi)^2 |\tilde{u}'_l(\xi)|^2 d\xi \\
 &\quad + \int_0^\infty (k(l)(k(l)+1) + (1+\xi)^2) |\tilde{u}_l(\xi)|^2 d\xi.
 \end{aligned}$$

The derivation of  $\hat{C}$  can be done by using standard techniques for  $H^1$ -conforming finite elements on the surface  $\Gamma$  (see [DE13]). Naturally, we expect  $\hat{C} \rightarrow 0$  for  $M \rightarrow \infty$ .

For the radial error, we obtain by a similar calculation as in (6.7)

$$\tilde{\varepsilon}^2 = \sum_{l=0}^K \int_0^\infty (1+\xi)^2 \left| (\tilde{u}_l^N)'(\xi) - \tilde{u}'_l(\xi) \right|^2 + \int_0^\infty (k(l)(k(l)+1) + (1+\xi)^2) |\tilde{u}_l^N(\xi) - \tilde{u}_l(\xi)|^2 d\xi.$$

This means that we have to find a bound for the radial best approximation error of the form

$$\inf_{\tilde{u}^N \in \tilde{\mathcal{X}}_N} \left\| h_k^{(1)}(\omega(1+\sigma\cdot)) - \tilde{u}^N \right\|_{\tilde{H}_k^1(\mathbb{R}_{>0})} \leq \tilde{C}(N) \left\| h_k^{(1)}(\omega(1+\sigma\cdot)) \right\|_{\tilde{H}_k^1(\mathbb{R}_{>0})}, \quad (6.8)$$

where the weighted norm is defined by

$$\|f\|_{\tilde{H}_k^1(\mathbb{R}_{>0})}^2 := \int_0^\infty (1+\xi)^2 |f'(\xi)|^2 + \int_0^\infty (k(k+1) + (1+\xi)^2) |f(\xi)|^2 d\xi, \quad (6.9)$$

for suitable functions  $f$ .

In the following sections we present a modal analysis, meaning that we show (6.8) with  $\tilde{C}(N) = \tilde{C}_k(N)$  depending on the Hankel index  $k$ . Note that for a full analysis we would need this bound to be uniform in the index.

### 6.5.1. General approximation results

In this section we present approximation results by Laguerre functions, which are independent of the fact that the radial components of the eigenfunctions are given by spherical Hankel functions. Recall that the discrete space  $\tilde{\mathcal{X}}_N$  is given by

$$\tilde{\mathcal{X}}_N = \text{span}(\{\phi_0, \dots, \phi_N\}) = \text{span}(\{\phi_{0,0}, \dots, \phi_{0,N}\})$$

(Definition 6.3). We shorten the notation by writing  $\psi_n := \phi_{n,0}$  for  $n \in \mathbb{N}_0$  and remind the reader that the functions  $\psi_n$  form a complete orthogonal system in  $L^2(\mathbb{R}_{>0})$ . Moreover, we

use the symbol  $\Pi_N$  for the orthogonal projection onto  $\tilde{\mathcal{X}}_N$  with respect to the  $L^2(\mathbb{R}_{>0})$ -inner product given by

$$\Pi_N f = 2 \sum_{n=0}^N (f, \psi_n)_{L^2(\mathbb{R}_{>0})} \psi_n, \quad (6.10)$$

for a function  $f \in L^2(\mathbb{R}_{>0})$ . From [STW11] we obtain the following result:

**Theorem 6.10.** *Let  $m, N \in \mathbb{N}$ ,  $m < N$  and  $f : \mathbb{R}_{>0} \rightarrow \mathbb{C}$  be a function such that  $\xi \mapsto \xi^m \left( \frac{\partial}{\partial \xi} + \mathbf{I} \right)^m f(\xi) \in L^2(\mathbb{R}_{>0})$ . Then*

$$\|\Pi_N f - f\|_{L^2(\mathbb{R}_{>0})}^2 \leq \frac{(N - m + 1)!}{(N + 1)!} \left\| \left( \frac{\partial}{\partial \cdot} + \mathbf{I} \right)^m f \right\|_{L^2(\mathbb{R}_{>0})}^2.$$

*Proof.* [STW11, Theorem 7.9] with  $\alpha = 1$  and  $l = 0$ . Note that the arguments of the basis functions in [STW11] are scaled by the factor  $\frac{1}{2}$  compared to the basis functions  $\phi_j$ .  $\square$

Using Stirling's approximation for the factorial gives

$$\frac{(N - m + 1)!}{(N + 1)!} \sim N^{-m}$$

for  $N \rightarrow \infty$ , which shows that the projection error decays super-algebraically in  $N$ . For a given function  $f \in L^2(\mathbb{R}_{>0})$  we write

$$c_n := 2 (f, \psi_n)_{L^2(\mathbb{R}_{>0})}. \quad (6.11)$$

Then the projection error and its norm are given by

$$\Pi_N f - f = \sum_{n=N+1}^{\infty} c_n \psi_n$$

and

$$\|\Pi_N f - f\|_{L^2(\mathbb{R}_{>0})}^2 = \frac{1}{2} \sum_{n=N+1}^{\infty} |c_n|^2.$$

From the considerations above it immediately follows that for  $m \in \mathbb{N}$  and a function  $f : \mathbb{R}_{>0} \rightarrow \mathbb{C}$  such that  $\xi \mapsto \xi^m \left( \frac{\partial}{\partial \xi} + \mathbf{I} \right)^m f(\xi) \in L^2(\mathbb{R}_{>0})$ , there exists  $\tilde{C}_m(f) > 0$  independent of  $n$  such that

$$|c_n| \leq \tilde{C}_m(f) n^{-\frac{m}{2}}$$

for every  $n \in \mathbb{N}$ . Thus, also the coefficients of the expansion of  $f$  converge to zero super-algebraically.

To obtain a bound in the weighted norm  $\|\cdot\|_{\tilde{H}_k^1(\mathbb{R}_{>0})}$  given by (6.9) we rewrite this norm by

$$\|\Pi_N f - f\|_{\tilde{H}_k^1(\mathbb{R}_{>0})}^2 = \frac{1}{2} \sum_{n,j=N+1}^{\infty} c_n \bar{c}_j \int_0^{\infty} (1 + \xi)^2 \psi'_n(\xi) \psi'_j(\xi) + (k(k+1) + (1 + \xi)^2 \psi_n(\xi) \psi_j(\xi)) d\xi \quad (6.12)$$

$$= \frac{1}{2} \sum_{n,j=N+1}^{\infty} c_n \bar{c}_j \left( \mathbf{S}_{n,j}^{(1+\xi)^2} + k(k+1) \frac{\delta_{n,j}}{2} + \mathbf{M}_{n,j}^{(1+\xi)^2} \right), \quad (6.13)$$

with

$$\mathbf{M}_{n,j}^{(1+\xi)^2} := \int_0^\infty (1+\xi)^2 \psi_n(\xi) \psi_j(\xi) d\xi, \quad \mathbf{S}_{n,j}^{(1+\xi)^2} := \int_0^\infty (1+\xi)^2 \psi'_n(\xi) \psi'_j(\xi) d\xi. \quad (6.14)$$

The lemma below states that the coefficients of the (infinite) matrices with entries  $\mathbf{S}_{n,j}^{(1+\xi)^2}$  and  $\mathbf{M}_{n,j}^{(1+\xi)^2}$  grow, at most, polynomially.

**Lemma 6.11.** *Let  $\mathbf{M}^{(1+\xi)^2}$ ,  $\mathbf{S}^{(1+\xi)^2}$  be the (infinite) matrices with entries given by (6.14). Then there exists a constant  $C > 0$  such that*

$$\left| \mathbf{S}_{n,j}^{(1+\xi)^2} \right|, \left| \mathbf{M}_{n,j}^{(1+\xi)^2} \right| \leq C \min\{j^2, n^2\}$$

for all  $n, j \in \mathbb{N}_0$ .

*Proof.* For  $n, j \in \mathbb{N}_0$  we decompose  $\mathbf{S}_{n,j}^{(1+\xi)^2}$  into

$$\mathbf{S}_{n,j}^{(1+\xi)^2} = \int_0^\infty \phi'_n(\xi) \phi'_j(\xi) d\xi + 2 \int_0^\infty \xi \phi'_n(\xi) \phi'_j(\xi) d\xi + \int_0^\infty \xi^2 \phi'_n(\xi) \phi'_j(\xi) d\xi.$$

Using the formula (Proposition A.11.(iii))

$$\psi'_n = -\psi_n - 2 \sum_{j=0}^{n-1} \psi_j,$$

we obtain

$$\begin{aligned} \int_0^\infty \phi'_n(\xi) \phi'_j(\xi) d\xi &= \int_0^\infty \left( \psi_n(\xi) + 2 \sum_{k=0}^{n-1} \psi_k(\xi) \right) \left( \psi_j(\xi) + 2 \sum_{l=0}^{j-1} \psi_l(\xi) \right) d\xi \\ &= \begin{cases} \frac{1}{2}(1+4n), & n=j, \\ \frac{1}{2}(2+4\min\{n,j\}), & n \neq j. \end{cases} \end{aligned}$$

Using (Proposition A.11.(i))

$$\int_0^\infty (2\xi)^k \phi_{n,k}(\xi) \phi_{j,k}(\xi) d\xi = \frac{(n+k)!}{2n!} \delta_{n,j}$$

and (Proposition A.11.(iii))

$$\psi'_n = -\phi_{n,1} - \phi_{n-1,1},$$

we obtain

$$\begin{aligned} 2 \int_0^\infty \xi \phi'_n(\xi) \phi'_j(\xi) d\xi &= \int_0^\infty 2\xi (\phi_{n,1}(\xi) + \phi_{n-1,1}(\xi)) (\phi_{j,1}(\xi) + \phi_{j-1,1}(\xi)) d\xi \\ &= \begin{cases} \frac{1}{2}(2n+1), & n=j, \\ \frac{1}{2}(n+1), & n+1=j, \\ \frac{1}{2}n, & n-1=j, \\ 0, & \text{else.} \end{cases} \end{aligned}$$

By performing similar calculations for the quadratic term and the expression  $\mathbf{M}_{n,j}^{(1+\xi)^2}$ , we obtain the claim.  $\square$

The final theorem of this section states that the best approximation error in the weighted norm decays super-algebraically as well.

**Theorem 6.12.** *Let  $m, N \in \mathbb{N}$  with  $m < N$ ,  $\Pi_N$  as in (6.10), and  $f$  as in Theorem 6.10. Then there exists a constant  $\tilde{C}_{m,k}(f) > 0$ , independent of  $N$ , such that*

$$\|\Pi_N f - f\|_{\tilde{H}_k^1(\mathbb{R}_{>0})} \leq \tilde{C}_{m,k}(f) N^{2-\frac{m}{2}}.$$

*Proof.* Let  $c_n$  be again the coefficients of the expansion of  $f$  in the basis functions  $\psi_n$  as in (6.11). Then for  $\mathbf{A}_{n,j} = \mathbf{M}_{n,j}^{(1+\xi)^2}, \mathbf{S}_{n,j}^{(1+\xi)^2}$

$$\begin{aligned} \left| \sum_{n=N+1}^{\infty} c_n \sum_{j=N+1}^{\infty} \mathbf{A}_{n,j} \bar{c}_j \right| &\leq \sum_{n=N+1}^{\infty} |c_n| \sum_{j=N+1}^{\infty} |\mathbf{A}_{n,j} \bar{c}_j| \\ &\leq C \tilde{C}_m^2(f) \sum_{n=N+1}^{\infty} n^{-\frac{m}{2}} \sum_{j=N+1}^{\infty} j^2 j^{-\frac{m}{2}} \\ &\leq C \tilde{C}_m^2(f) \sum_{n=N+1}^{\infty} n^{-\frac{m}{2}} \int_N^{\infty} x^{2-\frac{m}{2}} dx \\ &= C \tilde{C}_m^2(f) \sum_{n=N+1}^{\infty} n^{-\frac{m}{2}} \frac{1}{\frac{m}{2}-3} N^{3-\frac{m}{2}} \\ &\leq C \tilde{C}_m^2(f) \frac{1}{(\frac{m}{2}-3)(\frac{m}{2}-1)} N^{4-m} \end{aligned}$$

for any  $m < N$ . Using (6.12) and summing over the expressions and taking the square root finishes the proof.  $\square$

### 6.5.2. Approximation of spherical Hankel functions

In the previous section he have shown that the error in the weighted norm  $\|\cdot\|_{\tilde{H}_k^1(\mathbb{R}_{>0})}$  decays super-algebraically in the number of radial unknowns  $N$ . Although this gives us convergence of the complex-scaled infinite element method for Bessel equations, we do not obtain how the error depends on the scaling parameter  $\sigma$ . In the following we derive estimates for the  $L^2$ -error depending on the scaling. Error estimates in the weighted norm can then be obtained as in the previous section.

Again we use the notation  $\psi_n := \phi_{n,0}$ .

#### Best approximation in one dimension

Prior to the discussion of approximation results for the solutions in three dimensions, we state some results regarding the simpler one-dimensional problems.

**Theorem 6.13.** *For  $b \in \mathbb{C}$ ,  $\operatorname{Re}(b) > -1$  and  $n \in \mathbb{N}_0$ ,*

$$\int_0^{\infty} \exp(-b\xi) \psi_n(\xi) d\xi = \frac{(b-1)^n}{(b+1)^{n+1}}.$$

If, additionally,  $\operatorname{Re}(b) > 0$  and  $\xi \in \mathbb{R}_{>0}$ , we have

$$\exp(-b\xi) = \frac{2}{b+1} \sum_{n=0}^{\infty} \left(\frac{b-1}{b+1}\right)^n \psi_n(\xi).$$

Moreover, the  $L^2(\mathbb{R}_{>0})$ -orthogonal projection onto  $\tilde{\mathcal{X}}_N$  of the function  $\exp(-b\cdot)$  is given by

$$\Pi_N \exp(-b\cdot) = \frac{2}{b+1} \sum_{n=0}^N \left(\frac{b-1}{b+1}\right)^n \psi_n(\cdot).$$

*Proof.* It is easily shown by integration by parts and induction over  $j$  that for  $j \in \mathbb{N}, j \leq n+1$

$$\begin{aligned} \int_0^{\infty} \exp(-b\xi) \psi_n(\xi) d\xi &= \\ \frac{1}{b+1} \sum_{k=0}^{j-1} \left(\frac{2}{b+1}\right)^k L_{n,0}^{(k)}(0) &+ \left(\frac{2}{b+1}\right)^j \int_0^{\infty} \exp(-\xi(b+1)) L_{n,0}^{(j)}(2\xi) d\xi. \end{aligned}$$

For  $j = n+1$  we obtain

$$\begin{aligned} \int_0^{\infty} \exp(-b\xi) \psi_n(\xi) d\xi &= \frac{1}{b+1} \sum_{k=0}^n \left(\frac{2}{b+1}\right)^k L_{n,0}^{(k)}(0) \\ &\stackrel{\text{A.9.(iii)}}{=} \frac{1}{b+1} \sum_{k=0}^n \left(-\frac{2}{b+1}\right)^k L_{n-k,k}(0) \\ &= \frac{1}{b+1} \sum_{k=0}^n \left(-\frac{2}{b+1}\right)^k \binom{n}{k} \\ &= \frac{1}{b+1} \left(1 - \frac{2}{b+1}\right)^n \\ &= \frac{(b-1)^n}{(b+1)^{n+1}}. \end{aligned}$$

If  $\operatorname{Re}(b) > 0$ , we have  $\exp(-b\cdot) \in L^2(\mathbb{R}_{>0})$ . Since  $\{\psi_n, n \in \mathbb{N}_0\}$  is a complete orthogonal system of  $L^2(\mathbb{R}_{>0})$ , we have

$$\exp(-b\xi) = \sum_{n=0}^{\infty} \frac{(\psi_n, \exp(-b\cdot))_{L^2(\mathbb{R}_{>0})}}{(\psi_n, \psi_n)_{L^2(\mathbb{R}_{>0})}} \psi_n(x) = \frac{2}{b+1} \sum_{n=0}^{\infty} \left(\frac{b-1}{b+1}\right)^n \psi_n(\xi).$$

□

From Theorem 6.13 we obtain the following corollary for the best approximation error of decaying exponentials.

**Corollary 6.14.** For  $b \in \mathbb{C}$ ,  $\operatorname{Re}(b) > 0$  and  $N \in \mathbb{N}_0$

$$\inf_{u_N \in \tilde{\mathcal{X}}_N} \|\exp(-b\cdot) - u_N\|_{L^2(\mathbb{R}_{>0})} \leq \|(\mathbf{I} - \Pi_N) \exp(-b\cdot)\|_{L^2(\mathbb{R}_{>0})} = \frac{1}{\sqrt{2\operatorname{Re}(b)}} \left| \frac{b-1}{b+1} \right|^{N+1}.$$

*Proof.* We have

$$\begin{aligned}
\|(\mathbf{I} - \Pi_N) \exp(-b \cdot)\|_{L^2(\mathbb{R}_{>0})}^2 &= \left\| \frac{2}{b+1} \sum_{n=N+1}^{\infty} \left(\frac{b-1}{b+1}\right)^n \psi_n \right\|_{L^2(\mathbb{R}_{>0})}^2 \\
&= \left| \frac{2}{b+1} \right|^2 \sum_{n=N+1}^{\infty} \left| \frac{b-1}{b+1} \right|^{2n} \|\psi_n\|_{L^2(\mathbb{R}_{>0})}^2 \\
&= 2 \left| \frac{(b-1)^{N+1}}{(b+1)^{N+2}} \right|^2 \sum_{n=0}^{\infty} \left| \frac{b-1}{b+1} \right|^{2n} \\
&= 2 \left| \frac{(b-1)^{N+1}}{(b+1)^{N+2}} \right|^2 \frac{1}{1 - \left| \frac{b-1}{b+1} \right|^2} \\
&= \left| \frac{b-1}{b+1} \right|^{2N+2} \frac{1}{2\operatorname{Re}(b)}.
\end{aligned}$$

□

*Remark 6.15.* Because of the representation of the eigenfunctions for  $d = 1$  in the exterior (Definition 2.6)

$$u_{\text{ext}}(\xi) = \alpha \exp(\pm i\omega R) \exp(i\omega\sigma\xi),$$

Theorem 6.13 and Corollary 6.14 with  $b = -i\sigma\omega$  state that the approximation by Laguerre functions in the  $L^2$ -norm depends on the quantity  $\left| \frac{1+i\omega\sigma}{1-i\omega\sigma} \right|$ . It is exact if  $\omega\sigma = i$ . In particular we have for  $\operatorname{Im}(\sigma\omega) > 0$

$$\inf_{u_h \in \tilde{\mathcal{X}}_N} \|\exp(i\sigma\omega \cdot) - u_h\|_{L^2(\mathbb{R}_{>0})} \leq \frac{1}{\sqrt{2\operatorname{Im}(\sigma\omega)}} \left| \frac{1+i\sigma\omega}{1-i\sigma\omega} \right|^{N+1},$$

stating that the best approximation error of radiating eigenfunctions of the one-dimensional Helmholtz equation decreases exponentially with respect to the number of exterior degrees of freedom  $N$ .

### Best approximation of the zeroth spherical Hankel function

Since the radial part of the eigenfunctions of the three-dimensional Helmholtz resonance problem in the exterior domain consist of spherical Hankel functions of the first kind, we proceed by discussing the approximation of  $h_0^{(1)}$  by Laguerre functions. Suppose we want to approximate

$$h_0^{(1)}(\omega + i\xi) = \frac{-\exp(i\omega) \exp(-\xi)}{-i\omega + \xi}$$

using our basis functions  $\psi_n$ . This is the case when we apply a frequency-dependent complex scaling  $\sigma(\omega) = \frac{i}{\omega}$  (see Section 7.3). Then the approximation error is governed by the terms  $\left( \frac{\exp(-\cdot)}{a+\cdot}, \psi_n \right)_{L^2(\mathbb{R}_{>0})}$  with  $a = -i\omega$ . This motivates the following definition:



**Definition 6.16.** For  $a \in \mathbb{C} \setminus \mathbb{R}_{\leq 0}$  and  $n, k \in \mathbb{N}_0$ , we define

$$\alpha_{n,k}(a) := \int_0^\infty \frac{\exp(-\xi)}{(a + \xi)^k} \psi_n(\xi) d\xi.$$

The lemma below states that the numbers  $\alpha_{n,1}(a)$  can be computed by evaluating a single integral.

**Lemma 6.17.** For  $a \in \mathbb{C} \setminus \mathbb{R}_{\leq 0}$  and  $n \in \mathbb{N}_0$ , we have

$$\alpha_{n,1}(a) = \int_0^\infty \frac{\xi^n \exp(-\xi)}{(a + \xi)^{n+1}} d\xi.$$

The numbers  $2\alpha_{n,1}(a)$  are the coefficients of the expansion of  $\frac{\exp(-\cdot)}{a+\cdot}$  in the Laguerre functions  $\psi_n$  and therefore

$$\frac{\exp(-\xi)}{a + \xi} = 2 \sum_{n=0}^{\infty} \alpha_{n,1}(a) \psi_n(\xi).$$

*Proof.* It is easily shown by integration by parts and induction over  $j$  that for  $j \leq n$

$$\int_0^\infty \frac{t^n \exp(-t)}{(2a + t)^{n+1}} dt = \frac{(n-j)!}{n!} \int_0^\infty \frac{1}{(2a + t)^{n+1-j}} \frac{d^j}{dt^j} (\exp(-t) t^n) dt.$$

For  $j = n$ , we obtain

$$\begin{aligned} \int_0^\infty \frac{t^n \exp(-t)}{(2a + t)^{n+1}} dt &= \frac{1}{n!} \int_0^\infty \frac{1}{2a + t} \frac{d^n}{dt^n} (\exp(-t) t^n) dt \\ &\stackrel{\text{A.9.(v)}}{=} \int_0^\infty \frac{1}{2a + t} \exp(-t) L_{n,0}(t) dt \\ &= \int_0^\infty \frac{2 \exp(-t)}{2a + 2t} \psi_n(t) dt = \alpha_{n,1}(a). \end{aligned}$$

□

The following theorem gives an asymptotic expansion of the terms  $\alpha_{n,1}(a)$  with respect to  $n$ .

**Theorem 6.18** (asymptotic behavior of  $\alpha_{n,1}$ ). For  $a \in \mathbb{C} \setminus \mathbb{R}_{\leq 0}$ , we have

$$\alpha_{n,1}(a) = \exp\left(a - 2\sqrt{2a(n+1)}\right) \frac{\sqrt{\pi}}{(2a(n+1))^{\frac{1}{4}}} \left(1 + \mathcal{O}\left(\frac{1}{\sqrt{n+1}}\right)\right), \quad n \rightarrow \infty.$$

<sup>3</sup>

<sup>3</sup>The symbols  $\sqrt{z}$  and  $z^{\frac{1}{4}}$  for  $z \in \mathbb{C} \setminus \mathbb{R}_{\leq 0}$  assume their respective principal values (their image is symmetric with respect to the positive real axis).

*Proof.* Lemma 6.17 states that

$$\alpha_{n,1}(a) = n!U(n+1, 1, 2a),$$

where for  $n \in \mathbb{N}_0$ ,  $a \in \mathbb{C} \setminus \mathbb{R}_{\leq 0}$

$$U(n+1, m, a) = \frac{a^{1-m}}{n!} \int_0^\infty \frac{t^n \exp(-t)}{(a+t)^{n+2-m}} dt.$$

The function  $U$  is called *confluent hypergeometric function of the second kind* ([Tem96, Section 7.2]). Using (10.3.39) and (9.1.3) in [Tem15] we obtain

$$n!U(n+1, 1, 2a) = 2 \exp(a) \left( K_0(2\sqrt{2a(n+1)}) + \sqrt{\frac{2a}{n+1}} K_1(2\sqrt{2a(n+1)}) + \mathcal{O}\left(\frac{1}{\sqrt{n+1}}\right) \right)$$

for  $n \rightarrow \infty$  and

$$K_n(z) = \sqrt{\frac{\pi}{2z}} \exp(-z) \left( 1 + \mathcal{O}\left(\frac{1}{z}\right) \right),$$

for  $|z| \rightarrow \infty$ . All in all, we obtain

$$\begin{aligned} \alpha_{n,1}(a) &= n!U(n+1, 1, 2a) \\ &= \sqrt{\pi}(2a(n+1))^{-\frac{1}{4}} \exp\left(a - 2\sqrt{2a(n+1)}\right) \left( 1 + \mathcal{O}\left(\frac{1}{\sqrt{n+1}}\right) \right) \end{aligned}$$

for  $n \rightarrow \infty$ . □

Using the lemma above, we can now bound the best approximation error of  $h_0^{(1)}(\omega + i \cdot)$  by Laguerre functions.

**Lemma 6.19.** *Let  $N \in \mathbb{N}$  and  $\omega \in \mathbb{C} \setminus \{0\}$ . Then there exists a constant  $c > 0$  independent of  $N$ , such that*

$$\left\| (\mathbf{I} - \Pi_N) h_0^{(1)}(\omega + i \cdot) \right\|_{L^2(\mathbb{R}_{>0})} \leq \frac{c\sqrt{\pi}}{(2|\omega|)^{\frac{1}{4}}} \exp\left(-2\operatorname{Re}\left(\sqrt{\omega(N+1)}\right)\right).$$

*Proof.* We have

$$\begin{aligned} \left\| (\mathbf{I} - \Pi_N) h_0^{(1)}(\omega + i \cdot) \right\|_{L^2(\mathbb{R}_{>0})}^2 &= \left\| (\mathbf{I} - \Pi_N)(-1) \exp(i\omega R) \frac{\exp(-\cdot)}{-i\omega + \cdot} \right\|_{L^2(\mathbb{R}_{>0})}^2 \\ &= \sum_{n=N+1}^{\infty} |2\alpha_{n,1}(-i\omega)|^2 \|\psi_n\|^2 \\ &\leq 2c \sum_{n=N+1}^{\infty} \left| \exp\left(-i\omega - 2\sqrt{-2i\omega(n+1)}\right) \frac{\sqrt{\pi}}{(-2i\omega(n+1))^{\frac{1}{4}}} \right|^2 \\ &= c\pi \sqrt{\frac{2}{\omega}} \sum_{n=N+1}^{\infty} \frac{\exp\left(2\operatorname{Im}(\omega) - 4\operatorname{Re}\left(\sqrt{-2i\omega(n+1)}\right)\right)}{\sqrt{n+1}} \end{aligned}$$

for some  $c > 0$ . Since the summands are the values of a decreasing function in  $n$ , we can replace the sum with an integral and obtain

$$\begin{aligned} \left\| (\mathbf{I} - \Pi_N) h_0^{(1)}(\omega + i \cdot) \right\|_{L^2(\mathbb{R}_{>0})}^2 &\leq c\pi \exp(2\operatorname{Im}(\omega)) \sqrt{\frac{2}{\omega}} \int_{N+1}^{\infty} \frac{\exp(-4\operatorname{Re}(\sqrt{-2i\omega t}))}{\sqrt{t}} dt \\ &= 2c \exp(2\operatorname{Im}(\omega)) \pi \sqrt{\frac{2}{\omega}} \int_{\sqrt{N+1}}^{\infty} \exp(-4\operatorname{Re}(\sqrt{-2i\omega} s)) ds \\ &= \frac{c\pi \exp(2\operatorname{Im}(\omega))}{2\operatorname{Re}(\sqrt{-2i\omega})} \exp(-4\operatorname{Re}(\sqrt{-2i\omega(N+1)})). \end{aligned}$$

□

Lemma 6.19 only gives us the approximation error for a frequency-dependent complex scaling  $\sigma(\omega) = \frac{i}{\omega}$ , which leads to solutions with exponential decay  $\exp(-\cdot)$ . General scalings result in solutions with exponential decay  $\exp(\operatorname{Re}(i\omega\sigma))$  leading to an additional error term.

**Theorem 6.20.** *Let  $\omega \in \mathbb{C}$ ,  $\sigma \in \mathbb{C} \setminus \mathbb{R}_{<0}$  with  $\operatorname{Im}(\omega\sigma) > 0$ ,  $N \in \mathbb{N}$ , and  $\tilde{\mathcal{X}}_N$  as in Definition 6.3. Then there exist constants  $C_1, C_2 > 0$  independent of  $N$  such that the best approximation error of  $h_0^{(1)}(\omega + \omega\sigma \cdot)$  can be bounded by*

$$\inf_{u_N \in \tilde{\mathcal{X}}_N} \|h_0^{(1)}(\omega + \omega\sigma \cdot) - u_N\|_{L^2(\mathbb{R}_{>0})} \leq C_1 \left| \frac{1 + i\sigma\omega}{1 - i\sigma\omega} \right|^{N+1} + C_2 \varepsilon\left(N, \frac{1}{\sigma}, -i\omega\sigma\right),$$

with

$$\varepsilon(N, a, b) := \|(\mathbf{I} - \Pi_N) \frac{1}{a + \cdot} \Pi_N \exp(-b \cdot)\|_{L^2(\mathbb{R}_{>0})}. \quad (6.15)$$

*Proof.* We have

$$\begin{aligned} \|(\mathbf{I} - \Pi_N) h_0^{(1)}(\omega + \omega\sigma \cdot)\|_{L^2(\mathbb{R}_{>0})} &= \|(\mathbf{I} - \Pi_N) \frac{-i \exp(i\omega) \exp(i\omega\sigma \cdot)}{\omega\sigma} \frac{1}{\frac{1}{\sigma} + \cdot}\|_{L^2(\mathbb{R}_{>0})} \\ &\leq C_2 \|(\mathbf{I} - \Pi_N) \frac{1}{\frac{1}{\sigma} + \cdot} (\mathbf{I} - \Pi_N) \exp(i\omega\sigma \cdot)\|_{L^2(\mathbb{R}_{>0})} \\ &\quad + C_2 \underbrace{\|(\mathbf{I} - \Pi_N) \frac{1}{\frac{1}{\sigma} + \cdot} \Pi_N \exp(i\omega\sigma \cdot)\|_{L^2(\mathbb{R}_{>0})}}_{\varepsilon(N, \frac{1}{\sigma}, -i\omega\sigma)}, \end{aligned}$$

with  $C_2 = \left| \frac{\exp(i\omega)}{\omega\sigma} \right|$ . The first term can be bounded by

$$\begin{aligned} \|(\mathbf{I} - \Pi_N) \frac{1}{\frac{1}{\sigma} + \cdot} (\mathbf{I} - \Pi_N) \exp(i\omega\sigma \cdot)\|_{L^2(\mathbb{R}_{>0})} &\leq 2C \|(\mathbf{I} - \Pi_N) \exp(i\omega\sigma \cdot)\|_{L^2(\mathbb{R}_{>0})} \\ &\leq 2C \frac{1}{\sqrt{2\operatorname{Im}(\omega\sigma)}} \left| \frac{1 + i\omega\sigma}{1 - i\omega\sigma} \right|^{N+1} \end{aligned}$$

for some constant  $C > 0$  (cf. Corollary 6.14). □

To obtain a bound for the best approximation error of  $h_0^{(1)}$  in the space  $\tilde{\mathcal{X}}_N$ , we need to find a bound for the expression  $\varepsilon$ . Since for  $b \in \mathbb{C}$  and  $a \in \mathbb{C} \setminus \mathbb{R}_{\leq 0}$

$$(\mathbf{I} - \Pi_N) \frac{1}{a + \cdot} \Pi_N \exp(-b \cdot) = \sum_{n=N+1}^{\infty} \int_0^{\infty} \frac{1}{a + \xi} \sum_{k=0}^N \frac{(b-1)^k}{(b+1)^{k+1}} \psi_k(\xi) \psi_n(\xi) d\xi \psi_n(\cdot),$$

we need to know the asymptotic behavior of the expressions

$$\beta_{n,k}(a) := \int_0^{\infty} \frac{\psi_n(x) \psi_k(x)}{a + x} dx \quad (6.16)$$

for large  $n \in \mathbb{N}$ . Thus, we state the following lemma:

**Lemma 6.21.** *Let  $a \in \mathbb{C} \setminus \mathbb{R}_{<0}$ , and  $\beta_{n,k}$  given by (6.16). Then for  $n, k \in \mathbb{N}_0$  such that  $n \geq k$  there holds*

$$\beta_{n,k}(a) = \alpha_{n,1}(a) L_{k,0}(-2a). \quad (6.17)$$

*Proof.* We prove by induction in  $k$ . For  $k = 0$ , we have

$$\beta_{n,0}(a) = \alpha_{n,1}(a) = \alpha_{n,1}(a) L_{0,0}(-2a),$$

and for  $k = 1$ ,  $n \geq 1$

$$\begin{aligned} \beta_{n,1}(a) &= \int_0^{\infty} \frac{\exp(-x)(1-2x)}{a+x} \psi_n(x) dx \\ &= \alpha_{n,1}(a) - 2 \int_0^{\infty} \frac{x+a-a}{a+x} \exp(-x) \psi_n(x) dx \\ &= \alpha_{n,1}(a) - \delta_{n,0} + 2a\alpha_{n,1}(a) \\ &= (2a+1)\alpha_{n,1}(a) = L_{1,0}(-2a)\alpha_{n,1}(a). \end{aligned}$$

For  $n \geq k$ , we use the recursion from A.11.(vi) and write

$$\begin{aligned} \beta_{n,k}(a) &= \int_0^{\infty} \frac{\psi_n(x)}{a+x} \left( \frac{2k-1-2x}{k} \psi_{k-1}(x) - \frac{k-1}{k} \psi_{k-2}(x) \right) dx = \\ &= \frac{2k-1}{k} \beta_{n,k-1}(a) - \frac{k-1}{k} \beta_{n,k-2}(a) - \frac{2}{k} \int_0^{\infty} \frac{x+a-a}{a+x} \psi_n(x) \psi_{k-1}(x) dx \\ &= \frac{2k-1}{k} \beta_{n,k-1}(a) - \frac{k-1}{k} \beta_{n,k-2}(a) + \frac{2a}{k} \beta_{n,k-1}(a) \\ &= \alpha_{n,1}(a) \left( \frac{2k-1+2a}{k} L_{k-1,0}(-2a) - \frac{k-1}{k} L_{k-2,0}(-2a) \right) \\ &= \alpha_{n,1}(a) L_{k,0}(-2a). \end{aligned}$$

□

Now we are able to bound the term  $\varepsilon(N, a, b)$  given by (6.15).

**Lemma 6.22.** For  $a \in \mathbb{C} \setminus \mathbb{R}_{\leq 0}$ ,  $b \in \mathbb{C}$  and  $\operatorname{Re}(b) > 0$ , there exists  $C > 0$  independent of  $N$  such that

$$\varepsilon(N, a, b) \leq C \exp\left(-2\operatorname{Re}\left(\sqrt{2a(N+1)}\right)\right)$$

for  $\varepsilon$  as in (6.15).

*Proof.* Since

$$\Pi_N \exp(-bx) = \frac{2}{b+1} \sum_{k=0}^N \left(\frac{b-1}{b+1}\right)^k \psi_k(x),$$

we have

$$\begin{aligned} \varepsilon(N, a, b)^2 &= \left\| \sum_{n=N+1}^{\infty} \frac{4}{b+1} \sum_{k=0}^N \left(\frac{b-1}{b+1}\right)^k \left(\psi_n, \frac{\psi_k}{\cdot+a}\right)_{L^2(\mathbb{R}_{>0})} \psi_n \right\|_{L^2(\mathbb{R}_{>0})}^2 \\ &= \left\| \sum_{n=N+1}^{\infty} \frac{4}{b+1} \sum_{k=0}^N \left(\frac{b-1}{b+1}\right)^k \beta_{n,k}(a) \psi_n \right\|_{L^2(\mathbb{R}_{>0})}^2 \\ &= \frac{1}{2} \sum_{n=N+1}^{\infty} \left| \frac{4}{b+1} \alpha_{n,1}(a) \sum_{k=0}^N \left(\frac{b-1}{b+1}\right)^k L_{k,0}(-2a) \right|^2. \end{aligned}$$

Using the generating function of the Laguerre polynomials from Lemma A.9.(vi) we have, for some constant  $C$ , that

$$\begin{aligned} \sum_{k=0}^N \left(\frac{b-1}{b+1}\right)^k L_{k,0}(-2a) &\leq C \frac{1}{1-\frac{b-1}{b+1}} \exp\left(2a \frac{\frac{b-1}{b+1}}{1-\frac{b-1}{b+1}}\right) \\ &= C \frac{b+1}{2} \exp(a(b-1)) \end{aligned}$$

and thus

$$\varepsilon(N, a, b)^2 \leq 2C \sum_{n=N+1}^{\infty} |\alpha_{n,1}(a) \exp(a(b-1))|^2.$$

Substituting the asymptotic behavior of  $\alpha_{n,1}$  and repeating the arguments of the proof of Lemma 6.19, we find for some constant  $c \in \mathbb{R}$

$$\sum_{n=N+1}^{\infty} |\alpha_{n,1}(a)|^2 \leq c \left| \exp(2a) \frac{\pi}{\sqrt{2a}} \right| \frac{1}{2\operatorname{Re}(\sqrt{2a})} \exp\left(-4\operatorname{Re}\left(\sqrt{2a(N+1)}\right)\right).$$

All in all, this gives

$$\varepsilon(N, a, b) \leq \tilde{C} \frac{\exp(\operatorname{Re}(ab)) \sqrt{\pi}}{\sqrt{|2a|\operatorname{Re}(\sqrt{2a})}} \exp\left(-2\operatorname{Re}\left(\sqrt{2a(N+1)}\right)\right).$$

□

Using Theorem 6.20 and Lemma 6.22 we have proven the following theorem:

**Theorem 6.23.** *Let  $N \in \mathbb{N}$ ,  $\omega \in \mathbb{C}$ ,  $\sigma \in \mathbb{C} \setminus \mathbb{R}_{<0}$ , such that  $\text{Im}(\sigma\omega) > 0$  and  $\tilde{\mathcal{X}}_N$  as in Definition 6.3. Then we can bound the approximation error of the complex-scaled zeroth spherical Hankel function by*

$$\inf_{u_N \in \tilde{\mathcal{X}}_N} \left\| h_0^{(1)}(\omega(1 + \sigma \cdot)) - u_N \right\|_{L^2(\mathbb{R}_{>0})} \leq c_1 \left| \frac{1 + i\sigma\omega}{1 - i\sigma\omega} \right|^{N+1} + c_2 \exp\left(-2\text{Re}\left(\sqrt{\frac{2(N+1)}{\sigma}}\right)\right)$$

for some constants  $c_1, c_2 > 0$  independent of  $N$ .

Theorem 6.23 states that the approximation error of  $h_0^{(1)}(\omega + \sigma\omega \cdot)$  by Laguerre functions can be split up into two parts:

- An exponentially decaying part similar to the error of the one-dimensional problem, which is generated by the different exponential decay of the solution and the basis functions and
- a super-algebraic part due to the fact that we approximate the rational part of  $h_0^{(1)}$  by polynomials.

### Approximation of spherical Hankel functions with higher index

Up to now we have only dealt with the approximation of the complex-scaled Hankel function of the first kind with index zero. For Hankel functions with higher indices similar bounds for the approximation error can be derived. To avoid lengthy and technical calculations we merely give a short sketch of the results.

Similar to Theorem 6.18 one can show an asymptotic behavior of  $\alpha_{n,k}$  of the form

$$|\alpha_{n,k}(a)| \leq C_{k,a} \left| \exp\left(-2\sqrt{2a(n+1)}\right) \right| (n+1)^{-\frac{3}{4} + \frac{k}{2}}, \quad n \rightarrow \infty.$$

Using this and similar ideas as in the proofs of Theorem 6.20 and Lemma 6.22 leads to a bound of the best approximation error of the complex-scaled spherical Hankel function of the first kind with index  $n \in \mathbb{N}$

$$\inf_{u_N \in \tilde{\mathcal{X}}_N} \left\| h_n^{(1)}(\omega(1 + \sigma \cdot)) - u_N \right\|_{L^2(\mathbb{R}_{>0})} \leq c_1 \left| \frac{1 + i\sigma\omega}{1 - i\sigma\omega} \right|^{N+1} + c_2 \exp\left(-2\text{Re}\left(\sqrt{\frac{2(N+1)}{\sigma}}\right)\right) (N+1)^{\frac{n}{2}}$$

for some constants  $c_1, c_2 > 0$  independent of  $N$ .

## 7. Implementation

In this chapter we collect all the relevant information for readers who are interested in implementing our method. To implement the frequency-dependent complex scaling in exterior coordinates we have to

1. pick exterior coordinates and derive the according weak formulation of the complex-scaled equation,
2. pick a frequency-dependent scaling parameter  $\sigma : \Lambda \subset \mathbb{C} \rightarrow \mathbb{C} \setminus \{0\}$  and derive the according non-linear eigenvalue problem,
3. assemble the (in-)finite element matrices, and
4. solve the discrete non-linear eigenvalue problem.

We address the derivation of the weak formulation for three examples of exterior coordinates in Section 7.1 (see (7.3), (7.4), (7.5), (7.6), (7.7) and (7.8)).

In Section 7.2 we show how to derive eigenvalue problems that are rational in the frequency  $\omega$  for the given exterior coordinates from Section 7.1 and rational frequency-dependencies.

In Section 7.3 we give examples for choices of the frequency-dependency (see (7.14)). Moreover, for these frequency-dependencies, we explicitly calculate the subsets of the complex plane where the assumptions (S1) and (S2) are violated and therefore give descriptions for the possible location of the essential spectrum.

The task of assembling the (in-)finite element matrices is addressed in Section 7.4. For algorithms for the approximation of the eigenvalues and eigenfunctions of rational eigenvalue problems, we refer to Chapter 8.

In the following we assume that a suitable discretization of the interior domain  $\Omega_{\text{int}}$  and the interface  $\Gamma$  is already given (cf. Section 6.2.1) and merely focus on the discretization of the exterior domain  $\Omega_{\text{ext}}$ .

### 7.1. The complex-scaled Helmholtz equation in various exterior coordinates

In Chapter 5 we focused on the spherical scaling to present a detailed analysis. Since, in some configurations, it is advantageous to use different exterior coordinates and therefore different scalings, we give examples for the weak formulations of the complex-scaled Helmholtz equation for three different types of exterior coordinates.

To implement frequency-dependent complex scalings in exterior coordinates at least the weak formulation of the complex-scaled Helmholtz equation has to be known. We will

see that this means that we need explicit expressions of the inverse of the Jacobian of the coordinatization  $\Psi$  and its determinant. In the following we derive these expressions for a specific selection of exterior coordinates. Note that all of the following choices may be combined to create suitable exterior coordinates for a given problem, as long as the resulting exterior coordinates fulfill the assumptions (C1) and (C2). We emphasize that all the weak formulations in the following sections are still posed on infinite-dimensional spaces with infinite domains.

*Remark 7.1.* There are two reasons why we need an explicit expression of the inverse of the Jacobian of the complex scaling  $\check{\mathbf{x}}(\mathbf{x})$  and its determinant:

Firstly, due to the fact that we want to employ a suitable tensorization to assemble the discrete matrices, we need to split the respective sesquilinear forms into a generalized-radial and a surface part as in (6.1).

Secondly, we want to obtain a rational eigenvalue problem (as defined in Problem 8.1) to be able to apply the available efficient algorithms for rational or polynomial eigenvalue problems (see Chapter 8). Therefore, we need to derive a weak formulation of the complex-scaled equation which is a sum over rational functions in the frequency  $\omega$  times sesquilinear forms that are independent of  $\omega$ . Note that for a frequency-independent scaling this is always the case regardless of the choice of exterior coordinates.

Again we assume that the domains  $\Omega, \Omega_{\text{ext}}, \Omega_{\text{int}}, \Gamma$  are chosen such that the assumptions (D1–5) are fulfilled. Moreover, we assume that the mapping  $\mathbf{v}$  fulfills (C1) and (C2). We remind the reader that the exterior coordinatization  $\Psi : \mathbb{R}_{>0} \times \Gamma \rightarrow \Omega_{\text{ext}}$  is given by the mapping

$$\Psi(\xi, \hat{\mathbf{x}}) = \hat{\mathbf{x}} + \xi \mathbf{v}(\hat{\mathbf{x}}).$$

Since the choice of exterior coordinates is independent of the specific choice of the frequency-dependency of the scaling parameter  $\sigma(\cdot)$ , we omit this dependency in this section (except for Section 7.2) and simply write  $\sigma = \sigma(\omega)$ .

For the remainder of this section we use the following notation: Let  $M_j \subset \mathbb{R}^{d-1}$  and  $\varphi_j : M_j \subset \mathbb{R}^{d-1} \rightarrow \Gamma$  be an embedding (i.e., a diffeomorphism from  $M_j$  to  $\varphi_j(M_j)$ ). Then we define

$$\Psi_{\varphi_j} : \begin{cases} \mathbb{R}_{>0} \times M_j & \rightarrow \Omega_{\text{ext}}, \\ (\xi, \eta) & \mapsto \Psi(\xi, \varphi_j(\eta)). \end{cases} \quad (7.1)$$

Since  $\Gamma$  is a (piecewise smooth) manifold by assumption, there exists a family of embeddings such that  $\Gamma$  is covered. We define  $\Psi_{\varphi_j}^\sigma$  accordingly by

$$\Psi_{\varphi_j}^\sigma : \begin{cases} \mathbb{R}_{>0} \times M_j & \rightarrow \check{\Omega}_{\text{ext}}, \\ (\xi, \eta) & \mapsto \Psi^\sigma(\xi, \varphi_j(\eta)). \end{cases}$$

We emphasize that the embeddings  $\varphi_j$  are merely necessary for the derivation of the weak formulation and do not have to be known for the implementation of our method.

To, informally, derive a complex-scaled weak formulation of the Helmholtz resonance problem, we proceed as follows: Assume that  $(\omega, u)$  is an eigenpair of the strong formulation of the Helmholtz resonance problem (Problem 2.3) with homogeneous Neumann boundary



conditions on  $\partial\Omega$ . Moreover, we assume that  $u$  admits an analytic continuation  $U$  to some domain  $\Theta \subset \mathbb{C}^d$  such that  $\Omega_{\text{ext}} \subset \Theta$ ,  $\check{\Omega}_{\text{ext}} = \Psi^\sigma(\mathbb{R}_{>0}, \Gamma) \subset \Theta$  and such that  $U|_{\check{\Omega}_{\text{ext}}} \in H^1(\check{\Omega}_{\text{ext}})$ . We choose an analytic test function  $v : \Theta \rightarrow \mathbb{C}$  such that  $v|_{\Omega_{\text{ext}}} \in H^1(\Omega_{\text{ext}})$  and  $v|_{\check{\Omega}_{\text{ext}}} \in H^1(\check{\Omega}_{\text{ext}})$ . Then we multiply the homogeneous Helmholtz equation by  $\bar{v}$ , integrate over  $\Psi_{\varphi_j}(\mathbb{R}_{>0}, M_j)$ , and apply partial integration to obtain

$$\begin{aligned}
 0 &= \int_{\Psi_{\varphi_j}(\mathbb{R}_{>0}, M_j)} -\Delta u(\mathbf{x}) \overline{v(\mathbf{x})} - \omega^2 u(\mathbf{x}) \overline{v(\mathbf{x})} \, d\mathbf{x} \\
 &= \int_{\Psi_{\varphi_j}(\mathbb{R}_{>0}, M_j)} \nabla u(\mathbf{x}) \cdot \overline{\nabla v(\mathbf{x})} - \omega^2 u(\mathbf{x}) \overline{v(\mathbf{x})} \, d\mathbf{x} + \text{boundary terms} \\
 &= \int_{\mathbb{R}_{>0} \times M_j} \left( D\Psi_{\varphi_j}(\xi, \eta)^{-\top} \nabla u \circ \Psi_{\varphi_j}(\xi, \eta) \right) \cdot \left( D\Psi_{\varphi_j}(\xi, \eta)^{-\top} \overline{\nabla v \circ \Psi_{\varphi_j}(\xi, \eta)} \right) \\
 &\quad - \omega^2 u \circ \Psi_{\varphi_j}(\xi, \eta) \overline{v \circ \Psi_{\varphi_j}(\xi, \eta)} |\det(D\Psi_{\varphi_j}(\xi, \eta))| \, d(\xi, \eta) + \text{boundary terms}.
 \end{aligned} \tag{7.2}$$

The boundary terms vanish when we sum over sets  $M_j$  and embeddings  $\varphi_j$  for  $j$  in some index set  $J$  such that the sets  $\Psi_{\varphi_j}(\mathbb{R}_{>0}, M_j)$  are a disjoint decomposition of  $\Omega_{\text{ext}}$  and couple the exterior to the interior equation. If the integrand in (7.2) is holomorphic on a large enough complex domain, instead of integrating over  $\mathbb{R}_{>0}$ , we can integrate over the complex path  $\sigma\mathbb{R}_{>0}$  and obtain

$$\begin{aligned}
 0 &= \int_{\mathbb{R}_{>0} \times M} \sigma \left( \begin{pmatrix} \frac{1}{\sigma} & 0 \\ 0 & \mathbf{I} \end{pmatrix} D\Psi_{\varphi_j}(\sigma\xi, \eta)^{-\top} \nabla u \circ \Psi_{\varphi_j}(\sigma\xi, \eta) \right) \cdot \left( \begin{pmatrix} \frac{1}{\sigma} & 0 \\ 0 & \mathbf{I} \end{pmatrix} D\Psi_{\varphi_j}(\sigma\xi, \eta)^{-\top} \overline{\nabla v \circ \Psi_{\varphi_j}(\sigma\xi, \eta)} \right) \\
 &\quad - \omega^2 \sigma u \circ \Psi_{\varphi_j}(\sigma\xi, \eta) \overline{v \circ \Psi_{\varphi_j}(\sigma\xi, \eta)} r(\det(D\Psi_{\varphi_j}(\sigma\xi, \eta))) \, d(\xi, \eta) + \text{boundary terms},
 \end{aligned}$$

where  $r(\cdot)$  again denotes the analytic continuation of the modulus as in Remark 3.10.

The considerations above tell us that, to obtain a complex-scaled weak formulation in exterior coordinates, we need to explicitly determine the expressions

$$\left( D\Psi_{\varphi_j}(\xi, \eta) \right)^{-1}, \quad \det(D\Psi_{\varphi_j}(\xi, \eta)).$$

In the following sections we will perform these calculations for three different sets of coordinates.

To enhance the readability of the formulas, in the following sections, unlike in the previous sections, we write down the exterior sesquilinear forms for functions  $f, g : \mathbb{R}_{>0} \times \Gamma \rightarrow \mathbb{C}$  such that  $f \circ \Psi^{-1}, g \circ \Psi^{-1} \in H^1(\Omega_{\text{ext}})$ .

### 7.1.1. Uni-directional coordinates

A very simple example of (local) exterior coordinates are coordinates where the direction of the generalized-radial variable is constant (see Figure 7.1). Obviously, using one constant direction of the generalized-radial variable cannot lead to a parametrization of the whole exterior domain. Nevertheless, if this mapping is combined with suitable other exterior coordinates, it can lead to a useful complex scaling.

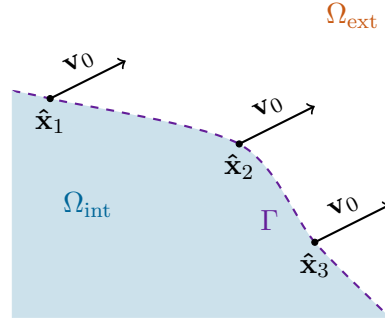


Figure 7.1.: An example for uni-directional coordinates in two dimensions.

**Definition 7.2.** We call exterior coordinates, as defined in Definition 3.1<sup>1</sup>, *uni-directional* on  $\Gamma_1 \subset \Gamma$  if  $\mathbf{v}(\hat{\mathbf{x}}) \equiv \mathbf{v}_0$  for some  $\mathbf{v}_0 \in \mathbb{R}^d$  and all  $\hat{\mathbf{x}} \in \Gamma_1$ .

For a given vector  $\mathbf{v}_0$  and a set  $\Gamma_1 \subset \Gamma$  to be local exterior coordinates, the restriction posed by assumption (C1) is that  $\mathbf{v}_0 \cdot \mathbf{n}(\hat{\mathbf{x}}) > 0$  for all  $\hat{\mathbf{x}} \in \Gamma_1$ . Assumption (C2) in general means that we require a sufficiently large distance between  $\Gamma_0$  and  $\Gamma_1$ .

**Theorem 7.3.** *The derivative of  $\Psi_{\varphi_j}$  for uni-directional coordinates given by Definition 7.2, its inverse, and its determinant can be calculated by*

$$\begin{aligned} D\Psi_{\varphi_j}(\xi, \eta) &= (\mathbf{v}_0, D\varphi_j(\eta)), \\ (D\Psi_{\varphi_j}(\xi, \eta))^{-1} &= \frac{1}{\mathbf{v}_0 \cdot \mathbf{n}(\varphi_j(\eta))} \begin{pmatrix} \mathbf{n}(\varphi_j(\eta))^\top \\ D\varphi_j(\eta)^\dagger \left( \mathbf{v}_0 \cdot \mathbf{n}(\varphi_j(\eta)) \mathbf{I}_d - \mathbf{v}_0 \mathbf{n}(\varphi_j(\eta))^\top \right) \end{pmatrix}, \\ \det D\Psi_{\varphi_j}(\xi, \eta) &= \sqrt{\det \left( D\varphi_j(\eta)^\top D\varphi_j(\eta) \right)} \mathbf{v}_0 \cdot \mathbf{n}(\varphi_j(\eta)). \end{aligned}$$

*Proof.* We use Corollary A.16 for the matrix  $(\mathbf{v}_0, D\varphi_j(\eta))$ , the facts that  $\mathbf{n}(\hat{\mathbf{x}}(\eta))$  is normalized and orthogonal to the columns of  $D\varphi_j(\eta)$  for  $\eta \in M_j$ , and  $\mathbf{v}_0 \cdot \mathbf{n} > 0$ .  $\square$

Using Theorem 7.3 we can compute the gradient in uni-directional coordinates of a function  $f \in C^1(\Omega_{\text{ext}})$  at a point  $\Psi(\xi, \hat{\mathbf{x}})$  by (see (1.8))

$$\nabla f(\Psi(\xi, \hat{\mathbf{x}})) = \frac{\mathbf{n}(\hat{\mathbf{x}})}{\mathbf{n}(\hat{\mathbf{x}}) \cdot \mathbf{v}_0} \frac{\partial f \circ \Psi}{\partial \xi}(\xi, \hat{\mathbf{x}}) + \left( \mathbf{I}_d - \frac{\mathbf{n}(\hat{\mathbf{x}}) \mathbf{v}_0^\top}{\mathbf{n}(\hat{\mathbf{x}}) \cdot \mathbf{v}_0} \right) \hat{\nabla} f \circ \Psi(\xi, \hat{\mathbf{x}}).$$

Thus, we can state the exterior part of the sesquilinear form of the weak formulation of the

<sup>1</sup>Here we have to weaken the assumption (C1) from  $\Psi$  being a bijective onto  $\Omega_{\text{ext}}$  to the assumption of  $\Psi : \mathbb{R}_{>0} \times \Gamma_1 \rightarrow \Omega_{\text{ext}}$  being a bijection onto a suitable subset of  $\Omega_{\text{ext}}$ .

complex-scaled Helmholtz equation in uni-directional coordinates by

$$\begin{aligned}
 a_\sigma^{\text{uni}}(\omega)(f, g) &:= \frac{1}{\sigma} \int_{\mathbb{R}_{>0} \times \Gamma_1} \frac{1}{\mathbf{n}(\hat{\mathbf{x}}) \cdot \mathbf{v}_0} \frac{\partial}{\partial \xi} f(\xi, \hat{\mathbf{x}}) \overline{\frac{\partial}{\partial \xi} g(\xi, \hat{\mathbf{x}})} d(\xi, \hat{\mathbf{x}}) \\
 &\quad - \int_{\mathbb{R}_{>0} \times \Gamma_1} \frac{\mathbf{v}_0}{\mathbf{n}(\hat{\mathbf{x}}) \cdot \mathbf{v}_0} \cdot \left( \hat{\nabla}(f(\xi, \hat{\mathbf{x}})) \overline{\frac{\partial}{\partial \xi} g(\xi, \hat{\mathbf{x}})} \right) d(\xi, \hat{\mathbf{x}}) \\
 &\quad - \int_{\mathbb{R}_{>0} \times \Gamma_1} \frac{\mathbf{v}_0}{\mathbf{n}(\hat{\mathbf{x}}) \cdot \mathbf{v}_0} \cdot \left( f(\xi, \hat{\mathbf{x}}) \overline{\hat{\nabla}(g(\xi, \hat{\mathbf{x}}))} \right) d(\xi, \hat{\mathbf{x}}) \\
 &\quad + \sigma \int_{\mathbb{R}_{>0} \times \Gamma_1} \left( \hat{\nabla} f(\xi, \hat{\mathbf{x}}) \right)^\top \left( \mathbf{n}(\hat{\mathbf{x}}) \cdot \mathbf{v}_0 \mathbf{I}_d + \frac{\mathbf{v}_0 \mathbf{v}_0^\top}{\mathbf{n}(\hat{\mathbf{x}}) \cdot \mathbf{v}_0} \right) \overline{\hat{\nabla} g(\xi, \hat{\mathbf{x}})} d(\xi, \hat{\mathbf{x}}) \\
 &\quad - \omega^2 \sigma \int_{\mathbb{R}_{>0} \times \Gamma_1} \mathbf{n}(\hat{\mathbf{x}}) \cdot \mathbf{v}_0 f(\xi, \hat{\mathbf{x}}) \overline{g(\xi, \hat{\mathbf{x}})} d(\xi, \hat{\mathbf{x}})
 \end{aligned} \tag{7.3}$$

for  $f, g : \mathbb{R}_{>0} \times \Gamma_1$  such that  $f \circ \Psi^{-1}, g \circ \Psi^{-1} \in H^1(\Omega_{\text{ext}})$ .

For  $d = 2$  we can simplify the term

$$\begin{aligned}
 &\int_{\mathbb{R}_{>0} \times \Gamma_1} \left( \hat{\nabla} f(\xi, \hat{\mathbf{x}}) \right)^\top \left( \mathbf{n}(\hat{\mathbf{x}}) \cdot \mathbf{v}_0 \mathbf{I}_2 + \frac{\mathbf{v}_0 \mathbf{v}_0^\top}{\mathbf{n}(\hat{\mathbf{x}}) \cdot \mathbf{v}_0} \right) \overline{\hat{\nabla} g(\xi, \hat{\mathbf{x}})} d(\xi, \hat{\mathbf{x}}) \\
 &= \int_{\mathbb{R}_{>0} \times \Gamma_1} \frac{\|\mathbf{v}_0\|^2}{\mathbf{n}(\hat{\mathbf{x}}) \cdot \mathbf{v}_0} \hat{\nabla} f(\xi, \hat{\mathbf{x}}) \cdot \overline{\hat{\nabla} g(\xi, \hat{\mathbf{x}})} d(\xi, \hat{\mathbf{x}}).
 \end{aligned}$$

To implement this scaling and assemble the corresponding matrices, the surface gradient  $\hat{\nabla}$  and the normal vector  $\mathbf{n}(\hat{\mathbf{x}})$  have to be evaluated at  $\hat{\mathbf{x}} \in \Gamma_1$ .

*Remark 7.4.* A very popular version of the complex scaling method is to use so-called cartesian scalings (see, e.g., [BP13]). Linear, cartesian scalings for  $d = 2$  and  $\Omega_{\text{int}} = [-1, 1] \times [-1, 1]$  are given by

$$\check{\mathbf{x}}(\mathbf{x}) = (\check{x}(x, y), \check{y}(x, y))^\top = \begin{pmatrix} x + \sigma(x-1)\chi_{\mathbb{R}_{\geq 1}}(x) + \sigma(x+1)\chi_{\mathbb{R}_{\leq -1}}(x) \\ y + \sigma(y-1)\chi_{\mathbb{R}_{\geq 1}}(y) + \sigma(y+1)\chi_{\mathbb{R}_{\leq -1}}(y) \end{pmatrix},$$

where  $\chi_M$  denotes the indicator function of a set  $M$ . Apart from the corner regions  $\{(x, y) \in \mathbb{R}^2 : |x|, |y| > 1\}$ , the cartesian scaling can be written in uni-directional coordinates where  $\mathbf{v}$  are the unit vectors in positive/negative  $x$  and  $y$  directions. In the corner regions, on the other hand, writing cartesian scalings in exterior coordinates is not possible due to the fact that the boundary corresponding to a corner region contains the corner point only. A possible workaround is to choose  $\Gamma_1$  as a curve inside of  $\Omega_{\text{ext}}$ , parallel to  $\Gamma$ , and with some suitable connection in the corner regions (e.g., quarter circles or straight lines) and allow also negative values of  $\xi$ . However, in this case coupling the interior to the exterior space is more involved.

### 7.1.2. Star-shaped coordinates

Star-shaped coordinates are a generalization of polar coordinates and are also used in [Hal16]. They describe the domain  $\Omega_{\text{ext}}$  by a surface coordinate and a generalized-radial

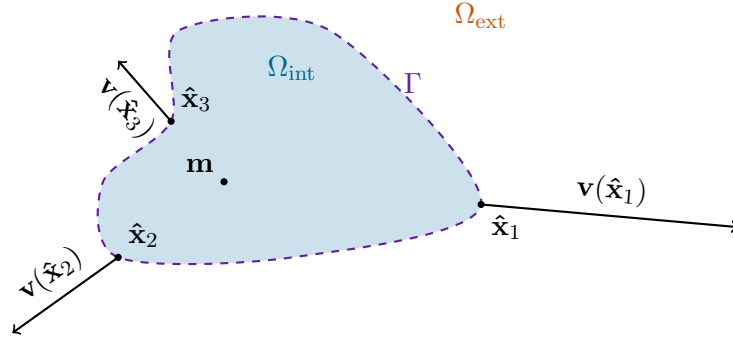


Figure 7.2.: An example for star-shaped coordinates in two dimensions.

coordinate with respect to some origin  $\mathbf{m} \in \Omega_{\text{int}}$  (see Figure 7.2). They have the property that, similar to the case of uni-directional coordinates (Section 7.1.3), only the normal vector  $\mathbf{n}(\hat{\mathbf{x}})$  has to be evaluated on the boundary. Moreover, they can be applied to cases where  $\Omega_{\text{int}}$  is star-shaped, whereas curvilinear coordinates (Section 7.1.3) can only be applied to cases where  $\Omega_{\text{int}}$  is convex. Nevertheless, for condition (C2) to hold it is, in general, necessary that there is a sufficient distance between  $\Gamma_0$  and  $\Gamma$ .

**Definition 7.5.** We call exterior coordinates, as given in Definition 3.1, *star-shaped* if  $\mathbf{v}(\hat{\mathbf{x}}) = \hat{\mathbf{x}} - \mathbf{m}$  for some point  $\mathbf{m} \in \Omega_{\text{int}}$ .

Again the inverse of the Jacobian and its determinant can be calculated directly.

**Theorem 7.6.** For star-shaped coordinates the derivative of  $\Psi_{\varphi_j}$ , its inverse, and its determinant can be calculated by

$$\begin{aligned}
 D\Psi_{\varphi_j}(\xi, \eta) &= (\varphi_j(\eta) - \mathbf{m}, (1 + \xi)D\varphi_j(\eta)), \\
 (D\Psi_{\varphi_j}(\xi, \eta))^{-1} &= \frac{1}{\mathbf{v}(\varphi_j(\eta)) \cdot \mathbf{n}(\varphi_j(\eta))} \begin{pmatrix} \mathbf{n}(\varphi_j(\eta))^\top \\ \frac{1}{1+\xi}D\varphi_j(\eta)^\top \left( \mathbf{v}(\varphi_j(\eta)) \cdot \mathbf{n}(\varphi_j(\eta)) \mathbf{I}_d - \mathbf{v}(\varphi_j(\eta)) \mathbf{n}(\varphi_j(\eta))^\top \right) \end{pmatrix}, \\
 \det D\Psi_{\varphi_j}(\xi, \eta) &= \sqrt{\det \left( D\varphi_j(\eta)^\top D\varphi_j(\eta) \right)} (1 + \xi)^{d-1} \mathbf{v}(\varphi_j(\eta)) \cdot \mathbf{n}(\varphi_j(\eta)).
 \end{aligned}$$

*Proof.* We use Corollary A.16 for the matrix

$$D\Psi_{\varphi_j}(\xi, \eta) = (\varphi_j(\eta) - \mathbf{m}, (1 + \xi)D\varphi_j(\eta))$$

and the fact that  $\mathbf{n}(\eta)$  is normalized and orthogonal to the columns of  $\varphi_j(\eta)$ .  $\square$

Similar to before we can calculate the according sesquilinear form

$$\begin{aligned}
 a_{\sigma}^{\text{star}}(\omega)(f, g) &:= \frac{1}{\sigma} \int_{\mathbb{R}_{>0} \times \Gamma} \frac{(1 + \sigma\xi)^{d-1}}{\mathbf{n}(\hat{\mathbf{x}}) \cdot \mathbf{v}(\hat{\mathbf{x}})} \frac{\partial}{\partial \xi} f(\xi, \hat{\mathbf{x}}) \overline{\frac{\partial}{\partial \xi} g(\xi, \hat{\mathbf{x}})} d(\xi, \hat{\mathbf{x}}) \\
 &\quad - \int_{\mathbb{R}_{>0} \times \Gamma} \frac{(1 + \sigma\xi)^{d-2} \mathbf{v}(\hat{\mathbf{x}})}{\mathbf{n}(\hat{\mathbf{x}}) \cdot \mathbf{v}(\hat{\mathbf{x}})} \cdot \left( \hat{\nabla}(f(\xi, \hat{\mathbf{x}})) \right) \overline{\frac{\partial}{\partial \xi} g(\xi, \hat{\mathbf{x}})} d(\xi, \hat{\mathbf{x}}) \\
 &\quad - \int_{\mathbb{R}_{>0} \times \Gamma} \frac{(1 + \sigma\xi)^{d-2} \mathbf{v}(\hat{\mathbf{x}})}{\mathbf{n}(\hat{\mathbf{x}}) \cdot \mathbf{v}(\hat{\mathbf{x}})} \cdot \left( \frac{\partial}{\partial \xi} f(\xi, \hat{\mathbf{x}}) \overline{\hat{\nabla}(g(\xi, \hat{\mathbf{x}}))} \right) d(\xi, \hat{\mathbf{x}}) \\
 &\quad + \sigma \int_{\mathbb{R}_{>0} \times \Gamma} (1 + \sigma\xi)^{d-3} \left( \hat{\nabla} f(\xi, \hat{\mathbf{x}}) \right)^{\top} \left( \mathbf{I}_d \mathbf{n}(\hat{\mathbf{x}}) \cdot \mathbf{v}(\hat{\mathbf{x}}) + \frac{\mathbf{v}(\hat{\mathbf{x}}) \mathbf{v}(\hat{\mathbf{x}})^{\top}}{\mathbf{n}(\hat{\mathbf{x}}) \cdot \mathbf{v}(\hat{\mathbf{x}})} \right) \overline{\hat{\nabla} g(\xi, \hat{\mathbf{x}})} d(\xi, \hat{\mathbf{x}}) \\
 &\quad - \omega^2 \sigma \int_{\mathbb{R}_{>0} \times \Gamma} (1 + \sigma\xi)^{d-1} \mathbf{n}(\hat{\mathbf{x}}) \cdot \mathbf{v}(\hat{\mathbf{x}}) f(\xi, \hat{\mathbf{x}}) \overline{g(\xi, \hat{\mathbf{x}})} d(\xi, \hat{\mathbf{x}})
 \end{aligned} \tag{7.4}$$

for  $f, g : \mathbb{R}_{>0} \times \Gamma$  such that  $f \circ \Psi^{-1}, g \circ \Psi^{-1} \in H^1(\Omega_{\text{ext}})$ . Again, similar to the case of uni-directional coordinates, the sesquilinear form for  $d = 2$  can be simplified by

$$\begin{aligned}
 a_{\sigma}^{\text{star},2}(\omega)(f, g) &:= \frac{1}{\sigma} \int_{\mathbb{R}_{>0} \times \Gamma} \frac{1 + \sigma\xi}{\mathbf{n}(\hat{\mathbf{x}}) \cdot \mathbf{v}(\hat{\mathbf{x}})} \frac{\partial}{\partial \xi} f(\xi, \hat{\mathbf{x}}) \overline{\frac{\partial}{\partial \xi} g(\xi, \hat{\mathbf{x}})} d(\xi, \hat{\mathbf{x}}) \\
 &\quad - \int_{\mathbb{R}_{>0} \times \Gamma} \frac{\mathbf{v}(\hat{\mathbf{x}})}{\mathbf{n}(\hat{\mathbf{x}}) \cdot \mathbf{v}(\hat{\mathbf{x}})} \cdot \left( \hat{\nabla}(f(\xi, \hat{\mathbf{x}})) \right) \overline{\frac{\partial}{\partial \xi} g(\xi, \hat{\mathbf{x}})} d(\xi, \hat{\mathbf{x}}) \\
 &\quad - \int_{\mathbb{R}_{>0} \times \Gamma} \frac{\mathbf{v}(\hat{\mathbf{x}})}{\mathbf{n}(\hat{\mathbf{x}}) \cdot \mathbf{v}(\hat{\mathbf{x}})} \cdot \left( \frac{\partial}{\partial \xi} f(\xi, \hat{\mathbf{x}}) \overline{\hat{\nabla}(g(\xi, \hat{\mathbf{x}}))} \right) d(\xi, \hat{\mathbf{x}}) \\
 &\quad + \sigma \int_{\mathbb{R}_{>0} \times \Gamma} \frac{\|\mathbf{v}(\hat{\mathbf{x}})\|^2}{\mathbf{n}(\hat{\mathbf{x}}) \cdot \mathbf{v}(\hat{\mathbf{x}}) (1 + \sigma\xi)} \left( \hat{\nabla} f(\xi, \hat{\mathbf{x}}) \right)^{\top} \cdot \overline{\hat{\nabla} g(\xi, \hat{\mathbf{x}})} d(\xi, \hat{\mathbf{x}}) \\
 &\quad - \omega^2 \sigma \int_{\mathbb{R}_{>0} \times \Gamma} (1 + \sigma\xi) \mathbf{n}(\hat{\mathbf{x}}) \cdot \mathbf{v}(\hat{\mathbf{x}}) f(\xi, \hat{\mathbf{x}}) \overline{g(\xi, \hat{\mathbf{x}})} d(\xi, \hat{\mathbf{x}}).
 \end{aligned} \tag{7.5}$$

*Remark 7.7.* The polar or spherical coordinates, used in Chapter 5 for the analysis of our method, are a special case of both, curvilinear and star-shaped coordinates with  $\Gamma = B_1$ . Plugging  $\mathbf{n}(\hat{\mathbf{x}}) = \mathbf{v}(\hat{\mathbf{x}}) = \hat{\mathbf{x}}$  into (7.4) gives

$$\begin{aligned}
 a_{\sigma}^{\text{polar}}(\omega)(f, g) &:= \frac{1}{\sigma} \int_{\mathbb{R}_{>0} \times \Gamma} (1 + \sigma\xi)^{d-1} \frac{\partial}{\partial \xi} f(\xi, \hat{\mathbf{x}}) \overline{\frac{\partial}{\partial \xi} g(\xi, \hat{\mathbf{x}})} d(\xi, \hat{\mathbf{x}}) \\
 &\quad + \sigma \int_{\mathbb{R}_{>0} \times \Gamma} (1 + \sigma\xi)^{d-3} \hat{\nabla} f(\xi, \hat{\mathbf{x}}) \cdot \overline{\hat{\nabla} g(\xi, \hat{\mathbf{x}})} d(\xi, \hat{\mathbf{x}}) \\
 &\quad - \omega^2 \sigma \int_{\mathbb{R}_{>0} \times \Gamma} (1 + \sigma\xi)^{d-1} f(\xi, \hat{\mathbf{x}}) \overline{g(\xi, \hat{\mathbf{x}})} d(\xi, \hat{\mathbf{x}}),
 \end{aligned} \tag{7.6}$$

since in this case  $\mathbf{v}$  is orthogonal to the surface gradient of a function.

### 7.1.3. Curvilinear coordinates

Curvilinear coordinates have also been used in [LS01]. They are based on the description of a point  $\mathbf{x} \in \Omega_{\text{ext}}$  by a normal and a tangential variable with respect to the boundary  $\Gamma$  (see Figure 7.3).

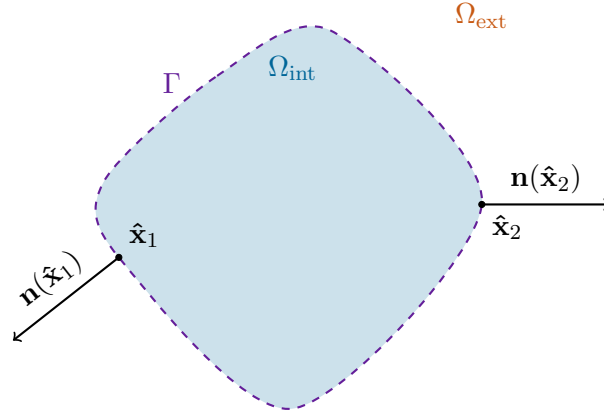


Figure 7.3.: An example for curvilinear coordinates in two dimensions.

**Definition 7.8.** We call exterior coordinates, as in Definition 3.1, *curvilinear* if  $\mathbf{v}(\hat{\mathbf{x}}) = \mathbf{n}(\hat{\mathbf{x}})$ .

Contrary to uni-directional (Section 7.1.1) and star-shaped (Section 7.1.2) coordinates where only the normal vector  $\mathbf{n}$  has to be evaluated on the boundary, when using curvilinear coordinates one also has to evaluate the curvature of  $\Gamma$ . Moreover, for assumption (C1) to be fulfilled  $\Omega_{\text{int}}$  has to be convex and the normal vector  $\mathbf{n}$  has to be continuous, (i.e.,  $\Gamma$  has to be at least  $C^1$ ). Assumption (C2), on the other hand, is always fulfilled for curvilinear coordinates.

For the remainder of this section we assume that the embeddings  $\varphi_j$  are such that the columns of its derivative

$$D\varphi_j(\eta) := (\mathbf{t}_1(\eta), \dots, \mathbf{t}_{d-1}(\eta)),$$

are orthonormal. Note that in this case we have

$$D\varphi_j(\eta)^\top D\varphi_j(\eta) = \mathbf{I}_{d-1}.$$

Then we can rewrite the derivative of the normal vector by

$$D\mathbf{n}(\eta) = (\kappa_1(\eta) \mathbf{t}_1(\eta), \dots, \kappa_{d-1}(\eta) \mathbf{t}_{d-1}(\eta))$$

for some functions  $\kappa_j$ . The functions  $\kappa_j$  are known as the main curvatures of the manifold  $\Gamma$ .

**Theorem 7.9.** For curvilinear coordinates, the derivative of  $\Psi_{\varphi_j}$ , its inverse, and its determinant can be calculated by

$$\begin{aligned} D\Psi_{\varphi_j}(\xi, \eta) &= (\mathbf{n}(\eta), (1 + \xi\kappa_1(\eta))\mathbf{t}_1(\eta), \dots, (1 + \xi\kappa_{d-1}(\eta))\mathbf{t}_{d-1}(\eta)), \\ (D\Psi_{\varphi_j}(\xi, \eta))^{-1} &= \left( \mathbf{n}(\eta), \frac{1}{1 + \xi\kappa_1(\eta)}\mathbf{t}_1(\eta), \dots, \frac{1}{1 + \xi\kappa_{d-1}(\eta)}\mathbf{t}_{d-1}(\eta) \right)^\top, \\ \det D\Psi_{\varphi_j}(\xi, \eta) &= \prod_{i=1}^{d-1} (1 + \xi\kappa_i(\eta)). \end{aligned}$$

*Proof.* The claim follows immediately from straightforward calculations and the fact that the columns of  $D\Psi_{\varphi_j}(\xi, \eta)$  are orthonormal.  $\square$

Using Theorem 7.9 we can calculate the gradient of a function  $f \in C^1(\Omega_{\text{ext}})$  in curvilinear coordinates at a point  $\Psi(\xi, \hat{\mathbf{x}})$  by

$$\nabla f(\Psi(\xi, \hat{\mathbf{x}})) = \mathbf{n}(\xi) \frac{\partial f \circ \Psi}{\partial \xi}(\xi, \hat{\mathbf{x}}) + \sum_{j=1}^{d-1} \frac{\mathbf{t}_j(\hat{\mathbf{x}}) \mathbf{t}_j(\hat{\mathbf{x}})^\top}{1 + \kappa_j(\hat{\mathbf{x}})} \hat{\nabla} f \circ \Psi(\xi, \hat{\mathbf{x}}).$$

The according sesquilinear form for  $d = 2$  is given by

$$\begin{aligned} a_\sigma^{\text{curv},2}(\omega)(f, g) &:= \frac{1}{\sigma} \int_{\mathbb{R}_{>0} \times \Gamma} (1 + \sigma \xi \kappa(\hat{\mathbf{x}})) \frac{\partial f}{\partial \xi}(\xi, \hat{\mathbf{x}}) \overline{\frac{\partial g}{\partial \xi}(\xi, \hat{\mathbf{x}})} d(\xi, \hat{\mathbf{x}}) \\ &\quad + \sigma \int_{\mathbb{R}_{>0} \times \Gamma} \frac{1}{1 + \sigma \xi \kappa(\hat{\mathbf{x}})} \hat{\nabla} f(\xi, \hat{\mathbf{x}}) \cdot \overline{\hat{\nabla} g(\xi, \hat{\mathbf{x}})} d(\xi, \hat{\mathbf{x}}) \\ &\quad - \omega^2 \sigma \int_{\mathbb{R}_{>0} \times \Gamma} (1 + \sigma \xi \kappa(\hat{\mathbf{x}})) f(\xi, \hat{\mathbf{x}}) \overline{g(\xi, \hat{\mathbf{x}})} d(\xi, \hat{\mathbf{x}}), \end{aligned} \quad (7.7)$$

where we used the notation  $\kappa := \kappa_1$  since we only have one main curvature. For  $d = 3$ , we obtain

$$\begin{aligned} a_\sigma^{\text{curv},3}(\omega)(f, g) &:= \frac{1}{\sigma} \int_{\mathbb{R}_{>0} \times \Gamma} (1 + \sigma \xi \kappa_1(\hat{\mathbf{x}}))(1 + \sigma \xi \kappa_2(\hat{\mathbf{x}})) \frac{\partial f}{\partial \xi}(\xi, \hat{\mathbf{x}}) \overline{\frac{\partial g}{\partial \xi}(\xi, \hat{\mathbf{x}})} d(\xi, \hat{\mathbf{x}}) \\ &\quad + \sigma \int_{\mathbb{R}_{>0} \times \Gamma} \frac{(1 + \sigma \xi \kappa_2(\hat{\mathbf{x}}))}{1 + \sigma \xi \kappa_1(\hat{\mathbf{x}})} \mathbf{t}_1(\hat{\mathbf{x}}) \cdot \hat{\nabla} f(\xi, \hat{\mathbf{x}}) \mathbf{t}_1(\hat{\mathbf{x}}) \cdot \overline{\hat{\nabla} g(\xi, \hat{\mathbf{x}})} d(\xi, \hat{\mathbf{x}}) \\ &\quad + \sigma \int_{\mathbb{R}_{>0} \times \Gamma} \frac{(1 + \sigma \xi \kappa_1(\hat{\mathbf{x}}))}{1 + \sigma \xi \kappa_2(\hat{\mathbf{x}})} \mathbf{t}_2(\hat{\mathbf{x}}) \cdot \hat{\nabla} f(\xi, \hat{\mathbf{x}}) \mathbf{t}_2(\hat{\mathbf{x}}) \cdot \overline{\hat{\nabla} g(\xi, \hat{\mathbf{x}})} d(\xi, \hat{\mathbf{x}}) \\ &\quad - \omega^2 \sigma \int_{\mathbb{R}_{>0} \times \Gamma} (1 + \sigma \xi \kappa_1(\hat{\mathbf{x}}))(1 + \sigma \xi \kappa_2(\hat{\mathbf{x}})) f(\xi, \hat{\mathbf{x}}) \overline{g(\xi, \hat{\mathbf{x}})} d(\xi, \hat{\mathbf{x}}). \end{aligned} \quad (7.8)$$

*Remark 7.10.* Unlike in the case of uni-directional or star-shaped coordinates, for the implementation of a complex scaling in curvilinear exterior coordinates and  $d = 2$ , also the curvature  $\kappa$  needs to be provided. For  $d = 3$ , apart from the curvatures  $\kappa_1, \kappa_2$ , also the tangential vectors  $\mathbf{t}_1, \mathbf{t}_2$  are needed. All this information is contained in the Weingarten tensor ([DE13, Definition 2.5])

$$\mathbf{W}(\hat{\mathbf{x}}) := \hat{\nabla} \mathbf{n}(\hat{\mathbf{x}})$$

since the eigenvalues and eigenvectors of  $\mathbf{W}(\hat{\mathbf{x}})$  are  $0, \kappa_1(\hat{\mathbf{x}}), \kappa_2(\hat{\mathbf{x}})$  and  $\mathbf{n}(\hat{\mathbf{x}}), \mathbf{t}_1(\hat{\mathbf{x}}), \mathbf{t}_2(\hat{\mathbf{x}})$ . Thus, a possible way to approximate the curvatures and tangential vectors if the normal vector is available is to project the normal vector onto the discrete surface space  $\mathcal{X} \subset H^1(\Gamma)$  (Section 6.2.2) and use a discrete gradient.

## 7.2. Derivation of rational eigenvalue problems

In the previous section we have derived explicit expressions for the exterior sesquilinear form  $a_{\text{ext}}(\omega)$  in various exterior coordinates. The goal of this section is to transform the

exterior bilinear forms from Section 7.1 into the following form: Let  $\Lambda \subset \mathbb{C} \rightarrow \mathbb{C} \setminus \{0\}$  be a given frequency-dependency and  $f, g \in H^1(\Omega)$  such that they allow a decomposition in  $\Omega_{\text{ext}}$  into

$$f \circ \Psi(\xi, \hat{\mathbf{x}}) = \tilde{f}(\xi) \hat{f}(\hat{\mathbf{x}}), \quad g \circ \Psi(\xi, \hat{\mathbf{x}}) = \tilde{g}(\xi) \hat{g}(\hat{\mathbf{x}})$$

for some functions  $\tilde{f}, \tilde{g} : \mathbb{R}_{>0} \rightarrow \mathbb{C}$  and  $\hat{f}, \hat{g} : \Gamma \rightarrow \mathbb{C}$ . Then we assume that we can decompose the exterior part of the sesquilinear form function  $a_\sigma$  into

$$a_{\text{ext}}(\omega)(f, g) = \sum_{j=0}^J \gamma_j(\omega) \tilde{a}_j(\tilde{f}, \tilde{g}) \hat{a}_j(\hat{f}, \hat{g}), \quad (7.9)$$

for some  $J \in \mathbb{N}_0$ , sesquilinear forms  $\tilde{a}_j, \hat{a}_j$ , acting on functions on  $\mathbb{R}_{>0}$  and  $\Gamma$  respectively, and rational functions  $\gamma_j : \Lambda \rightarrow \mathbb{C}$ . We require the generalized-radial and surface sesquilinear forms  $\tilde{a}_j$  and  $\hat{a}_j$  to be independent of  $\omega$ .

This decomposition is necessary for two reasons (cf. Remark 7.1):

- To be able to assemble the matrices for the exterior problem by a suitable tensorization of matrices, corresponding to the generalized-radial parts  $\tilde{a}_j$  and matrices corresponding to the surface parts  $\hat{a}_j$ , we already required the exterior bilinear form of the complex-scaled Helmholtz problem to be of the form (6.1), which is a weaker assumption than (7.9).
- While there exist methods to approximate or solve matrix eigenvalue problems with a general holomorphic dependency of the matrix function on the eigenvalue parameter, we shall see in Chapter 8 that it is considerably less computationally expensive to consider rational eigenvalue problems. A Galerkin discretization, as in Section 6.1, of the eigenvalue problem corresponding to a sesquilinear form of the form (7.9) leads to a rational eigenvalue problem, in the sense of Problem 8.1.

For the use of a frequency-independent complex scaling in exterior coordinates only assumption (6.1) has to be met.

### 7.2.1. Uni-directional coordinates

If we assume a rational frequency-dependency  $\sigma(\cdot)$ , the sesquilinear form (7.3) is already of the form (7.9). Thus, it can immediately be used for assembling the discretization matrices and we obtain a rational eigenvalue problem (Problem 8.1).

### 7.2.2. Star-shaped coordinates

For a rational function  $\sigma(\cdot)$  the exterior sesquilinear form for star-shaped coordinates for  $d = 3$  (see (7.4)) is of the form (7.9) after an expansion of the factors  $(1 + \sigma(\omega) \xi)^2$ .

For  $d = 2$ , on the other hand, the sesquilinear form  $a_\sigma^{\text{star}}$  (see (7.5)) merely fulfills assumption (6.1) of Chapter 6 (i.e., it can be decomposed into a generalized-radial and a surface part). Due to the factor  $\frac{1}{1 + \sigma(\omega) \xi}$  it cannot be decomposed as in (7.9) and therefore does not lead to a rational eigenvalue problem in the sense of Chapter 8 (Problem 8.1).



To obtain a rational problem in this case, one can scale the solution (or trial function) and the test function in  $\Omega_{\text{ext}}$  by the factor  $(1 + \xi(\mathbf{x}))^{1/2}$  before applying the complex scaling. An application of the product rule leads to the sesquilinear form

$$\begin{aligned}
 a_{\sigma}^{\text{star sc.}}(\omega)(f, g) &:= \frac{1}{\sigma(\omega)} \int_{\mathbb{R}_{>0} \times \Gamma} \frac{(1 + \sigma(\omega) \xi)^2}{\mathbf{n}(\hat{\mathbf{x}}) \cdot \mathbf{v}(\hat{\mathbf{x}})} \frac{\partial}{\partial \xi} f(\xi, \hat{\mathbf{x}}) \overline{\frac{\partial}{\partial \xi} g(\xi, \hat{\mathbf{x}})} d(\xi, \hat{\mathbf{x}}) \\
 &\quad - \frac{\sigma(\omega)}{4} \int_{\mathbb{R}_{>0} \times \Gamma} \frac{1}{\mathbf{n}(\hat{\mathbf{x}}) \cdot \mathbf{v}(\hat{\mathbf{x}})} f(\xi, \hat{\mathbf{x}}) \overline{g(\xi, \hat{\mathbf{x}})} d(\xi, \hat{\mathbf{x}}) \\
 &\quad - \int_{\mathbb{R}_{>0} \times \Gamma} \frac{(1 + \sigma(\omega) \xi) \mathbf{v}(\hat{\mathbf{x}})}{\mathbf{n}(\hat{\mathbf{x}}) \cdot \mathbf{v}(\hat{\mathbf{x}})} \cdot \left( \hat{\nabla} f(\xi, \hat{\mathbf{x}}) \right) \overline{\frac{\partial}{\partial \xi} g(\xi, \hat{\mathbf{x}})} d(\xi, \hat{\mathbf{x}}) \\
 &\quad - \int_{\mathbb{R}_{>0} \times \Gamma} \frac{(1 + \sigma(\omega) \xi) \mathbf{v}(\hat{\mathbf{x}})}{\mathbf{n}(\hat{\mathbf{x}}) \cdot \mathbf{v}(\hat{\mathbf{x}})} \cdot \left( \frac{\partial}{\partial \xi} f(\xi, \hat{\mathbf{x}}) \overline{\hat{\nabla} g(\xi, \hat{\mathbf{x}})} \right) d(\xi, \hat{\mathbf{x}}) \\
 &\quad - \frac{\sigma(\omega)}{2} \int_{\mathbb{R}_{>0} \times \Gamma} \frac{\mathbf{v}(\hat{\mathbf{x}})}{\mathbf{n}(\hat{\mathbf{x}}) \cdot \mathbf{v}(\hat{\mathbf{x}})} \cdot \hat{\nabla} \left( f(\xi, \hat{\mathbf{x}}) \overline{g(\xi, \hat{\mathbf{x}})} \right) d(\xi, \hat{\mathbf{x}}) \\
 &\quad + \sigma(\omega) \int_{\mathbb{R}_{>0} \times \Gamma} \frac{\|\mathbf{v}(\hat{\mathbf{x}})\|^2}{\mathbf{n}(\hat{\mathbf{x}}) \cdot \mathbf{v}(\hat{\mathbf{x}})} \left( \hat{\nabla} f(\xi, \hat{\mathbf{x}}) \right)^{\top} \cdot \overline{\hat{\nabla} g(\xi, \hat{\mathbf{x}})} d(\xi, \hat{\mathbf{x}}) \\
 &\quad - \frac{1}{2} \int_{\Gamma} \frac{1}{\mathbf{n}(\hat{\mathbf{x}}) \cdot \mathbf{v}(\hat{\mathbf{x}})} \text{tr}_0 f(\hat{\mathbf{x}}) \overline{\text{tr}_0 g(\hat{\mathbf{x}})} d\hat{\mathbf{x}} \\
 &\quad - \omega^2 \sigma(\omega) \int_{\mathbb{R}_{>0} \times \Gamma} (1 + \sigma(\omega) \xi)^2 \mathbf{n}(\hat{\mathbf{x}}) \cdot \mathbf{v}(\hat{\mathbf{x}}) f(\xi, \hat{\mathbf{x}}) \overline{g(\xi, \hat{\mathbf{x}})} d(\xi, \hat{\mathbf{x}}),
 \end{aligned} \tag{7.10}$$

where  $\text{tr}_0$  denotes the trace at  $\xi = 0$ . The additional boundary term in (7.10) is due to the fact that the scaling factor is merely applied in  $\Omega_{\text{ext}}$  and not in  $\Omega_{\text{int}}$ .

Note that, unlike in [NW18, Section 3.2] where we scaled solely the test function, we are able to preserve the symmetry<sup>2</sup> of the problem by scaling the test and trial function. For the special case of polar or spherical coordinates (see (5.1) and (7.6)) we obtain

$$\begin{aligned}
 a_{\sigma}^{\text{polar sc.}}(\omega)(f, g) &:= \frac{1}{\sigma(\omega)} \int_{\mathbb{R}_{>0} \times \Gamma} (1 + \sigma(\omega) \xi)^2 \frac{\partial}{\partial \xi} f(\xi, \hat{\mathbf{x}}) \overline{\frac{\partial}{\partial \xi} g(\xi, \hat{\mathbf{x}})} d(\xi, \hat{\mathbf{x}}) \\
 &\quad - \frac{\sigma(\omega)}{4} \int_{\mathbb{R}_{>0} \times \Gamma} f(\xi, \hat{\mathbf{x}}) \overline{g(\xi, \hat{\mathbf{x}})} d(\xi, \hat{\mathbf{x}}) \\
 &\quad + \sigma(\omega) \int_{\mathbb{R}_{>0} \times \Gamma} \left( \hat{\nabla} f(\xi, \hat{\mathbf{x}}) \right)^{\top} \cdot \overline{\hat{\nabla} g(\xi, \hat{\mathbf{x}})} d(\xi, \hat{\mathbf{x}}) \\
 &\quad - \frac{1}{2} \int_{\Gamma} \text{tr}_0 f(\hat{\mathbf{x}}) \overline{\text{tr}_0 g(\hat{\mathbf{x}})} d\hat{\mathbf{x}} \\
 &\quad - \omega^2 \sigma(\omega) \int_{\mathbb{R}_{>0} \times \Gamma} (1 + \sigma(\omega) \xi)^2 f(\xi, \hat{\mathbf{x}}) \overline{g(\xi, \hat{\mathbf{x}})} d(\xi, \hat{\mathbf{x}}).
 \end{aligned} \tag{7.11}$$

<sup>2</sup>in a sense that  $a^{\text{star sc.}}(\omega)$  is symmetric for real-valued functions  $f, g$

### 7.2.3. Curvilinear coordinates

In the case of curvilinear coordinates, in general, the sesquilinear forms  $a_\sigma^{\text{curv},2}(\omega)$  and  $a_\sigma^{\text{curv},3}(\omega)$  from (7.7) and (7.8) cannot be decomposed into a generalized-radial and a surface part in the sense of (6.1). Thus, obviously they do not fulfill (7.9) either. A scaling similar to the case of star-shaped coordinates of the solution and test function would have to be a multiplication by a factor containing  $1 + \kappa(\hat{\mathbf{x}}) \sigma(\omega) \xi$ . Therefore, such a scaling is not reasonable in this case since it would lead to additional terms containing also the derivatives of the curvatures.

A possible way to obtain a rational problem is to introduce additional unknowns. For  $d = 2$  we introduce the additional unknown function  $u_\tau \in L^2(\Omega_{\text{ext}})$  that fulfills

$$(1 + \sigma(\omega) \kappa(\hat{\mathbf{x}}) \xi) u_\tau(\xi, \hat{\mathbf{x}}) := \mathbf{t}(\hat{\mathbf{x}}) \cdot \hat{\nabla} u(\xi, \hat{\mathbf{x}}).$$

In weak form this leads to the augmented sesquilinear form

$$\begin{aligned} a_\sigma^{\text{curv}, \text{mixed}}(\omega)((f, f_\tau), (g, g_\tau)) &:= \frac{1}{\sigma(\omega)} \int_{\mathbb{R}_{>0} \times \Gamma} (1 + \sigma(\omega) \xi \kappa(\hat{\mathbf{x}})) \frac{\partial f}{\partial \xi}(\xi, \hat{\mathbf{x}}) \overline{\frac{\partial g}{\partial \xi}(\xi, \hat{\mathbf{x}})} d(\xi, \hat{\mathbf{x}}) \\ &+ \sigma(\omega) \int_{\mathbb{R}_{>0} \times \Gamma} f_\tau(\xi, \hat{\mathbf{x}}) \mathbf{t}(\hat{\mathbf{x}}) \cdot \overline{\hat{\nabla} g(\xi, \hat{\mathbf{x}})} d(\xi, \hat{\mathbf{x}}) \\ &+ \sigma(\omega) \int_{\mathbb{R}_{>0} \times \Gamma} \mathbf{t}(\hat{\mathbf{x}}) \cdot \overline{\hat{\nabla} f(\xi, \hat{\mathbf{x}})} \overline{g_\tau(\xi, \hat{\mathbf{x}})} d(\xi, \hat{\mathbf{x}}) \\ &- \sigma(\omega) \int_{\mathbb{R}_{>0} \times \Gamma} (1 + \sigma(\omega) \xi \kappa(\hat{\mathbf{x}})) f_\tau(\xi, \hat{\mathbf{x}}) \overline{g_\tau(\xi, \hat{\mathbf{x}})} d(\xi, \hat{\mathbf{x}}) \\ &- \sigma(\omega) \int_{\mathbb{R}_{>0} \times \Gamma} \omega^2 (1 + \sigma(\omega) \xi \kappa(\hat{\mathbf{x}})) f(\xi, \hat{\mathbf{x}}) \cdot \overline{g(\xi, \hat{\mathbf{x}})} d(\xi, \hat{\mathbf{x}}), \end{aligned} \quad (7.12)$$

for  $f, f_\tau, g, g_\tau$  such that  $f \circ \Psi^{-1}, g \circ \Psi^{-1} \in H^1(\Omega_{\text{ext}})$  and  $f_\tau \circ \Psi^{-1}, g_\tau \circ \Psi^{-1} \in L^2(\Omega_{\text{ext}})$ . Note that the augmented sesquilinear form above is still symmetric for real-valued test and ansatz functions.

*Remark 7.11.* The discrete space of the auxiliary variable has to be picked in a way that the tangential part of the surface derivative of a discrete function is an element of this space. In our examples in Chapter 9 we choose a similar tensor product approach as described in Section 6.2 by choosing  $\hat{\mathcal{X}}_N \otimes \hat{\mathcal{Y}}_L$  with a surface space  $\hat{\mathcal{Y}}_L \subset L^2(\Gamma)$  such that  $\mathbf{t}(\hat{\mathbf{x}}) \cdot \hat{\nabla} \hat{f}(\hat{\mathbf{x}}) \in \hat{\mathcal{Y}}_L$  for all  $f \in \hat{\mathcal{X}}_M$ .

For  $d = 3$ , similar techniques can be applied although in this case it is not straightforward to preserve the symmetry.

## 7.3. Specific frequency-dependencies and their essential spectra

As shown in Chapter 4, the choice of the frequency-dependency  $\sigma : \Lambda \subset \mathbb{C} \rightarrow \mathbb{C} \setminus \{0\}$  heavily affects the approximation of the resonances and resonance functions. Although in general any holomorphic function can be used, we focus on functions  $\sigma$  that are rational in

the frequency  $\omega$  to obtain rational matrix eigenvalue problems. Using frequency-dependent scaling parameters is common for scattering problems (and necessary for problems in time domain cf. Section 10.2.4). In his original publication [Ber94] Bereng er used a function<sup>3</sup>

$$\sigma(\omega) := 1 + \frac{i\alpha}{\omega},$$

with  $\alpha > 0$ . In [NW18] we used the simpler scaling  $\sigma(\omega) := \frac{\sigma_0}{\omega}$  for some complex parameter  $\sigma_0 \in \mathbb{C} \setminus \{0\}$ . More involved frequency-dependencies are used in the engineering community (mostly in connection with finite difference schemes) under the name of CPML<sup>4</sup> (e.g., [DG07, RG00]).

If we consider the possible locations of the two parts of the essential spectrum (cf. (S1) and (S2) and Sections 5.3.1, 5.3.2) and the fact that we want to have similar approximation properties of the eigenfunctions for a range of frequencies which is as wide as possible, we have to pick the function  $\sigma$  in a way that

- $\text{Im}(\sigma(\omega)\omega) > 0$  and  $\arg(\sigma(\omega)) \notin [\pi - \mu, \pi + \mu]$  for frequencies  $\omega$  we are interested in and
- $\sigma(\omega)\omega$  is bounded for  $|\omega| \rightarrow \infty$ .

In the following we consider frequency-dependencies of the form

$$\sigma(\omega) = \frac{\alpha + \beta}{\gamma + \delta\omega}, \quad (7.13)$$

with  $\alpha, \beta, \gamma, \delta \in \mathbb{C}$  such that  $|\alpha| + |\beta|, |\gamma| + |\delta| \neq 0$ . Notable special cases of this choice are

$$\sigma_0(\omega) := \beta, \quad (7.14a)$$

$$\sigma_v(\omega) := \frac{\alpha}{\omega}, \quad (7.14b)$$

$$\sigma_b(\omega) := \beta + \frac{\alpha}{\omega}, \quad (7.14c)$$

$$\sigma_c(\omega) := \frac{\beta}{\gamma + \delta\omega}. \quad (7.14d)$$

We know from the analysis of our method in Section 5.3 that we have to expect an essential spectrum in regions where  $\text{Re}(\sigma(\omega)\omega) = 0$  and  $\arg(\sigma(\omega)) \notin [\pi - \mu, \pi + \mu]$ , where  $\mu \in [0, \frac{\pi}{2}]$  (see Section 5.4). Thus, we have to identify the set

$$\Xi := \{\omega \in \Lambda : \text{Im}(\sigma(\omega)\omega) > 0, \arg(\sigma(\omega)) \notin [\pi - \mu, \pi + \mu]\},$$

which is bounded by the sets

$$\begin{aligned} \Lambda_{\text{sing}} &:= \Lambda_{\text{sing}}^+ \cup \Lambda_{\text{sing}}^-, \\ \Sigma_{\text{dec}} &= \{\omega \in \Lambda : \text{Im}(\sigma(\omega)\omega) = 0\}, \end{aligned}$$

<sup>3</sup>Note that in [Ber94] the sign of the Fourier transform is inverted.

<sup>4</sup>The abbreviation CPML (short for convolutional PML) is used due to the fact that the term  $\frac{1}{1+i\omega}$  leads to a convolution operator in time-domain.

with

$$\begin{aligned}\Lambda_{\text{sing}}^+ &:= \{\omega \in \Lambda : \arg(\sigma(\omega)) = \pi + \mu\}, \\ \Lambda_{\text{sing}}^- &:= \{\omega \in \Lambda : \arg(\sigma(\omega)) = \pi - \mu\}.\end{aligned}$$

To this end, we have to invert the mappings  $\omega \mapsto \sigma(\omega)$  and  $\omega \mapsto \tau(\omega) := \sigma(\omega)\omega$ .

For scalings of the form (7.13), the function  $\tau$  is a Möbius transformation (Definition A.18). Therefore, in this case the set  $\Sigma_{\text{dec}}$  is a subset of either a circle or a straight line.

For scalings of the form (7.14) the function  $\sigma$  is a Möbius transformation as well. Therefore, for such scalings the sets  $\Lambda_{\text{sing}}^\pm$  are subsets of circles and/or straight lines as well. In the following we determine these sets explicitly for the scalings given in (7.14).

### The frequency-independent scaling $\sigma_0$

The scaling  $\sigma_0(\omega) \equiv \beta \neq 0$  is the one most commonly used for resonance problems (e.g., [Hal19, HN09, KP09]). Its domain is  $\Lambda = \mathbb{C}$  and for  $\arg(\beta) \notin [\pi - \mu, \pi + \mu]$  it leads to

$$\Sigma_{\text{dec}} = \frac{1}{\beta}\mathbb{R}$$

and therefore for  $\text{Im}(\beta) > 0$

$$\Xi = \{\omega \in \mathbb{C} : \arg(\omega) \notin [\pi - \arg(\beta), 2\pi - \arg(\beta)]\}$$

(see Figure 7.4).

### The scaling $\sigma_v$

In the simplest frequency-dependent case of  $\sigma_v$  from (7.14b) with  $\alpha \notin \mathbb{R}$  we have the domain  $\Lambda = \mathbb{C} \setminus \{0\}$ . The set  $\Lambda_{\text{sing}}$  is given by

$$\Lambda_{\text{sing}}^\pm = \sigma_v^{-1}(\exp(i(\pi \pm \mu))\mathbb{R}_{\geq 0}) = \frac{\alpha}{\exp(i(\pi \pm \mu))}\mathbb{R}_{\geq 0} = -\alpha \exp(\mp i\mu)\mathbb{R}_{\geq 0}.$$

We have

$$\tau_v(\omega) = \sigma_v(\omega)\omega = \alpha \notin \mathbb{R} \tag{7.15}$$

and thus ([NW18, Section 3.1]),

$$\Sigma_{\text{dec}} = \emptyset.$$

For  $\arg(\alpha) < \pi - \mu$  the set where we can expect approximations to radiating resonances is given by (see Figure 7.5)

$$\Xi = \{\omega \in \mathbb{C} \setminus \{0\} : \arg(\omega) \notin [\pi + \arg(\alpha) - \mu, \pi + \arg(\alpha) + \mu]\}.$$

The set where  $\Sigma_{\text{sing}}$  is located is a wedge, which is symmetric with respect to the line  $-\alpha\mathbb{R}_{\geq 0}$  and has an opening angle  $2\mu$ . Moreover, in the case of a spherical scaling, because of (7.15), the complex-scaled (spherical) Hankel functions have a uniform exponential decay and oscillatory behavior for all frequencies  $\omega \neq 0$ .

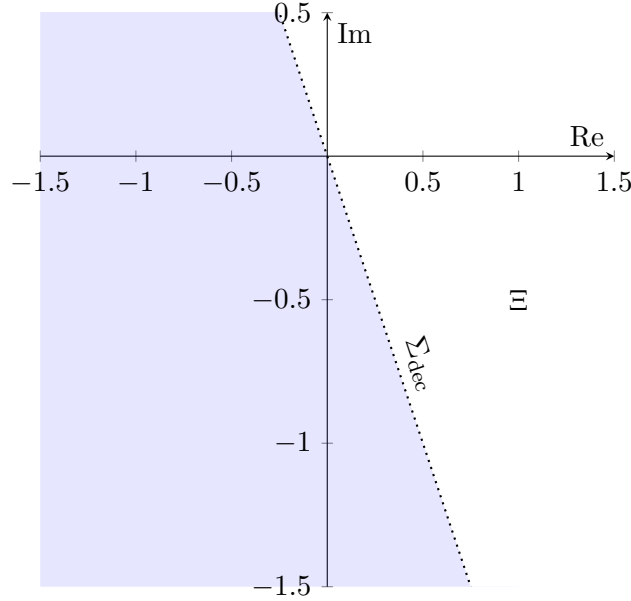


Figure 7.4.: The essential spectrum (dotted) and the area  $\Xi$  where eigenvalues corresponding to radiating eigenfunctions are approximated (white) for a constant scaling  $\sigma(\omega) = 1 + 2i$ . The area where the non-radiating resonances are approximated is colored in blue.

### The scaling $\sigma_b$

We assume that  $\alpha, \beta \neq 0$ , otherwise our scaling is already covered by the previous considerations. Like in the previous case, the domain is  $\Lambda = \mathbb{C} \setminus \{0\}$ . The sets  $\Lambda_{\text{sing}}^{\pm}$  can be calculated by

$$\Lambda_{\text{sing}}^{\pm} = \sigma_b^{-1}(-\exp(\pm i\mu) \mathbb{R}_{\geq 0}).$$

Because of

$$\sigma_b^{-1}(t) = \frac{\alpha}{t - \beta},$$

we may apply Lemma A.19 and obtain that  $\Lambda_{\text{sing}}^{\pm}$  are subsets of circular lines connecting the points  $-\frac{\alpha}{\beta}$  and 0 with center  $\frac{\alpha\bar{\mu}}{\beta\mu - \beta\bar{\mu}}$  and  $\frac{\alpha\mu}{\beta\bar{\mu} - \beta\mu}$  respectively. Moreover, because of

$$\tau_b^{-1}(t) = \frac{t - \alpha}{\beta},$$

the set  $\Sigma_{\text{dec}}$  is given by

$$\Sigma_{\text{dec}} = -\frac{\alpha}{\beta} + \frac{t}{\beta} : t \in \mathbb{R}$$

and is therefore a straight line (see Figure 7.6). Contrary to before, in this case the quantity  $\sigma_b(\omega)\omega$  is not bounded for large  $|\omega|$ . Therefore, we cannot expect uniform approximation properties of eigenfunctions in the frequency (see also Figure 4.2b).

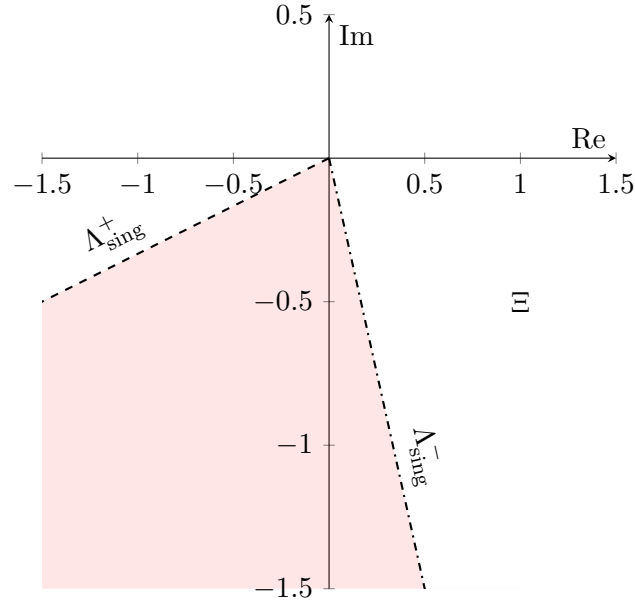


Figure 7.5.: The possible location of the essential spectrum  $\Sigma_{\text{sing}}$  (red) and the area  $\Xi$  (white) where eigenvalues corresponding to radiating eigenfunctions are approximated for the scaling  $\sigma_v(\omega) = \frac{1+2j}{\omega}$  with  $\mu = \frac{\pi}{4}$ .

### The scaling $\sigma_c$

We assume that  $\beta, \gamma, \delta \neq 0$ . Otherwise, the scaling is already covered by the previous considerations. Because of

$$\sigma_c^{-1}(t) = \frac{\beta - \gamma t}{\delta t},$$

we obtain that the sets  $\Lambda_{\text{sing}}^{\pm}$  are given by

$$\Lambda_{\text{sing}}^{\pm} = -\frac{\gamma}{\delta} - \exp(\mp i\mu) \frac{\beta}{\delta} \mathbb{R}_{\geq 0}.$$

Therefore,  $\Sigma_{\text{sing}}$  is contained in a wedge with edge at  $-\frac{\gamma}{\delta}$  and angle  $2\mu$ , which is symmetric with respect to the line  $-\frac{\gamma}{\delta} - \frac{\beta}{\delta} \mathbb{R}_{\geq 0}$  (see Figure 7.7). Using Lemma A.19 for the mapping

$$\tau_c^{-1}(t) = \frac{\gamma t}{\beta - \delta t},$$

we obtain that  $\Sigma_{\text{dec}}$  is a circle with center  $\frac{\gamma\bar{\beta}}{\beta\delta - \beta\delta}$  and radius  $\left| \frac{\gamma\beta}{\beta\delta - \beta\delta} \right|$ .

## 7.4. Assembling the infinite element matrices

To apply numerical methods for solving or approximating the non-linear matrix eigenvalue problems (Chapter 8), resulting from a Galerkin discretization by the use of (in-)finite elements (Chapter 6), we need to assemble the matrices  $\mathbf{M}(\omega)$  with entries

$$\mathbf{M}_{k,j}(\omega) := a_{\sigma}(\omega)(b_j, b_k)$$

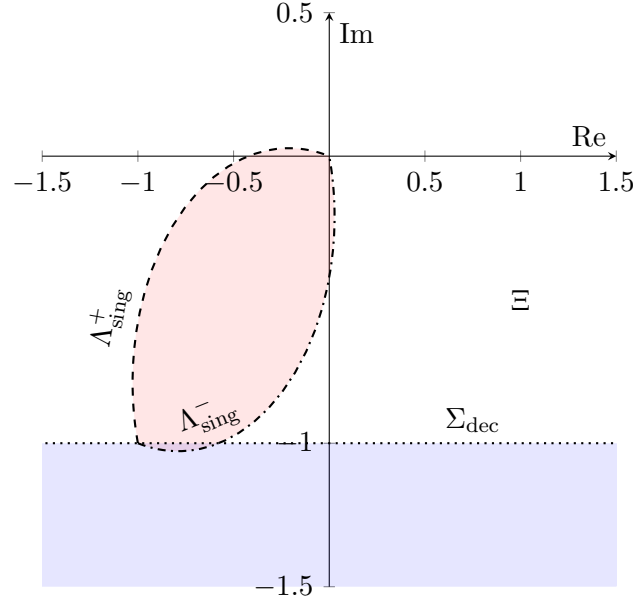


Figure 7.6.: The possible location of the essential spectrum and the area  $\Xi$  (white) where eigenvalues corresponding to radiating eigenfunctions are approximated for the scaling  $\sigma_b(\omega) = 1 + \frac{1+i}{\omega}$  with  $\mu = \frac{\pi}{3}$ .

for given frequencies  $\omega$  and a given basis  $B_{\mathcal{N}} = \{b_0, \dots, b_{\mathcal{N}}\} \subset \mathcal{X}_{\mathcal{N}}$  (cf. Section 6.2.3).

By Section 6.2.2 our basis functions in  $\Omega_{\text{ext}}$  in exterior coordinates are products of a generalized-radial and a surface component. Therefore, by (6.1) (and (7.9)) the exterior parts of our sesquilinear forms can be decomposed into generalized-radial and surface parts and we may assemble these parts separately and tensorize them appropriately.

Plugging basis functions  $\phi_j(\xi) b_k(\hat{\mathbf{x}})$ ,  $\phi_l(\xi) b_m(\hat{\mathbf{x}})$ , for generalized-radial and surface basis functions as in Sections 6.2.3 and 6.3, for instance, into the sesquilinear form  $a_{\sigma}^{\text{polar}}(\omega)$  for  $d = 3$  (see 7.6) results in

$$\begin{aligned} a_{\sigma}^{\text{polar}}(\omega)(\phi_j \otimes b_k, \phi_l \otimes b_m) &:= \frac{1}{\sigma(\omega)} \int_{\mathbb{R}_{>0}} (1 + \sigma(\omega) \xi)^2 \phi_j'(\xi) \phi_l'(\xi) d\xi \int_{\Gamma} b_k(\hat{\mathbf{x}}) b_m(\hat{\mathbf{x}}) d\hat{\mathbf{x}} \\ &+ \sigma(\omega) \int_{\mathbb{R}_{>0}} \phi_j(\xi) \phi_l(\xi) d\xi \int_{\Gamma} \hat{\nabla} b_k(\hat{\mathbf{x}}) \cdot \hat{\nabla} b_m(\hat{\mathbf{x}}) d\hat{\mathbf{x}} \\ &+ \sigma(\omega) \omega^2 \int_{\mathbb{R}_{>0}} (1 + \sigma(\omega) \xi)^2 \phi_j(\xi) \phi_l(\xi) d\xi \int_{\Gamma} b_k(\hat{\mathbf{x}}) b_m(\hat{\mathbf{x}}) d\hat{\mathbf{x}}. \end{aligned}$$

The surface parts can be assembled using usual techniques for (surface) finite elements. The generalized-radial parts consist of matrices with entries of the form

$$\int_{\mathbb{R}_{>0}} \xi^a \phi_j^{(b)}(\xi) \phi_l^{(b)}(\xi) d\xi$$

for  $a \in \mathbb{N}_0$  and  $b \in \{0, 1\}$ , where  $\cdot^{(n)}$  denotes the  $n$ -th derivative. For other coordinates

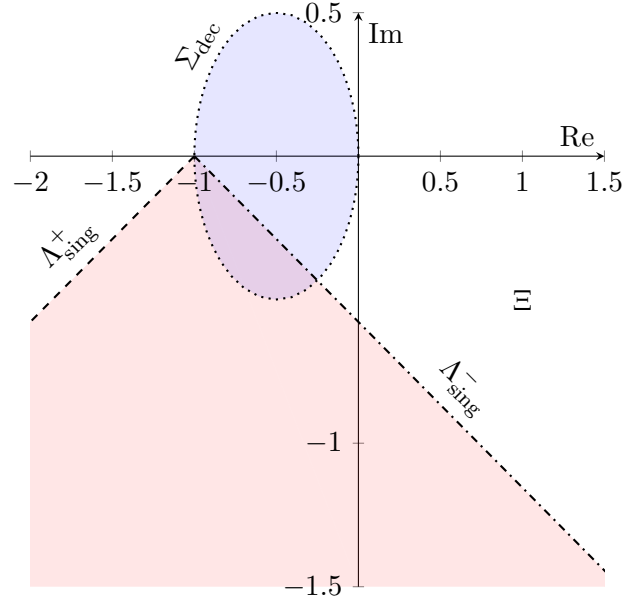


Figure 7.7.: The possible location of the essential spectrum and the area  $\Xi$  (white) where eigenvalues corresponding to radiating eigenfunctions are approximated for the scaling  $\sigma_c(\omega) = \frac{2i}{1+\omega}$  with  $\mu = \frac{\pi}{3}$ .

also non-symmetric terms might occur (cf. (7.3), (7.4), and (7.5)). Therefore, we define the following matrices:

**Definition 7.12.** For  $N, n \in \mathbb{N}_0$ , let  $\phi_0, \dots, \phi_N$  be as in Definition 6.3. Then we define the matrices  $\tilde{\mathbf{M}}^n, \tilde{\mathbf{S}}^n, \tilde{\mathbf{D}}^n \in \mathbb{R}^{N+1 \times N+1}$  by

$$\begin{aligned}\tilde{\mathbf{M}}^n &:= \left( \tilde{\mathbf{M}}_{j,k}^n \right)_{j,k=0,\dots,N} := \int_{\mathbb{R}_{>0}} \xi^n \phi_k(\xi) \phi_j(\xi) d\xi, \\ \tilde{\mathbf{S}}^n &:= \left( \tilde{\mathbf{S}}_{j,k}^n \right)_{j,k=0,\dots,N} := \int_{\mathbb{R}_{>0}} \xi^n \phi'_k(\xi) \phi'_j(\xi) d\xi, \\ \tilde{\mathbf{D}}^n &:= \left( \tilde{\mathbf{D}}_{j,k}^n \right)_{j,k=0,\dots,N} := \int_{\mathbb{R}_{>0}} \xi^n \phi'_k(\xi) \phi_j(\xi) d\xi.\end{aligned}$$

#### 7.4.1. Explicit formulas

We use the orthogonality from Proposition A.11.(i) and the recursion (ii) from the same proposition to obtain for  $j, k \in \mathbb{N}_0$

$$\tilde{\mathbf{M}}_{j,k}^0 = \int_0^\infty \phi_k(\xi) \phi_j(\xi) d\xi = \int_0^\infty (\psi_k(\xi) - \psi_{k-1}(\xi)) (\psi_j(\xi) - \psi_{j-1}(\xi)) d\xi = \begin{cases} \frac{1}{2}, & k = j = 0, \\ 1, & k = j > 0, \\ -\frac{1}{2}, & |k - j| = 1, \\ 0, & \text{else.} \end{cases}$$



Similarly, we obtain, by using Proposition A.11.(iii), that

$$\tilde{\mathbf{S}}_{j,k}^0 = \int_0^\infty \phi'_k(\xi) \phi'_j(\xi) d\xi = \int_0^\infty (-\psi_k(\xi) - \psi_{k-1}(\xi)) (-\psi_j(\xi) - \psi_{j-1}(\xi)) d\xi = \begin{cases} \frac{1}{2}, & k = j = 0, \\ 1, & k = j > 0, \\ \frac{1}{2}, & |k - j| = 1, \\ 0, & \text{else} \end{cases}$$

and

$$\tilde{\mathbf{D}}_{j,k}^0 = \int_0^\infty \phi'_k(\xi) \phi_j(\xi) d\xi = \int_0^\infty (-\psi_k(\xi) - \psi_{k-1}(\xi)) (\psi_j(\xi) - \psi_{j-1}(\xi)) d\xi = \begin{cases} -\frac{1}{2}, & k = j = 0, \\ 0, & k = j > 0, \\ \mp \frac{1}{2}, & k - j = \pm 1, \\ 0, & \text{else.} \end{cases}$$

The above in matrix form reads

$$\tilde{\mathbf{M}}^0 = \frac{1}{2} \begin{pmatrix} 1 & -1 & & & \\ -1 & 2 & \ddots & & \\ & \ddots & \ddots & \ddots & \\ & & & -1 & 2 \\ & & & & -1 & 2 \end{pmatrix}, \quad \tilde{\mathbf{S}}^0 = \frac{1}{2} \begin{pmatrix} 1 & 1 & & & \\ 1 & 2 & \ddots & & \\ & \ddots & \ddots & \ddots & 1 \\ & & & 1 & 2 \end{pmatrix}, \quad \tilde{\mathbf{D}}^0 = \frac{1}{2} \begin{pmatrix} 1 & -1 & & & \\ 1 & 0 & \ddots & & \\ & \ddots & \ddots & \ddots & -1 \\ & & & 1 & 0 \end{pmatrix}.$$

The matrices corresponding to sesquilinear forms with non-constant polynomial coefficients can be obtained by similar calculations.

*Remark 7.13.* In some cases (e.g., for the frequency-independent scaling in polar coordinates for  $d = 2$ , see (7.6)) it is necessary to compute matrices  $\tilde{\mathbf{A}} = (\tilde{\mathbf{A}}_{l,j})_{l,j=0,\dots,N}$  with entries of the form

$$\tilde{\mathbf{A}}_{l,j} = \int_{\mathbb{R}_{>0}} \frac{1}{1 + \sigma_0 \xi} \phi_j^{(b)}(\xi) \phi_l^{(c)}(\xi) d\xi,$$

with  $b, c \in \{0, 1\}$  and some  $\sigma_0 \in \mathbb{C} \setminus \mathbb{R}_{<0}$ . In [HN09] this is done in the following way: The matrix  $\tilde{\mathbf{A}}$  for  $b, c = 0$  is approximated by the matrix

$$\tilde{\mathbf{A}} \approx \mathbf{B}^\top \mathbf{T}^{-1} \mathbf{B},$$

where  $\mathbf{B}$  is the representation of the basis functions  $\phi_j = \phi_{j,-1}, j = 0, \dots, N$ , with respect to the orthogonal basis function  $\psi_j = \phi_{j,0}, j = 0, \dots, N$  and  $\mathbf{T}$  is the matrix corresponding to the multiplication operator by  $\xi \mapsto 1 + \sigma_0 \xi$ , with respect to the basis  $\psi_0, \dots, \psi_N$ . Note, however, that this gives merely an approximation of the correct matrix.

### 7.4.2. Numerical integration

Alternatively, we can compute the generalized-radial discretization matrices from Definition 7.12 by using quadrature rules. This is particularly useful for the case where we consider potentials  $\rho$  that are not constant in the exterior domain  $\Omega_{\text{ext}}$  (Section 10.2.1). Since the radial basis functions are of the form  $\exp(-\xi) q(2\xi)$  for certain polynomials  $q$ , also their

## 7. Implementation

derivatives are of this form. Thus, after applying the substitution  $\xi \mapsto \frac{\xi}{2}$  to the integrals in Definition 7.12, we have to find a quadrature rule  $w_j, \xi_j \in \mathbb{R}, j = 0, \dots, M$  such that

$$\int_{\mathbb{R}_{>0}} \exp(-\xi) q(\xi) d\xi = \sum_{j=0}^M w_j q(\xi_j)$$

for all polynomials  $q$  up to some degree. An obvious choice for this task are Gauss rules with respect to the weight function  $\exp(-\cdot)$ . These integration rules are given by the following theorem:

**Theorem 7.14.** For  $M \in \mathbb{N}$ , let  $\xi_0, \dots, \xi_M$  be the roots of the Laguerre polynomial  $L_{M+1,0}$ . Moreover, let

$$w_j := \frac{\xi_j}{(M+1)^2 L_{M,0}(\xi_j)^2}, \quad j = 0, \dots, M.$$

Then

$$\int_0^\infty \exp(-\xi) q(\xi) d\xi = \sum_{j=0}^M w_j q(\xi_j)$$

for all polynomials  $q \in \mathcal{P}_{2M+1}$ .

*Proof.* See [STW11, Theorem 7.1] with  $\alpha = 0$ . □

The weights and quadrature points can be calculated using the following theorem:

**Theorem 7.15.** For  $M \in \mathbb{N}$ , the quadrature points  $\xi_0, \dots, \xi_M$  of the Gauss-Laguerre quadrature as in Theorem 7.14 are the eigenvalues of the matrix

$$\begin{pmatrix} 1 & -1 & & & & & \\ -1 & 3 & -2 & & & & \\ & \ddots & \ddots & \ddots & & & \\ & & -M+1 & 2M-1 & -M & & \\ & & & -M & 2M+1 & & \end{pmatrix}.$$

The weights  $w_0, \dots, w_M$  are the squares of the first entries of the according eigenvectors.

*Proof.* See [STW11, Section 7.1.3]. □

## 8. Non-Linear Eigenvalue Problems

In this chapter we present methods to efficiently approximate the eigenvalues and eigenvectors of the discrete, non-linear eigenvalue problems that result from the discretization of the complex-scaled Helmholtz equation using frequency-dependent scalings (see Section 7.2).

General non-linear eigenvalue problems appear in a wide range of applications in mathematics, physics, and engineering (e.g., [BHM<sup>+</sup>13]). Numerical methods for such problems are, for example, discussed in [Ruh73], [MV04] (subspace iteration), and [SS03, Bey12] (methods based on contour integrals).

A helpful property of the non-linear eigenvalue problems in question is the fact that they consist of sums over constant matrices times scalar rational functions in the frequency. Therefore, they allow a linear representation<sup>1</sup> (cf., e.g., [MV04, Section 2] and Section 8.2.1), which is a larger, but in some sense equivalent, generalized-linear eigenvalue problem.

Although for the linear representation of a non-linear eigenvalue problem, known methods like an Arnoldi iteration can be applied, it is, in many cases, advised against doing so (e.g., [MV04, Introduction]) since the linear representation is usually considerably larger than the original problem. Moreover, it is not straightforward to preserve desirable properties like symmetry (cf. [DPVD19] for structure preserving linear representations of polynomial eigenvalue problems).

Nevertheless, we use linear representations to derive a method for efficiently approximating the eigenvalues and eigenvectors of the rational eigenvalue problems. Our method is nearly as efficient as solving linear eigenvalue problems using the shift-and-invert Arnoldi method since the main effort also consists of applying the inverse of the particular matrix function (cf. Problem 8.1) evaluated at a given shift once per iteration (see Table 8.1).

This chapter is structured as follows: After the proper definition of the rational eigenvalue problems we want to solve (Problem 8.1) we briefly discuss the shift-and-invert Arnoldi algorithm for the special case of generalized-linear eigenvalue problems (Section 8.1). In Section 8.2.1 we deal with linear representations of rational eigenvalue problems and show in Sections 8.2.2 and 8.2.3 how the shift-and-invert Arnoldi algorithm can be efficiently applied to linear representations.

For the remainder of this chapter, we consider the following problems:

**Problem 8.1.** For  $\Lambda \subset \mathbb{C}$ ,  $n \in \mathbb{N}_0$ , and  $N \in \mathbb{N}$ , let  $\gamma_0, \dots, \gamma_n : \Lambda \rightarrow \mathbb{C}$  and  $\mathbf{M}^0, \dots, \mathbf{M}^n \in \mathbb{C}^{N \times N}$ . Then we call the problem to

$$\text{find eigenpairs } (\omega, \mathbf{u}) \in \Lambda \times \mathbb{C}^N \setminus \{\mathbf{0}\} \text{ such that } \mathbf{M}(\omega) \mathbf{u} := \sum_{j=0}^n \gamma_j(\omega) \mathbf{M}^j \mathbf{u} = \mathbf{0} \quad (8.1)$$

<sup>1</sup>In the literature the term *linearization* is widely used. Nevertheless, we refrain from using this term since it might lead the reader to the belief that we apply some form of linear approximation.

a *non-linear eigenvalue problem with scalar coefficients*. A problem of this form is called *rational* if  $\gamma_0, \dots, \gamma_n$  are rational functions. We call the set

$$\Sigma(\mathbf{M}) := \{\omega \in \Lambda : \mathbf{M}(\omega) \text{ is singular}\}$$

the spectrum of the generalized eigenvalue problem,  $\omega \in \Sigma(\mathbf{M})$  an eigenvalue, and  $\mathbf{u} \in \ker(\mathbf{M}(\omega)) \setminus \{\mathbf{0}\}$  a corresponding eigenvector.

In our case the matrices  $\mathbf{M}^j$  typically are large and sparse and, as shown in Section 7.2, we can assume that the eigenvalue problems are rational. Moreover, we are not interested in the full set of eigenvalues, but rather in the ones in the vicinity of a given shift  $\omega_0 \in \mathbb{C}$ .

We start by discussing the special case of generalized-linear eigenvalue problems.

## 8.1. Generalized-linear eigenvalue problems

Linear eigenvalue problems, which are the problems to

$$\text{find } (\omega, \mathbf{u}) \in \mathbb{C} \times \mathbb{C}^N \setminus \{\mathbf{0}\} \text{ such that } \mathbf{M}^0 \mathbf{u} = \omega \mathbf{u}$$

and generalized-linear eigenvalue problems, which are the problems to

$$\text{find } (\omega, \mathbf{u}) \in \mathbb{C} \times \mathbb{C}^N \setminus \{\mathbf{0}\} \text{ such that } \mathbf{M}^0 \mathbf{u} = \omega \mathbf{M}^1 \mathbf{u} \quad (8.2)$$

for matrices  $\mathbf{M}^0, \mathbf{M}^1 \in \mathbb{C}^{N \times N}$  are clearly special cases of non-linear (and rational) eigenvalue problems (see Problem 8.1). For such problems, the set  $\Lambda$  can always be chosen as  $\Lambda = \mathbb{C}$ .

To find eigenpairs  $(\mu, \mathbf{u})$  of the shift-and-inverted problem, we use the so-called Arnoldi algorithm (see, e.g., [Saa11, Section 6.2]), stated in Algorithm 1 in its simplest form. For a given matrix  $\mathbf{A}$ , this algorithm computes orthonormal vectors  $\mathbf{v}^0, \dots, \mathbf{v}^K$  and an upper Hessenberg matrix  $\mathbf{H} \in \mathbb{C}^{(K+1) \times (K+1)}$  that is the projection of  $\mathbf{A}$  onto the subspace spanned by these vectors. The eigenvalues of  $\mathbf{H}$  are approximations to the eigenvalues of  $\mathbf{A}$  with the largest absolute values and the corresponding eigenvectors are the representations of approximations to the according eigenvectors of  $\mathbf{A}$  in the basis  $\{\mathbf{v}^0, \dots, \mathbf{v}^K\}$ . The algorithm terminates if for some index  $j < K$  the set  $\mathbf{v}^0, \dots, \mathbf{v}^j$  is an invariant subspace with respect to the matrix  $\mathbf{A}$ . A convergence analysis for the Arnoldi algorithm can be found in [Saa11, Section 6.7].

An important idea for the treatment of large and sparse generalized-linear eigenvalue problems (8.2) is using a so-called shift-and-invert. Instead of looking for eigenpairs of (8.2), we look for the eigenvalues  $\mu$  with the largest absolute values of the shift-and-inverted linear problem to

$$\text{find } (\mu, \mathbf{u}) \in \mathbb{C} \setminus \{0\} \times \mathbb{C}^N \setminus \{\mathbf{0}\} \text{ such that } (\mathbf{M}^0 - \omega_0 \mathbf{M}^1)^{-1} \mathbf{M}^1 \mathbf{u} = \mu \mathbf{u} \quad (8.3)$$

for a given fixed shift  $\omega_0 \in \mathbb{C}$  such that  $\omega_0$  is no eigenvalue. It is easy to verify that the eigenvalues  $\mu$  with the largest absolute values of the shift-and-inverted problem (8.3)

**Algorithm 1** Arnoldi algorithm**Input:**  $\mathbf{A} \in \mathbb{C}^{N \times N}$ ,  $K \in \mathbb{N}$ **Output:** approximations  $(\lambda_0, \mathbf{u}^0), \dots, (\lambda_K, \mathbf{u}^K)$  to eigenpairs of  $\mathbf{A}$ 

```

1: pick a normalized random vector  $\mathbf{v}^0 \in \mathbb{C}^N$ 
2:  $\mathbf{H} \leftarrow \mathbf{0} \in \mathbb{C}^{(K+1) \times (K+1)}$ 
3: for  $k = 1, \dots, K + 1$  do
4:    $\mathbf{t} \leftarrow \mathbf{A}\mathbf{v}^{k-1}$ 
5:   for  $j = 0, \dots, k - 1$  do
6:      $\mathbf{H}_{j,k-1} \leftarrow \overline{\mathbf{v}^j} \cdot \mathbf{t}$ 
7:      $\mathbf{t} \leftarrow \mathbf{t} - \mathbf{H}_{j,k-1} \mathbf{v}^j$ 
8:   end for
9:   if  $\mathbf{t} = \mathbf{0}$  then
10:    break
11:  end if
12:  if  $k < K + 1$  then
13:     $\mathbf{H}_{k,k-1} \leftarrow \|\mathbf{t}\|$ 
14:     $\mathbf{v}^k \leftarrow \frac{\mathbf{t}}{\mathbf{H}_{k,k-1}}$ 
15:  end if
16: end for
17:  $(\lambda_0, \mathbf{w}^0), \dots, (\lambda_K, \mathbf{w}^K) \in \mathbb{C} \times \mathbb{C}^{K+1} \leftarrow$  eigenpairs of  $\mathbf{H}$ 
18: for  $j = 0, \dots, K$  do
19:    $\mathbf{u}^j \leftarrow (\mathbf{v}^0, \dots, \mathbf{v}^K) \mathbf{w}^j$ 
20: end for

```

correspond to the eigenvalues  $\omega$  of the initial problem (8.2) closest to the shift  $\omega_0$  via the relation

$$\omega = \frac{1}{\mu} + \omega_0 \quad (8.4)$$

and the eigenvectors  $\mathbf{u}$  of the corresponding eigenvalues  $\omega$  and  $\mu$  coincide.

If we apply Algorithm 1 to the setting described above, namely, to the matrix  $\mathbf{A} = (\mathbf{M}^0 - \omega_0 \mathbf{M}^1)^{-1} \mathbf{M}^1$ , we end up with Algorithm 2. Note that in Algorithm 2, as in the following algorithms, we omit explicitly stating the computation of the eigenpairs of the projected matrix  $\mathbf{H}$  and the computation of the vectors  $\mathbf{u}^j$  since it can be done as in Algorithm 1 (lines 14–20). Subsequently, the eigenvalues can be shifted back using (8.4).

If we assume that  $N \gg K$ , the main computational effort of Algorithm 2 is the factorization and application of the large inverse matrix in lines 3 and 5, where the effort for the factorization is considerably more costly than the application. The computational effort for the orthogonalization (lines 6–15) and the effort for finding the eigenvalues and eigenvectors of the matrix  $\mathbf{H} \in \mathbb{C}^{(K+1) \times (K+1)}$ , which has to be performed afterwards, is not as significant.

**Algorithm 2** Shift-and-invert Arnoldi algorithm

---

**Input:**  $\mathbf{M}^0, \mathbf{M}^1 \in \mathbb{C}^{N \times N}$ ,  $K \in \mathbb{N}$ ,  $\omega_0 \in \mathbb{C}$   
**Output:**  $\mathbf{v}^0, \dots, \mathbf{v}^K \in \mathbb{C}^N$ ,  $\mathbf{H} \in \mathbb{C}^{(K+1) \times (K+1)}$

- 1: pick a normalized random vector  $\mathbf{v}^0 \in \mathbb{C}^N$
- 2:  $\mathbf{H} \leftarrow \mathbf{0} \in \mathbb{C}^{(K+1) \times (K+1)}$
- 3: factorize  $(\mathbf{M}^0 - \omega_0 \mathbf{M}^1)^{-1}$
- 4: **for**  $k = 1, \dots, K + 1$  **do**
- 5:    $\mathbf{t} \leftarrow (\mathbf{M}^0 - \omega_0 \mathbf{M}^1)^{-1} \mathbf{M}^1 \mathbf{v}^{k-1}$
- 6:   **for**  $j = 0, \dots, k - 1$  **do**
- 7:      $\mathbf{H}_{j,k-1} \leftarrow \overline{\mathbf{v}^j} \cdot \mathbf{t}$
- 8:      $\mathbf{t} \leftarrow \mathbf{t} - \mathbf{H}_{j,k-1} \mathbf{v}^j$
- 9:   **end for**
- 10:   **if**  $\mathbf{t} = \mathbf{0}$  **then**
- 11:     break
- 12:   **end if**
- 13:   **if**  $k < K + 1$  **then**
- 14:      $\mathbf{H}_{k,k-1} \leftarrow \|\mathbf{t}\|$
- 15:      $\mathbf{v}^k \leftarrow \frac{\mathbf{t}}{\mathbf{H}_{k,k-1}}$
- 16:   **end if**
- 17: **end for**

---

## 8.2. Rational eigenvalue problems

To be able to use the ideas from Section 8.1 for non-linear eigenvalue problems of the form (8.1) as well, we introduce additional unknowns to transform (8.1) into a generalized-linear eigenvalue problem of the form (8.2). Although this makes the shift-and-invert Arnoldi algorithm 2 applicable to rational eigenvalue problems, the resulting problem is much more costly to solve compared to linear problems with the same dimensions. In the following we construct an algorithm that applies the procedure described above, with no significant extra costs compared to Algorithm 2, for generalized-linear problems of the same dimensions.

### 8.2.1. Linear representations

We define the linear representation of a non-linear eigenvalue problem as follows:

**Definition 8.2.** Let  $N \in \mathbb{N}$  and  $\mathbf{M} : \Lambda \subset \mathbb{C} \rightarrow \mathbb{C}^{N \times N}$ . Moreover, let  $M \in \mathbb{N}$  and  $\mathbf{T} : \Lambda \rightarrow \mathbb{C}^{(N+M) \times (N+M)}$ ,  $\mathbf{V} : \Lambda \rightarrow \mathbb{C}^{N \times (N+M)}$  be affine matrix functions<sup>2</sup> such that  $\mathbf{T}(\omega)$  is regular for all  $\omega \in \Lambda_0 \subset \Lambda$  and

$$\mathbf{M}(\omega) \mathbf{u} = \mathbf{V}(\omega) \mathbf{T}(\omega)^{-1} \begin{pmatrix} \mathbf{u} \\ \mathbf{0} \end{pmatrix}$$

for all  $\omega \in \Lambda_0$  and  $\mathbf{u} \in \mathbb{C}^N$ . Then we call  $\mathbf{V}, \mathbf{T}, \Lambda_0$  a *linear representation* of  $\mathbf{M}$ .

<sup>2</sup>For a matrix function  $\omega \mapsto \mathbf{A}(\omega)$ , the term "affine" has to be understood with respect to the variable  $\omega$  (i.e., in a sense that  $\mathbf{A}(\omega) = \hat{\mathbf{A}} - \omega \tilde{\mathbf{A}}$  for two constant matrices  $\hat{\mathbf{A}}, \tilde{\mathbf{A}}$  with suitable dimensions and  $\omega$  in the respective domain).

In the following we frequently use the decomposition of the matrix functions  $\mathbf{T}$  and  $\mathbf{V}$  into

$$\mathbf{V} = (\mathbf{V}^0, \mathbf{V}^1), \quad \mathbf{T} = \begin{pmatrix} \mathbf{T}^{0,0} & \mathbf{T}^{0,1} \\ \mathbf{T}^{1,0} & \mathbf{T}^{1,1} \end{pmatrix}, \quad (8.5)$$

with affine matrix functions  $\mathbf{V}^0 : \Lambda \rightarrow \mathbb{C}^{N \times N}$ ,  $\mathbf{V}^1 : \Lambda \rightarrow \mathbb{C}^{N \times M}$ ,  $\mathbf{T}^{0,0} : \Lambda \rightarrow \mathbb{C}^{N \times N}$ ,  $\mathbf{T}^{0,1} : \Lambda \rightarrow \mathbb{C}^{N \times M}$ ,  $\mathbf{T}^{1,0} : \Lambda \rightarrow \mathbb{C}^{M \times N}$ ,  $\mathbf{T}^{1,1} : \Lambda \rightarrow \mathbb{C}^{M \times M}$ .

To illustrate Definition 8.2 and for later use, we give an example of a linear representation.

*Example 8.3.* Consider the rational eigenvalue problem corresponding to the matrix function

$$\mathbf{M} : \begin{cases} \mathbb{C} \setminus \{1\} & \rightarrow \mathbb{C}^{N \times N}, \\ \omega & \mapsto \mathbf{M}^0 + \frac{1}{1-\omega} \mathbf{M}^1 + \omega^3 \mathbf{M}^2 \end{cases} \quad (8.6)$$

for some matrices  $\mathbf{M}^0, \mathbf{M}^1, \mathbf{M}^2 \in \mathbb{C}^{N \times N}$  and some  $N \in \mathbb{N}$ . To find a linear representation of  $\mathbf{M}$ , one can introduce additional unknowns

$$\mathbf{u}^0 := \mathbf{u}, \quad \mathbf{u}^1 := \frac{1}{1-\omega} \mathbf{u}^0, \quad \mathbf{u}^2 := \omega \mathbf{u}^0, \quad \mathbf{u}^3 := \omega \mathbf{u}^2 = \omega^2 \mathbf{u}^0,$$

which are linear combinations of each other with an affine dependency on  $\omega$  and find the matrix  $\mathbf{T}(\omega) \in \mathbb{C}^{4N \times 4N}$  such that

$$\mathbf{T}(\omega) \begin{pmatrix} \mathbf{u}^0 \\ \mathbf{u}^1 \\ \mathbf{u}^2 \\ \mathbf{u}^3 \end{pmatrix} = \begin{pmatrix} \mathbf{u} \\ \mathbf{0} \\ \mathbf{0} \\ \mathbf{0} \end{pmatrix}.$$

For (8.6), a linear representation is then given by the matrix functions

$$\mathbf{T}(\omega) := \begin{pmatrix} \mathbf{I}_N & \mathbf{0} & \mathbf{0} & \mathbf{0} \\ -\mathbf{I}_N & (1-\omega)\mathbf{I}_N & \mathbf{0} & \mathbf{0} \\ -\omega\mathbf{I}_N & \mathbf{0} & \mathbf{I}_N & \mathbf{0} \\ \mathbf{0} & \mathbf{0} & -\omega\mathbf{I}_N & \mathbf{I}_N \end{pmatrix}, \quad \mathbf{V}(\omega) := (\mathbf{M}^0, \mathbf{M}^1, \mathbf{0}, \omega\mathbf{M}^2)$$

for  $\omega \in \mathbb{C}$ . Since  $\det(\mathbf{T}(\omega)) = 1 - \omega$  for all  $\omega \in \mathbb{C}$ , we can pick  $\Lambda_0 = \Lambda = \mathbb{C} \setminus \{1\}$ . Straightforward computations show that  $\mathbf{T}, \mathbf{V}, \Lambda_0$  is indeed a linear representation of  $\mathbf{M}$

since

$$\begin{aligned}
 \mathbf{V}(\omega) \mathbf{T}(\omega)^{-1} \begin{pmatrix} \mathbf{u} \\ \mathbf{0} \\ \mathbf{0} \\ \mathbf{0} \end{pmatrix} &= (\mathbf{M}^0, \mathbf{M}^1, \mathbf{0}, \omega \mathbf{M}^2) \begin{pmatrix} \mathbf{I}_N & \mathbf{0} & \mathbf{0} & \mathbf{0} \\ -\mathbf{I}_N & (1-\omega)\mathbf{I}_N & \mathbf{0} & \mathbf{0} \\ -\omega\mathbf{I}_N & \mathbf{0} & \mathbf{I}_N & \mathbf{0} \\ \mathbf{0} & \mathbf{0} & -\omega\mathbf{I}_N & \mathbf{I}_N \end{pmatrix}^{-1} \begin{pmatrix} \mathbf{u} \\ \mathbf{0} \\ \mathbf{0} \\ \mathbf{0} \end{pmatrix} \\
 &= (\mathbf{M}^0, \mathbf{M}^1, \mathbf{0}, \omega \mathbf{M}^2) \begin{pmatrix} \mathbf{I}_N & \mathbf{0} & \mathbf{0} & \mathbf{0} \\ \frac{1}{1-\omega}\mathbf{I}_N & \frac{1}{1-\omega}\mathbf{I}_N & \mathbf{0} & \mathbf{0} \\ \omega\mathbf{I}_N & \mathbf{0} & \mathbf{I}_N & \mathbf{0} \\ \omega^2\mathbf{I}_N & \mathbf{0} & \omega\mathbf{I}_N & \mathbf{I}_N \end{pmatrix} \begin{pmatrix} \mathbf{u} \\ \mathbf{0} \\ \mathbf{0} \\ \mathbf{0} \end{pmatrix} \\
 &= (\mathbf{M}^0, \mathbf{M}^1, \mathbf{0}, \omega \mathbf{M}^2) \begin{pmatrix} \mathbf{u} \\ \frac{1}{1-\omega}\mathbf{u} \\ \omega\mathbf{u} \\ \omega^2\mathbf{u} \end{pmatrix} \\
 &= \left( \mathbf{M}^0 + \frac{1}{1-\omega}\mathbf{M}^1 + \omega^3\mathbf{M}^2 \right) \mathbf{u} = \mathbf{M}(\omega) \mathbf{u}
 \end{aligned}$$

for  $\mathbf{u} \in \mathbb{C}^N$  and  $\omega \in \mathbb{C} \setminus \{1\}$ .

*Remark 8.4.* Example 8.3 shows the linear representation of a rational eigenvalue problem with scalar coefficients. Note, however, that the linear representations from Definition 8.2 may also be applied to non-linear eigenvalue problems of a more involved form than sums over constant matrices times scalar functions (i.e., than the ones given in Problem 8.1).

The following lemma shows that a linear representation is, in some sense, equivalent to the initial non-linear problem.

**Lemma 8.5.** *Let  $\mathbf{V}, \mathbf{T}, \Lambda_0$  be a linear representation of  $\mathbf{M}$  as in Definition 8.2 and (8.5). Then*

$$\Sigma(\mathbf{M}) \cap \Lambda_0 = \Sigma \left( \begin{pmatrix} \mathbf{V}^0 & \mathbf{V}^1 \\ \mathbf{T}^{1,0} & \mathbf{T}^{1,1} \end{pmatrix} \right) \cap \Lambda_0.$$

*Proof.* Let  $\omega \in \Sigma(\mathbf{M}) \cap \Lambda_0$ . Then there exists a vector  $\mathbf{u} \in \mathbb{C}^N \setminus \{\mathbf{0}\}$  such that

$$\mathbf{M}(\omega) \mathbf{u} = \mathbf{0}.$$

Since  $\mathbf{V}, \mathbf{T}, \Lambda_0$  is a linear representation and  $\omega \in \Lambda_0$ , we have

$$\mathbf{0} = \mathbf{M}(\omega) \mathbf{u} = \mathbf{V}(\omega) \mathbf{T}(\omega)^{-1} \begin{pmatrix} \mathbf{u} \\ \mathbf{0} \end{pmatrix}.$$

Because  $\mathbf{T}(\omega)$  is regular and  $\mathbf{u} \neq \mathbf{0}$ , we have  $\mathbf{z} := \mathbf{T}(\omega)^{-1} \begin{pmatrix} \mathbf{u} \\ \mathbf{0} \end{pmatrix} \neq \mathbf{0}$  and since

$$\begin{pmatrix} \mathbf{u} \\ \mathbf{0} \end{pmatrix} = \mathbf{T}(\omega) \mathbf{z},$$

we have that  $(\mathbf{T}^{1,0}, \mathbf{T}^{1,1})(\omega) \mathbf{z} = \mathbf{0}$  and therefore also

$$\begin{pmatrix} \mathbf{V}^0(\omega) & \mathbf{V}^1(\omega) \\ \mathbf{T}^{1,0}(\omega) & \mathbf{T}^{1,1}(\omega) \end{pmatrix} \mathbf{z} = \mathbf{0}.$$



Thus,  $(\omega, \mathbf{z})$  is an eigenpair of  $\begin{pmatrix} \mathbf{V}^0 & \mathbf{V}^1 \\ \mathbf{T}^{1,0} & \mathbf{T}^{1,1} \end{pmatrix}$ .

Let  $(\omega, \mathbf{z}) \in \Lambda_0 \times \mathbb{C}^{N+M} \setminus \{\mathbf{0}\}$  be an eigenpair of  $\begin{pmatrix} \mathbf{V}^0 & \mathbf{V}^1 \\ \mathbf{T}^{1,0} & \mathbf{T}^{1,1} \end{pmatrix}$ , meaning that

$$\begin{pmatrix} \mathbf{V}^0(\omega) & \mathbf{V}^1(\omega) \\ \mathbf{T}^{1,0}(\omega) & \mathbf{T}^{1,1}(\omega) \end{pmatrix} \mathbf{z} = \mathbf{0}.$$

It follows that

$$\mathbf{T}(\omega) \mathbf{z} = \begin{pmatrix} (\mathbf{T}^{0,0}(\omega), \mathbf{T}^{0,1}(\omega)) \mathbf{z} \\ (\mathbf{T}^{1,0}(\omega), \mathbf{T}^{1,1}(\omega)) \mathbf{z} \end{pmatrix} =: \begin{pmatrix} \mathbf{y} \\ \mathbf{0} \end{pmatrix},$$

with  $\mathbf{y} \neq \mathbf{0}$ , since  $\mathbf{T}(\omega)$  is regular by assumption and  $\mathbf{z} \neq \mathbf{0}$ . All in all, we have that

$$\mathbf{M}(\omega) \mathbf{y} = \mathbf{V}(\omega) \mathbf{T}(\omega)^{-1} \begin{pmatrix} \mathbf{y} \\ \mathbf{0} \end{pmatrix} = \mathbf{V}(\omega) \mathbf{T}(\omega)^{-1} \mathbf{T}(\omega) \mathbf{z} = \mathbf{V}(\omega) \mathbf{z} = \mathbf{0},$$

stating that  $(\omega, \mathbf{y})$  is an eigenpair of  $\mathbf{M}$ . □

The matrix function  $\mathbf{T}$  of the linear representation in Example 8.3 is of the form

$$\mathbf{T}(\omega) = \begin{pmatrix} \mathbf{I}_N & \mathbf{0} \\ \mathbf{T}^{1,0}(\omega) & \mathbf{T}^{1,1}(\omega) \end{pmatrix}, \quad (8.7)$$

stating that the eigenvectors are, essentially, not changed during the process of deriving the linear representation. In this case, if we find an eigenvalue  $\omega$  of the matrix function  $\begin{pmatrix} \mathbf{V}^0 & \mathbf{V}^1 \\ \mathbf{T}^{1,0} & \mathbf{T}^{1,1} \end{pmatrix}$  for a linear representation as in Lemma 8.5, we merely need to check whether  $\mathbf{T}^{1,1}(\omega)$  is regular. If this is the case, by Lemma 8.5,  $\omega$  is an eigenvalue of the non-linear problem corresponding to  $\mathbf{M}$ . If  $\mathbf{T}^{1,1}(\omega)$  is singular we have no information whether  $\omega$  is an eigenvalue of the non-linear problem as well.

### 8.2.2. The Arnoldi algorithm for linear representations

Since the matrix function

$$\mathbf{L}^{\mathbf{V}, \mathbf{T}} := \begin{pmatrix} \mathbf{V}^0 & \mathbf{V}^1 \\ \mathbf{T}^{1,0} & \mathbf{T}^{1,1} \end{pmatrix}, \quad (8.8)$$

induced by a linear representation of a non-linear eigenvalue problem as given in Definition 8.2, is affine, the according eigenvalue problem is of the form (8.2). Thus, we may apply the shift-and-invert Arnoldi algorithm (Algorithm 2) to the eigenvalue problem corresponding to the matrix function  $\mathbf{L}^{\mathbf{V}, \mathbf{T}}$  from (8.8) to approximate eigenvalues and eigenvectors of the non-linear problem corresponding to  $\mathbf{M}$  (cf. Lemma 8.5).

As noted before, the factorization of the inverse matrix (in this case the inverse of  $\mathbf{L}^{\mathbf{V}, \mathbf{T}}(\omega)$  from (8.8)) contributes the main computational effort of this algorithm. Therefore, we attempt to make the factorization and application of this inverse more efficient. To this end, we state the following definition:

**Definition 8.6.** Let  $\mathbf{V}, \mathbf{T}, \Lambda_0$  be a linear representation of  $\mathbf{M}$  as in Definition 8.2 and (8.5). Then we write  $\hat{\cdot}$  and  $\tilde{\cdot}$  for the constant part and first derivative respectively, of all the affine matrix functions involved (e.g.,  $\mathbf{V}(\omega) = \hat{\mathbf{V}} - \omega\tilde{\mathbf{V}}$ ). We also adopt this notation for further occurring affine matrix functions. Moreover, for  $\mathbf{L}^{\mathbf{V},\mathbf{T}}$  as in (8.8) and  $\mathbf{u} \in \mathbb{C}^N$ , we write

$$\mathbf{n}^{\mathbf{M},\omega}(\mathbf{u}) := \mathbf{L}^{\mathbf{V},\mathbf{T}}(\omega)^{-1} \tilde{\mathbf{L}}^{\mathbf{V},\mathbf{T}} \mathbf{u} = \begin{pmatrix} \mathbf{V}^0(\omega) & \mathbf{V}^1(\omega) \\ \mathbf{T}^{1,0}(\omega) & \mathbf{T}^{1,1}(\omega) \end{pmatrix}^{-1} \begin{pmatrix} \tilde{\mathbf{V}}^0 & \tilde{\mathbf{V}}^1 \\ \mathbf{T}^{\tilde{1},0} & \mathbf{T}^{\tilde{1},1} \end{pmatrix} \mathbf{u}$$

for the next vector in the shift-and-invert Arnoldi algorithm (Algorithm 2) applied to the generalized-linear eigenvalue problem corresponding to the affine matrix function  $\mathbf{L}^{\mathbf{V},\mathbf{T}}$  (Algorithm 2, line 5).

The following lemma states that the inverse of the matrix  $\mathbf{M}(\omega)$  is exactly the Schur complement of the matrix  $\mathbf{L}^{\mathbf{V},\mathbf{T}}(\omega)$  and therefore gives us a formula for the inverse involved in the computation of  $\mathbf{n}^{\mathbf{M},\omega}(\mathbf{u})$ .

**Lemma 8.7.** Let  $\mathbf{T}, \mathbf{V}, \Lambda_0$  a linear representation of  $\mathbf{M}$  as in Definition 8.2 that fulfills (8.5) and (8.7) and  $\mathbf{L}^{\mathbf{V},\mathbf{T}}$  as in (8.8). Then for  $\omega \in \Lambda_0$

$$\mathbf{M}(\omega) = \mathbf{V}^0(\omega) - \mathbf{V}^1(\omega) \mathbf{T}^{1,1}(\omega)^{-1} \mathbf{T}^{1,0}(\omega)$$

(i.e.,  $\mathbf{M}(\omega)$  is the Schur complement of the matrix  $\mathbf{L}^{\mathbf{V},\mathbf{T}}(\omega)$  from (8.8)). Moreover, for  $\omega \in \Lambda_0 \setminus \Sigma(\mathbf{M})$  and  $\mathbf{z}^0 \in \mathbb{C}^N, \mathbf{z}^1 \in \mathbb{C}^M$ , we have

$$\mathbf{L}^{\mathbf{V},\mathbf{T}}(\omega)^{-1} \begin{pmatrix} \mathbf{z}^0 \\ \mathbf{z}^1 \end{pmatrix} = \begin{pmatrix} \mathbf{M}(\omega)^{-1} (\mathbf{z}^0 - \mathbf{V}^1(\omega) \mathbf{T}^{1,1}(\omega)^{-1} \mathbf{z}^1) \\ \mathbf{T}^{1,1}(\omega)^{-1} (\mathbf{z}^1 - \mathbf{T}^{1,0}(\omega) \mathbf{n}^0) \end{pmatrix},$$

where  $\mathbf{n}^0 \in \mathbb{C}^N$  consists of the first  $N$  entries of the vector  $\mathbf{L}^{\mathbf{V},\mathbf{T}}(\omega)^{-1} \begin{pmatrix} \mathbf{z}^0 \\ \mathbf{z}^1 \end{pmatrix}$ .

*Proof.* For  $\omega \in \Lambda_0$ , the matrix  $\mathbf{T}(\omega)$ , and therefore also  $\mathbf{T}^{1,1}(\omega)$ , is regular and we have

$$\mathbf{T}(\omega)^{-1} = \begin{pmatrix} \mathbf{I}_N & \mathbf{0} \\ -\mathbf{T}^{1,1}(\omega)^{-1} \mathbf{T}^{1,0}(\omega) & \mathbf{T}^{1,1}(\omega)^{-1} \end{pmatrix}.$$

Thus, for arbitrary  $\mathbf{u} \in \mathbb{C}^N$

$$\begin{aligned} \mathbf{M}(\omega) \mathbf{u} &= \mathbf{V}(\omega) \begin{pmatrix} \mathbf{I}_N & \mathbf{0} \\ -\mathbf{T}^{1,1}(\omega)^{-1} \mathbf{T}^{1,0}(\omega) & \mathbf{T}^{1,1}(\omega)^{-1} \end{pmatrix} \begin{pmatrix} \mathbf{u} \\ \mathbf{0} \end{pmatrix} \\ &= \mathbf{V}(\omega) \begin{pmatrix} \mathbf{u} \\ -\mathbf{T}^{1,1}(\omega)^{-1} \mathbf{T}^{1,0}(\omega) \mathbf{u} \end{pmatrix} \\ &= \left( \mathbf{V}^0(\omega) - \mathbf{V}^1(\omega) \mathbf{T}^{1,1}(\omega)^{-1} \mathbf{T}^{1,0}(\omega) \right) \mathbf{u}. \end{aligned}$$

It follows that  $\mathbf{M}(\omega)$  is the Schur complement of the Matrix

$$\mathbf{L}^{\mathbf{V},\mathbf{T}}(\omega) = \begin{pmatrix} \mathbf{V}^0(\omega) & \mathbf{V}^1(\omega) \\ \mathbf{T}^{1,0}(\omega) & \mathbf{T}^{1,1}(\omega) \end{pmatrix}.$$

The second claim follows by Lemma A.17. □

Lemma 8.7 states that, to undertake the computations in the lines 3 and 5 in Algorithm 2, applied to  $\mathbf{L}^{\mathbf{V},\mathbf{T}}$  from (8.8), we can employ a factorization of the matrix  $\mathbf{M}(\omega)$  (i.e., as in the case of a generalized-linear problem (8.2), the according matrix function evaluated at the shift). Therefore, desirable properties of the matrix that has to be inverted (like, e.g., symmetry or skew-symmetry) are preserved. In general, this is not the case if simply the matrix  $\mathbf{L}^{\mathbf{V},\mathbf{T}}$  is used. The additional costs for the inversion and the application of the inverse for a linear representation compared to a generalized-linear problem consist mostly of the factorization and application of the inverse of the matrix  $\mathbf{T}^{1,1}(\omega) \in \mathbb{C}^{M \times M}$ .

Nevertheless, if the dimension  $M$  of the matrix  $\mathbf{T}^{1,1}(\omega)$  is as large as or larger than the dimension of the problem  $N$ , we still end up with the additional factorization of a large.

### 8.2.3. Linear representations by scalar multiples

We motivate the following section by applying Lemma 8.7 to the problem from Example 8.3.

*Example 8.3 (contd.).* Recall the linear representation

$$\mathbf{T}(\omega) = \begin{pmatrix} \mathbf{I}_N & \mathbf{0} & \mathbf{0} & \mathbf{0} \\ -\mathbf{I}_N & (1-\omega)\mathbf{I}_N & \mathbf{0} & \mathbf{0} \\ -\omega\mathbf{I}_N & \mathbf{0} & \mathbf{I}_N & \mathbf{0} \\ \mathbf{0} & \mathbf{0} & -\omega\mathbf{I}_N & \mathbf{I}_N \end{pmatrix}, \quad \mathbf{V}(\omega) = (\mathbf{M}^0, \mathbf{M}^1, \mathbf{0}, \omega\mathbf{M}_3)$$

of the matrix function (8.6).

Note that  $\mathbf{T}$  is of the form

$$\mathbf{T}(\omega) = \begin{pmatrix} 1 & \mathbf{0} \\ \mathbf{t}(\omega) & \mathbf{S}(\omega) \end{pmatrix} \otimes \mathbf{I}_N, \quad (8.9)$$

with

$$\mathbf{t}(\omega) := \begin{pmatrix} -1 \\ -\omega \\ 0 \end{pmatrix} \in \mathbb{C}^3, \quad \mathbf{S}(\omega) := \begin{pmatrix} 1-\omega & 0 & 0 \\ 0 & 1 & 0 \\ 0 & -\omega & 1 \end{pmatrix} \in \mathbb{C}^{3 \times 3},$$

where the Kronecker product  $\mathbf{A} \otimes \mathbf{B} \in \mathbb{C}^{NK \times ML}$  for two matrices  $\mathbf{A} = (\mathbf{A}_{i,j})_{i=1,\dots,N,j=1,\dots,M} \in \mathbb{C}^{N \times M}$ ,  $\mathbf{B} \in \mathbb{C}^{K \times L}$  and  $M, N, K, L \in \mathbb{N}$  is defined by

$$\mathbf{A} \otimes \mathbf{B} := \begin{pmatrix} \mathbf{A}_{1,1}\mathbf{B} & \dots & \mathbf{A}_{1,M}\mathbf{B} \\ \vdots & \ddots & \vdots \\ \mathbf{A}_{N,1}\mathbf{B} & \dots & \mathbf{A}_{N,M}\mathbf{B} \end{pmatrix}.$$

If we only introduce new unknowns that are scalar multiples of our original unknowns as in the present example, the matrix function  $\mathbf{T}$  of the according linear representation will always be of the form (8.9). This makes the computation and application of

$$\mathbf{T}^{1,1}(\omega)^{-1} = \mathbf{S}(\omega)^{-1} \otimes \mathbf{I}_N$$

straightforward and computationally cheap if the matrix  $\mathbf{S}(\omega)$  is small. This motivates the following definition:

**Definition 8.8.** We call a linear representation  $\mathbf{V}, \mathbf{T}, \Lambda_0$  of  $\mathbf{M} : \Lambda \subset \mathbb{C} \rightarrow \mathbb{C}^{N \times N}$  for  $N \in \mathbb{N}$  a *linear representation by scalar multiples* if the matrix function  $\mathbf{T} \in \mathbb{C}^{(m+1)N \times (m+1)N}$  for some  $m \in \mathbb{N}$  is of the form

$$\mathbf{T}(\omega) = \begin{pmatrix} \mathbf{T}^{0,0}(\omega) & \mathbf{T}^{0,1}(\omega) \\ \mathbf{T}^{1,0}(\omega) & \mathbf{T}^{1,1}(\omega) \end{pmatrix} = \begin{pmatrix} \mathbf{I}_N & \mathbf{0} \\ \mathbf{t}(\omega) \otimes \mathbf{I}_N & \mathbf{S}(\omega) \otimes \mathbf{I}_N \end{pmatrix}$$

for some matrix functions

$$\mathbb{C}^m \ni \mathbf{t}(\omega) = \hat{\mathbf{t}} - \omega \tilde{\mathbf{t}}, \quad \mathbb{C}^{m \times m} \ni \mathbf{S}(\omega) = \hat{\mathbf{S}} - \omega \tilde{\mathbf{S}}$$

and  $\omega \in \Lambda_0$ . We change the notation of  $\mathbf{V}$  slightly, compared to (8.5), by writing

$$\mathbf{V}(\omega) = (\mathbf{V}^0(\omega), \dots, \mathbf{V}^m(\omega))$$

for affine matrix functions  $\mathbf{V}^0, \dots, \mathbf{V}^m : \Lambda \rightarrow \mathbb{C}^{N \times N}$ . Moreover, we introduce the matrix functions

$$\begin{aligned} \mathbb{C}^{m \times (m+1)} \ni \mathbf{A}(\omega) &= \begin{pmatrix} \mathbf{A}_{1,0}(\omega) & \dots & \mathbf{A}_{1,m}(\omega) \\ \vdots & \ddots & \vdots \\ \mathbf{A}_{m,0}(\omega) & \dots & \mathbf{A}_{m,m}(\omega) \end{pmatrix} := \mathbf{S}(\omega)^{-1} \begin{pmatrix} \tilde{\mathbf{t}}, \tilde{\mathbf{S}} \end{pmatrix}, \\ \mathbb{C}^m \ni \mathbf{a}(\omega) &= \begin{pmatrix} \mathbf{a}_1(\omega) \\ \vdots \\ \mathbf{a}_m(\omega) \end{pmatrix} := \mathbf{S}(\omega)^{-1} \mathbf{t}(\omega), \end{aligned} \tag{8.10}$$

for all  $\omega \in \Lambda_0$ .

In the case of a linear representation by scalar multiples (Definition 8.8), the following theorem shows how to efficiently compute the next vector  $\mathbf{n}^{\mathbf{M}, \omega}$  (Definition 8.6) in the shift-and-invert Arnoldi algorithm.

**Theorem 8.9.** *Let  $\mathbf{V}, \mathbf{T}, \Lambda_0$  be a linear representation by scalar multiples of  $\mathbf{M}$  as in Definition 8.8 and  $\omega \in \Lambda_0 \setminus \Sigma(\mathbf{M})$ . Then the vector*

$$\mathbf{n}^{\mathbf{M}, \omega}(\mathbf{u}) = \left( (\mathbf{n}^0)^\top, \dots, (\mathbf{n}^m)^\top \right)^\top$$

from Definition 8.6 for

$$\mathbb{C}^{N(m+1)} \ni \mathbf{u} = \left( (\mathbf{u}^0)^\top, \dots, (\mathbf{u}^m)^\top \right)^\top$$

with  $\mathbf{u}^j, \mathbf{n}^j \in \mathbb{C}^N, j = 0, \dots, m$  can be computed by

$$\mathbb{C}^N \ni \mathbf{x}^i := \sum_{j=0}^m \mathbf{A}_{i,j}(\omega) \mathbf{u}^j, \quad i = 1, \dots, m,$$

$$\mathbb{C}^N \ni \mathbf{n}^0 = \mathbf{M}(\omega)^{-1} \left( \tilde{\mathbf{V}} \mathbf{u} - \sum_{i=1}^m \mathbf{V}^i(\omega) \mathbf{x}^i \right),$$

$$\mathbf{n}^i = \mathbf{x}^i - \mathbf{a}_i \mathbf{n}^0, \quad i = 1, \dots, m$$

with  $\mathbf{a}, \mathbf{A}$  as in (8.10).

*Proof.* For

$$\mathbf{z}^0 := \tilde{\mathbf{V}}\mathbf{u} = \left( \tilde{\mathbf{V}}^0, \dots, \tilde{\mathbf{V}}^m \right) \mathbf{u}, \quad \mathbf{z}^1 := \left( \tilde{\mathbf{T}}^{1,0}, \tilde{\mathbf{T}}^{1,1} \right) \mathbf{u} = \left( \tilde{\mathbf{t}}, \tilde{\mathbf{S}} \right) \otimes \mathbf{I}_N \mathbf{u}$$

we obtain, by applying Lemma 8.7<sup>3</sup> and using  $\mathbf{T}^{1,1}(\omega) = \mathbf{S}(\omega) \otimes \mathbf{I}_N$  and  $\mathbf{T}^{1,0}(\omega) = \mathbf{t}(\omega) \otimes \mathbf{I}_N$ , that

$$\begin{aligned} \mathbf{n}^{\mathbf{M},\omega}(\mathbf{u}) &= \begin{pmatrix} \mathbf{M}(\omega)^{-1} \left( \mathbf{z}^0 - (\mathbf{V}^1(\omega), \dots, \mathbf{V}^m(\omega)) \mathbf{T}^{1,1}(\omega)^{-1} \mathbf{z}^1 \right) \\ \mathbf{T}^{1,1}(\omega)^{-1} \left( \mathbf{z}^1 - \mathbf{T}^{1,0}(\omega) \mathbf{n}^0 \right) \end{pmatrix} \\ &= \begin{pmatrix} \mathbf{M}(\omega)^{-1} \left( \tilde{\mathbf{V}} - (\mathbf{V}^1(\omega), \dots, \mathbf{V}^m(\omega)) \mathbf{S}(\omega)^{-1} \left( \tilde{\mathbf{t}}, \tilde{\mathbf{S}} \right) \otimes \mathbf{I}_N \right) \mathbf{u} \\ \mathbf{S}(\omega)^{-1} \left( \left( \tilde{\mathbf{t}}, \tilde{\mathbf{S}} \right) \otimes \mathbf{I}_N \mathbf{u} - \mathbf{t}(\omega) \otimes \mathbf{I}_N \mathbf{n}^0 \right) \end{pmatrix} \\ &= \begin{pmatrix} \mathbf{M}(\omega)^{-1} \left( \tilde{\mathbf{V}} - (\mathbf{V}^1(\omega), \dots, \mathbf{V}^m(\omega)) \mathbf{A}(\omega) \otimes \mathbf{I}_N \right) \mathbf{u} \\ \mathbf{A}(\omega) \otimes \mathbf{I}_N \mathbf{u} - \mathbf{a}(\omega) \otimes \mathbf{I}_N \mathbf{n}^0 \end{pmatrix} \\ &= \begin{pmatrix} \mathbf{M}(\omega)^{-1} \left( \tilde{\mathbf{V}}\mathbf{u} - (\mathbf{V}^1(\omega), \dots, \mathbf{V}^m(\omega)) \begin{pmatrix} \mathbf{x}^1 \\ \vdots \\ \mathbf{x}^m \end{pmatrix} \right) \\ \mathbf{x}^1 - \mathbf{a}_1(\omega) \mathbf{n}^0 \\ \vdots \\ \mathbf{x}^m - \mathbf{a}_m(\omega) \mathbf{n}^0 \end{pmatrix}. \end{pmatrix} \end{aligned}$$

□

Theorem 8.9 immediately leads to Algorithm 3. This version of the shift-and-invert Arnoldi algorithm for linear representations is more efficient, compared to inverting the whole linear system matrix  $\mathbf{L}^{\mathbf{V},\mathbf{T}}(\omega) \in \mathbb{C}^{(m+1)N \times (m+1)N}$ , since only the matrix  $\mathbf{M}(\omega) \in \mathbb{C}^{N \times N}$  of the non-linear problem evaluated at the shift has to be inverted. Although it involves only the factorization and application of one large inverse matrix (lines 5 and 11), the vectors that have to be orthonormalized in each step are of the dimension  $(m+1)N$  (instead of  $N$  in the generalized-linear case).

Moreover, there are still many computations with large vectors involved in each step (lines 7–10 and lines 12–14).

The efficiency of Algorithm 3 depends on the number  $m$ , which depends on the choice of the linear representation. For rational functions  $\gamma_j$  with high orders, this number can get large compared to the number  $n+1$  of the involved matrices.

The matrices  $\hat{\mathbf{V}}, \tilde{\mathbf{V}}$  in Example 8.3 consist of scalar multiples of the constant matrices  $\mathbf{M}^j$  of the given problem. This observation can be formally put by assuming that the affine matrix functions  $\mathbf{V}^j : \Lambda \rightarrow \mathbb{C}^{N \times N}$  from

$$\mathbf{V}(\omega) = (\mathbf{V}^0(\omega), \dots, \mathbf{V}^m(\omega)) = \left( \hat{\mathbf{V}}^0, \dots, \hat{\mathbf{V}}^m \right) - \omega \left( \tilde{\mathbf{V}}^0, \dots, \tilde{\mathbf{V}}^m \right)$$

for  $\omega \in \Lambda$ , are given by

$$\hat{\mathbf{V}}^j = \sum_{i=0}^n \hat{\mathbf{P}}_{i,j} \mathbf{M}^i, \quad \tilde{\mathbf{V}}^j = \sum_{i=0}^n \tilde{\mathbf{P}}_{i,j} \mathbf{M}^i, \quad j = 1, \dots, m \quad (8.11)$$

<sup>3</sup>remember that we have to replace  $\mathbf{V}^1$  by  $(\mathbf{V}^1, \dots, \mathbf{V}^m)$

for matrices  $\hat{\mathbf{P}}, \tilde{\mathbf{P}} \in \mathbb{C}^{(n+1) \times (m+1)}$ .

*Remark 8.10.* Recall the matrix function

$$\mathbf{T}(\omega) = \begin{pmatrix} 1 & 0 & 0 & 0 \\ -1 & 1-\omega & 0 & 0 \\ -\omega & 0 & 1 & 0 \\ 0 & 0 & -\omega & 1 \end{pmatrix} \otimes \mathbf{I}_N$$

and its inverse

$$\mathbf{T}(\omega)^{-1} = \begin{pmatrix} 1 & 0 & 0 & 0 \\ \frac{1}{1-\omega} & \frac{1}{1-\omega} & 0 & 0 \\ \omega & 0 & 1 & 0 \\ \omega^2 & 0 & \omega & 1 \end{pmatrix} \otimes \mathbf{I}_N$$

of the linear representation of the matrix function

$$\mathbf{M}(\omega) = \sum_{j=0}^2 \gamma_j(\omega) \mathbf{M}^j = \mathbf{M}^0 + \frac{1}{1-\omega} \mathbf{M}^1 + \omega^3 \mathbf{M}^2$$

for  $\omega \in \mathbb{C} \setminus \{1\}$ .

For this linear representation the matrices from 8.11 are given by

$$\hat{\mathbf{P}} = \begin{pmatrix} 1 & 0 & 0 & 0 \\ 0 & 1 & 0 & 0 \\ 0 & 0 & 0 & 0 \end{pmatrix}, \quad \tilde{\mathbf{P}} = \begin{pmatrix} 0 & 0 & 0 & 0 \\ 0 & 0 & 0 & 0 \\ 0 & 0 & 0 & 1 \end{pmatrix}$$

since  $\mathbf{V}(\omega) = (\mathbf{M}^0, \mathbf{M}^1, \mathbf{0}, \omega \mathbf{M}^2)$ .

The fact that the coefficient functions  $\gamma_j$  are entries of the first column of  $\mathbf{T}(\omega)^{-1}$  suggests that we can evaluate the coefficients  $\gamma_j$  at a point  $\omega \in \Lambda_0$  by using a given linear representation.

Indeed, for a linear representation by scalar multiples  $\mathbf{T}, \mathbf{V}, \Lambda_0$  of  $\mathbf{M}(\omega) = \sum_{j=0}^n \gamma_j(\omega) \mathbf{M}^j$ , we obtain, by Lemma 8.7, for  $\omega \in \Lambda_0$

$$\begin{aligned} \mathbf{M}(\omega) &= \mathbf{V}^0(\omega) - (\mathbf{V}^1(\omega), \dots, \mathbf{V}^m(\omega)) \mathbf{T}^{1,1}(\omega)^{-1} \mathbf{T}^{1,0}(\omega) \\ &= \sum_{i=0}^n \mathbf{M}^i (\hat{\mathbf{P}}_{i,0} - \omega \tilde{\mathbf{P}}_{i,0}) - \sum_{j=1}^m \sum_{i=0}^n \mathbf{M}^i (\hat{\mathbf{P}}_{i,j} - \omega \tilde{\mathbf{P}}_{i,j}) \mathbf{a}_j(\omega) \\ &= (\mathbf{M}^0, \dots, \mathbf{M}^n) (\hat{\mathbf{P}} - \omega \tilde{\mathbf{P}}) \begin{pmatrix} 1 \\ -\mathbf{a}(\omega) \end{pmatrix}. \end{aligned}$$

It follows that

$$(\gamma_0(\omega), \dots, \gamma_n(\omega))^T = (\hat{\mathbf{P}} - \omega \tilde{\mathbf{P}}) \begin{pmatrix} 1 \\ -\mathbf{a}(\omega) \end{pmatrix}.$$

These considerations also show that linear representations by scalar multiples (Definition 8.8) can only exist for rational eigenvalue problems (Problem 8.1) since the function  $\mathbf{a}(\cdot) = \mathbf{S}(\cdot)^{-1} \mathbf{t}(\cdot)$  is always rational.

Due to the formulas for the computation of the next vector in the shift-and-invert Arnoldi algorithm for a linear representation by scalar multiples from Theorem 8.9, it is clear that all the components  $\mathbf{n}^j, j = 0, \dots, m$  of the vector  $\mathbf{n}^{\mathbf{M}, \omega}(\mathbf{u})$  can be written as linear combinations of the component  $\mathbf{n}^0$  and the components of the previous vector  $\mathbf{u}$ . The following, a little technical, theorem utilizes this fact and the assumption (8.11) to derive a more efficient version of Algorithm 3.

**Theorem 8.11.** *Let  $\mathbf{T}, \mathbf{V}, \Lambda_0$  be a linear representation by scalar multiples of the matrix function  $\mathbf{M} : \Lambda \rightarrow \mathbb{C}^{N \times N}$ ,  $N \in \mathbb{N}$ , and  $\omega \in \Lambda_0 \setminus \Sigma(\mathbf{M})$  such that (8.11) holds. Moreover, let  $k \in \mathbb{N}$ ,  $\mathbf{b}^0, \dots, \mathbf{b}^{k-1} \in \mathbb{C}^N$  be normalized and orthogonal,*

$$\mathbf{n}^{\mathbf{M}}(\mathbf{u}, \omega) = \left( (\mathbf{n}^0)^\top, \dots, (\mathbf{n}^m)^\top \right)^\top,$$

as in Definition 8.6, and

$$\mathbf{u} = \left( (\mathbf{u}^0)^\top, \dots, (\mathbf{u}^m)^\top \right)^\top \in \mathbb{C}^{N(m+1)}$$

with  $\mathbf{u}^j, \mathbf{n}^j \in \mathbb{C}^N, j = 0, \dots, m$  such that  $\mathbf{u}^j = (\mathbf{b}^0, \dots, \mathbf{b}^{k-1}) \mathbf{c}^j$  for  $j = 0, \dots, m$  and  $\mathbf{c}^j \in \mathbb{C}^k$ .

Then there exist vectors  $\mathbf{d}^0, \dots, \mathbf{d}^m \in \mathbb{C}^{k+1}$  such that

$$\mathbf{n}^{\mathbf{M}}(\mathbf{u}, \omega) = \begin{pmatrix} (\mathbf{b}^0, \dots, \mathbf{b}^k) \mathbf{d}^0 \\ \vdots \\ (\mathbf{b}^0, \dots, \mathbf{b}^k) \mathbf{d}^m \end{pmatrix},$$

where  $\mathbf{b}^k$  is the orthonormalization of  $\mathbf{n}^0$  against  $\mathbf{b}^0, \dots, \mathbf{b}^{k-1}$  which defines  $\mathbf{d}^0$ . Moreover, with

$$\mathbf{w}^{j,l} := \mathbf{M}^j \mathbf{b}^l \in \mathbb{C}^N, \quad j = 0, \dots, n, l = 0, \dots, k-1,$$

and  $\mathbf{a}, \mathbf{A}$  as in Definition 8.8, the vectors  $\mathbf{n}^0$  and  $\mathbf{d}^1, \dots, \mathbf{d}^m$  can be computed by

$$\begin{aligned} \mathbf{n}^0 &= \mathbf{M}^{-1}(\omega) \sum_{j=0}^n \left( \mathbf{w}^{j,0}, \dots, \mathbf{w}^{j,k-1} \right) \mathbf{e}^j, \\ (\mathbf{d}^1, \dots, \mathbf{d}^m) &= \begin{pmatrix} (\mathbf{c}^0, \dots, \mathbf{c}^m) \mathbf{A}(\omega)^\top \\ \mathbf{0} \end{pmatrix} - \mathbf{d}^0 \mathbf{a}(\omega)^\top, \end{aligned}$$

with

$$\begin{aligned} \mathbb{C}^{(n+1) \times (m+1)} \ni \mathbf{F}(\omega) &:= \tilde{\mathbf{P}} - \left( \hat{\mathbf{P}} - \omega \tilde{\mathbf{P}} \right) \begin{pmatrix} \mathbf{0} \\ \mathbf{A}(\omega) \end{pmatrix}, \\ \mathbb{C}^{k \times (n+1)} \ni (\mathbf{e}^0, \dots, \mathbf{e}^n) &:= (\mathbf{c}^0, \dots, \mathbf{c}^m) \mathbf{F}(\omega)^\top. \end{aligned}$$

*Proof.* From Theorem 8.9 it is clear that the components  $\mathbf{n}^1, \dots, \mathbf{n}^m$  are linear combinations of the components of  $\mathbf{u}$  and  $\mathbf{n}^0$  and therefore also of  $\mathbf{b}^0, \dots, \mathbf{b}^k$ . For the remainder, we use the formula for  $\mathbf{n}^0$  from Theorem 8.9

$$\mathbf{n}^0 = \mathbf{M}^{-1}(\omega) \left( \tilde{\mathbf{V}} - (\mathbf{V}^1(\omega), \dots, \mathbf{V}^m(\omega)) \mathbf{A}(\omega) \otimes \mathbf{I}_N \right) \mathbf{u}$$

to compute

$$\begin{aligned}
 \mathbf{M}(\omega) \mathbf{n}^0 &= \sum_{j=0}^m \tilde{\mathbf{V}}^j \mathbf{u}^j - \sum_{k=1}^m (\hat{\mathbf{V}}^k - \omega \tilde{\mathbf{V}}^k) \sum_{j=0}^m \mathbf{A}_{k,j}(\omega) \mathbf{u}^j \\
 &= \sum_{j=0}^m \tilde{\mathbf{V}}^j (\mathbf{b}^0, \dots, \mathbf{b}^{k-1}) \mathbf{c}^j - \sum_{k=1}^m (\hat{\mathbf{V}}^k - \omega \tilde{\mathbf{V}}^k) \sum_{j=0}^m \mathbf{A}_{k,j}(\omega) (\mathbf{b}^0, \dots, \mathbf{b}^{k-1}) \mathbf{c}^j \\
 &= \sum_{j=0}^m \sum_{i=0}^n \tilde{\mathbf{P}}_{i,j} \mathbf{M}^i (\mathbf{b}^0, \dots, \mathbf{b}^{k-1}) \mathbf{c}^j \\
 &\quad - \sum_{k=1}^m \sum_{i=0}^n (\hat{\mathbf{P}}_{i,k} - \omega \tilde{\mathbf{P}}_{i,k}) \mathbf{M}^i (\mathbf{b}^0, \dots, \mathbf{b}^{k-1}) \sum_{j=0}^m \mathbf{A}_{k,j}(\omega) \mathbf{c}^j \\
 &= \sum_{i=0}^n (\mathbf{w}^{i,0}, \dots, \mathbf{w}^{i,k-1}) \left( \sum_{j=0}^m \tilde{\mathbf{P}}_{i,j} \mathbf{c}^j - \sum_{k=1}^m (\hat{\mathbf{P}}_{i,k} - \omega \tilde{\mathbf{P}}_{i,k}) \sum_{j=0}^m \mathbf{A}_{k,j}(\omega) \mathbf{c}^j \right) \\
 &= \sum_{i=0}^n (\mathbf{w}^{i,0}, \dots, \mathbf{w}^{i,k-1}) \underbrace{\left( \sum_{j=0}^m \mathbf{F}_{i,j}(\omega) \mathbf{c}^j \right)}_{\mathbf{e}^i},
 \end{aligned}$$

with

$$\mathbf{F}(\omega) := \tilde{\mathbf{P}} - (\hat{\mathbf{P}} - \omega \tilde{\mathbf{P}}) \begin{pmatrix} \mathbf{0} \\ \mathbf{A}(\omega) \end{pmatrix}.$$

Thus, the formula for  $\mathbf{n}^0$  is proven. Using the formulas for  $\mathbf{n}^i, i = 1, \dots, m$  from Theorem 8.9, we obtain

$$\begin{aligned}
 \mathbf{n}^i &= \sum_{j=0}^m \mathbf{A}_{i,j}(\omega) \mathbf{u}^j - \mathbf{a}_i(\omega) \mathbf{n}^0 \\
 &= \sum_{j=0}^m \mathbf{A}_{i,j}(\omega) (\mathbf{b}^0, \dots, \mathbf{b}^{k-1}) \mathbf{c}^j - \mathbf{a}_i(\omega) (\mathbf{b}^0, \dots, \mathbf{b}_k) \mathbf{d}^0 \\
 &= (\mathbf{b}^0, \dots, \mathbf{b}^k) \left( \sum_{j=0}^m \mathbf{A}_{i,j}(\omega) \begin{pmatrix} \mathbf{c}^j \\ 0 \end{pmatrix} - \mathbf{a}_i(\omega) \mathbf{d}^0 \right).
 \end{aligned}$$

Therefore,

$$(\mathbf{n}^1, \dots, \mathbf{n}^m) = (\mathbf{b}^0, \dots, \mathbf{b}^k) \left( \begin{pmatrix} (\mathbf{c}^0, \dots, \mathbf{c}^m) \mathbf{A}(\omega)^\top \\ \mathbf{0} \end{pmatrix} - \mathbf{d}^0 \mathbf{a}(\omega)^\top \right).$$

□

The main idea of Algorithm 4 is to utilize the fact that the  $m + 1$  components of the vectors  $\mathbf{u}^j \in \mathbb{C}^{(m+1)N}$  from Algorithm 3 can be written as linear combinations of the basis vectors  $\mathbf{b}^j \in \mathbb{C}^N$  (cf. Theorem 8.11). The only necessary additional assumption is that



the components of the first vector  $\mathbf{u}^0 \in \mathbb{C}^{(m+1)N}$  are scalar multiples of a vector  $\mathbf{b}^0 \in \mathbb{C}^N$ . Since the vectors  $\mathbf{b}^0, \dots, \mathbf{b}^k$  are already orthonormal, we merely have to orthonormalize the smaller vectors  $\left( (\mathbf{d}^0)^\top, \dots, (\mathbf{d}^m)^\top \right)^\top \in \mathbb{C}^{(K+1)(m+1)}$  (cf. Theorem 8.11) against the coefficient vectors of the previous large vectors. This leads to Algorithm 4.

### Discussion of Algorithm 4

Lines 1–6 in Algorithm 4 are pre-computations that have to be carried out only once, involving only small vectors and matrices. Lines 7 and 14 contain the, usually expensive, factorization and application of the inverse of the large matrix  $\mathbf{M}(\omega)$ . Lines 15–24 correspond to the orthonormalization of the next basis vector  $\mathbf{b}^k$  and are exactly as expensive as in the Arnoldi algorithm for the (generalized-)linear case (Algorithm 2). Line 25–36 involve only small vectors and are negligible with respect to their computational costs if  $n, m, K \ll N$ .

The only parts involving large vectors that are more expensive than in the linear case, are the lines 9–11 (in each step we have to multiply every matrix  $\mathbf{M}^j$  by the new basis vector) and the sum in line 14.

Since Algorithm 4 is, in exact arithmetic, equivalent to the shift-and-invert Arnoldi algorithm for the linear representation, the analysis of Algorithm 4 can be done using the analysis presented, for example, in [Saa11] for the Arnoldi algorithm.

### Comparison of Algorithms 2–4

Table 8.1 shows a comparison of the computational costs of the algorithms presented in this chapter. Under the reasonable assumption that  $n \leq m + 1 \ll N$  we can summarize that, with respect to the main contribution to the numerical costs, namely, the factorization and application of the large inverse matrix, Algorithms 3 and 4 for rational problems are as efficient as Algorithm 2 for generalized-linear problems. Due to its high costs for the factorization, applying Algorithm 2 to the linear representation  $\mathbf{L}^{\mathbf{V}, \mathbf{T}}$  is not advisable.

The computational costs for the orthonormalization grow quadratic in  $K$ . Thus, the higher costs for the orthonormalization of the larger vectors in Algorithm 3 can be relevant for larger values of  $K$ . Note, however, that Algorithm 4 also requires  $k(n + 1)$  additions in each step which leads to a quadratic growth in  $K$  as well. Nevertheless, while for small values of  $m$  and  $K$ , Algorithm 3 might be as efficient as Algorithm 4, in general, Algorithm 4 is the most efficient choice.

<sup>4</sup>where we counted a scalar multiplication together with a vector addition as one and also counted vector assignments

	Alg. 2 for $\mathbf{M}(\omega) = \mathbf{M}^0 - \omega\mathbf{M}^1$	Alg. 2 for $\mathbf{L}^{\mathbf{V},\mathbf{T}}$	Alg. 3	Alg. 4
dimension of the inverse matrix	$N$	$(m+1)N$	$N$	$N$
dimension of the vectors that are orthonormalized	$N$	$(m+1)N$	$(m+1)N$	$N$
number of applications of matrices with dim. $N$	1	$(m+1)^2$	$3m+1$	$n+1$
number of additions of vectors with dim. $N^4$	0	$(m+1)^2$	$(m+1)^2 + 2m$	$k(n+1)$

Table 8.1.: Comparison of the computational efficiency of the algorithms for generalized-linear and rational eigenvalue problems per iteration step, where  $N$  is the dimension of the matrix function,  $m$  is the number of additional unknowns,  $n+1$  the number of large matrices, and  $k$  the step. All computations involving no large vectors of dimension  $N$  are neglected, as well as the computation of the eigenvectors (lines 14–20 in Algorithm 1), since they are identical for all of the algorithms.

---

**Algorithm 3** Shift-and-invert Arnoldi algorithm for linear representations by scalar multiples with smart inverse

---

**Input:**  $\mathbf{M}, \tilde{\mathbf{V}}, \hat{\mathbf{V}}, \tilde{\mathbf{S}}, \hat{\mathbf{S}}, \tilde{\mathbf{t}}, \hat{\mathbf{t}}$  as in Definition 8.8,  $\omega \in \Lambda_0$ ,  $K \in \mathbb{N}$

**Output:**  $\mathbf{u}^0, \dots, \mathbf{u}^K \in \mathbb{C}^{N(m+1)}, \mathbf{H} \in \mathbb{C}^{(K+1) \times (K+1)}$

- 1: choose a normalized random vector  $\mathbf{u}^0 = \left( (\mathbf{u}^{0,0})^\top, \dots, (\mathbf{u}^{0,m})^\top \right)^\top \in \mathbb{C}^{N(m+1)}$
- 2:  $\mathbf{A} \leftarrow \left( \hat{\mathbf{S}} - \omega \tilde{\mathbf{S}} \right)^{-1} \left( \tilde{\mathbf{t}}, \tilde{\mathbf{S}} \right)$
- 3:  $\mathbf{a} \leftarrow \left( \hat{\mathbf{S}} - \omega \tilde{\mathbf{S}} \right)^{-1} \left( \hat{\mathbf{t}} - \omega \tilde{\mathbf{t}} \right)$
- 4:  $\mathbf{H} \leftarrow \mathbf{0} \in \mathbb{C}^{(K+1) \times (K+1)}$
- 5: factorize  $\mathbf{M}(\omega)^{-1}$
- 6: **for**  $k = 1, \dots, K + 1$  **do**
- 7:   **for**  $i = 1, \dots, m$  **do**
- 8:      $\mathbf{x}^i \leftarrow \sum_{l=0}^m \mathbf{A}_{i,l} \mathbf{u}^{k-1,l}$
- 9:   **end for**
- 10:  $\mathbf{y} \leftarrow \tilde{\mathbf{V}} \mathbf{u}^{k-1} - \sum_{l=1}^m \left( \hat{\mathbf{V}}^l - \omega \tilde{\mathbf{V}}^l \right) \mathbf{x}^l$
- 11:  $\mathbf{n}^0 \leftarrow \mathbf{M}(\omega)^{-1} \mathbf{y}$
- 12:   **for**  $i = 1, \dots, m$  **do**
- 13:      $\mathbf{n}^i \leftarrow \mathbf{x}^i - \mathbf{a}_i \mathbf{n}^0$
- 14:   **end for**
- 15:   **for**  $j = 0, \dots, k - 1$  **do**
- 16:      $\mathbf{H}_{j,k-1} \leftarrow \mathbf{u}^j \cdot \mathbf{n}$
- 17:      $\mathbf{n} = \left( (\mathbf{n}^0)^\top, \dots, (\mathbf{n}^m)^\top \right)^\top \leftarrow \mathbf{n} - \mathbf{H}_{j,k-1} \mathbf{u}^j$
- 18:   **end for**
- 19:   **if**  $\mathbf{n} = \mathbf{0}$  **then**
- 20:     break
- 21:   **end if**
- 22:   **if**  $k < K + 1$  **then**
- 23:      $\mathbf{H}_{k,k-1} \leftarrow \|\mathbf{n}\|$
- 24:      $\mathbf{u}^k \leftarrow \frac{\mathbf{n}}{\mathbf{H}_{k,k-1}}$
- 25:   **end if**
- 26: **end for**

---

---

**Algorithm 4** Optimized shift-and-invert Arnoldi algorithm for linear representations by scalar multiples

---

**Input:**  $\mathbf{M}^0, \dots, \mathbf{M}^n, \hat{\mathbf{P}}, \tilde{\mathbf{P}}, \hat{\mathbf{S}}, \tilde{\mathbf{S}}, \hat{\mathbf{t}}, \tilde{\mathbf{t}}$  as in Definition 8.8 and (8.11),  $\omega \in \Lambda_0$ ,  $K \in \mathbb{N}$

**Output:**  $\mathbf{b}^0, \dots, \mathbf{b}^K \in \mathbb{C}^N, \mathbf{c}^0, \dots, \mathbf{c}^K \in \mathbb{C}^{(K+1)(m+1)}, \mathbf{H} \in \mathbb{C}^{(K+1) \times (K+1)}$

- 1: pick a normalized rand. vectors  $\mathbf{b}^0 \in \mathbb{C}^N, \mathbf{c}^0 = \left( (\mathbf{c}^{0,0})^\top, \dots, (\mathbf{c}^{0,m})^\top \right)^\top \in \mathbb{C}^{(K+1)(m+1)}$ , with  $\mathbf{c}^{0,j} = \left( \mathbf{c}_0^{0,j}, \mathbf{0} \right)^\top \in \mathbb{C}^{K+1}$  and  $\mathbf{c}_0^{0,j} \in \mathbb{C}$  for  $j = 0, \dots, m$
  - 2:  $\mathbf{H} \leftarrow \mathbf{0} \in \mathbb{C}^{(K+1) \times (K+1)}$
  - 3:  $\mathbf{A} \leftarrow \left( \hat{\mathbf{S}} - \omega \tilde{\mathbf{S}} \right)^{-1} \left( \tilde{\mathbf{t}}, \tilde{\mathbf{S}} \right)$
  - 4:  $\mathbf{a} \leftarrow \left( \hat{\mathbf{S}} - \omega \tilde{\mathbf{S}} \right)^{-1} \left( \hat{\mathbf{t}} - \omega \tilde{\mathbf{t}} \right)$
  - 5:  $\mathbf{F} \leftarrow \tilde{\mathbf{P}} - \left( \hat{\mathbf{P}} - \omega \tilde{\mathbf{P}} \right) \begin{pmatrix} \mathbf{0} \\ \mathbf{A} \end{pmatrix}$
  - 6:  $(\gamma_0, \dots, \gamma_n)^\top \leftarrow \left( \hat{\mathbf{P}} - \omega \tilde{\mathbf{P}} \right) \begin{pmatrix} 1 \\ -\mathbf{a} \end{pmatrix}$
  - 7: factorize  $\mathbf{M}(\omega)^{-1} = \left( \sum_{i=0}^n \mathbf{M}^i \gamma_i \right)^{-1}$
  - 8: **for**  $k = 1, \dots, K + 1$  **do**
  - 9:   **for**  $i = 0, \dots, n$  **do**
  - 10:      $\mathbf{w}^{i,k-1} \leftarrow \mathbf{M}^i \mathbf{b}^{k-1}$
  - 11:   **end for**
  - 12:    $(\mathbf{e}^0, \dots, \mathbf{e}^n) \leftarrow (\mathbf{c}^{k-1,0}, \dots, \mathbf{c}^{k-1,m}) \mathbf{F}^\top$
  - 13:    $\mathbf{d}^0 \leftarrow \mathbf{0} \in \mathbb{C}^{K+1}$
  - 14:    $\mathbf{n} \leftarrow \mathbf{M}(\omega)^{-1} \sum_{i=0}^n \sum_{j=0}^{k-1} \mathbf{w}^{i,j} \mathbf{e}_j^i$
  - 15:   **for**  $j = 0, \dots, k - 1$  **do**
  - 16:      $\mathbf{d}_j^0 \leftarrow \overline{\mathbf{b}^j} \cdot \mathbf{n}$
  - 17:      $\mathbf{n} \leftarrow \mathbf{n} - \mathbf{d}_j^0 \mathbf{b}^j$
  - 18:   **end for**
-

---

```

19: if  $\mathbf{n} = \mathbf{0}$  then
20:     break
21: end if
22:  $l \leftarrow \|\mathbf{n}\|$ 
23:  $\mathbf{b}^k \leftarrow \frac{\mathbf{n}}{l}$ 
24:  $\mathbf{d}_k^0 \leftarrow l$ 
25:  $(\mathbf{d}^1, \dots, \mathbf{d}^m) \leftarrow (\mathbf{c}^{k-1,0}, \dots, \mathbf{c}^{k-1,m}) \mathbf{A}^\top - \mathbf{d}^0 \mathbf{a}^\top$ 
26:  $\mathbf{d} \leftarrow \left( (\mathbf{d}^0)^\top, \dots, (\mathbf{d}^m)^\top \right)^\top$ 
27: for  $j = 0, \dots, k-1$  do
28:      $\mathbf{H}_{j,k-1} \leftarrow \overline{\mathbf{c}^j} \cdot \mathbf{d}$ 
29:      $\mathbf{d} \leftarrow \mathbf{d} - \mathbf{H}_{j,k-1} \mathbf{c}^j$ 
30: end for
31: if  $\mathbf{d} = \mathbf{0}$  then
32:     break
33: end if
34: if  $k < K + 1$  then
35:      $\mathbf{H}_{k,k-1} \leftarrow \|\mathbf{d}\|$ 
36:      $\mathbf{c}^k \leftarrow \frac{\mathbf{d}}{\mathbf{H}_{k,k-1}}$ 
37: end if
38: end for

```

---



Die approbierte gedruckte Originalversion dieser Dissertation ist an der TU Wien Bibliothek verfügbar.  
The approved original version of this doctoral thesis is available in print at TU Wien Bibliothek.

## 9. Numerical Experiments

In this chapter we discuss the results of numerical experiments that show how the three main ideas of this thesis, namely,

- frequency-dependent complex scaling,
- tensor product discretizations generated by exterior coordinates, and
- complex-scaled infinite elements,

affect the performance of our method, compared to standard techniques.

In Section 9.2 we show that frequency-dependent scalings lead to a larger number of well-approximated resonances than frequency-independent scalings (Figures 9.4, 9.5, and 9.6). Moreover, we show that the use of curvilinear coordinates can help to considerably reduce the number of unknowns of the discrete problem (Figure 9.7 and Table 9.1). In Section 9.3 we perform experiments that exhibit the superior computational efficiency of complex-scaled infinite elements compared to certain PML approximations. Moreover, we numerically compute the condition numbers of the generalized-radial discretization matrices to show that they depend polynomially on the number of unknowns of the infinite element spaces (Section 9.1).

All of the experiments were done using an implementation along the lines of Chapter 7 based on the software package Netgen/NGsolve [Sch97, Sch14]. To solve the rational eigenvalue problems we used the shift-and-invert Arnoldi algorithm 4 from Chapter 8, where we applied a, once per shift pre-computed, Cholesky factorization for symmetric, non-hermitian problems to solve the linear system of equations in each step of the method.

We note that our implementation, as described in Chapter 7, is done in a way that it can be applied to problems with potential functions  $\rho$  that are non-constant in the exterior domain as well, as long as they allow a suitable decomposition in exterior coordinates (see Section 10.2.1).

### 9.1. Condition numbers

In Section 6.3 requirement (R6) for basis functions  $\phi_j$  was that they lead to well-conditioned discretization matrices. Figure 9.1 shows the condition numbers of the discretization matrices  $\tilde{\mathbf{A}}^{n,N}$  for a fixed scaling parameter  $\sigma_0 \in \mathbb{C} \setminus \{0\}$ , given by

$$\begin{aligned}
 \tilde{\mathbf{A}}_{j,k}^{n,N} := & \frac{1}{\sigma_0} \int_{\mathbb{R}_{>0}} (1 + \sigma_0 \xi)^2 \phi_j'(\xi) \phi_k'(\xi) d\xi \\
 & + \sigma_0 \int_{\mathbb{R}_{>0}} (n(n+1) - \omega^2(1 + \sigma_0 \xi)^2) \phi_j(\xi) \phi_k(\xi) d\xi, \quad (9.1)
 \end{aligned}$$

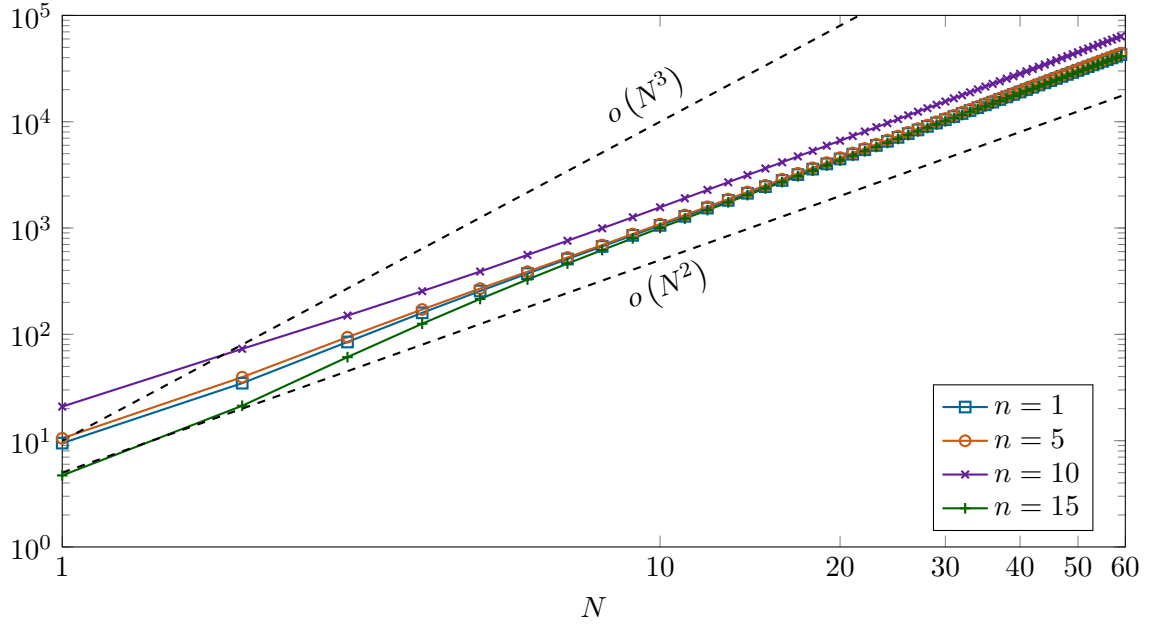


Figure 9.1.: Spectral condition numbers of the discretization matrices  $\tilde{\mathbf{A}}^{n,N}$  given by (9.1), with parameter  $\sigma_0 = 0.3 + 0.3i$  and frequency  $\omega = 10 - 0.5i$ .

with respect to different infinite element orders  $N \in \mathbb{N}$ . These matrices correspond to discretizations of the complex-scaled spherical Bessel equations with index  $n$ . We observe that the condition numbers grow slower than  $o(N^3)$ . For  $N = 60$  degrees of freedom the condition number is about  $10^5$ . Nevertheless, since the best approximation error decays at least super-algebraically (Section 6.5), we expect that the mild grow in the condition number is dominated by the fast convergence of the approximation error.

## 9.2. Comparison of different scalings

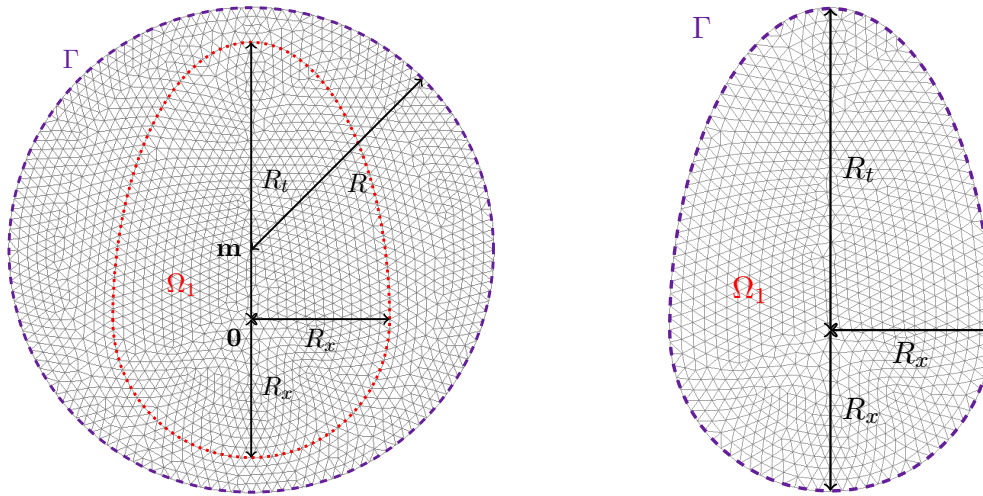
Similar to Section 4.2, we choose two-dimensional numerical examples with  $\Omega = \mathbb{R}^2$  and  $\rho = \rho_0 \chi_{\Omega_1}$ , and  $\rho_0 > -1$ , where  $\chi_{\Omega_1}$  denotes the indicator function of a set  $\Omega_1 \subset \mathbb{R}^2$  (Figures 9.2 and 9.3).

### Spherical scaling

Figure 9.4 shows the discrete resonances for spherical, frequency-independent scalings and infinite elements. We can observe that only the first two resonances are approximated with an approximation quality depending on the choice of the parameter. Moreover, we can observe the discretization of the essential spectrum  $\Sigma_{\text{dec}}$  (Sections 5.3.2 and 7.3) close to the imaginary axis.

Figure 9.5 shows discrete resonances computed using frequency-dependent scalings  $\sigma_\nu$  (see (7.14b)). Compared to the frequency-independent scaling in Figure 9.4, more resonances are approximated. Moreover, we can observe the essential spectrum  $\Sigma_{\text{sing}}$ . Note





(a) Geometry for the circular scaling. The dotted, red line marks the jump in the potential function  $\rho$ . (b) Geometry for the curvilinear scaling.

Figure 9.2.: Geometry with different choices of  $\Gamma$ . The upper part of  $\Omega_1$  consists of half of an ellipse with main semi-axis sizes  $R_t$  and  $R_x$ . The lower part is a half circle.

that although the set  $\Sigma_{\text{sing}}$  takes the shape derived in Section 7.3, it does not fill the whole region. This does not contradict our analysis from Chapter 5 since the essential spectrum  $\Sigma_{\text{sing}}$  therein was only derived for the case of a spherical scatterer. The lines  $\Lambda_{\text{sing}}^{\pm}$  delimit the area where the essential spectrum would occur for a circular scatterer surrounding  $\Omega_1$ . Since the set  $\Sigma_{\text{dec}}$  is empty in this case, we do not observe it here.

We emphasize again that the computations shown in Figure 9.5 were done using an identical mesh and the same number of degrees of freedom as the computations shown in Figure 9.4 (see also Table 9.1). The better results are solely a result of the more pleasant behavior of the complex-scaled eigenfunctions due to the frequency-dependent scaling.

Figure 9.6 shows discrete resonances obtained by using a spherical, frequency-dependent scaling  $\sigma_c$  (see (7.14d)). We observe a similar approximation quality as in Figure 9.5. This time the circular shaped essential spectrum  $\Sigma_{\text{dec}}$  is also present.

### Curvilinear scaling

To reduce the number of degrees of freedom, we use a curvilinear scaling (Section 7.1.3 and (7.12)) to be able to choose  $\Gamma := \partial \text{supp}(\rho)$  (Figure 9.2b). Note that this choice is not covered by our theory since we required a positive distance between the support of the potential  $\rho$  and the boundary  $\Gamma$  (Remark 2.5). Nevertheless, Figure 9.7 shows that this choice leads to better results than the application of spherical scalings.

Table 9.1 shows a comparison of the numbers of degrees of freedom for the spherical (Figures 9.4–9.6 and 9.2a) and the curvilinear scaling (Figures 9.7 and 9.2b). The use of

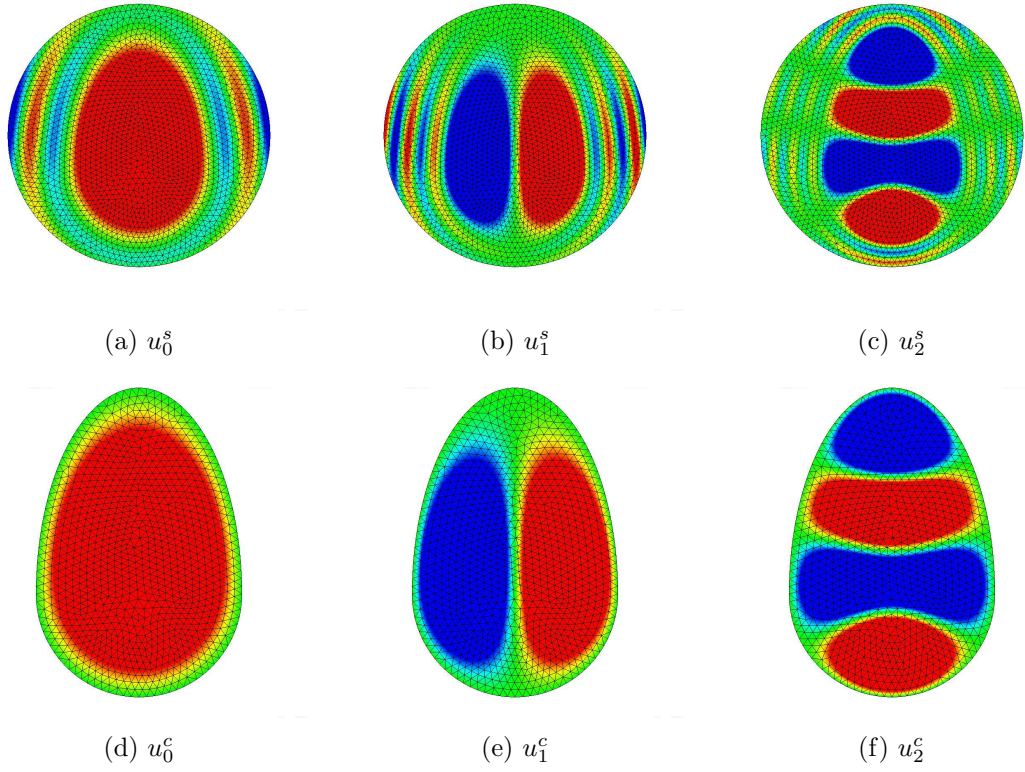


Figure 9.3.: Real parts of the resonance functions corresponding to resonances  $\omega_0 \approx 5.1262664193 - 0.4639832795i$ ,  $\omega_1 \approx 8.8930913382 - 0.4891699190i$ ,  $\omega_2 \approx 11.9748826324 - 0.3852545391i$  in  $\Omega_{\text{int}}$ . We used parameters  $R_t = 4$ ,  $R_x = 2$ ,  $\rho_0 = -0.8$  (see Figure 9.2) and the frequency-dependent scaling  $\sigma(\omega) = \frac{1+i}{\omega}$  and spherical ( $\mathbf{m} = (0, 1)^\top$ ,  $R = 3.5$ , Figures a–c, cf. Figure 9.5a) and curvilinear coordinates (Figures d–f, cf. Figure 9.7). The colors red, blue, and green correspond to positive, negative, and neutral values respectively. Note that the resonance functions in  $\Omega_{\text{ext}}$  are not pictured.

the curvilinear scaling considerably reduces the overall number of degrees of freedom due to the fact that only about half the number of interior degrees of freedom are needed. The number of exterior degrees of freedom is higher in the curvilinear case, since we need to introduce an additional unknown to obtain a rational problem (see Section 7.2 and (7.12)). Nevertheless, since the basis functions corresponding to the additional unknown are  $L^2$ -basis functions, they lead to more sparsity in the matrix structure than the degrees of freedom corresponding to the  $H^1$ -basis functions.

### 9.3. Comparison of infinite elements to PMLs

In this subsection we reproduce the results of [NW19, Section 6.2]. Contrary to the previous sections, we choose a three-dimensional example to compare the computational costs of the

	spherical	curvilinear
interior dofs	17 764	9 196
boundary $H^1$ -dofs	444	318
boundary $L^2$ -dofs		318
exterior $H^1$ -dofs	9 324	6 678
exterior $L^2$ -dofs		6 678
exterior dofs	8 880	13 038
total dofs	26 644	22 234

Table 9.1.: Comparison of the degrees of freedom (dofs) used for the experiments in Figures 9.4–9.6 (spherical scaling) and 9.7 (curvilinear scaling).

infinite elements to the ones of a PML. We approximate the resonances of the Helmholtz equation on  $\Omega_{\text{ext}} := \Omega := \mathbb{R}^3 \setminus \overline{B_1}$  with homogeneous Neumann boundary conditions on  $\partial\Omega$ . In this case the resonances are given by the roots of the spherical Hankel functions (Lemma 5.16) and the eigenfunctions are given by (5.12).

All of the computations in this section were done on a desktop computer with an Intel i3 CPU with 2x3.5GHz and 16GiB memory. All of the given times are for the factorization of the system matrix only since this factorization contributes the main computational effort to the used algorithm (see Chapter 8).

Figure 9.8 shows the error of the resonances plotted against the factorization times for infinite elements and a PML using the tensor product method described in Section 6.3.1, with one-dimensional, high-order finite element basis functions in radial direction on an interval  $[0, T]$ . We applied  $h$ -refinement to obtain a succession of discretizations, with an initial mesh consisting of one single element.

In Figures 9.8a and 9.8c the error generated by the truncation of the exterior domain can be observed at approximately  $10^{-3}$ . In Figures 9.8c and 9.8d the infinite elements already reach the error generated by the surface discretization, which is approximately  $10^{-7}$ . All of the experiments show that the infinite elements are clearly superior to the used PML discretizations with respect to the computational efficiency.

Note that, due to the fact that we used the tensor product ansatz also for the PML discretizations, this version of PML is already more efficient than a typical linear PML based on an unstructured exterior mesh. On the other hand, the efficiency of the PML can be increased by using more involved scaling profiles than the simple linear scaling functions we make use of. Moreover, an adapted one-dimensional mesh could be used to obtain better approximation properties in radial direction.

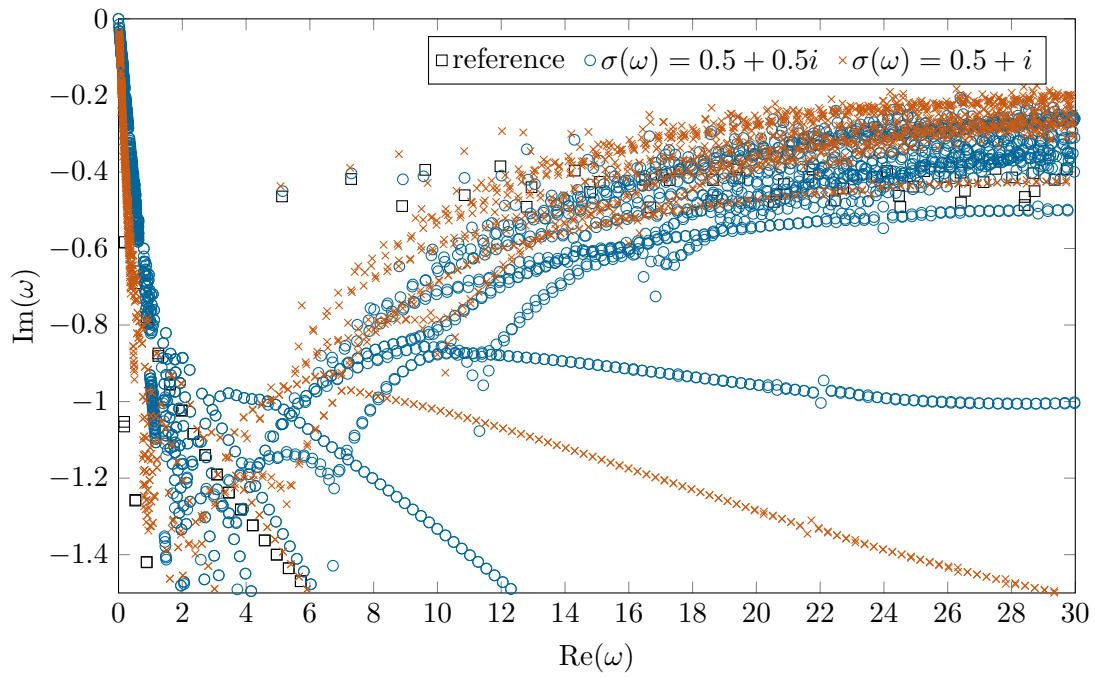
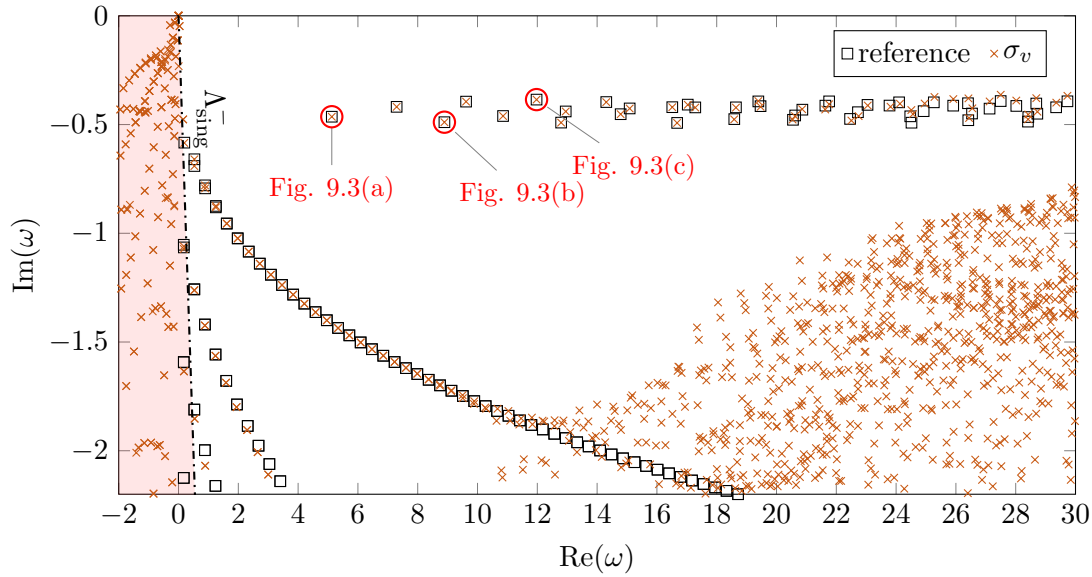
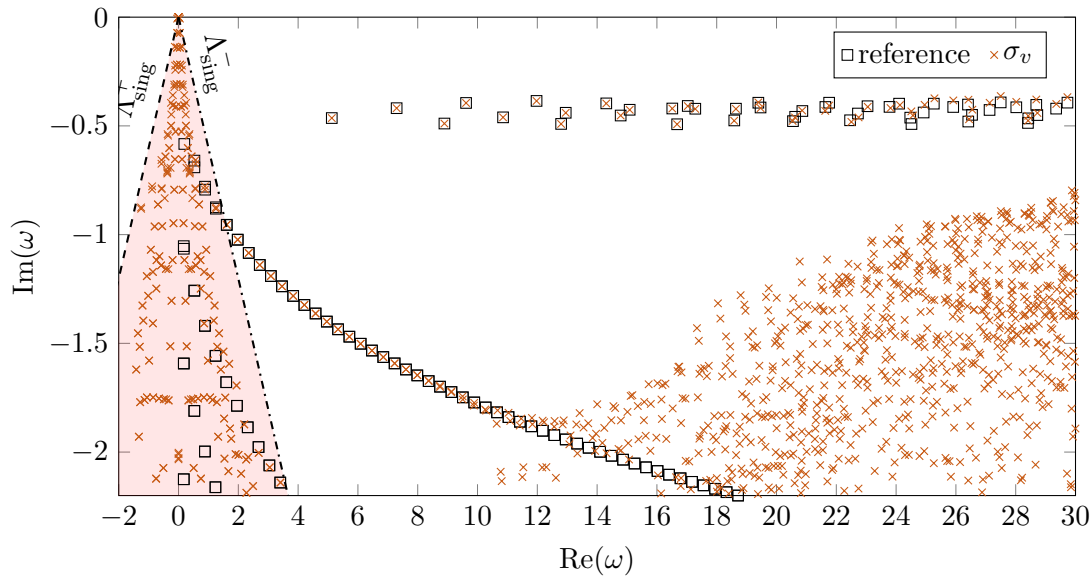


Figure 9.4.: Resonances for a spherical, frequency-independent scaling with  $R_t = 4$ ,  $R_x = 2$ ,  $R = 3.5$ ,  $\rho_0 = -0.8$ , and  $\mathbf{m} = (0, 1)^\top$ . The discretization parameters are  $N = 20$  and polynomial order 3 where we used the mesh from Figure 9.2a for the interior and surface discretization.



(a)  $\sigma_v(\omega) = \frac{1+i}{\omega}$



(b)  $\sigma_v(\omega) = \frac{i}{\omega}$

Figure 9.5.: Resonances for a spherical, frequency-dependent scaling  $\sigma_v$  with  $R_t = 4$ ,  $R_x = 2$ ,  $R = 3.5$ ,  $\rho_0 = -0.8$ ,  $\mathbf{m} = (0, 1)^\top$ . The discretization parameters are  $N = 20$  and polynomial order 3, where we used the mesh from Figure 9.2a. The dashdotted lines indicate the region where we expect the essential spectrum  $\Sigma_{\text{sing}}$ .



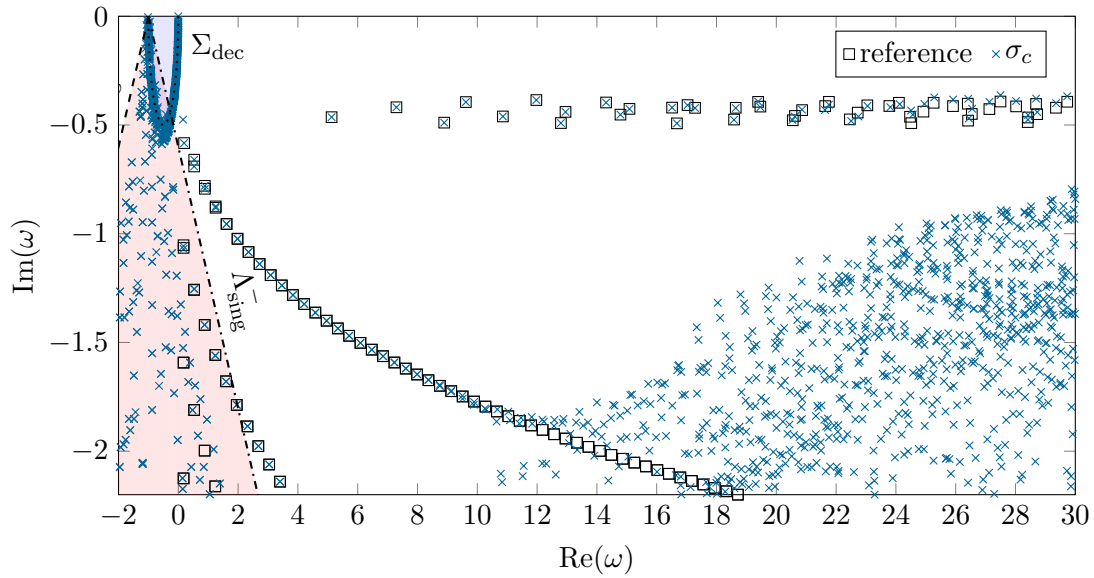


Figure 9.6.: Resonances for a spherical, frequency-dependent scaling  $\sigma_c(\omega) = \frac{i}{1+\omega}$  with  $R_t = 4$ ,  $R_x = 2$ ,  $R = 3.5$ ,  $\rho_0 = -0.8$ ,  $\mathbf{m} = (0, 1)^\top$ . The discretization parameters are  $N = 20$  and polynomial order 3, where we used the mesh from Figure 9.2a. The dashdotted and dotted lines indicate the regions where we expect the subsets of the essential spectrum  $\Sigma_{\text{sing}}$  and  $\Sigma_{\text{dec}}$  respectively.

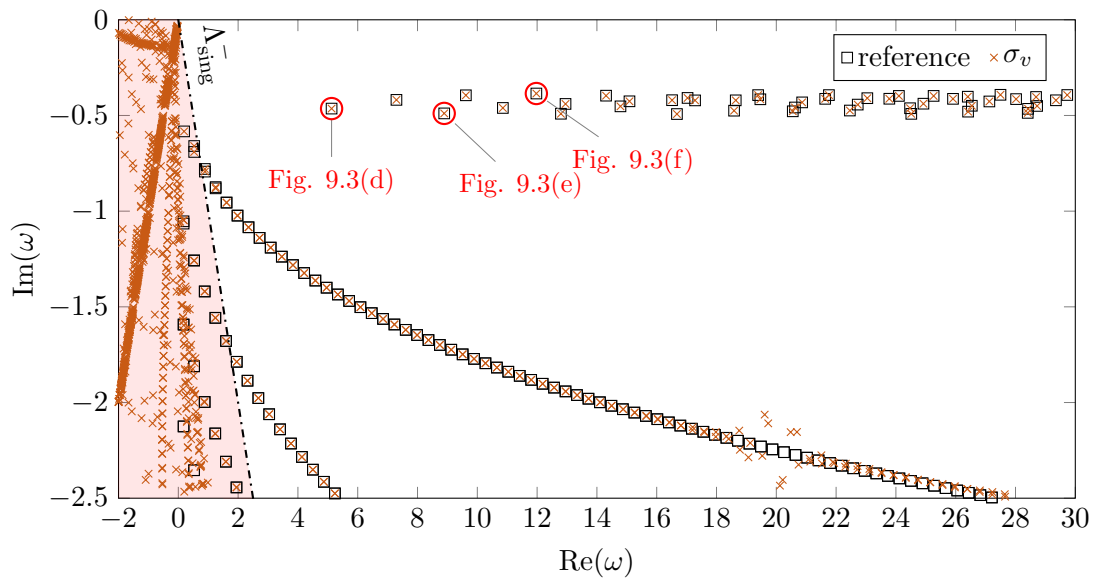
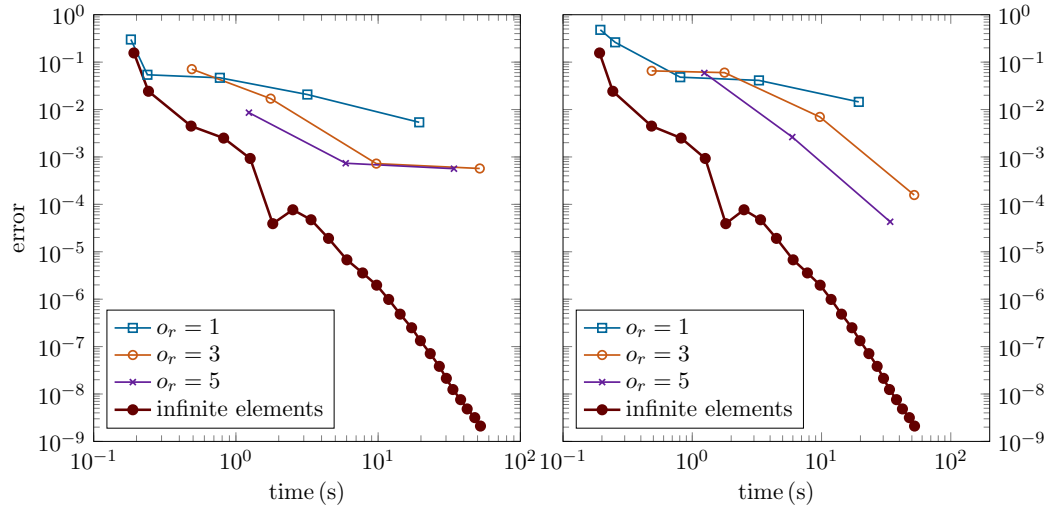
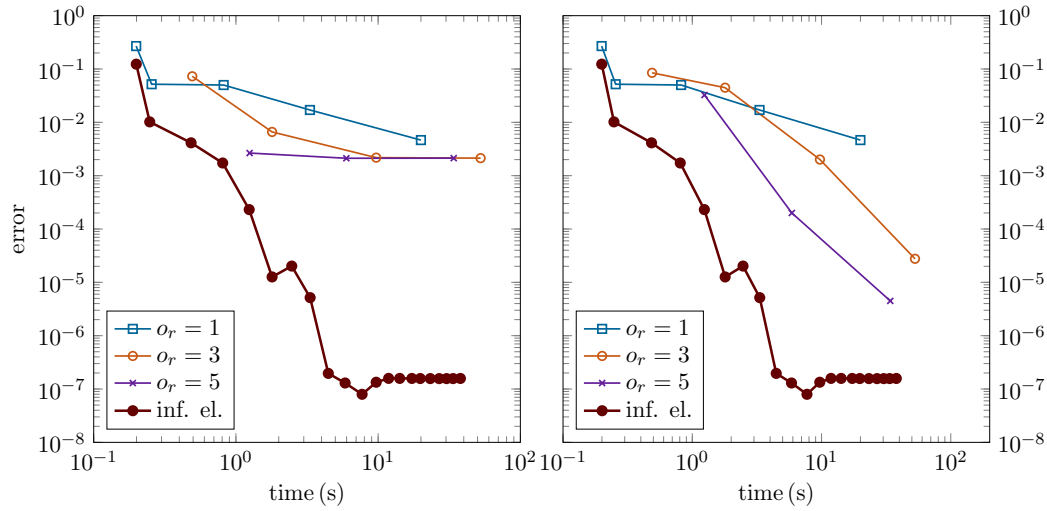


Figure 9.7.: Resonances for a curvilinear frequency-dependent scaling  $\sigma_v(\omega) = \frac{1+i}{\omega}$  with  $R_t = 4$ ,  $R_x = 2$ ,  $\rho_0 = -0.8$ ,  $\mathbf{m} = (0, 1)^\top$ . The discretization parameters are  $N = 20$  and polynomial order 3 (and 2 for the auxiliary  $L^2$ -space) and we used the mesh from Figure 9.2b. The dashdotted line indicates the region where we expect the essential spectrum  $\Sigma_{\text{sing}}$ .



(a)  $T = 5$ ,  
 $\omega \approx 2.90391653245 - 1.20186645975i$

(b)  $T = 8$ ,  
 $\omega \approx 2.90391653245 - 1.20186645975i$



(c)  $T = 5$ ,  
 $\omega \approx 5.77658328455 - 1.41788771722i$

(d)  $T = 8$ ,  
 $\omega \approx 5.77658328455 - 1.41788771722i$

Figure 9.8.: Comparison of the errors of selected resonances  $\omega$  against factorization times. We used a surface discretization with order  $o = 5$  and mesh-size  $h = 0.3$ ,  $\sigma(\omega) = \frac{1+i}{\omega}$ , and different exterior discretizations. The PMLs were truncated at  $T > 0$  and discretized with radial elements of order  $o_r$ .



Die approbierte gedruckte Originalversion dieser Dissertation ist an der TU Wien Bibliothek verfügbar.  
The approved original version of this doctoral thesis is available in print at TU Wien Bibliothek.



# 10. Conclusion and Outlook

In this final chapter we give a short summary of our findings (Section 10.1). Moreover, we explain a few additional scenarios where our method might be a good choice and present ideas on how to apply it (Section 10.2). In Section 10.3 we address some open questions for future research.

## 10.1. Conclusion

We have presented the derivation, analysis, and implementation of the method of frequency-dependent complex-scaled infinite elements for exterior Helmholtz resonance problems. Throughout this work we have shown, in our numerical experiments in Chapters 4 and 9, that the use of a frequency-dependent complex scaling can make the method more robust in the frequency. Therefore, a single computation produces a larger number of well-approximated discrete resonances, compared to the use of a frequency-independent scaling.

In our analysis in Chapter 5, we have shown that the use of a frequency-dependent complex scaling affects the essential spectrum of the problem. This has to be taken into account for the choice of the scaling parameters. Using exterior coordinates (Section 7.1) for generating the complex scaling is useful for the following reasons: Primarily, these coordinates enable us to use curvilinear and star-shaped complex scalings. These scalings can be used to adapt the shape of the interface between the exterior and interior domain to the geometry of the given problem. Therefore, the interior domain can be chosen small to reduce the number of unknowns of the resulting discrete problem (see Table 9.1). Moreover, exterior coordinates can be used to define the discretization of the exterior domain by the use of tensor product basis functions (Section 6.2). Thus, it is not necessary to explicitly generate a mesh of the exterior domain.

We have introduced complex-scaled infinite elements (Section 6.3) for the discretization of the exterior problem. These infinite elements exhibit super-algebraic approximation properties for the eigenfunctions of the complex-scaled Helmholtz equation (cf. Section 6.5) and are, therefore, very well-suited to efficiently treat the resonance problems at hand. Moreover, the complex-scaled infinite elements unite many preferable properties, including well-conditioned, sparse discretization matrices (Section 9.1) and the possibility to use numerical integration (Section 6.3.2) for assembling said matrices.

Lastly, in Chapter 8 we have presented numerical procedures to efficiently solve the rational eigenvalue problems which appear due to the use of frequency-dependent complex scalings.

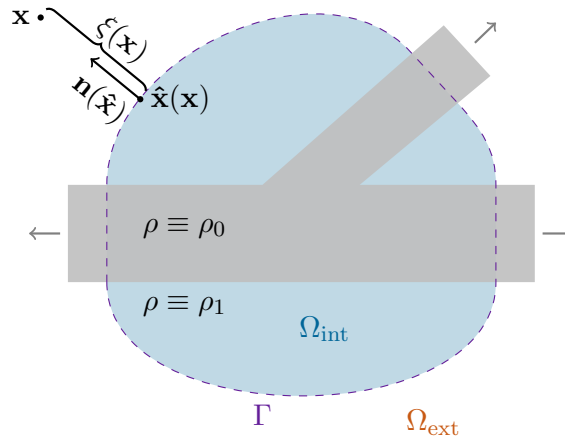


Figure 10.1.: An example of a problem with non-constant potential  $\rho(\cdot) = \hat{\rho}(\hat{\mathbf{x}}(\cdot))$  in  $\Omega_{\text{ext}}$  that can be treated using curvilinear coordinates. Note that the jumps in the potential function are aligned with the normal vector  $\mathbf{n}$  of the interface  $\Gamma$ .

## 10.2. Applications and extensions

In the following we give an overview of problems, in addition to the scenarios studied in this work, where our method could be applied.

### 10.2.1. Inhomogeneous exterior

Contrary to the discretization matrices of Hardy space infinite elements, which are, in some sense, equivalent to the complex-scaled infinite elements (Section 6.4), the discretization matrices of the complex-scaled infinite elements can also be computed using numerical integration (Section 7.4.2). This can be applied in situations where the potential  $\rho$  is not only supported in a bounded domain ([SHK<sup>+</sup>07, NS11]). If we assume that the potential  $\rho$  can be written in  $\Omega_{\text{ext}}$  by

$$\rho(\mathbf{x}) = \tilde{\rho}(\xi(\mathbf{x})) \hat{\rho}(\hat{\mathbf{x}}(\mathbf{x})),$$

we can still compute the discretization matrices by an appropriate tensorization and solve the discrete eigenvalue problem. Configurations where this is useful include, for example, open waveguides (see Figure 10.1, where the potential depends only on the surface variable  $\hat{\mathbf{x}}$ ) or potentials that have also a dependency on the generalized-radial coordinate. Resonances for the latter situation were computed, experimentally, in [NW19], although a proper analysis of this problem has yet to be done. Note that, in this case, it is not even straightforward to define an appropriate radiation condition (cf. [NS11]).

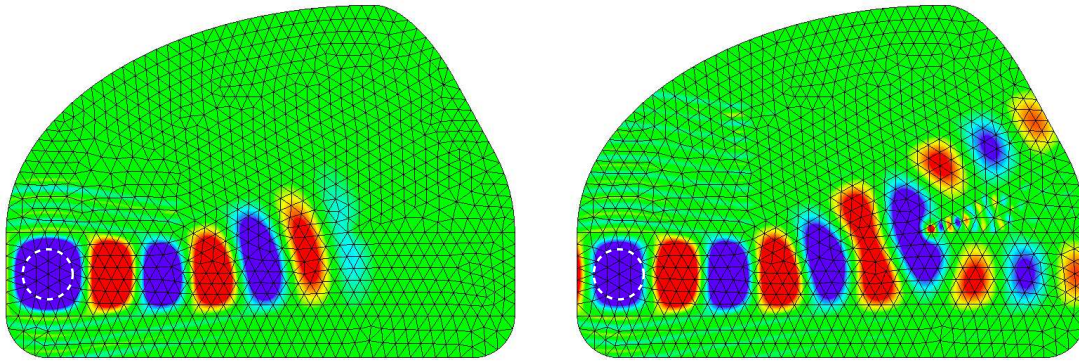


Figure 10.2.: Snapshots of a time-domain example with inhomogeneous exterior potential  $\rho$  (see Figure 10.1). The dashed, white circle marks the location of the source.

### 10.2.2. Frequency-dependent materials

An interesting topic is the study of waves in metamaterials. In some applications these materials can be modeled by frequency-dependent material parameters, where the frequency-dependency is usually chosen as a rational function ([GV17]). In this case the complex scaling has to be chosen dependent on the frequency as well ([BFJ03, BJV18, BK17]). Since the according non-linear eigenvalue problems are very similar to the ones in our case, they could also be treated using the methods from Chapter 8.

### 10.2.3. Other wave-type equations

The Hardy space infinite element method has been successfully applied to electromagnetic ([NHSS13]) and elastic ([HN15a]) wave problems in the time-harmonic regime. Therefore, it is straightforward to use complex-scaled infinite elements for these equations as well. In the elastic case also so-called two pole Hardy space infinite elements are used ([HN18, HHNS16]). It remains an open question whether these elements allow a representation as complex-scaled infinite elements as well.

### 10.2.4. Time-domain

Another situation where it is mandatory to use a frequency-dependent complex scaling is the discretization of problems in time-domain. The scaling needs to be frequency-dependent due to the fact that it has to work for all frequencies  $\omega \in \mathbb{R}$ , since in the derivation of the problem, the inverse Fourier transform is applied to the time-harmonic problem. The frequency-dependencies given in Section 7.3 have already successfully been used for the time-discretization together with infinite elements ([NTW19]). Using exterior coordinates makes the treatment of interesting geometries, such as open waveguides (see Figures 10.1, and 10.2) possible. Future work could include combining these ideas with discontinuous Galerkin methods and explicit time-discretization schemes for fast matrix-free implementations. Moreover, a thorough study of the effects of the various frequency-dependencies in time-domain could be conducted, since, also in time-domain, the choice of the frequency-

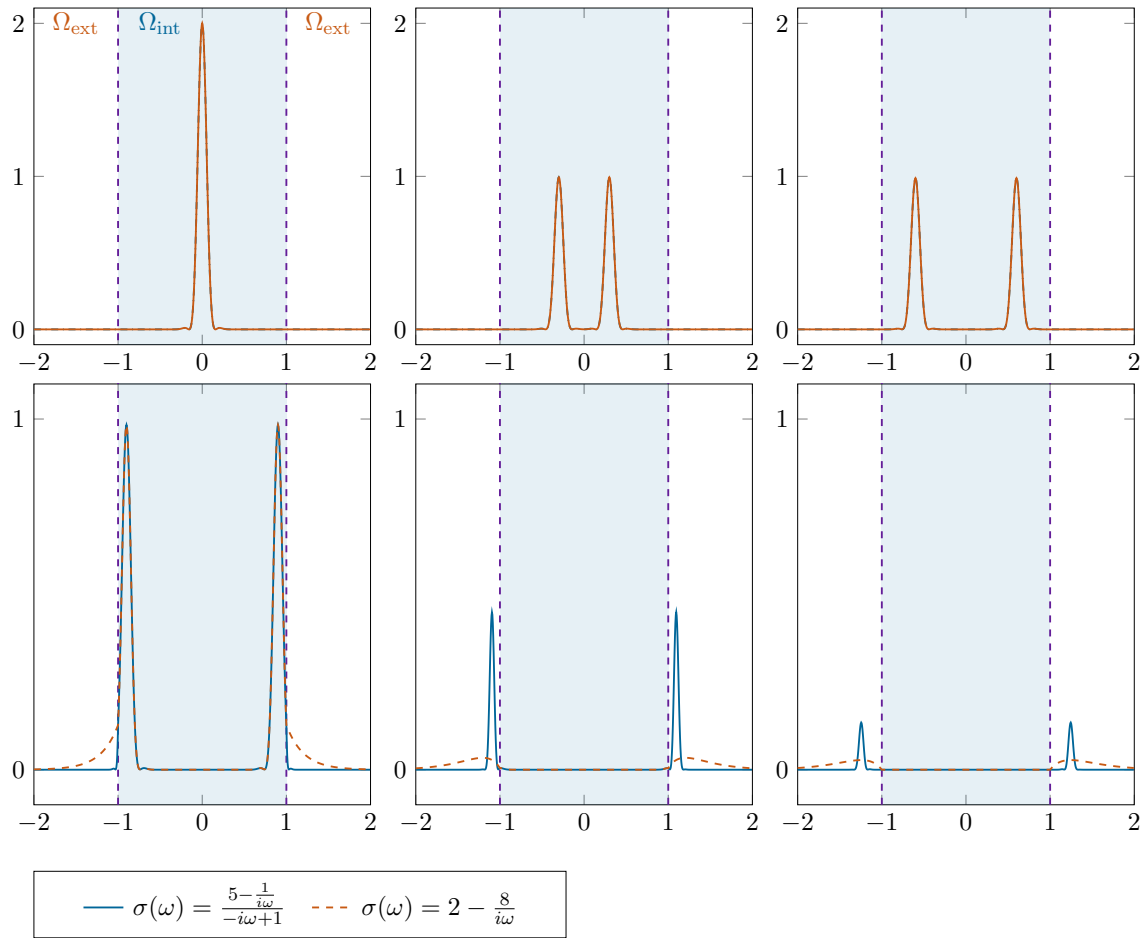


Figure 10.3.: Successive snapshots of a one-dimensional time-domain example using PMLs with different frequency-dependencies.

dependency heavily affects the behavior of the wave in the exterior domain (see Figure 10.3). Although different frequency-dependencies are used in the engineering community (e.g., [DG07, RG00]), to our knowledge the issue of the mathematical analysis thereof has not attracted much attention.

### 10.2.5. Preconditioning

Another interesting topic for future research is the application of preconditioned iterative solvers to our method for non-linear eigenvalue problems. The matrix that needs to be inverted for the application of our algorithm is identical to the one of an according scattering problem. Therefore, any preconditioner for (complex-scaled) Helmholtz scattering problems may be applied. Established preconditioners for such problems are sweeping preconditioners (e.g., [EY11b, EY11a, GZ19]) and shifted Laplace preconditioners (e.g., [BGT83]).

### 10.3. Further open questions

Although we have presented an analysis of our method for the case of a spherical scaling in three dimensions, there are still some gaps to fill.

There is a gap between the region in the complex plane where we can show Fredholmness of the operator function and the region where we can show the existence of an essential spectrum. Moreover, the results regarding the essential spectrum  $\Sigma_{\text{sing}}$  should be refined and generalized to other configurations. In addition to these gaps, the analysis should be extended to the case of general scalings in exterior coordinates.

Lastly, we have presented only a modal analysis of the approximation properties of our basis functions. For a comprehensive analysis, bounds that are uniform in the Bessel index have to be found.



Die approbierte gedruckte Originalversion dieser Dissertation ist an der TU Wien Bibliothek verfügbar.  
The approved original version of this doctoral thesis is available in print at TU Wien Bibliothek.

# A. Appendix

## A.1. Special functions

In this section we give an overview of the special functions we use throughout our work. For a useful summary of most of these functions and their properties we refer to [AS64]. For more comprehensive references see, for example, [Leb65, Tem96, AW01].

### A.1.1. (Spherical) Hankel functions

The Hankel functions of the first and second kind  $H_\alpha^{(1,2)}$  of order  $\alpha \in \mathbb{R}$  play an important role in a wide variety of applications. Most notably, in our context they appear in the separation of the Helmholtz and wave equations into polar coordinates.

The spherical Hankel functions  $h_\alpha^{(1,2)}$  are the counterparts of the Hankel functions for three dimensions and spherical coordinates. In the literature the (spherical) Hankel functions of the first and second kind are commonly also referred to as (spherical) Bessel functions of the third (and fourth) kind. A classical reference for these functions is [Wat44]. All of the following properties can also be found in [AS64, Chapters 9 and 10], [Leb65, Chapter 5] and [Tem96, Chapter 9]. For an overview of the properties of the spherical Hankel functions we refer to [CK98, Section 2.4].

One way to define the Hankel functions is to use integral representations (cf. [Tem96, Equation (9.2)]). The spherical Hankel functions can then be defined by

$$h_\alpha^{(1,2)}(z) := \sqrt{\frac{\pi}{2z}} H_{\alpha+\frac{1}{2}}^{(1,2)}(z)$$

for  $z \in \mathbb{C} \setminus \{0\}$ .

In the following we state a few properties of the (spherical) Hankel functions which are proven in the given references or follow as easy corollaries.

**Proposition A.1.** *Let  $n \in \mathbb{N}_0$ . Then*

- (i) *the Hankel functions  $H_n^{(1,2)}$  are analytic on  $\mathbb{C} \setminus \{0\}$  with a branch point at 0 and*
- (ii)  *$H_n^{(1)}$  and  $H_n^{(2)}$  are linearly independent solutions of Bessel's differential equation*

$$z^2 u''(z) + zu'(z) + (z^2 - n^2)u(z) = 0.$$

**Proposition A.2.** *Let  $n \in \mathbb{N}_0$ . Then*

- (i)

$$h_n^{(1,2)} = \frac{\exp(\pm iz)}{(\pm i)^{n+1} z} \sum_{m=0}^n \frac{1}{(\mp 2iz)^m} \frac{(n+m)!}{m!(n-m)!},$$

(ii) the functions  $h_n^{(1,2)}$  are holomorphic functions on  $\mathbb{C} \setminus \{0\}$  with a pole of order  $n + 1$  at 0, and

(iii) the functions  $h_n^{(1,2)}$  are linearly independent solutions of Bessel's spherical differential equation

$$z^2 u''(z) + 2z u'(z) + (z^2 - n(n+1)) u(z) = 0. \quad (\text{A.1})$$

The (spherical) Hankel functions and their derivatives have the following asymptotic behavior for large arguments and large orders:

**Proposition A.3.** *Let  $n, k \in \mathbb{N}_0$ . Then*

$$\begin{aligned} \frac{\partial^k}{\partial z^k} H_n^{(1,2)}(z) &= (\pm i)^k \sqrt{\frac{2}{\pi z}} \exp\left(\pm i \left(z - \frac{(2n+1)\pi}{4}\right)\right) \left(1 + O\left(\frac{1}{z}\right)\right), & |z| \rightarrow \infty, \\ \frac{\partial^k}{\partial z^k} h_n^{(1,2)}(z) &= \frac{(\pm i)^{k-n-1}}{z} \exp(\pm iz) \left(1 + O\left(\frac{1}{z}\right)\right), & |z| \rightarrow \infty. \end{aligned}$$

**Proposition A.4** (Asymptotics of the (spherical) Hankel functions for large order). *We have*

$$\lim_{n \rightarrow \infty} \frac{h_n(z) i z^{n+1}}{(2n-1)!!} = 1$$

and

$$\lim_{n \rightarrow \infty} \frac{h'_n(z) i z^{n+2}}{(2n-1)!!(n+1)} = -1,$$

uniformly on compact subsets of  $\mathbb{C} \setminus \{0\}$ .

### A.1.2. (Spherical) harmonics

Spherical and cylindrical harmonics are orthogonal systems on the surfaces of the unit sphere and circle respectively. References for these functions include [Leb65, Chapter 7], [AW01, Section 12.6], and [CK98, Section 2.3].

**Definition A.5** (Spherical and cylindrical harmonics). For  $n \in \mathbb{N}_0, m \in \mathbb{Z}$  with  $|m| \leq n$ , the spherical harmonics can be defined on  $S_1 \subset \mathbb{R}^3$  by

$$Y_n^m : \begin{cases} \Gamma & \rightarrow \mathbb{R}, \\ \hat{\mathbf{x}} & \mapsto \sqrt{\frac{(2n+1)(n-|m|!)}{4\pi(n+|m|)!}} p_n^{|m|}(\cos(\theta(\hat{\mathbf{x}}))) \exp(im\phi(\hat{\mathbf{x}})), \end{cases}$$

where  $p_n^{|m|}$  are the associated Legendre functions and  $\theta, \phi$  are the polar angles. Moreover, we define the cylindrical harmonics on  $S_1 \subset \mathbb{R}^2$  by

$$\Phi_n(\hat{\mathbf{x}}) := \exp(in\theta(\hat{\mathbf{x}})),$$

where  $\theta \in [0, 2\pi)$  is the polar angle.



**Proposition A.6.**

(i) The spherical harmonics are a complete orthonormal system with respect to the  $L^2(S_1)$ -inner product. Moreover, they are a complete orthogonal system with respect to the  $H^1(S_1)$ -inner product.

(ii) For all  $n \in \mathbb{N}_0$  and  $\hat{\mathbf{x}} \in B_1$ ,

$$|Y_n^0(\hat{\mathbf{x}})| \leq \sqrt{2n+1}.$$

**A.1.3. (Generalized) Laguerre polynomials and functions**

The generalized Laguerre polynomials form orthogonal systems for certain weighted  $L^2$ -spaces on the set  $\mathbb{R}_{>0}$ . References for these functions include [STW11, Section 7.1], [AS64, Chapter 22], and [Leb65, Section 4.17].

**Definition A.7.** For  $n, m \in \mathbb{Z}$ , we define the generalized Laguerre polynomials by

$$L_{n,m}(x) := \sum_{k=0}^n \binom{n+m}{n-k} \frac{(-x)^k}{k!},$$

where the binomial coefficient for  $\alpha \in \mathbb{C}, k \in \mathbb{N}_0$  is defined by

$$\binom{\alpha}{k} := \prod_{j=1}^k \frac{\alpha - j + 1}{j}. \tag{A.2}$$

We use the convention that an empty sum equals zero and an empty product equals one.

*Remark A.8.* Since an empty sum equals zero we have for  $n < 0$

$$L_{n,m}(x) = 0.$$

An empty product equals one which leads to

$$\binom{\alpha}{0} = 1$$

for all  $\alpha \in \mathbb{C}$ . Moreover, for  $n, k \in \mathbb{N}_0$  with  $k > n$ , we have

$$\binom{n}{k} = 0.$$

Thus, the Laguerre polynomials  $L_{n,-m}$  with  $n > 0$  and negative index  $-m$  have vanishing coefficients of  $x^k$  for  $k \leq m$ .

**Proposition A.9** (properties of the generalized Laguerre polynomials). *Let  $n, m \in \mathbb{Z}$ . Then we have*

(i) for  $x \in \mathbb{C}$

$$nL_{n,m}(x) = (2n + m - 1 - x)L_{n-1,m}(x) - (n + m - 1)L_{n-2,m}(x),$$

(ii)

$$L_{n,m-1} = L_{n,m} - L_{n-1,m},$$

(iii) for  $k \in \mathbb{N}_0$ ,  $x \in \mathbb{C}$

$$\frac{d^k}{dx^k} L_{n,m}(x) = (-1)^k L_{n-k,m+k}(x),$$

(iv)

$$L'_{n,m} = -L_{n-1,m+1} = -\sum_{k=0}^{n-1} L_{k,m},$$

(v) for  $n \in \mathbb{N}_0$ ,  $x \in \mathbb{C}$

$$L_{n,m}(x) = \frac{\exp(x)}{x^m n!} \frac{d^n}{dx^n} (\exp(-x) x^{n+m}),$$

and

(vi) for  $t, x \in \mathbb{C}$ ,  $|t| < 1$ ,

$$\sum_{k=0}^{\infty} L_{k,0}(x) t^k = \frac{\exp\left(-\frac{tx}{1-t}\right)}{1-t}.$$

**Definition A.10.** We define the generalized Laguerre functions for  $n, m \in \mathbb{Z}$  by

$$\phi_{n,m}(x) := \exp(-x) L_{n,m}(2x).$$

We shorten the notation by writing and  $\phi_n := \phi_{n,-1}$ ,  $\psi_n := \phi_{n,0}$ .

**Proposition A.11** (properties of the generalized Laguerre functions). *Let  $n \in \mathbb{N}_0$ ,  $m \in \mathbb{Z}$ . Then*

(i) for  $k \in \mathbb{N}_0$ , the functions  ${}^k\phi_{n,m} \in L^2(\mathbb{R}_{>0})$  and

$$\int_0^{\infty} \xi^m \phi_{n,m}(\xi) \phi_{j,m}(\xi) d\xi = \frac{(n+m)!}{2^{m+1} n!} \delta_{n,j},$$

(ii)

$$\phi_{n,m-1} = \phi_{n,m} - \phi_{n-1,m},$$

(iii)

$$\phi'_{n,m} = -\phi_{n,m} - 2\phi_{n-1,m+1} = -\phi_{n,m+1} - \phi_{n-1,m+1} = -\phi_{n,m} - 2 \sum_{k=0}^{n-1} \phi_{k,m},$$

(iv)

$$\phi_{n,-1}(0) = \delta_{0,n},$$

(v) for  $j, l \in \mathbb{N}_0$  such that  $|j - n| > l + 1$  and  $p \in \mathcal{P}_l$ ,

$$(p\phi'_n, \phi'_j)_{L^2(\mathbb{R}_{>0})} = (p\phi_n, \phi_j)_{L^2(\mathbb{R}_{>0})} = 0,$$

and

(vi) for  $x \in \mathbb{C}$ ,

$$k\phi_{k,m}(x) = (2k + m - 1 - 2x)\phi_{k-1,m}(x) - (k + m - 1)\phi_{k-2,m}(x).$$

## A.2. Further necessary results and technical computations

In this section we state and prove results that were omitted in the main text for the sake of a clear presentation.

**Theorem A.12.** *Let  $D \subset \mathbb{R}^d$  be a smooth, open domain such that  $D^c$  is bounded. Then there exists a bounded operator*

$$\mathrm{tr}_{\partial D} : H^1(D) \rightarrow H^{1/2}(\partial D)$$

such that for  $f \in C(\overline{D}) \cap H^1(D)$  we have  $\mathrm{tr}_{\partial D} f = f|_{\partial D}$ .

*Proof.* Let  $R > 0$  be such that  $D^c \subset B_R$ . Then the set  $D_R := D \cap B_R$  is a bounded, open domain with smooth boundary. Thus, we have a well-defined and bounded trace operator

$$\mathrm{tr}_{\partial D_R} : H^1(D_R) \rightarrow H^{1/2}(\partial D_R)$$

that fulfills

$$\|\mathrm{tr}_{\partial D_R} f\|_{H^{1/2}(\partial D_R)} \leq \|\mathrm{tr}_{\partial D_R}\| \|f\|_{H^1(D_R)}$$

for every  $f \in H^1(D_R)$ , where  $\|\mathrm{tr}_{\partial D_R}\| > 0$  denotes the operator norm of  $\mathrm{tr}_{\partial D_R}$ .

For  $f \in H^1(D)$ , we have  $f|_{D_R} \in H^1(D_R)$  and thus, we may define

$$\mathrm{tr}_{\partial D} f := (\mathrm{tr}_{\partial D_R} f)|_{\partial D}.$$

Because of

$$\|\mathrm{tr}_{\partial D} f\|_{H^{1/2}(\partial D)} \leq \|\mathrm{tr}_{\partial D_R} f\|_{H^{1/2}(\partial D_R)} \leq \|\mathrm{tr}_{\partial D_R}\| \|f\|_{H^1(D_R)} \leq \|\mathrm{tr}_{\partial D_R}\| \|f\|_{H^1(\Omega)},$$

the operator  $\mathrm{tr}_{\partial D}$  is also bounded with norm  $\|\mathrm{tr}_{\partial D}\| \leq \|\mathrm{tr}_{\partial D_R}\|$ . □

**Lemma A.13.** Let  $n \in \mathbb{N}$ ,  $a \in \mathbb{C}$ ,  $\mathbf{b}, \mathbf{d} \in \mathbb{C}^n$ , and  $\mathbf{C} \in \mathbb{C}^{n \times n}$  such that  $\mathbf{C}$  is regular. Then the determinant of  $\mathbf{M} := \begin{pmatrix} a & \mathbf{b}^\top \\ \mathbf{d} & \mathbf{C} \end{pmatrix}$  can be computed by

$$\det(\mathbf{M}) = (a - \mathbf{b}^\top \mathbf{C}^{-1} \mathbf{d}) \det(\mathbf{C}).$$

Moreover, if  $a \neq \mathbf{b}^\top \mathbf{C}^{-1} \mathbf{d}$ , the matrix  $\mathbf{M}$  is regular and

$$\mathbf{M}^{-1} = \frac{\det(\mathbf{C})}{\det(\mathbf{M})} \begin{pmatrix} 1 & -\mathbf{b}^\top \mathbf{C}^{-1} \\ -\mathbf{C}^{-1} \mathbf{d} & \mathbf{C}^{-1} \mathbf{d} \mathbf{b}^\top \mathbf{C}^{-1} \end{pmatrix} + \begin{pmatrix} 0 & \mathbf{0} \\ \mathbf{0} & \mathbf{C}^{-1} \end{pmatrix}.$$

*Proof.* We have

$$\mathbf{M} = \begin{pmatrix} a & \mathbf{b}^\top \\ \mathbf{d} & \mathbf{C} \end{pmatrix} = \begin{pmatrix} a - \mathbf{b}^\top \mathbf{C}^{-1} \mathbf{d} & \mathbf{b}^\top \mathbf{C}^{-1} \\ \mathbf{0} & \mathbf{I}_n \end{pmatrix} \begin{pmatrix} 1 & \mathbf{0} \\ \mathbf{d} & \mathbf{C} \end{pmatrix}$$

which proves the statement about the determinant. Moreover, if  $a \neq \mathbf{b}^\top \mathbf{C}^{-1} \mathbf{d}$  the determinant of  $\mathbf{M}$  is non-zero and

$$\begin{aligned} \mathbf{M} \frac{\det(\mathbf{C})}{\det(\mathbf{M})} \begin{pmatrix} 1 & -\mathbf{b}^\top \mathbf{C}^{-1} \\ -\mathbf{C}^{-1} \mathbf{d} & \mathbf{C}^{-1} \mathbf{d} \mathbf{b}^\top \mathbf{C}^{-1} \end{pmatrix} \\ = \frac{1}{a - \mathbf{b}^\top \mathbf{C}^{-1} \mathbf{d}} \begin{pmatrix} a - \mathbf{b}^\top \mathbf{C}^{-1} \mathbf{d} & -a \mathbf{b}^\top \mathbf{C}^{-1} + \mathbf{b}^\top \mathbf{C}^{-1} \mathbf{d} \mathbf{b}^\top \mathbf{C}^{-1} \\ \mathbf{0} & \mathbf{0} \end{pmatrix} \\ = \begin{pmatrix} 1 & -\mathbf{b}^\top \mathbf{C}^{-1} \\ \mathbf{0} & \mathbf{0} \end{pmatrix} = \mathbf{I}_{n+1} - \mathbf{M} \begin{pmatrix} 0 & \mathbf{0} \\ \mathbf{0} & \mathbf{C}^{-1} \end{pmatrix}. \end{aligned}$$

□

**Lemma A.14.** Let  $m, n \in \mathbb{N}$ ,  $m < n$ , and  $\mathbf{T} \in \mathbb{C}^{n \times m}$  such that  $\mathbf{T}$  has full rank. Then  $\mathbf{T} \mathbf{T}^\dagger$  is the matrix of the orthogonal projection onto  $V := \text{span}(\mathbf{T})$ , where  $\mathbf{T}^\dagger := (\mathbf{T}^\top \mathbf{T})^{-1} \mathbf{T}^\top$  and  $\text{span}(\mathbf{T})$  denotes the space spanned by the columns of  $\mathbf{T}$ .

*Proof.* For  $\mathbf{v} \in \mathbb{C}^n$ , the vector  $\mathbf{T} \mathbf{T}^\dagger \mathbf{v}$  is in  $V$ . Moreover, we have

$$\mathbf{T}^\top (\mathbf{T} \mathbf{T}^\dagger \mathbf{v} - \mathbf{v}) = \mathbf{T}^\top \mathbf{v} - \mathbf{T}^\top \mathbf{v} = \mathbf{0}.$$

□

**Theorem A.15.** Let  $\mathbf{v} \in \mathbb{C}^n$ ,  $\mathbf{T} \in \mathbb{C}^{n \times n-1}$  such that  $\mathbf{T}$  has full rank (i.e.,  $\mathbf{T}^\top \mathbf{T}$  is regular), and  $\mathbf{n} \in \mathbb{C}^n$  such that  $\|\mathbf{n}\| = 1$  and  $\mathbf{T}^\top \mathbf{n} = \mathbf{0}$ . Then

$$\det \left( \begin{pmatrix} \mathbf{v}^\top \\ \mathbf{T}^\top \end{pmatrix} (\mathbf{v}, \mathbf{T}) \right) = \det(\mathbf{T}^\top \mathbf{T}) (\mathbf{v} \cdot \mathbf{n})^2.$$

Moreover, if  $\mathbf{v} \cdot \mathbf{n} \neq 0$ , the matrix  $\begin{pmatrix} \mathbf{v}^\top \\ \mathbf{T}^\top \end{pmatrix} (\mathbf{v}, \mathbf{T})$  is regular and

$$\left( \begin{pmatrix} \mathbf{v}^\top \\ \mathbf{T}^\top \end{pmatrix} (\mathbf{v}, \mathbf{T}) \right)^{-1} = \frac{1}{(\mathbf{v} \cdot \mathbf{n})^2} \begin{pmatrix} 1 & -(\mathbf{T}^\dagger \mathbf{v})^\top \\ -\mathbf{T}^\dagger \mathbf{v} & \mathbf{T}^\dagger \mathbf{v} (\mathbf{T}^\dagger \mathbf{v})^\top \end{pmatrix} + \begin{pmatrix} 0 & \mathbf{0} \\ \mathbf{0} & \mathbf{T}^\dagger (\mathbf{T}^\dagger)^\top \end{pmatrix}.$$

*Proof.* Since  $\mathbf{T}^\top \mathbf{T}$  is regular, we can apply the first part of Lemma A.13 to the matrix

$$\mathbf{M} := \begin{pmatrix} \mathbf{v}^\top \\ \mathbf{T}^\top \end{pmatrix} (\mathbf{v}, \mathbf{T}) = \begin{pmatrix} \mathbf{v}^\top \mathbf{v} & \mathbf{v}^\top \mathbf{T} \\ \mathbf{T}^\top \mathbf{v} & \mathbf{T}^\top \mathbf{T} \end{pmatrix}$$

to obtain

$$\det(\mathbf{M}) = \det \left( \begin{pmatrix} \mathbf{v}^\top \mathbf{v} & \mathbf{v}^\top \mathbf{T} \\ \mathbf{T}^\top \mathbf{v} & \mathbf{T}^\top \mathbf{T} \end{pmatrix} \right) = (\mathbf{v} \cdot \mathbf{v} - \mathbf{v}^\top \mathbf{T} \mathbf{T}^\top \mathbf{v}) \det(\mathbf{T}^\top \mathbf{T}) = (\mathbf{v} \cdot \mathbf{n})^2 \det(\mathbf{T}^\top \mathbf{T}).$$

If  $\mathbf{v} \cdot \mathbf{n} \neq 0$ , the matrix  $\mathbf{M}$  is regular and we can apply the second part of Lemma A.13 to obtain

$$\begin{aligned} \mathbf{M}^{-1} &= \frac{1}{(\mathbf{v} \cdot \mathbf{n})^2} \begin{pmatrix} 1 & -\mathbf{v}^\top \mathbf{T} (\mathbf{T}^\top \mathbf{T})^{-1} \\ -(\mathbf{T}^\top \mathbf{T})^{-1} \mathbf{T}^\top \mathbf{v} & (\mathbf{T}^\top \mathbf{T})^{-1} \mathbf{T}^\top \mathbf{v} \mathbf{v}^\top \mathbf{T} (\mathbf{T}^\top \mathbf{T})^{-1} \end{pmatrix} + \begin{pmatrix} 0 & \mathbf{0} \\ \mathbf{0} & (\mathbf{T}^\top \mathbf{T})^{-1} \end{pmatrix} \\ &= \frac{1}{(\mathbf{v} \cdot \mathbf{n})^2} \begin{pmatrix} 1 & -(\mathbf{T}^\dagger \mathbf{v})^\top \\ -\mathbf{T}^\dagger \mathbf{v} & \mathbf{T}^\dagger \mathbf{v} \mathbf{v}^\top (\mathbf{T}^\dagger)^\top \end{pmatrix} + \begin{pmatrix} 0 & \mathbf{0} \\ \mathbf{0} & \mathbf{T}^\dagger (\mathbf{T}^\dagger)^\top \end{pmatrix}, \end{aligned}$$

since

$$\mathbf{T}^\dagger (\mathbf{T}^\dagger)^\top = (\mathbf{T}^\top \mathbf{T})^{-1} \mathbf{T}^\top \mathbf{T} (\mathbf{T}^\top \mathbf{T})^{-1} = (\mathbf{T}^\top \mathbf{T})^{-1}.$$

□

**Corollary A.16.** *Let  $\mathbf{n}, \mathbf{v} \in \mathbb{C}^n$ , and  $\mathbf{T} \in \mathbb{C}^{n \times n-1}$  such that  $\mathbf{T}$  has full rank,  $\|\mathbf{n}\| = 1$ ,  $\mathbf{T}^\top \mathbf{n} = \mathbf{0}$ , and  $\mathbf{v} \cdot \mathbf{n} \neq 0$ . Then  $(\mathbf{v}, \mathbf{T})$  is regular,*

$$(\mathbf{v}, \mathbf{T})^{-1} = \frac{1}{\mathbf{v} \cdot \mathbf{n}} \begin{pmatrix} \mathbf{n}^\top \\ -\mathbf{T}^\dagger \mathbf{v} \mathbf{n}^\top \end{pmatrix} + \begin{pmatrix} 0 \\ \mathbf{T}^\dagger \end{pmatrix},$$

and

$$|\det(\mathbf{v}, \mathbf{T})| = \sqrt{|\det(\mathbf{T}^\top \mathbf{T})|} |\mathbf{v} \cdot \mathbf{n}|.$$

*Proof.* Since for any regular matrix  $\mathbf{M} \in \mathbb{C}^{n \times n}$  we have  $\mathbf{M}^{-1} = (\mathbf{M}^\top \mathbf{M})^{-1} \mathbf{M}^\top$ , we obtain for  $\mathbf{M} = (\mathbf{v}, \mathbf{T})$ , by Theorem A.15, that

$$\begin{aligned} \mathbf{M}^{-1} &= \left( \frac{1}{(\mathbf{v} \cdot \mathbf{n})^2} \begin{pmatrix} 1 & -(\mathbf{T}^\dagger \mathbf{v})^\top \\ -\mathbf{T}^\dagger \mathbf{v} & \mathbf{T}^\dagger \mathbf{v} \mathbf{v}^\top (\mathbf{T}^\dagger)^\top \end{pmatrix} + \begin{pmatrix} 0 & \mathbf{0} \\ \mathbf{0} & \mathbf{T}^\dagger (\mathbf{T}^\dagger)^\top \end{pmatrix} \right) \begin{pmatrix} \mathbf{v}^\top \\ \mathbf{T}^\top \end{pmatrix} \\ &= \frac{1}{(\mathbf{v} \cdot \mathbf{n})^2} \begin{pmatrix} \mathbf{v}^\top (\mathbf{I}_n - (\mathbf{T} \mathbf{T}^\dagger)^\top) \\ -\mathbf{T}^\dagger \mathbf{v} \mathbf{v}^\top (\mathbf{I}_n - (\mathbf{T} \mathbf{T}^\dagger)^\top) \end{pmatrix} + \begin{pmatrix} 0 \\ \mathbf{T}^\dagger \end{pmatrix}. \end{aligned}$$

Since, by Lemma A.14,  $(\mathbf{I}_n - \mathbf{T} \mathbf{T}^\dagger)$  is the projection onto the space  $\text{span}(\mathbf{T})^\perp = \text{span}(\mathbf{n})$ , we have

$$(\mathbf{I}_n - \mathbf{T} \mathbf{T}^\dagger) \mathbf{v} = \mathbf{v} \cdot \mathbf{n} \mathbf{n}$$

and therefore the assertion follows. The formula for the determinant follows from taking the square root of the determinant of  $\mathbf{M}^\top \mathbf{M}$ . □

**Lemma A.17.** For  $N, M \in \mathbb{N}$ , let  $\mathbf{A} \in \mathbb{C}^{N \times N}$ ,  $\mathbf{B} \in \mathbb{C}^{N \times M}$ ,  $\mathbf{C} \in \mathbb{C}^{M \times N}$ , and  $\mathbf{D} \in \mathbb{C}^{M \times M}$  such that  $\mathbf{D}$  is regular and

$$\mathbf{S} := \mathbf{A} - \mathbf{B}\mathbf{D}^{-1}\mathbf{C}$$

is regular. Then  $\begin{pmatrix} \mathbf{A} & \mathbf{B} \\ \mathbf{C} & \mathbf{D} \end{pmatrix}$  is regular and for  $\mathbf{x}_0 \in \mathbb{C}^N$ ,  $\mathbf{x}_1 \in \mathbb{C}^M$ , we have

$$\begin{pmatrix} \mathbf{y}_0 \\ \mathbf{y}_1 \end{pmatrix} := \begin{pmatrix} \mathbf{A} & \mathbf{B} \\ \mathbf{C} & \mathbf{D} \end{pmatrix}^{-1} \begin{pmatrix} \mathbf{x}_0 \\ \mathbf{x}_1 \end{pmatrix} = \begin{pmatrix} \mathbf{S}^{-1}(\mathbf{x}_0 - \mathbf{B}\mathbf{D}^{-1}\mathbf{x}_1) \\ \mathbf{D}^{-1}(\mathbf{x}_1 - \mathbf{C}\mathbf{y}_0) \end{pmatrix}.$$

*Proof.* We have

$$\begin{pmatrix} \mathbf{S}^{-1}(\mathbf{x}_0 - \mathbf{B}\mathbf{D}^{-1}\mathbf{x}_1) \\ \mathbf{D}^{-1}(\mathbf{x}_1 - \mathbf{C}\mathbf{S}^{-1}(\mathbf{x}_0 - \mathbf{B}\mathbf{D}^{-1}\mathbf{x}_1)) \end{pmatrix} = \begin{pmatrix} \mathbf{S}^{-1} & -\mathbf{S}^{-1}\mathbf{B}\mathbf{D}^{-1} \\ -\mathbf{D}^{-1}\mathbf{C}\mathbf{S}^{-1} & (\mathbf{I}_M + \mathbf{D}^{-1}\mathbf{C}\mathbf{S}^{-1}\mathbf{B})\mathbf{D}^{-1} \end{pmatrix} \begin{pmatrix} \mathbf{x}_0 \\ \mathbf{x}_1 \end{pmatrix}.$$

Moreover, due to

$$\begin{aligned} \mathbf{A}\mathbf{S}^{-1} - \mathbf{B}\mathbf{D}^{-1}\mathbf{C}\mathbf{S}^{-1} &= \mathbf{S}\mathbf{S}^{-1} = \mathbf{I}_N, \\ -\mathbf{A}\mathbf{S}^{-1}\mathbf{B}\mathbf{D}^{-1} + \mathbf{B}(\mathbf{I}_M - \mathbf{D}^{-1}\mathbf{C}\mathbf{S}^{-1}\mathbf{B})\mathbf{D}^{-1} &= (-\mathbf{A}\mathbf{S}^{-1} + \mathbf{I}_M + \mathbf{B}\mathbf{D}^{-1}\mathbf{C}\mathbf{S}^{-1})\mathbf{B}\mathbf{D}^{-1} = 0, \\ \mathbf{C}\mathbf{S}^{-1} - \mathbf{D}\mathbf{D}^{-1}\mathbf{C}\mathbf{S}^{-1} &= 0 \end{aligned}$$

and

$$-\mathbf{C}\mathbf{S}^{-1}\mathbf{B}\mathbf{D}^{-1} + \mathbf{I}_M + \mathbf{C}\mathbf{S}^{-1}\mathbf{B}\mathbf{D}^{-1} = \mathbf{I}_M,$$

we obtain

$$\begin{pmatrix} \mathbf{A} & \mathbf{B} \\ \mathbf{C} & \mathbf{D} \end{pmatrix} \begin{pmatrix} \mathbf{S}^{-1}(\mathbf{x}_0 - \mathbf{B}\mathbf{D}^{-1}\mathbf{x}_1) \\ \mathbf{D}^{-1}(\mathbf{x}_1 - \mathbf{C}\mathbf{S}^{-1}(\mathbf{x}_0 - \mathbf{B}\mathbf{D}^{-1}\mathbf{x}_1)) \end{pmatrix} = \begin{pmatrix} \mathbf{x}_0 \\ \mathbf{x}_1 \end{pmatrix}.$$

□

**Definition A.18.** For complex numbers  $a, b, c, d \in \mathbb{C}$  such that  $|c| + |d| \neq 0$ , we define the Möbius transformation  $m$  by

$$m : \begin{cases} \mathbb{C} \setminus \{-\frac{d}{c}\} & \rightarrow \mathbb{C}, \\ z & \mapsto \frac{az+b}{cz+d}. \end{cases}$$

**Lemma A.19.** Let  $\mu \in \mathbb{C} \setminus \{0\}$  and  $a, b, c, d \in \mathbb{C}$  such that  $c, d \neq 0$  and  $m$  as in Definition A.18. Then the set

$$m(\mu\mathbb{R})$$

is a subset of the circle in the complex plane with center

$$m_0 := \frac{(bc - ad)\bar{\mu}c}{c(d\bar{c}\bar{\mu} - \bar{d}c\mu)} + \frac{a}{c} = \frac{b\bar{\mu}c - a\bar{d}\mu}{d\bar{c}\bar{\mu} - \bar{d}c\mu}$$

and radius

$$r := \left| \frac{(bc - ad)\mu}{d\bar{c}\bar{\mu} - \bar{d}c\mu} \right|.$$

*Proof.* For  $t \in \mathbb{R}$ , we have

$$\begin{aligned}
 |m_0 - m(\mu t)| &= \left| \frac{(bc - ad)\bar{\mu}\bar{c}}{c(d\bar{c}\bar{\mu} - \bar{d}c\mu)} + \frac{a}{c} - \frac{at\mu + b}{ct\mu + d} \right| \\
 &= \left| \frac{(bc - ad)\bar{\mu}|c|^2}{c^2(d\bar{c}\bar{\mu} - \bar{d}c\mu)} + \frac{a(ct\mu + d) - (at\mu + b)c}{c(ct\mu + d)} \right| \\
 &= \left| \frac{(bc - ad)\bar{\mu}|c|^2}{c^2(d\bar{c}\bar{\mu} - \bar{d}c\mu)} + \frac{ad - bc}{c(ct\mu + d)} \right| \\
 &= \left| \frac{(bc - ad)\bar{\mu}|c|^2(ct\mu + d) + (ad - bc)c(d\bar{c}\bar{\mu} - \bar{d}c\mu)}{c^2(d\bar{c}\bar{\mu} - \bar{d}c\mu)(ct\mu + d)} \right| \\
 &= \left| \frac{(bc - ad)(\bar{\mu}|c|^2(ct\mu + d) - c(d\bar{c}\bar{\mu} - \bar{d}c\mu))}{c^2(d\bar{c}\bar{\mu} - \bar{d}c\mu)(ct\mu + d)} \right| \\
 &= \left| \frac{(bc - ad)\mu(\bar{\mu}|c|^2ct + \bar{d}c^2)}{c^2(d\bar{c}\bar{\mu} - \bar{d}c\mu)(ct\mu + d)} \right|.
 \end{aligned}$$

Because of

$$\left| \frac{\bar{\mu}|c|^2ct + \bar{d}c^2}{ct\mu + d} \right| = \left| \frac{\bar{\mu}c^2\bar{c}t + \bar{d}c^2}{ct\mu + d} \right| = |c|^2 \left| \frac{\bar{\mu}\bar{c}t + \bar{d}}{ct\mu + d} \right| = |c|^2,$$

we have

$$|m_0 - m(\mu t)| = \left| \frac{(bc - ad)\mu}{d\bar{c}\bar{\mu} - \bar{d}c\mu} \right| = r.$$

□



Die approbierte gedruckte Originalversion dieser Dissertation ist an der TU Wien Bibliothek verfügbar.  
The approved original version of this doctoral thesis is available in print at TU Wien Bibliothek.



# Bibliography

- [Arn51] W. E. Arnoldi. The principle of minimized iteration in the solution of the matrix eigenvalue problem. *Quart. Appl. Math.*, 9:17–29, 1951.
- [AS64] Milton Abramowitz and Irene A. Stegun. *Handbook of mathematical functions with formulas, graphs, and mathematical tables*, volume 55 of *National Bureau of Standards Applied Mathematics Series*. For sale by the Superintendent of Documents, U.S. Government Printing Office, Washington, D.C., 1964.
- [AW01] George B. Arfken and Hans J. Weber. *Mathematical methods for physicists*. Harcourt/Academic Press, Burlington, MA, fifth edition, 2001.
- [BBDF18] Anne-Sophie Bonnet-Ben Dhia, Sonia Fliss, and Antoine Tonnoir. The half-space matching method: a new method to solve scattering problems in infinite media. *J. Comput. Appl. Math.*, 338:44–68, 2018.
- [Ber94] Jean-Pierre Berenger. A perfectly matched layer for the absorption of electromagnetic waves. *J. Comput. Phys.*, 114(2):185–200, 1994.
- [Bey12] Wolf-Jürgen Beyn. An integral method for solving nonlinear eigenvalue problems. *Linear Algebra Appl.*, 436(10):3839–3863, 2012.
- [BFJ03] E. Bécache, S. Fauqueux, and P. Joly. Stability of perfectly matched layers, group velocities and anisotropic waves. *J. Comput. Phys.*, 188(2):399–433, 2003.
- [BGT83] Alvin Bayliss, Charles I. Goldstein, and Eli Turkel. An iterative method for the Helmholtz equation. *J. Comput. Phys.*, 49(3):443–457, 1983.
- [BHM<sup>+</sup>13] Timo Betcke, Nicholas J. Higham, Volker Mehrmann, Christian Schröder, and Françoise Tisseur. NLEVP: a collection of nonlinear eigenvalue problems. *ACM Trans. Math. Software*, 39(2):Art. 7, 28, 2013.
- [BHNPRr08] A. Bermúdez, L. Hervella-Nieto, A. Prieto, and R. Rodríguez. An exact bounded perfectly matched layer for time-harmonic scattering problems. *SIAM J. Sci. Comput.*, 30(1):312–338, 2007/08.
- [BJV18] Éliane Bécache, Patrick Joly, and Valentin Vinoles. On the analysis of perfectly matched layers for a class of dispersive media and application to negative index metamaterials. *Math. Comp.*, 87(314):2775–2810, 2018.

- [BK17] Eliane Bécache and Maryna Kachanovska. Stable perfectly matched layers for a class of anisotropic dispersive models. Part I: Necessary and sufficient conditions of stability. *ESAIM: Mathematical Modelling and Numerical Analysis*, 51(6):2399 – 2434, December 2017. Extended Version.
- [BP13] James H. Bramble and Joseph E. Pasciak. Analysis of a Cartesian PML approximation to acoustic scattering problems in  $\mathbb{R}^2$  and  $\mathbb{R}^3$ . *J. Comput. Appl. Math.*, 247:209–230, 2013.
- [Cia02] Philippe G. Ciarlet. *The finite element method for elliptic problems*, volume 40 of *Classics in Applied Mathematics*. Society for Industrial and Applied Mathematics (SIAM), Philadelphia, PA, 2002. Reprint of the 1978 original [North-Holland, Amsterdam; MR0520174 (58 #25001)].
- [CK98] David Colton and Rainer Kress. *Inverse acoustic and electromagnetic scattering theory*, volume 93 of *Applied Mathematical Sciences*. Springer-Verlag, Berlin, second edition, 1998.
- [CM98] Francis Collino and Peter Monk. The perfectly matched layer in curvilinear coordinates. *SIAM J. Sci. Comput.*, 19(6):2061–2090 (electronic), 1998.
- [Dav02] E. B. Davies. Non-self-adjoint differential operators. *Bull. London Math. Soc.*, 34(5):513–532, 2002.
- [DE13] Gerhard Dziuk and Charles M. Elliott. Finite element methods for surface PDEs. *Acta Numer.*, 22:289–396, 2013.
- [DG07] Francis H. Drossaert and Antonios Giannopoulos. Complex frequency shifted convolution pml for fdtd modelling of elastic waves. *Wave Motion*, 44(7):593 – 604, 2007.
- [DPVD19] Froilán M. Dopico, Javier Pérez, and Paul Van Dooren. Structured backward error analysis of linearized structured polynomial eigenvalue problems. *Math. Comp.*, 88(317):1189–1228, 2019.
- [EE87] D. E. Edmunds and W. D. Evans. *Spectral theory and differential operators*. Oxford Mathematical Monographs. The Clarendon Press, Oxford University Press, New York, 1987. Oxford Science Publications.
- [EG15] Christian Engström and Luka Grubišić. A subspace iteration algorithm for Fredholm valued functions. *Math. Probl. Eng.*, pages Art. ID 459895, 14, 2015.
- [Eva10] Lawrence C. Evans. *Partial differential equations*, volume 19 of *Graduate Studies in Mathematics*. American Mathematical Society, Providence, RI, second edition, 2010.
- [EY11a] Björn Engquist and Lexing Ying. Sweeping preconditioner for the Helmholtz equation: hierarchical matrix representation. *Comm. Pure Appl. Math.*, 64(5):697–735, 2011.

- [EY11b] Björn Engquist and Lexing Ying. Sweeping preconditioner for the Helmholtz equation: moving perfectly matched layers. *Multiscale Model. Simul.*, 9(2):686–710, 2011.
- [GGO20] Jay Gopalakrishnan, Luka Grubišić, and Jeffrey Owall. Spectral discretization errors in filtered subspace iteration. *Math. Comp.*, 89(321):203–228, 2020.
- [Giv01] Dan Givoli. High-order nonreflecting boundary conditions without high-order derivatives. *J. Comput. Phys.*, 170(2):849–870, 2001.
- [Giv04] D. Givoli. High-order local non-reflecting boundary conditions: a review. *Wave Motion*, 39:319–326, 2004.
- [GS11] Martin J. Gander and Achim Schädle. The pole condition: a Padé approximation of the Dirichlet to Neumann operator. In *Domain decomposition methods in science and engineering XIX*, volume 78 of *Lect. Notes Comput. Sci. Eng.*, pages 125–132. Springer, Heidelberg, 2011.
- [GV17] Mauricio Garcia Vergara. *Impulsions électromagnétiques dans des milieux ultra-dispersifs nanostructurés : une approche théorique et numérique*. PhD thesis, 2017. Thèse de doctorat dirigée par Zolla, Frédéric et Demésy, Guillaume Physique et sciences de la matière. Optique, photonique et traitement d’image Aix-Marseille 2017.
- [GZ19] Martin J. Gander and Hui Zhang. A class of iterative solvers for the Helmholtz equation: factorizations, sweeping preconditioners, source transfer, single layer potentials, polarized traces, and optimized Schwarz methods. *SIAM Rev.*, 61(1):3–76, 2019.
- [Hal16] Martin Halla. Convergence of hardy space infinite elements for helmholtz scattering and resonance problems. *SIAM Journal on Numerical Analysis*, 54(3):1385–1400, 2016.
- [Hal19] Martin Halla. *Analysis of radial complex scaling methods for scalar resonance problems in open systems*. PhD. thesis, TU Vienna, Wien, 2019.
- [HHNS16] Martin Halla, Thorsten Hohage, Lothar Nannen, and Joachim Schöberl. Hardy space infinite elements for time harmonic wave equations with phase and group velocities of different signs. *Numer. Math.*, 133(1):103–139, 2016.
- [HN09] Thorsten Hohage and Lothar Nannen. Hardy space infinite elements for scattering and resonance problems. *SIAM J. Numer. Anal.*, 47(2):972–996, 2009.
- [HN15a] Martin Halla and Lothar Nannen. Hardy space infinite elements for time-harmonic two-dimensional elastic waveguide problems. *Wave Motion*, 59:94–110, 2015.

- [HN15b] Thorsten Hohage and Lothar Nannen. Convergence of infinite element methods for scalar waveguide problems. *BIT Numerical Mathematics*, 55(1):215–254, 2015.
- [HN18] Martin Halla and Lothar Nannen. Two scale Hardy space infinite elements for scalar waveguide problems. *Adv. Comput. Math.*, 44(3):611–643, 2018.
- [HS96] P. D. Hislop and I. M. Sigal. *Introduction to spectral theory*, volume 113 of *Applied Mathematical Sciences*. Springer-Verlag, New York, 1996. With applications to Schrödinger operators.
- [HSZ03a] Thorsten Hohage, Frank Schmidt, and Lin Zschiedrich. Solving time-harmonic scattering problems based on the pole condition. I. Theory. *SIAM J. Math. Anal.*, 35(1):183–210, 2003.
- [HSZ03b] Thorsten Hohage, Frank Schmidt, and Lin Zschiedrich. Solving time-harmonic scattering problems based on the pole condition. II. Convergence of the PML method. *SIAM J. Math. Anal.*, 35(3):547–560, 2003.
- [Ihl98] Frank Ihlenburg. *Finite element analysis of acoustic scattering*, volume 132 of *Applied Mathematical Sciences*. Springer-Verlag, New York, 1998.
- [Kar96a] Otto Karma. Approximation in eigenvalue problems for holomorphic Fredholm operator functions. I. *Numer. Funct. Anal. Optim.*, 17(3-4):365–387, 1996.
- [Kar96b] Otto Karma. Approximation in eigenvalue problems for holomorphic Fredholm operator functions. II. (Convergence rate). *Numer. Funct. Anal. Optim.*, 17(3-4):389–408, 1996.
- [Kat95] Tosio Kato. *Perturbation theory for linear operators*. Classics in Mathematics. Springer-Verlag, Berlin, 1995. Reprint of the 1980 edition.
- [Kim09] Seungil Kim. *Analysis of a pml method applied to computation of resonances in open systems and acoustic scattering problems*. ProQuest LLC, Ann Arbor, MI, 2009. Thesis (Ph.D.)—Texas A&M University.
- [Kim14] Seungil Kim. Cartesian PML approximation to resonances in open systems in  $\mathbb{R}^2$ . *Appl. Numer. Math.*, 81:50–75, 2014.
- [KP09] Seungil Kim and Joseph E. Pasciak. The computation of resonances in open systems using a perfectly matched layer. *Math. Comp.*, 78(267):1375–1398, 2009.
- [KP10a] Seungil Kim and Joseph E. Pasciak. Analysis of a Cartesian PML approximation to acoustic scattering problems in  $\mathbb{R}^2$ . *J. Math. Anal. Appl.*, 370(1):168–186, 2010.

- [KP10b] Seungil Kim and Joseph E. Pasciak. Analysis of the spectrum of a Cartesian perfectly matched layer (PML) approximation to acoustic scattering problems. *J. Math. Anal. Appl.*, 361(2):420–430, 2010.
- [Kre99] Rainer Kress. *Linear integral equations*, volume 82 of *Applied Mathematical Sciences*. Springer-Verlag, New York, second edition, 1999.
- [Leb65] N. N. Lebedev. *Special functions and their applications*. Revised English edition. Translated and edited by Richard A. Silverman. Prentice-Hall, Inc., Englewood Cliffs, N.J., 1965.
- [LS01] Matti Lassas and Erkki Somersalo. Analysis of the PML equations in general convex geometry. *Proc. Roy. Soc. Edinburgh Sect. A*, 131(5):1183–1207, 2001.
- [MV04] Volker Mehrmann and Heinrich Voss. Nonlinear eigenvalue problems: a challenge for modern eigenvalue methods. *GAMM Mitt. Ges. Angew. Math. Mech.*, 27(2):121–152 (2005), 2004.
- [N01] Jean-Claude Nédélec. *Acoustic and electromagnetic equations*, volume 144 of *Applied Mathematical Sciences*. Springer-Verlag, New York, 2001. Integral representations for harmonic problems.
- [Nan17] Lothar Nannen. High order transport boundary conditions for the Helmholtz equation. In *Modern solvers for Helmholtz problems*, Geosyst. Math., pages 27–52. Birkhäuser/Springer, Cham, 2017.
- [NHSS13] Lothar Nannen, Thorsten Hohage, Achim Schädle, and Joachim Schöberl. Exact sequences of high order Hardy space infinite elements for exterior Maxwell problems. *SIAM J. Sci. Comput.*, 35(2):A1024–A1048, 2013.
- [NS11] Lothar Nannen and Achim Schädle. Hardy space infinite elements for Helmholtz-type problems with unbounded inhomogeneities. *Wave Motion*, 48(2):116–129, 2011.
- [NTW19] Lothar Nannen, Karoline Tichy, and Markus Wess. Complex scaled infinite elements for wave equations in heterogeneous open systems. In Manfred Kaltenbacher, J. Markus Melenk, Lothar Nannen, and Florian Toth, editors, *14th International Conference on Mathematical and Numerical Aspects of Wave Propagation. Book of Abstracts*, pages 520–521, 2019.
- [NW18] Lothar Nannen and Markus Wess. Computing scattering resonances using perfectly matched layers with frequency dependent scaling functions. *BIT*, 58(2):373–395, 2018.
- [NW19] Lothar Nannen and Markus Wess. Complex scaled infinite elements for exterior Helmholtz problems, 2019. arXiv.
- [RG00] J. Alan Roden and Stephen D. Gedney. Convolution pml (cpml): An efficient fdtd implementation of the cfs-pml for arbitrary media. *Microwave and Optical Technology Letters*, 27(5):334–339, 2000.

- [RSS13] Daniel Ruprecht, Achim Schädle, and Frank Schmidt. Transparent boundary conditions based on the pole condition for time-dependent, two-dimensional problems. *Numer. Methods Partial Differential Equations*, 29(4):1367–1390, 2013.
- [Ruh73] Axel Ruhe. Algorithms for the nonlinear eigenvalue problem. *SIAM J. Numer. Anal.*, 10:674–689, 1973.
- [Saa11] Yousef Saad. *Numerical methods for large eigenvalue problems*, volume 66 of *Classics in Applied Mathematics*. Society for Industrial and Applied Mathematics (SIAM), Philadelphia, PA, 2011. Revised edition of the 1992 original [1177405].
- [Sch97] Joachim Schöberl. Netgen - an advancing front 2d/3d-mesh generator based on abstract rules. *Comput. Visual.Sci*, 1:41–52, 1997.
- [Sch14] Joachim Schöberl. C++11 implementation of finite elements in ngsolve. Preprint 30/2014, Institute for Analysis and Scientific Computing, TU Wien, 2014.
- [SD95] F. Schmidt and P. Deuffhard. Discrete transparent boundary conditions for the numerical solution of Fresnel’s equation. *Comput. Math. Appl.*, 29(9):53–76, 1995.
- [SHK<sup>+</sup>07] F. Schmidt, T. Hohage, R. Klose, A. Schädle, and L. Zschiedrich. Pole condition: A numerical method for Helmholtz-type scattering problems with inhomogeneous exterior domain. *J. Comput. Appl. Math.*, 2007. at press.
- [Sim79] B. Simon. The definition of molecular resonance curves by the method of exterior complex scaling. *Phys. Lett. A*, 71A(2, 3), 1979.
- [SS03] Tetsuya Sakurai and Hiroshi Sugiura. A projection method for generalized eigenvalue problems using numerical integration. In *Proceedings of the 6th Japan-China Joint Seminar on Numerical Mathematics (Tsukuba, 2002)*, volume 159, pages 119–128, 2003.
- [SS11] Stefan A. Sauter and Christoph Schwab. *Boundary element methods*, volume 39 of *Springer Series in Computational Mathematics*. Springer-Verlag, Berlin, 2011. Translated and expanded from the 2004 German original.
- [STW11] Jie Shen, Tao Tang, and Li-Lian Wang. *Spectral methods*, volume 41 of *Springer Series in Computational Mathematics*. Springer, Heidelberg, 2011. Algorithms, analysis and applications.
- [SU12] O. Steinbach and G. Unger. Convergence analysis of a Galerkin boundary element method for the Dirichlet Laplacian eigenvalue problem. *SIAM J. Numer. Anal.*, 50:710–728, 2012.
- [SY97] Frank Schmidt and David Yevick. Discrete transparent boundary conditions for Schrödinger-type equations. *J. Comput. Phys.*, 134(1):96–107, 1997.



- [SZ99] Johannes Sjöstrand and Maciej Zworski. Asymptotic distribution of resonances for convex obstacles. *Acta Math.*, 183(2):191–253, 1999.
- [Tem96] Nico M. Temme. *Special functions*. A Wiley-Interscience Publication. John Wiley & Sons, Inc., New York, 1996. An introduction to the classical functions of mathematical physics.
- [Tem15] Nico M. Temme. *Asymptotic methods for integrals*, volume 6 of *Series in Analysis*. World Scientific Publishing Co. Pte. Ltd., Hackensack, NJ, 2015.
- [Tja19] Yohanes Tjandrawidjaja. *Some contributions to the analysis of the Half-Space Matching Method for scattering problems and extension to 3D elastic plates*. Thesis, ENSTA PARISTECH UNIVERSITÉ PARIS SACLAY, December 2019.
- [TP14] Ping Tak Peter Tang and Eric Polizzi. FEAST as a subspace iteration eigensolver accelerated by approximate spectral projection. *SIAM J. Matrix Anal. Appl.*, 35(2):354–390, 2014.
- [Wat44] G. N. Watson. *A Treatise on the Theory of Bessel Functions*. Cambridge University Press, Cambridge, England; The Macmillan Company, New York, 1944.
- [Won01] R. Wong. *Asymptotic approximations of integrals*, volume 34 of *Classics in Applied Mathematics*. Society for Industrial and Applied Mathematics (SIAM), Philadelphia, PA, 2001. Corrected reprint of the 1989 original.
- [Zwo99] Maciej Zworski. Resonances in physics and geometry. *Notices Amer. Math. Soc.*, 46(3):319–328, 1999.



Die approbierte gedruckte Originalversion dieser Dissertation ist an der TU Wien Bibliothek verfügbar.  
The approved original version of this doctoral thesis is available in print at TU Wien Bibliothek.



# Curriculum Vitae

## Persönliche Daten

Name	<b>Markus Wess</b>
Geburtsdatum	20.12.1987
Geburtsort	Wien
Nationalität	Österreich
Email	markus.wess@tuwien.ac.at

---

## Ausbildung

seit 10/2014	Universitätsassistent am Institut für Analysis und Scientific Computing, TU Wien, Österreich
2011–2014	Masterstudium Mathematik in Technik und Naturwissenschaften, TU Wien, Österreich
2009–2012	Bachelorstudium Jazztrompete, Konservatorium Wien, Österreich
2007–2011	Bachelorstudium Mathematik in Technik und Naturwissenschaften, TU Wien, Österreich
1997–2006	Realgymnasium, BG & BRG Keimgasse, Mödling, Österreich

---

Wien, am 22. Mai 2020

---

Dipl.-Ing. Markus Wess